UNIVERSITÉ DU QUÉBEC EN ABITIBI-TÉMISCAMINGUE

DÉSULFURATION ENVIRONNEMENTALE DES REJETS MINIERS POUR LE CONTRÔLE DE LA GÉNÉRATION DU DRAINAGE MINIER CONTAMINÉ

THÈSE

PRÉSENTÉE

COMME EXIGENCE PARTIELLE

DU DOCTORAT EN SCIENCES DE L'ENVIRONNEMENT

PAR

YASSINE AIT KHOUIA

DÉCEMBRE 2022

REMERCIEMENTS

Je tiens à remercier toutes les personnes que j'ai côtoyées durant ces années d'études et qui m'ont soutenu et aidé. Mes remerciements vont d'abord à mes directeurs de thèse Isabelle Demers et Mostafa Benzaazoua de m'avoir donné l'opportunité de réaliser un tel projet de doctorat dans des conditions meilleures. Je tiens à les remercier pour leurs encadrements et apport scientifiques, encouragements, implications, disponibilités et soutien tout au long de la thèse. Sans leur précieuse aide, ce travail n'aurait pas abouti.

J'adresse aussi mes remerciements à toute l'équipe de l'IRME/URSTM pour leur soutien. Les travaux de laboratoire ont été réalisés dans les meilleures conditions grâce à la collaboration du personnel de l'URSTM : Je remercie chaleureusement Elvin pour son aide apportée au laboratoire et disponibilité durant mes tests de flottation et gravimétrie, Alain pour son aide aussi durant la réalisation de mes tests cinétiques. Merci également à Lilas et Joël pour leurs disponibilités et bonne humour. Un grand merci aussi est adressé à Guillaume Noirant pour son aide à faire fonctionner l'appareil DRIFTS et le partage de la documentation. Merci également à toute l'équipe : Sylvette, Mathieu, Gwendoline, Mélinda, Pierre-Alain, Jean-Christophe et Roch.

Des remerciements spéciaux partent à mon ami Abdelilah de m'avoir aidé dans la purification des minéraux purs et la réalisation de quelques tests de caractérisation surfaciques des minéraux purs, Benjamin De Castro pour sa disponibilité et ses belles images de microscopie optique, Abdellatif Elghali pour ses conseils et ses recommandations précieuses. Je remercie également mes amis (es) et collègues que j'ai côtoyés durant ce doctorat, particulièrement Abdelilah, Hicham, Noureddine, Marouen, Chloé, Safa, Faneiva, Alban, Simon, Khadija, Youssef et Mahya. Je m'excuse d'avance auprès de ceux et elles que je n'ai pas cités, mais je n'oublie pas dans ma pensée.

Un grand merci est adressé également à Aurélie Chopard, Raphael Mermillod Blondin pour leur aide à la réussite de ce projet de doctorat, leurs réponses aux nombreuses questions posées. J'exprime aussi mes reconnaissances à Ievgeniia Morozova et au personnel de NIKON METROLOGY pour leur collaboration et leur aide dans l'analyse CT (computed tomography), à Yassine Taha et Manar Derhy pour leur aide dans les tests de zétamétrie. Enfin, un grand merci au laboratoire XPS de Sudbury (Canada) pour son aide dans la réalisation de l'analyse QEMSCAN.

DÉDICACE

À la mémoire de ma mère, mon père, ma femme, mon fils, mes frères et mes soeurs

AVANT-PROPOS

Cette thèse a été rédigée sous forme d'articles scientifiques et elle est composée de neuf chapitres. Il sera ainsi possible pour le lecteur de trouver quelques redondances dans certaines parties de la thèse. Cependant, cette particularité ne nuit pas au suivi des travaux réalisés et à leur compréhension ainsi qu'aux résultats obtenus.

La conception générale de ce projet de thèse a été réalisée principalement par les directeurs de thèse Isabelle Demers et Mostafa Benzaazoua avec une contribution de l'auteur principal Yassine Ait Khouia.

Cinq articles scientifiques ont été proposés. Ils constituent ainsi le corps de document. Parmi eux, deux sont déjà publiés (Minerals engineering Journal), deux sont acceptés pour publication après des corrections mineures dans « Minerals Engineering journal » et « Journal of Geochemical exploration», alors que le cinquième est soumis pour évaluation à « Journal of Geochemical Exploration ». Il est à mentionner que l'élaboration des protocoles expérimentaux, le travail de laboratoire et les essais effectués dans ces papiers ainsi que leur rédaction ont été réalisés par l'auteur de cette thèse. En effet, la place d'auteur principal lui est attribuée. Mes directeurs de thèse ont contribué à la conception du projet, à la supervision, à l'analyse et l'interprétation des résultats et à la révision et la correction du manuscript.

Il est également judicieux de mentionner que quelques collaborations avec d'autres auteurs (selon le sujet spécifique traité) avaient lieu. Ainsi, Abdelilah Elbouazzaoui et Yassine Taha ont participé/aidé à la réalisation de quelques tests de laboratoire du chapitre IV, c'est pourquoi les places de deuxième et troisième auteurs lui ont été attribuées. Au niveau du chapitre V, Aurélie Chopard et Abdellatif Elghali ont participé à la relecture et la correction du papier. Morozova Ievgeniia à son tour a contribué à la réalisation de quelques analyses de tomographie 3D (chapitre VI) , c'est pourquoi la troisième place lui a été attribuée.

TABLE DES MATIÈRES

LISTE DES FIGURES

LISTE DES TABLEAUX

LISTE DES ABRÉVIATIONS, DES SIGLES ET DES ACRONYMES

A : Absorbance

Ce : Concentrtion résiduelle de collecteur (mol/L)

DMA : Drainage minier acide

DMC : Drainage minier contaminé

DNC : Drainage neutre contaminé

DRIFTS : Spectroscopie Infrarouge à Transformée de Fourier en mode Réflexion Diffuse

DRX : Diffraction des rayons X

EDS : microanalyse en spectroscopie de dispersion des énergies de photons X

FRX : Fluorescence des rayons X

ICP-AES : Spectrométrie d'émission atomique - Plasma à Couplage Inductif

ICP-MS : Spectroscopie de masse - Plasma à Couplage Inductif

L : Largueur de la cellule du spectrophotomètre (cm)

MIBC : Méthyl isobutyl carbinol

PA : Potentiel d'acidité

PAX : Potassium amyl xanthate (ou KAX)

PCN : Point de charge nulle

PN : Potentiel de neutralisation

QEMSCAN : évaluation quantitative de minéraux par microscope électronique à balayage

S/C : Soufre et carbone total

T : Transmittance

UV : Ultraviolet

X : Xanthate

X2 : Dixanthogène

ε : Coefficient d'extinction molaire (L/mol/cm)

RÉSUMÉ

La gestion des rejets miniers, tant pour les résidus que pour les roches stériles, constitue un véritable défi environnemental pour l'industrie minière autant par le volume de ces derniers que par leur diversité, leur potentiel contaminant et leur hétérogénéité. L'entreposage de ces rejets doit être conforme aux normes environnementales qui sont de plus en plus strictes, afin de minimiser leurs impacts sur l'environnement, notamment en matière de génération du drainage minier contaminé.

Cette présente thèse a pour objectif principal d'approfondir le cadre d'application de la désulfuration environnementale (par flottation et/ou gravimétrie) en tant que technique de gestion intégrée des rejets miniers, pour le contrôle de la génération des contaminants (e.g., As, Ni), qui peut émaner à la suite de l'oxydation de certains minéraux (e.g., sulfosels) contenus dans les rejets miniers. Cette étude s'inscrit également dans la continuité des travaux permettant une meilleure compréhension des mécanismes surfaciques fondamentaux inhérents à la séparation par flottation de certains minéraux porteurs de contaminants (e.g., gersdorffite, skutterudite, nickéline) sous diverses conditions physico-chimiques. Cet exercice a permis de déterminer les conditions optimales nécessaires de leur flottation. Ces résultats fondamentaux ont été validés par une application sur des résidus miniers (Amaruq) porteurs de la gersdorffite (NiAsS).

Quant aux stériles miniers, cette étude a permis de définir le DPLS (diamètre d'encapsulation physique des sulfures) par le biais de techniques minéralogiques avancées combinées à des tests géochimiques. Ce paramètre permet de séparer le stérile minier étudié en deux fractions de réactivités différentes : une fraction >DPLS=2.5mm à faible risque et une fraction < DPLS génératrice de contaminants et de volume réduit. Les travaux ont également permis de proposer une méthodologie de gestion durable de ce rejet avant son entreposage. De nouvelles pratiques permettant de décontaminer la fraction réactivevet de la stocker de manière plus durable ont été développées. Les résultats obtenus ont montré que la séparation en milieu dense (DMS centrifuge) et le procédé combinant la flottation et la gravimétrie présentent une efficacité de décontamination intéressante de la fraction problématique, , ce qui permet d'élaborer de nouvelles pratiques concrètes.

Mots clés :

Rejets miniers, sulfures/sulfosels, skutteruditte, gersdorffite, nickéline, DRIFTS, UV-Visible, drainage minier contaminé, désulfuration environnementale, flottation, gravimétrie, DPLS, DMS, essais cinétiques, gestion intégrée des rejets miniers

CHAPITRE 1

INTRODUCTION

Dans l'objectif d'extraire le minerai doté de valeur économique, l'activité minière génère des quantités importantes de rejets miniers dont la gestion des risques qui y sont associés est devenue un véritable défi environnemental (Aubertin et al., 2002, Elghali et al., 2019a). Cette problématique est amenée à s'intensifier en raison de l'exploitation récente intensive de gisements à grand tonnage et à faible teneur renfermant des minéraux sulfureux porteurs de contaminants (Elghali et al., 2019a; José Neto et al., 2019; Taskinen et al., 2018). Ainsi, l'industrie minière est appelée à réévaluer régulièrement ses pratiques de gestion des rejets miniers tout en les adaptant aux directives gouvernementales et guides de bonne pratiques qui cadrent cette activité (à l'image de la Directive 019 au Canada) afin de réduire et contrôler son impact sur l'environnement.

Ces rejets miniers comprennent une variété de produits dont on en distingue principalement les roches stériles appelées communément stériles miniers (waste rock) et les rejets de concentrateur appelés également résidus miniers. Les stériles miniers sont des roches non économiques fragmentées et extraites pour accéder à un corps minéralisé (gisement) et dont la teneur en élément de valeur est inférieure à la fameuse teneur de coupure. Ainsi, le terme « stérile » ne signifie pas que ces rejets sont dépourvus des éléments d'intérêt (valorisables), mais plutôt que leur abondance est trop limitée pour être exploités de façon rentable économiquement à l'usine. Ils sont le plus souvent produits en immenses quantité lors des exploitations à ciel ouvert mais aussi, à un rythme moindre, lors des travaux d'accès aux zones minéralisées pour le cas des mines souterraines. Ce sont des matériaux grossiers (avec une distribution granulométrique étalée) caractérisés par une hétérogénéité de leurs propriétés physiques (Amos et al., 2015; Bussière, 2007; Bussière et al., 2004) et présentant des

anisotropies des propriétés chimiques, minéralogiques et géochimiques (Aubertin et al., 2008; Elghali et al., 2019a; Jamieson et al., 2015). Quant aux résidus miniers, qui sont des rejets desquels la valeur commerciale est retirée à l'usine, se caractérisent par une granulométrie fine (particules broyées à l'usine) et sont considérés comme des matériaux homogènes (Bussière, 2007 ; Amos et al., 2015). Les modes de gestion respectifs de ces deux types de rejets sont conséquemment différents. Quand ils ne sont pas réutilisés pour le remblayage des vides exploités, les stériles miniers sont généralement déposés en surface sous forme de grandes haldes à stériles. Cependant, les résidus miniers sont le plus souvent gérés à l'état de pulpe plus ou moins densifiée et déposés généralement dans des aires de stockage appelées « parcs à résidus ».

La gestion durable de ces rejets est une préoccupation environnementale majeure pour l'industrie minière en raison des risques d'instabilité physique et/ou géochimique qu'ils peuvent engendrer suite à des altérations météoriques. Dépendamment du contexte géologique des gisements exploités, ces rejets peuvent contenir des minéraux sulfureux et/ou sulfosels de différentes réactivités vis-à-vis les conditions météorologiques. L'exposition de ces rejets à l'air et à l'eau peut générer du drainage minier acide (DMA) si leur contenu en minéraux neutralisant est insuffisant pour neutraliser l'acidité produite par les réactions d'oxydation des sulfures/sulfosels (Benzaazoua et al., 2004; Blowes et al., 1998). Cette réactivité entraîne le relargage de métaux et métalloïdes toxiques en solution et par conséquent, la contamination des sols et la pollution de l'environnement avoisinant (faune, flore, eaux souterraines et de surface) (Alloway, 1995; Dold, 2017; Förstner et Wittmann, 2012). Dans le cas où le rejet minier contient suffisamment de minéraux neutralisants, les eaux de drainage minier sont caractérisées par des pH neutres ou proches de la neutralité, et ne pouvant induire qu'une contamination plus ou moins prononcée (non respect de la réglemntation environnementale) appelée drainage neutre contaminé (DNC) (Mayes et al. 2009, Plante 2010b). Conséquemment, les minières sont amenées à gérer leurs rejets miniers solides de manière à stabiliser leur comportement géochimique avant la fermeture

définitive du site minier. Pour cette raison, différentes approches ont été développées dans ce sens. Bien que nombreuses, ces dernières interviennent au niveau de l'un ou plusieurs facteurs déclenchant la formation du drainage minier (DMA/DNC), à savoir une des composantes de la réaction d'oxydation : le ou les sulfures/sulfosels, l'eau et l'oxygène.

La désulfuration environnementale par flottation non sélective, ayant beaucoup gagné en popularité au cours des deux dernières décennies, fait partie de ces approches en tant que technique de gestion intégrée des résidus miniers (Benzaazoua et al., 2000; Demers et al., 2009) ayant comme principe l'enlèvement des sulfures et sulfosels présents dans les rejets. Ce procédé vise ainsi à séparer l'espèce minérale d'intérêt (sulfures et sulfosels: concentré de flottation) de la gangue (rejet de flottation). Afin de réaliser cette séparation minéralogique, les surfaces minérales doivent être le plus souvent modifiées de façon sélective par le biais de différents additifs pour hydrophobiser les minéraux cibles (sulfures et sulfosels). En séparant les sulfures des autres minéraux de gangue, on peut réduire et limiter l'ampleur des importants volumes de rejets miniers générateurs du drainage minier contaminé (DMC) (Benzaazoua et Kongolo, 2003; Benzaazoua et al., 2000b; Broadhurst et al., 2015; Demers et al., 2008; Derycke, 2012; Kongolo et al., 2004; Mermillod-Blondin, 2005). Il est à souligner que, dans le cas des mines polymétalliques, les résidus miniers, issus des circuits de traitement minéralurgique, sont généralement problématiques à cause de leur potentiel contaminant. Ainsi, la désulfuration a été investiguée sur plusieurs types de résidus miniers à travers le monde pour prévenir la génération de DMA (Benzaazoua et al., 1998; Derycke, 2012; Kongolo et al., 2004; Leppinen et al., 1997; Mermillod-Blondin, 2005). Cependant, son application pour prévenir la génération de DNC est beaucoup moins étudiée (Derycke, 2012). En effet, la plupart des études menées dans le domaine de la désulfuration environnementale des résidus miniers ont toujours visé le contrôle de la génération de l'acidité plus que le contrôle de la contamination en métaux et métalloïdes de façon générale. Les concentrés de sulfures produit lors du processus de

la désulfuration peuvent être réutilisés ou valorisés s'ils renferment des teneurs en éléments de valeur économiquement viables. De plus, leurs volumes étant moindres, ils peuvent être gérés plus facilement en les incorporant par exemple comme remblai en pâte souterrain (Benzaazoua et al., 1999; Benzaazoua et al., 2000). Quant aux rejets désulfurés, ils peuvent être valorisés par exemple dans les couvertures utilisées dans la restauration des parcs à résidus miniers (Bois et al., 2005b; Bussière et al., 2002a; Demers et al., 2009b; Rey et al., 2016).

Bien que l'application de la désulfuration par flottation en fin de circuit de traitement de minerai ait été menée avec succès sur différents minerais à travers le monde (Benzaazoua et al., 2000; Mermillod-Blondin 2005), il n'en demeure pas moins que son efficacité dépend de plusieurs facteurs, à savoir les propriétés minéralogiques (composition et texture) et granulométriques des rejets à désulfurer. De plus, l'efficacité de la désulfuration environnementale par flottation est aussi tributaire des mécanismes surfaciques fondamentaux inhérents à la formation d'un film hydrophobe autour des minéraux cibles (sulfures et sulfosels) qui est à la base de leur flottation. Ces mécanismes sont directement dépendant des conditions physico-chimiques imposées par le traitement antérieur (Derycke et al., 2013). En effet, la caractérisation de l'évolution des espèces formées en surface des sulfures et sulfosels suite à leur oxydation superficielle et les mécanismes d'adsorption des xanthates à leurs surfaces (à l'échelle moléculaire) permet d'améliorer les pratiques relatives au procédé de flottation et par conséquent la désulfuration environnementale (Deryck, 2013; Mermillod Blondin, 2005).

De point de vue stériles miniers produits aussi en grande quantités par les exploitations minières, il est à noter que leur gestion est actuellement assez complexe techniquement et très couteuse économiquement (Amar et al., 2020). En effet, le développement de nouvelles techniques fiables et moins onéreuses devient un besoin pressant afin de prévenir le potentiel contaminant que présentent ces rejets sur l'environnement

(Benzaazoua et al., 2008). Sachant que la taille des grains de ce type de rejet s'étend de quelques microns à des blocs métriques, il est convenu que la fraction fine est celle responsable de la réactivité globale de la halde à stérile (Elghali et al., 2018; Amar et al., 2021). Est-il alors possible de déterminer la taille des grains qui pourra séparer le stérile minier en question en deux fractions distinctes de réactivité géochimiques différentes? C'est-à-dire la granulométrie au-dessus de la laquelle les minéraux sulfureux sont majoritairement encapsulés dans des matrices imperméables et sont alors moins disponibles à la réaction générant du drainage minier contaminé?

Des études récentes menées par Elghali et al. (2019a) et Amar et al. (2021) ont pu définir, à l'aide d'un système de minéralogie automatisé couplé aux tests géochimiques, cette granulométrie/ paramètre appelée « diamètre d'encapsulation physique des sulfures (DPLS) ». Le tri des stériles par criblage, après le dynamitage, en fonction du diamètre critique DPLS pourrait être une technique efficace pour la gestion globale des stériles miniers. Basé sur ce paramètre, le coût économique lié à la gestion des haldes à stériles sera bien réduit vu la quantité réduite de stériles réactifs à gérer (Amar et al., 2020; Elghali et al., 2019a). Un principe similaire utilisé in situ en mines à ciel ouvert, a été développé pour la récupération du minerai par l'australien CRCore et appelé grade engineering (Carrasco et al., 2016). La fraction grossière (> DPLS) pourra être valorisée dans le domaine du génie civil ou de la céramique ou être stockée sous forme de haldes à stériles vu son inertie géochimique, alors que la fraction fine (< DPLS) censée être réactive et potentiellement génératrice d'acide et/ou de contamination, sera retraitée et désulfurée (Amar et al., 2020; Elghali et al., 2019).

Les rejets miniers, objets de ce projet de doctorat, proviennent de la mine d'Amaruq située au Nunavut (Canada). Dans ce cas, la désulfuration environnementale est envisagée comme alternative pour la gestion environnementale de ses rejets (résidus et stériles miniers) pour les fins de contrôle du DMC et, par conséquence, de la réduction des impacts potentiels sur l'environnement de l'exploitation minière. Dans ce cas du

gisement d'Amaruq, les rejets sont connus pour contenir de la gersdorffite comme sulfosel réactif (Chopard et al., 2015), donc susceptible de générer un DMC en arsenic, nickel et cobalt.

Il est judicieux de mentionner que les études antérieures réalisées portant sur la désulfuration environnementale des rejets miniers ont pu démontrer que cette technique est bien efficace pour contrôler la génération de DMA par le biais de sulfures communément rencontrés dans les rejets miniers (pyrite, pyrrhotite, arsénopyrite). Le cas de l'arsénopyrite dans les rejets de la mine Lapa (Derycke, 2012) ou le cas de la pentlandite dans résidus de la mine Raglan (Benzaazoua et al., 2017) sont quelques exemples. Toutefois, son application pour le contrôle de la génération du potentiel contaminant (DNC) à partir de certains sulfures et sulfosels en faibles quantités et moins prépondérant, n'a pas encore été abordée suffisamment. Il s'agit d'une multitude de minéraux capables de se solubiliser sous l'action de l'oxygène entre autres. Pour cela, le présent projet vise donc la désulfuration environnementale des rejets (résidus et stériles miniers) qui renferment ces sulfures et sulfosels moins communs (à l'image de la gersdorffite) pour une gestion durable et intégrée. Les résultats qui seront issus de ce projet de recherche combleront des lacunes scientifiques et des besoins en recherche importants.

Cette thèse est présentée par articles, et est structurée en neuf chapitres. Les trois premiers chapitres correspondent à la présente introduction, à la revue de littérature, et aux objectifs de l'étude et hypothèses de travail. Le corps de la thèse est composé de quatre articles scientifiques (soit un article par chapitre) présentant les différents résultats et avancées scientifiques dans le domaine de recherche. Cette mise en forme a été choisie pour faciliter la publication des différents résultats obtenus. Les deux derniers chapitres sont consacrés à la discussion, aux conclusions générales ainsi qu'aux recommandations et perspectives de recherche.

Le chapitre « revue de littérature » offrira dans un premier temps une synthèse exhaustive des connaissances et avancées scientifiques dans le domaine de la désulfuration environnementale comme approche de gestion intégrée des rejets miniers. Elle mettra également en évidence les principales caractéristiques des rejets miniers (résidus et stériles) pour ressortir les différents défis liés à leur désulfuration. Cette revue de littérature visera également à évaluer l'adéquation de différentes techniques minéralurgiques à la désulfuration environnementale des rejets miniers pour contrôler la génération du DMC (autre que la flottation largement utilisée). Les différentes exigences inhérentes aux différentes techniques de séparation minéralurgique pour une opération de désulfuration efficace ont fait aussi l'objet d'états de l'art. L'apport des caractérisations physiques, chimiques et minéralogiques pour le choix d'une telle technique pour une désulfuration efficace des deux types de rejets miniers a été également discuté.

Il est ainsi judicieux de mentionner ici que le chapitre « Matériels et méthodes » n'a pas été présenté dans ce rapport de thèse vu que son contenu se retrouve en détails dans les différents chapitres (articles de revues scientifiques).

Le chapitre 4 concerne la caractérisation surfacique de la skutterudite, la gersdorffite et la nickéline pures (minéraux moins communs pouvant générer du DNC en As et Ni) afin de décrire l'évolution de leurs états de surface à travers diverses conditions physico-chimiques (broyage sec, oxydation à l'air, conditionnement à pH naturel et à pH alcalin (pH = 10,5), activation par les sulfates de cuivre, et interaction avec les xanthates comme collecteur de flottation). Cette étude de la physico-chimie de surface permet l'identification et la compréhension des mécanismes fondamentaux inhérents à la flottation de ces minéraux (meilleures conditions de flottation).

Le chapitre 5 porte sur des aspects plus appliqués de la désulfuration environnementale par flottation. Il examine l'optimisation et la faisabilité de la désulfuration environnementale par flottation appliquée à un cas spécifique de résidu minier Whale

Tail (porteur de la gersdorffite) issu de la mine d'Amaruq (Nunavut, Canada), pour prévenir la formation de DNC à l'arsenic et au nickel. Les tests de flottation ont été réalisés à l'échelle du laboratoire en cellule Denver pour déterminer les conditions optimales qui maximisent la récupération des sulfures/sulfosels (gersdorffite entre autres) en utilisant la modélisation et l'optimisation par des plans d'expériences. Ce chapitre permet également de valider les conclusions mises en évidence dans le chapitre 4 (partie fondamentale). Ainsi, l'évaluation de l'efficacité de la désulfuration environnementale pour la prévention du DNC à l'arsenic et au nickel par une caractérisation environnementale des produits désulfurés, fait partie des points développés dans ce chapitre.

Les chapitres 6 et 7 permettent de s'intéresser au second type de rejet miniers qui est les stériles miniers. Ces chapitres visent à relever les défis liés à la gestion durable des stériles miniers (renfermant spécifiquement la gersdorffite). L'influence de la taille des particules et le degré de libération des sulfures/sulfosels et des carbonates sur la géochimie de rejet minier étudié est soigneusement examinée dans le chapitre 6. Des techniques avancées d'analyse minéralogique automatisée (QEMSCAN® et CT) combinées à une approche cinétique (cellules humides) ont été utilisées dans ce sens. Le principal résultat de ce chapitre réside dans la détermination du DPLS (diamètre d'encapsulation physique des sulfures) qui permet de séparer le stérile minier en question en deux fractions de réactivités différentes (une fraction > DPLS inerte et une fraction < DPLS réactive) et par conséquent de proposer une méthodologie de gestion durable de ces rejets.

Le chapitre 7 vise le développement de nouvelles pratiques permettant la décontamination (désulfuration environnementale) de la fraction fine réactive (<DPLS), la concentration de l'or résiduel, la stabilisation et le stockage en toute sécurité de ces roches stériles. La séparation par milieu dense (DMS), la spirale/table à secousse et la combinaison de la gravimétrie (DMS/concentrateur Knelson) avec de la flottation sont

les trois approches de décontamination testées dans ce cadre pour la prévention de la génération du DNC à l'arsenic. Une évaluation de l'efficacité de ces techniques par caractérisation environnementale est aussi parmi les points traités dans ce chapitre.

Une discussion est proposée au huitième chapitre. Enfin, le chapitre 9 rassemble les différentes conclusions rappelant tous les résultats saillants issus de ce travail de doctorat et les avancées réalisées. Ainsi, des perspectives de recherche (recommandations) sont également proposées dans ce dernier chapitre.

CHAPITRE 2

REVUE DE LITTÉRATURE : ENVIRONMENTAL DESULFURIZATION OF MINE WASTES USING VARIOUS MINERAL PROCESSING TECHNIQUES: RECENT ADVANCES AND OPPORTUNITIES

Préambule : Cet article a été publié dans la revue Minerals Engineering. Volume 174, 1 décembre 2021, 107225. DOI: 10.1016/j.mineng.2021.107225

Yassine Ait-Khouia[a] , Mostafa Benzaazoua[a,b,*] , Isabelle Demers[a]
[a] Research Institute on Mines and Environment (RIME), University of Quebec in Abitibi Témiscamingue, 445, boul. de l' université, Rouyn-Noranda J9X 5E4, Quebec, Canada

[b] Mohammed VI Polytechnic University (UM6P), Mining Environment & Circular Economy, Lot 660, Hay Moulay Rachid, Ben Guerir 43150, Morocco

* Corresponding author. E-mail address: mostafa.benzaazoua@uqat.ca

2.1 Abstract

Management of mine wastes (e.g., waste rock and tailings) is becoming an increasing global environmental concern for mining industries around the world. With environmental regulations becoming more restrictive, there is a continuously growing need to develop efficient and clean integrated techniques to sustainably manage mine wastes. Mines wastes often contain acid-forming minerals, such as sulfides and sulfosalts that are responsible for generating contamination. Environmental desulfurization using non-selective flotation has recently been implemented as an integrated management approach for mine tailings. Furthermore, physical separation techniques, commonly used in mineral processing and offering a remarkable potential

for sulfur and valuable minerals enrichment, are rarely used to manage mine wastes. The separation methods for sulfides and sulfosalts, which are based on the physical properties of the minerals, can achieve the same performance as flotation. These physical properties are mainly related to: i) the particle size distribution, ii) the difference in density between the targeted minerals (i.e., sulfides and sulfosalts) and those of the gangue minerals, iii) the magnetic properties, iv) the electrical attributes, and v) the response to specific sensing. Based on the discrepancy between mineral properties, various methods are proposed, including sieving/screening, hydrodynamic classification, gravity concentration, dense medium separation, magnetic and electrical separation, and sensor-based sorting. These techniques could be considered to be more efficient, less expensive, and more respectful of the environment than flotation. This critical review aims to evaluate the suitability of these physical separation techniques, other than the widely used flotation, to mine waste environmental desulfurization. The paper includes a brief description of these techniques, a discussion of their advantages, and their limitations for the removal of the most common sulfides and sulfosalts (mainly responsible for contaminated mine drainage). Indeed, the application of one or more of these mineral processing techniques requires specific conditions, which depend on the size-by-size mineralogical characterization of each mine waste. The specific requirements for the application of each technique are explored.

Keywords: Mine wastes, Sulfides, Sulfosalts, Contaminated mine drainage, Environmental desulfurization, Flotation, size-by-size mineralogy, Mineral processing techniques.

Résumé

La gestion des rejets miniers (stériles et résidus) est devenue une préoccupation environnementale mondiale croissante pour les industries minières. Vu les réglementations environnementales qui deviennent de plus en plus restrictives, le

développement des techniques intégrées, efficaces et propres pour gérer durablement ces rejets miniers est devenu un besoin croissant pour les minières. Ces rejets contiennent le plus souvent des minéraux acidifiants, tels que des sulfures et des sulfosels responsables du drainage minier contaminé. La désulfuration environnementale par flottation non sélective, comme approche de gestion intégrée des résidus miniers, est la technique la plus utilisée. De plus, les techniques de séparation physique, couramment utilisées dans le traitement des minerais et offrant un potentiel remarquable quant à l'enrichissement des sulfures et minéraux précieux, sont rarement utilisées pour gérer les rejets miniers. Les méthodes de séparation des sulfures et des sulfosels, basées sur les propriétés physiques des minéraux, peuvent atteindre les mêmes performances que la flottation. Ces propriétés physiques se rapportent essentiellement à : i) la distribution granulométrique, ii) la différence de densité entre les minéraux cibles (sulfures et sulfosels) et ceux de la gangue, iii) au caractère magnétique, iv) aux attributs électriques , et v) la réponse à une détection spécifique. Sur la base de ces particularités, différents procédés sont proposés. On en distingue : le tamisage/criblage, la classification hydrodynamique, la concentration gravimétrique, la séparation en milieu dense, la séparation magnétique et électrique et le tri par capteur. Ces techniques pourront être autant efficaces, moins onéreuses et surtout plus respectueuses de l'environnement que la flottation. Cette revue critique vise à évaluer l'adéquation de ces techniques de séparation physique, autres que la flottation largement utilisée, à la désulfuration environnementale des rejets miniers. L'article comprend une brève description de ces techniques, une discussion de leurs avantages et de leurs limites pour l'enlevement des sulfures et des sulfosels les plus communs dans les rejets mniers (principaux responsables du drainage minier contaminé). En effet, l'application d'une ou plusieurs de ces techniques de traitement du minerai nécessite des conditions particulières, qui se trouvent en relation directe avec les résultats de la caractérisation granulo-minéralogique de chaque rejet minier. Ainsi, les exigences particulières à l'application des différentes technologies sont exposées.

Mots-clés : Rejets miniers, Sulfures, Sulfosels, Drainage minier contaminé, Désulfuration environnementale, Flottation, Granulo-minéralogie, Techniques de traitement du minerai.

2.2 Introduction

The mining industry is facing many challenges due to environmental impacts. These challenges are becoming harder to overcome, with increasingly restrictive legislation and growing social awareness (Taha et al., 2016). Significant amounts of mine wastes are generated by exploiting deposits to produce ore with economic value. The management of the associated risks has become a real environmental challenge (Aubertin et al., 2002; Simate and Ndlovu, 2014). Over the last few decades, this problem has intensified due to the recent exploitation of high-tonnage/low-grade ores containing sulfurous minerals carrying contaminants (Elghali et al., 2019a; José Neto et al., 2019; Taskinen et al., 2018). These mine wastes include a variety of products but are composed mainly mine waste rock (product from the ore extraction stage) and tailings (generated during ore processing). Waste rock is often deposited in unsaturated piles that can be hundreds of meters in height and cover thousands of hectares, while tailings are generally managed in the form of a slurry and often stored in engineered dams and impoundments (Elghali et al., 2019a). The sustainable management of these wastes is a major environmental concern for the mining industry because of their geotechnical and geochemical instability. Depending on the geological context of polymetallic and precious metal deposits, mine wastes may contain significant residual sulfide and sulfosalt content, with different reactivity under atmospheric conditions (Chopard et al., 2017). Pyrite and pyrrhotite are the most abundant minerals found in these deposits (Blowes et al., 2014; Elghali et al., 2019a). In fact, in the absence of a sufficient quantity of neutralizing minerals, sulfides and sulfosalts exposed to atmospheric oxygen and water can be oxidized through the following reaction and produce acidic effluents:

$$\text{Sulfide(s) / Sulfosalt(s)} + \text{Water} + \text{Oxygen} \rightarrow \text{AMD } (H^+, SO_4^{2-}, \text{Metals/metalloids}) \quad (1)$$

These effluents tend to be loaded with various heavy metals/metalloids and sulfates in concentrations above the regulatory criteria (Amar et al., 2020b; Benzaazoua et al., 2004; Blowes et al., 1998; Bouzahzah et al., 2014; Dold, 2017; Elghali et al., 2019b; Mafra et al., 2020). This phenomenon is known as acid mine drainage (AMD), resulting in soil contamination and pollution of the surrounding environment (fauna, flora, groundwater, and surface water) (Dold, 2017; Förstner and Wittmann, 2012).

If sufficient quantities of neutralizing minerals (e.g., carbonates) are present, mine waste oxidation generates circumneutral drainage effluent. However, the quality of the effluent (metals release) may still exceed the existing environmental criteria even at neutral pH and could result in several environmental issues (Mayes et al., 2009; Plante, 2010); this phenomenon is called contaminated neutral drainage (CND). Consequently, the mining companies are required to manage their mine wastes to stabilize the geochemical behavior before the definitive closure of the mine site. Indeed, to ensure that this contamination does not adversely affect the environment, the mining industry must use on-site measures to prevent and control the problem. So, different approaches and management strategies have been developed by many researchers from all around the world. Although numerous, these strategies are generally based on limiting the availability of one or more of three main components of the sulfide (or sulfosalt) oxidation reaction shown above: atmospheric oxygen, water, and sulfides/sulfosalts minerals (through environmental desulfurization). Figure 2.1 illustrates these different factors and the different techniques that can be applied to prevent the formation of contaminated mine drainage.

The environmental desulfurization of tailings is one approach that has gained much popularity in the last two decades. It was defined as an alternative, integrated tailings management technique that can be accomplished through froth flotation (Benzaazoua et al., 2000; Demers et al., 2009). This method aims to remove sulfide and sulfosalt

minerals (flotation concentrate) from gangue minerals (e.g., silicates and carbonates as a flotation rejection) using froth flotation, thus producing desulfurized tailings that do not generate CMD.

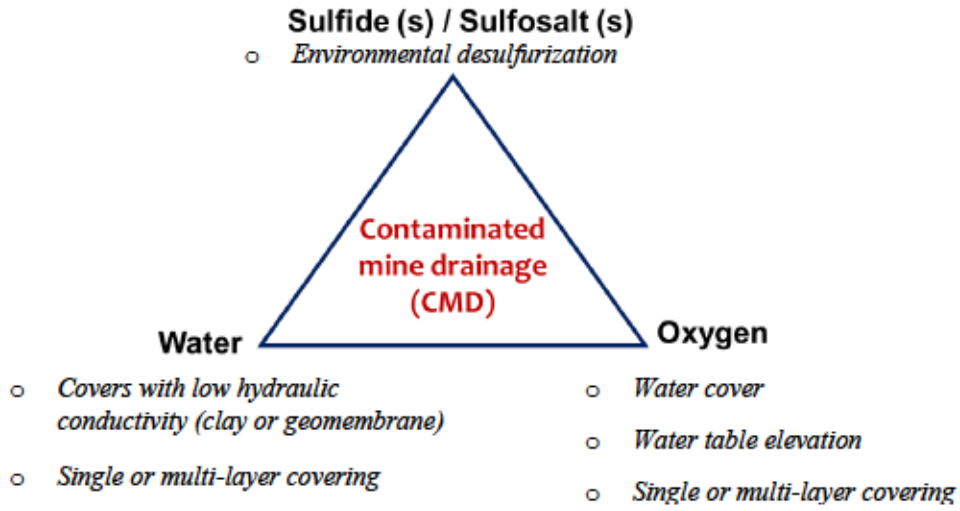

Figure 2.1 Trigger components of CMD generation and some control methods

Mine waste desulfurization using bulk sulfide flotation has already been proven to successfully control CMD generation from the laboratory and small scale to the industrial scale (Amar et al., 2020a; Benzaazoua et al., 2017; Benzaazoua et al., 2000; Bois et al., 2005; Broadhurst and Harrison, 2015; Demers et al., 2008; Nadeif et al., 2019; Nakhaei and Irannajad, 2017; Noirant et al., 2019). Nevertheless, the flotation process faces some limitations related to particle size distribution of mine wastes. This method is more suitable for finely ground materials (Derycke et al., 2013), although the effectiveness depends on several factors, including the granulo-mineralogy and the surface chemistry of the particles to be floated. Thus, researchers are interested in the development of other desulfurization techniques that are more effective, cleaner, eco-friendly, and less costly than flotation to manage these mine wastes sustainably. In this context, physical mineral processing techniques commonly used for ore enrichment could offset some of the limitations observed in environmental desulfurization of mine

waste by flotation and already can show important efficiency. These processes are based on the difference in the physical properties of minerals, which mainly relate to: i) the particle size, ii) the difference in density between the targeted minerals (sulfides and sulfosalts) and those of the gangue, iii) the ferromagnetic character, iv) the electrical attributes, and v) the response to electromagnetic radiation.

This paper aims to study the applicability of these techniques to sulfidic mine wastes for environmental desulfurization. To do so, the latest physical methods are evaluated by providing a critical analysis of their advantages and their limits to remove the most common sulfides and sulfosalts in mine wastes. Firstly, a review was conducted of the different mineral processing techniques that can provide similar desulfurization objectives as flotation. Secondly, each technology was examined by assessing its potential in the context of mine waste reprocessing, particularly environmental desulfurization of mine wastes.

2.3 Typology of Mine Wastes

Mining industries around the world generate significant amounts of mine wastes in the form of waste rock, tailings, and slags (Figure 2.2). This paper only focuses on the waste rock and tailings. Waste rock is non-economic rock that must be mined and extracted to access a mineralized ore body (or deposit). It is most often produced in large quantities during open-pit operations, but also, at a slower rate, during access work to mineralized zones in the case of underground mines.

Waste rocks are coarse materials characterized by high internal structural heterogeneity, particularly with regards to particle size distribution (PSD). Because of the way these materials are deposited, waste rocks present some anisotropies of their physical, chemical, mineralogical, and geochemical properties, especially in comparison to tailings (Amar et al., 2020b; Amos et al., 2015; Elghali et al., 2018; Elghali et al., 2019a; Jamieson et al., 2015). These heterogeneities are caused by pile construction as well as

by particle segregation that could take place inside the piles due to water infiltration (Elghali et al., 2019a; McLemore et al., 2006).

Figure 2.2 The operating cycle of a mine and the main typologies of mine wastes.

Tailings are ground rock particles from which the commercial value has been extracted at the concentrator. They are characterized by relatively homogenous particle-size distribution and are considered to be homogeneous materials (Amos et al., 2015; Bussière, 2007). The management methods for each category of mine wastes is therefore different. Waste rocks are usually deposited in the form of surface waste rock piles if they are not reused for mine backfill. Tailings are generally managed in the form of pulp, usually with an initial solids content between 25% and 45% that settles with time. Tailings are transported from the concentrator to a dedicated area called a tailings impoundment, where they are deposited. This area is partly or wholly surrounded by dykes that retain both the solid tailings and liquid effluent (Bussière, 2007).

From a physical point of view, the particle size of the waste rock can vary from a few micrometers (clay and silt) to several tens of centimeters (blocks) (Elghali et al., 2019a; Fala et al., 2005). This particle size distribution changes according to the blasting method used during the exploitation (firing diagram) and the hardness of the rocks. McKeown et al. (2000) studied the PSD of waste rock from different mining sites.

According to this study, waste rock corresponds to relatively coarse materials. Indeed, the D10 value (particle size corresponding to 10% passing over the PSD curve) is generally between 0.2 mm and 3 mm, and the D60 is between 1 and 80 mm (Peregoedova, 2012). Their uniformity coefficient ($C_U = D_{60}/D_{10}$) can reach 30 or more (Aubertin et al., 2002; Gamache-Rochette, 2004; Peregoedova, 2012). This coefficient characterizes the particle size spread of materials. Figure 2.3 shows the size distribution of the waste rock and of the tailings. The relative density (Dr) of the grains is between 2.4 and 6 (and more) depending on the mineralogy of the rock (Bussière, 2007). For example, the mineralized waste rock (e.g., ilmenite) from the Havre Saint-Pierre mine (Canada) shows a relative density between 3.9 and 4.2 (Peregoedova, 2012) and the non-mineralized waste rock (e.g., anorthosite) between 2.7 and 2.9 (Plante, 2010).

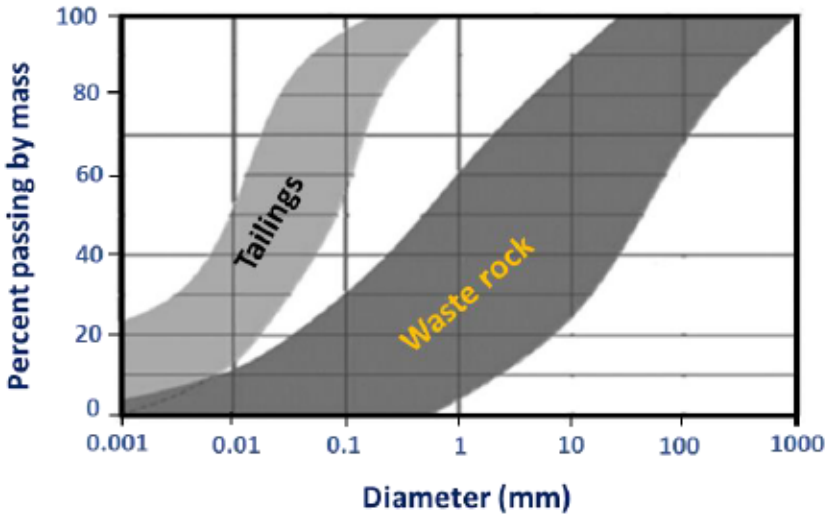

Figure 2.3 Size distributions of mine wastes. Adapted from James et al. (2013).

Tailings have a D_{10} that varies between 0.001 and 0.004 mm, while D_{60} varies between 0.01 and 0.05 mm (Bussière, 2007). The corresponding uniformity coefficient C_U varies between 8 and 18. The Dr of solid grains also is dependent on the mineralogy. For instance, Dr values for sulfide tailings can range from 2.9 to more than 4.5; for

gold mines where the ore is mainly in quartz veins, the Dr is generally between 2.6 and 2.9 (Bussière, 2007).

The environmental behavior of both mine waste types is controlled by their chemical, mineralogical, and physical properties (Aubertin et al., 2008; Jamieson et al., 2015; Nordstrom, 2000) as well as by other external factors (Parbhakar-Fox and Lottermoser, 2015). Both categories of mine wastes often contain sulfur minerals (e.g., pyrite, pyrrhotite, arsenopyrite, gersdorffite) that, when exposed to oxygen and water, are oxidized and generate CMD. The quality of mine drainage depends on the mineralogy of the waste as well as on the dissolution rates of the minerals (acidifiers and neutralizers), which are very variable (Blowes et al., 2014; Paktunc and Davé, 2000). Several previous studies also suggest that the particle size, the specific surface area, and the degree of mineral liberation are essential factors controlling the geochemical reactivity of mine wastes (Benzaazoua et al., 2017; Elghali et al., 2019c; Erguler and Erguler, 2015; Mafra et al., 2020; Parbhakar-Fox et al., 2011). Indeed, the particle size is closely linked to the specific surface area (Mbonimpa et al., 2009) and subsequently to the liberation degree of minerals. In this context, Erguler and Erguler (2015) studied the geochemical behavior of mine waste at three different particle sizes. Results showed that the geochemistry of the leachate was different and depended on the particle size. Thus, the lag time (i.e., time necessary for the start of the acidity generation after the exhaustion of the neutralizing potential) was positively correlated with particle size (Fig. 1S) (Annexe A).

Generally, when the granulometry of a material is finer, its specific surface area becomes large and its reactivity increases. This result can be explained by the large proportion of sulfides exposed to oxidation reactions (liberation degree) in a fine sample compared to a coarse sample. This result was confirmed by Elghali et al. (2018), who examined the influence of the particle size of three waste rock from the Canadian Malartic mine (Canada) and the degree of liberation of the sulfides and carbonates on

the geochemistry of this type of waste. This relationship was also confirmed by the recent study of Amar et al. (2020b). In the case of mine tailings, the effect of mineral liberation is not as remarkable as for waste rock because of the difference in particle size between the two wastes.

2.4 Environmental Desulfurization

Environmental desulfurization is an approach proposed by several authors to limit and prevent CMD generation from mine wastes (Amar et al., 2020a; Benzaazoua et al., 2017; Benzaazoua and Kongolo, 2003; Bois et al., 2005; Mermillod-Blondin et al., 2005; Noirant et al., 2019). It consists of separating the sulfides or sulfosalts (acid-generating) and non-sulfide minerals (gangue) and managing both fractions accordingly. This operation is performed using mineral processing techniques, usually through froth flotation (Benzaazoua et al., 2000; Demers et al., 2009). This technique has been demonstrated to be economically and technically effective to prevent CMD.

As illustrated in Figure 2.4, environmental desulfurization allows a decrease in the volume of CMD-generating wastes requiring surface storage. The integration of an environmental desulfurization step at the concentrator allows an integrated management of mine wastes.

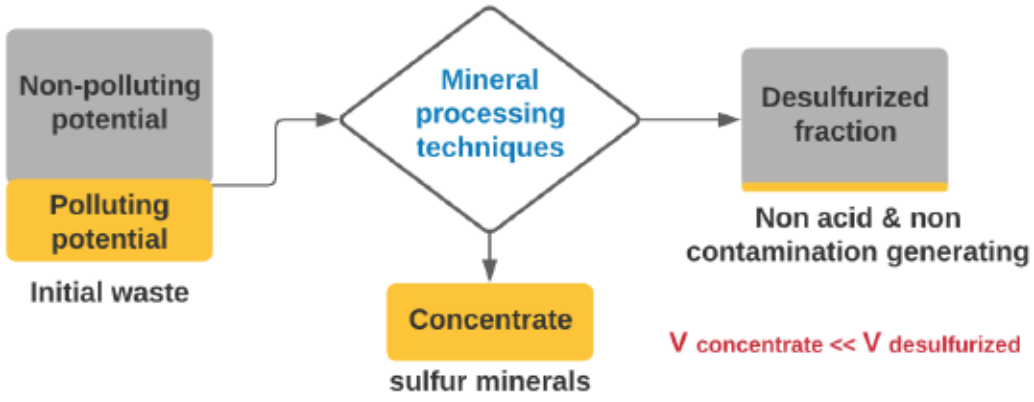

Figure 2.4 Principle of environmental desulfurization of mine wastes

With this process, there are two fractions to manage: a smaller volume of enriched tailings that is acid generating (concentrate), and a large volume sulfide-lean fraction (non-acid generating tailings).

The sulfide concentrate could be placed to reduced and dedicated sealed tailings impoundment (equipped with a geomembrane) as required by Canadian laws for acid generating wastes. It could also be stored underground as a cemented paste backfill (Benzaazoua et al., 2008; Benzaazoua et al., 1999; Smith et al., 2013) which ensure chemical and physical stability. Pastefill becomes nowadays used by all modern mining companies exploiting hard rock ores.

The sulfide concentrate can also be processed further into useful by-products such as sulfuric acid or valorized for metal recovery (Amar et al., 2020a; Broadhurst and Harrison, 2015; Nadeif et al., 2019). Because the desulfurized fraction is non-acid generating, it can be stored at the surface using conventional or emerging tailings disposal approaches, and/or sent to be placed in underground to fill open stopes. It can be also valorized as material for dam construction or cover to prevent and control AMD generation (Bois et al., 2004; Bussière et al., 2004; Demers et al., 2008; Lessard et al., 2018; Rey et al., 2016). Indeed, this approach can help minimize considerably the

volume of the problematic tailings to be stored at the surface, especially when the concentrate will be stored underground as a cemented paste backfill. It also provides opportunities for value recovery and reallocation of unavoidable wastes as feedstock for other uses.

Environmental desulfurization is usually accomplished through non-selective flotation. It is a mineralogical separation technique frequently used for sulfide concentration in ore processing. It takes advantage of differences in the surface properties of the minerals. As a basic principle, the slurried tailings are conditioned with numerous reagents, such as flotation collectors and activators. Collectors are organic compounds that selectively adsorb on target mineral surfaces and form a hydrophobic layer around the particle (Wills and Finch, 2016). Aeration in the flotation cells allows the transport of these hydrophobic particles as a mineralized froth to the surface where it can be scraped off and recovered.

Environmental desulfurization by froth flotation has been successfully carried out on numerous mine tailings around the world from small to industrial scale (Benzaazoua et al., 2000; Mermillod-Blondin et al., 2005). Nonetheless, the effectiveness depends on several factors. Physicochemical parameters imposed by the previous treatment, the mineralogical composition, the textures, and the particle size distribution of the wastes are the main factors. Despite these limitations, flotation remains the most widely used technique for desulfurization of mine tailings. However, recent studies show that this type of process could also be applied to mine waste rock (Amar et al., 2020a). In addition to flotation, other techniques could be used for desulfurization, such as gravimetric methods (Amar et al., 2020a; Amar et al., 2020b; Atrafi et al., 2012; Falconer, 2003).

2.5 Physical Separation Techniques

In the mineral processing field, physical separation has been widely used for centuries to separate the target minerals from gangue minerals by exploiting the differences in their physical properties. Physical separation techniques can also be used to upgrade or preconcentrate the ore before the enrichment process when target minerals are at low concentrations, or when their separation would be uneconomical (Farrokhpay, 2020). Physical separation, when appropriate, provides high efficiency, low investment, low operating costs, and the general absence of the use of chemicals resulting in less environmental risk (Farrokhpay, 2020).

The physical properties exploited relate mainly to: i) the size of the particles, ii) the difference in density between the target and gangue minerals, iii) the ferromagnetic character, iv) the electrical attributes, v) the response to electromagnetic radiation, and vi) the character of hydrophobicity (Grewal et al., 2014; Mercier et al., 2001; Rezvanipour et al., 2018). Based on these properties, various physical separation methods have been developed for ore processing (Figure 2.5). Particle size classification, automatic sorting (known as sensor-based sorting), gravity concentration, dense medium separation, and magnetic and electrical separations are the typical mineral separation techniques mostly used by the mining industry. Each process is adopted according to the physical characteristics of the minerals or particles to be treated (Dermont et al., 2008).

Table 2.1 summarizes the typical classes of techniques, specifying their main uses, the principles of separation, and the various implemented technologies. According to some researchers (Farrokhpay, 2020; Rikers et al., 1998), mineral processing techniques can be used for more specific purposes such as decontamination (desulfurization) of soils and mine wastes.

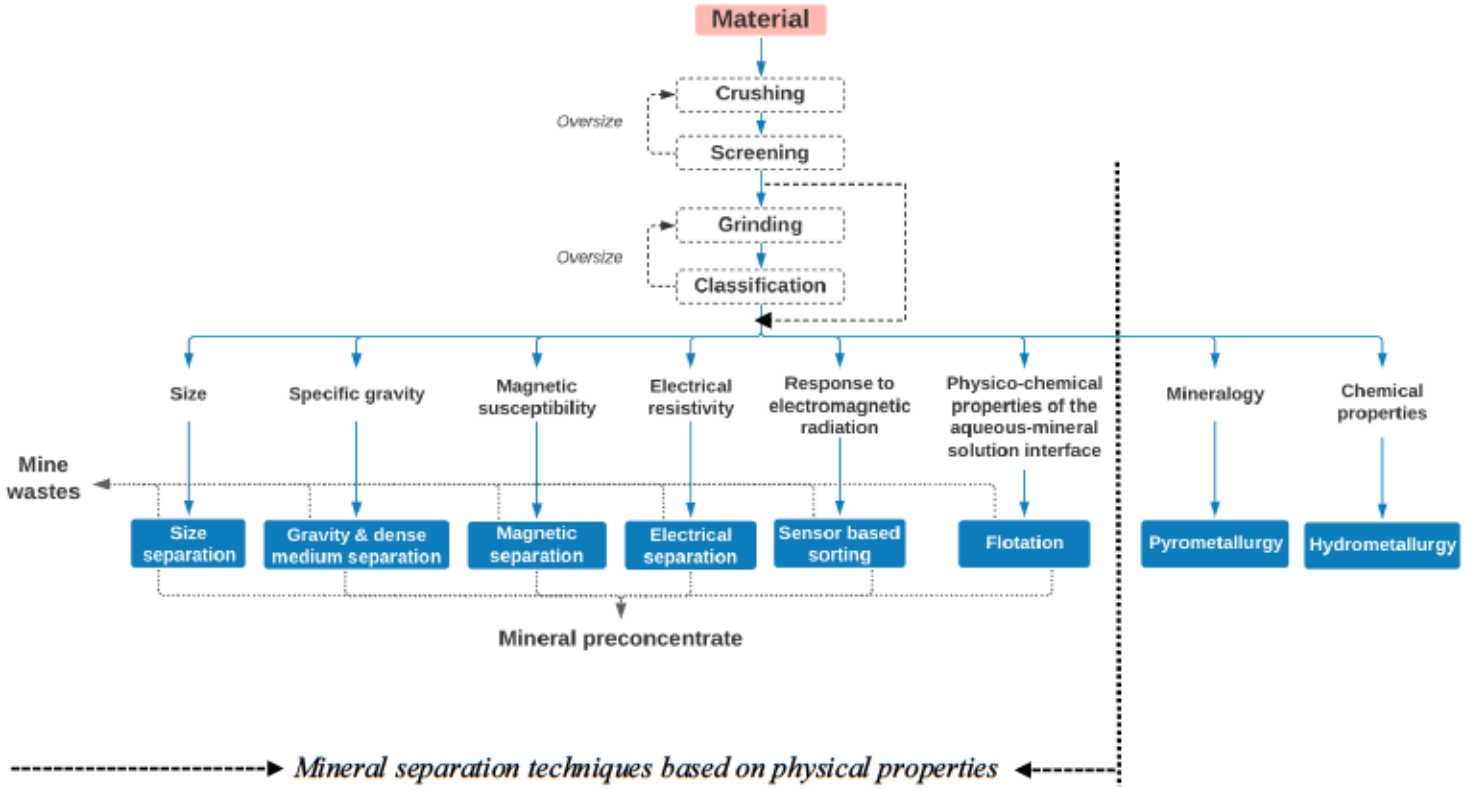

Figure. 2.5 Different mineral processing techniques developed by the mining industry

Table 2.1 Summary of physical separation classes

Technique		Principle	Description	Comments	Some implemented technologies	References
Size classification	***Mechanical screening***	Separation based on particle sizes	Mechanical screening is based on the exclusion of particle size through a physical barrier to provide suitable dimensions for further processing	Widely used. It is generally done wet or dry and requires the use of screens or sieves for the grainy fractions (> 250 µm)	Grizzly; barrel trommel; vibrating or gyratory screens	Tripathy et al., 2015 Dermont et al., 2008
	Hydrodynamic classification	Separation based on the particle settling velocity	This technique achieves almost the same objectives as sieving, but the principle is entirely different. It separates the particles by the difference of settling velocity or by centrifugal forces into a water flow	Widely used. Hydrocyclone is the most preferred classifier in the mineral industry	Hydrocyclones, hydraulic classifiers, mechanical classifiers (screw classifier)	Heiskanen, 1993 Dermont et al., 2008
Gravity concentration		Separation based on the difference of particle density and their settling velocity	Gravimetric technologies separate high-density from low-density minerals in a slurry (with relatively high solid concentration)	Widely used in two modes: gravitational and centrifugal	Jig; spirals; shaking tables; knelson; falcon; kelsey; MGS mozley, etc.	Roy, 2009 Marion et al., 2018
DMS (dense medium separation)		Separation based on the difference of particle density	Also known as heavy medium separation, the DMS is a technique of enrichment or physical separation of the particles according to their densities in a medium whose density is intermediate between that of the desired minerals and that of the gangue	Widely used in the mining industry, especially for the concentration of coal and diamonds and the preconcentration of some minerals (e.g., cassiterite)	Dense medium cyclone; water-only cyclone; Dyna Whirlpool, etc.	Marion et al., 2017 Ndlovu et al., 2017 Khalil et al., 2019
Magnetic separation		Separation based on the difference of the magnetic properties of particles	Exploits the susceptibility of materials to magnetism, which reflects the behavior of a mineral or a material when it is subjected to a magnetic field	Moderately used in the mining industry and showing high efficiency	Dry or wet separators using high intensity (HIMS) or low intensity (LIMS)	Gillet, 2004) Grewal et al., 2016 Taskinen et al., 2018
Electrical separation		Separation based on the difference of electrical conductivity of particles	Electrical separation exploits the differences of surface electrical conductivity between the different minerals or the various particles to be separated	Rarely used due to the required processing conditions. The particles to be separated must be completely dry	Electrostatic and electrodynamic separators	Dance and Morrison, 1992 Gill, 1991
Sensor-based sorting		Separation based on the different properties of the particles (e.g., color, reflectance, reflection and absorption of IR, etc.)	Automated sorting systems often inspect particles in spectral ranges invisible to the naked eye, to determine the value of some properties using non-contact (non-destructive) measurements in real-time	Still emerging technologies with a limited number of industrial applications	X-ray transmission (XRT) detector, electromagnetic sensor (EM), X-ray luminescence, etc.	Von Ketelhodt, 2009 Dalm et al., 2014 Robben and Wotruba, 2019

Based on a literature review and on typical use, the different physical separation techniques present various advantages and disadvantages/limitations in the context of environmental desulfurization (Table 2.2). The two main advantages of these techniques are that they are well established and that their operating principles are well known in the ore processing industry. These techniques can be used to decontaminate ores and wastes in the continuous processing system (Dermont et al., 2008). Thus, these techniques make it possible to recover sulfides and sulfosalts, either valuable or not, and to reduce the volumes of wastes for more economical and safer management. These techniques are environmentally friendly, especially as no chemical reagents are required (except for DMS). In addition, the operating and implementation costs are generally low compared to other separation techniques such as flotation.

In some cases, the recovered sulfur minerals can be recycled by sending them to the upgrading and extraction processes. It should also be noted that the processing circuits are easily modular, and certain mobile unit systems are available (Dermont et al., 2008). However, for large-scale applications the environmental desulfurization of mining wastes by physical separation methods has certain limitations:

- it requires extensive equipment and large spaces for certain technologies;
- the heterogeneous nature, both in terms of chemical and mineralogical composition and in terms of particle size, presents a constraint on separation efficiency (Gosselin et al., 1999); and,
- it becomes difficult when the degree of liberation of residual sulfides and sulfosalts is low.

Table 2.2 Advantages and limitations of physical separation techniques in the context of environmental desulfurization

Technique	(*Technology*)	Advantages	Limitations	References
Conventional gravimetric concentration	**Jigs Spirals Shaking tables**	- Treatment of wastes whose particle sizes are between 75 µm and 15 mm (i.e., waste rock and tailings): wide range of particle size - Economical and efficient - Generally low investment and operating costs - No chemical reagents are required	-Difference between the densities of sulfides and gangue minerals must be greater than 1 g/cm^3 - High degree of liberation required for sulfides/sulfosalts - Relatively narrow particle size distribution required - Requires pretreatment (sieving, hydro classification) - Ineffective for fine particles < 75 µm - Limited performance when the reject contains more than 30% clay material (fineness)	Gosselin et al., 1999 Mercier et al., 2001 Falconer, 2003 Gülsoy and Gülcan, 2019 Ndlovu et al., 2017 Wills, 2016
Centrifugal gravimetric concentration	**MGS Mosley**	- About 25 g is achievable - Capable of treating fine particles (10 - 75 µm): tailings - No chemical reagents are required	- Low capacity - Not suitable for the desulfurization of coarse particles and especially waste rock	Das and Sarkar, 2018 Falconer, 2003 Göktepe, 2005 Gosselin et al., 1999
	Knelson	- About 60 g is achievable - High separation efficiency and recovery rate - Losses are minimized by washing with water - Batch and continuous units are available	- Wastewater treatment is difficult due to the suspension of very fine particles and requires special filters, centrifuges, or thickeners.	Koppalkar, 2009 Zhu et al., 2017 Falconer, 2003 Das and Sarkar, 2018
	Falcon	- About 300 g is achievable - High capacity - Good mineral processing performance - Capable of handling fine particle size (15-20 µm)	- Requires a screened or sieved feed to a size smaller than the opening size of the ports to prevent clogging	Falconer, 2003 Das and Sarkar, 2018 Honaker et al., 1996 Gosselin et al., 1999
	Kelsey jig	- About 60 g is achievable - High capacity - Capable of handling fine particle size (10 µm) - Narrow specific gravity difference accepted	- Relatively high investment and operating costs	Napier-Munn, 1997 Falconer, 2003 Das and Sarkar, 2018

Table 2.3 Advantages and limitations of physical separation techniques in the context of environmental desulfurization (Continued)

Technique	Advantages	Limitations	References
Dense medium separation (DMS)	- Ability to make clean separations at any required density with a high degree of efficiency - The separation density can be controlled - The separation density can be changed very quickly to respond to variations in operating conditions - Ability to handle a wide range of particle sizes - Relatively low investment and operating costs - High processing capacity - Recycling and reuse of dense medium - Low space occupation	- Desulfurization performance directly dependent on the density of the medium: poor control of the medium density will cause low performance, - Particle sizes smaller than 0.5 mm are not desired. - This size is difficult to concentrate by DMS and can increase the apparent viscosity of the medium and negatively influence the separation performance	Gosselin et al., 1999 Wills, 2016 Williford and Bricka, 2000
Magnetic separation	- Moderately expensive - Respectful of the environment - Possibility to adjust the intensity of the magnetic field by varying the intensity of the electric current when desired	- Requires particle sizes greater than 75 µm - Medium liberation degree of contaminants required - High investment and operating costs	Mercier et al., 2001 Rikers et al., 1998 Gosselin et al., 1999 Rezvanipour et al., 2018 Wills, 2016
Electrical separation	- Clean and respectful of the environment - More suitable for sizes ranging from 60 to 500 µm - Good mineral processing performance	- The particles must be perfectly dry - The presence of moisture alters the behavior of particles - The liberation degree of contaminants (sulfides / sulfosalts) must be high with a difference in electrical conductivity - A step of selective development of the charges on the mineral particles is required	Gosselin et al., 1999 Wills, 2016 Haldar, 2018
Sensor-based sorting	- Different minerals properties can be exploited according to the sensor(s) used - Can be applied to relatively coarse particles (0.5 - 350 mm): generally to waste rock	- Complex system: hard to set up and operate - Not applicable to taillings - Relatively high investment and operating costs	Dalm et al., 2014 Robben and Wotruba, 2019 Wills, 2016

2.5.1 Particle Size Classification

The unit operations implemented in the mineral separation processes are often coupled or preceded by classifying the material into different particle size fractions. These unitary ore enrichment operations do not always guarantee excellent efficiencies except on well-defined grain size materials (Farrokhpay, 2020; Gosselin et al., 1999; Kelly and Spottiswood, 1982). Table 2.4 presents the characteristics of some classification techniques, their main uses, and the conditions under which the associated equipment is employed.

Table 2.4 Sizing techniques used in mining industry

Sieving & screening

Process	Principle	Uses	References
Dry/Wet	Gravity	i) Crushing circuits: Scalping of crushers feed to reduce their circular load; control of the grain size ii) Grinding circuits (rarely) iii) Water removal	Farrokhpay, 2020 Tripathy et al., 2015 Wills, 2016

Equipment	Particle size	Remarks	References
Grizzly	20 - 300 mm	Large blocks – Tilt: 35 to 45 °	Gosselin et al., 1999
Trommels	6 - 55 mm	Lots of space - Low capacity	Gosselin et al., 1999
Vibratory	0.25 - 250 mm	Most used in mining industry	Wills, 2016
Gyratory	0.04 - 12 mm	especially intended for fine sieving	Gosselin et al., 1999

Hydroclassification

Process	Principle	Uses	References
Slurry	Gravity & Centrifugation	Grinding circuits Thickening and desliming	Farrokhpay, 2020 Tripathy et al., 2015

Equipment	Cut-off point	Flow rate	References
Screw classifier	45 µm to 1 mm	5 - 850 t/h	Kelly and Spottiswood, 1982
Hydraulic classifier	100 µm to 850 µm	10 - 120 t/h	Gosselin et al., 1999
Hydrocyclone	5 µm to 300 µm	< 20 m^3/min	Wills, 2016

Hydro classification (or hydrodynamic classification) is the classification type most commonly used in the mineral industry. It is based on the differential particle settling velocity in water (Heiskanen, 1993). There are several classification technologies: mechanical classifiers (e.g., screw), where separation is done mechanically; and non-mechanical classifiers (e.g., hydro-cyclone), the principle of which is based on gravitational or centrifugal forces.

The conical and the centrifuge are other types of classifiers and are by far the most frequently used in the mineral industry. Hydrocyclone is the most preferred and widely used classifier in the mineral industry because it is inexpensive and requires very little space to be installed (Dermont et al., 2008; Gosselin et al., 1999). Hydrocyclone is a device with a cylindroconical shape that can effectively separate multi-phase mixtures of particles with different sizes and densities based on centrifugal sedimentation principles (Farrokhpay, 2020; Jiang et al., 2019; Zhang et al., 2019). It is generally used for the classification of particles smaller than 1400 µm.

Applicability to environmental desulfurization

Recent studies on waste rock using an automated mineralogy system coupled with geochemical tests have been able to define a parameter called "diameter of physical locking of sulfides" (DPLS) for particle separation (Amar et al., 2020b; Elghali et al., 2018). It represents the particle size above which the sulfides and sulfosalts are mainly encapsulated in impermeable matrices and are less available to react and generate CMD. Indeed, DPLS separates the waste rock material according to its geochemical reactivity into two fractions: i) the fraction below DPLS considered as the fine reactive fraction, and ii) the fraction above DPLS referred to as the coarsest and non-reactive fraction. As illustrated in Figure 2.6, screening waste rock material after blasting according to the critical DPLS could be an effective technique for global mine waste rock management. A decrease in the quantity of reactive waste rock material resulting from

this technique can be linked to a decrease in the economic cost of waste rock pile reclamation (Amar et al., 2020a; Elghali et al., 2019a). Likewise, a similar principle called "grade engineering" has been already used in situ in open-pit mines, which has been developed for the recovery of ores by the Australian CRCore (Carrasco et al., 2016). The fine fraction (<DPLS) will be processed and desulphurized. In contrast, the coarse fraction (>DPLS) can be used in the field of civil engineering or ceramics or be stored in the form of waste rock dumps due to its non-reactivity (Amar et al., 2020a; Amar et al., 2020b; Elghali et al., 2019a).

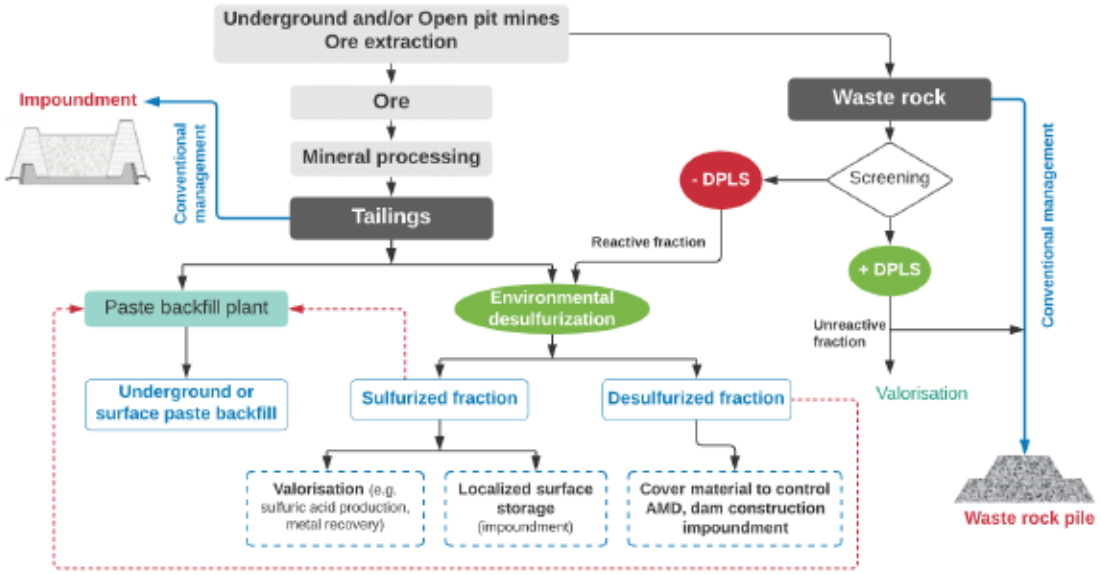

Figure 2.6 Approaches to reach an integrated mine waste management

2.5.2 Gravity Separation

Gravity separation, as the oldest industrial technique widely used, is still one of the most important routes in mineral processing. This operation of concentration consists of differential decantation of mineral particles in a fluid (water or air). Ease of operation, low operating costs (no reagent costs), ability to process coarse grain sizes at high flow rates, and ecofriendly aspects are the main benefits associated with its use (Marion et

al., 2018; Roy, 2009). This technique can be considered when the target minerals have densities sufficiently different from those of gangue minerals (Gülsoy and Gülcan, 2019). Gravity separation takes place in a field of forces combining gravity and other forces such as the resistance offered by the fluid to the movement of particles. When the effect of gravity is insufficient, the action of centrifugal force is required for better separation. After years of research and development, a variety of gravity separation equipment and technologies were developed for mineral separation. **Fig. 2.7** summarizes the common equipment frequently used in mineral processing field.

According to the simplest theoretical model, the movement of particles in a fluid can be characterized by a limited settling rate, which is a function of the density of the particle but is also strongly dependent on particle size. Taggart proposed a concentration criterion (C_T) to empirically assess opportunities as well as difficulties of an ore to be amenable by a gravity separation (Wills, 2016):

$$C_T = \frac{\rho_1 - \rho_f}{\rho_2 - \rho_f} \tag{2}$$

where ρ_1 is the density of the heaviest mineral, ρ_2 is the density of the lightest mineral (gangue), and ρ_f is the density of the fluid medium.

Table 2.5 presents the relative ease of mineral particle separation using gravity techniques, based on the particle size and concentration criterion (Wills, 2016). This relationship remains valid in hindered settling, such as pulps with a solid concentration between 5 and 30%.

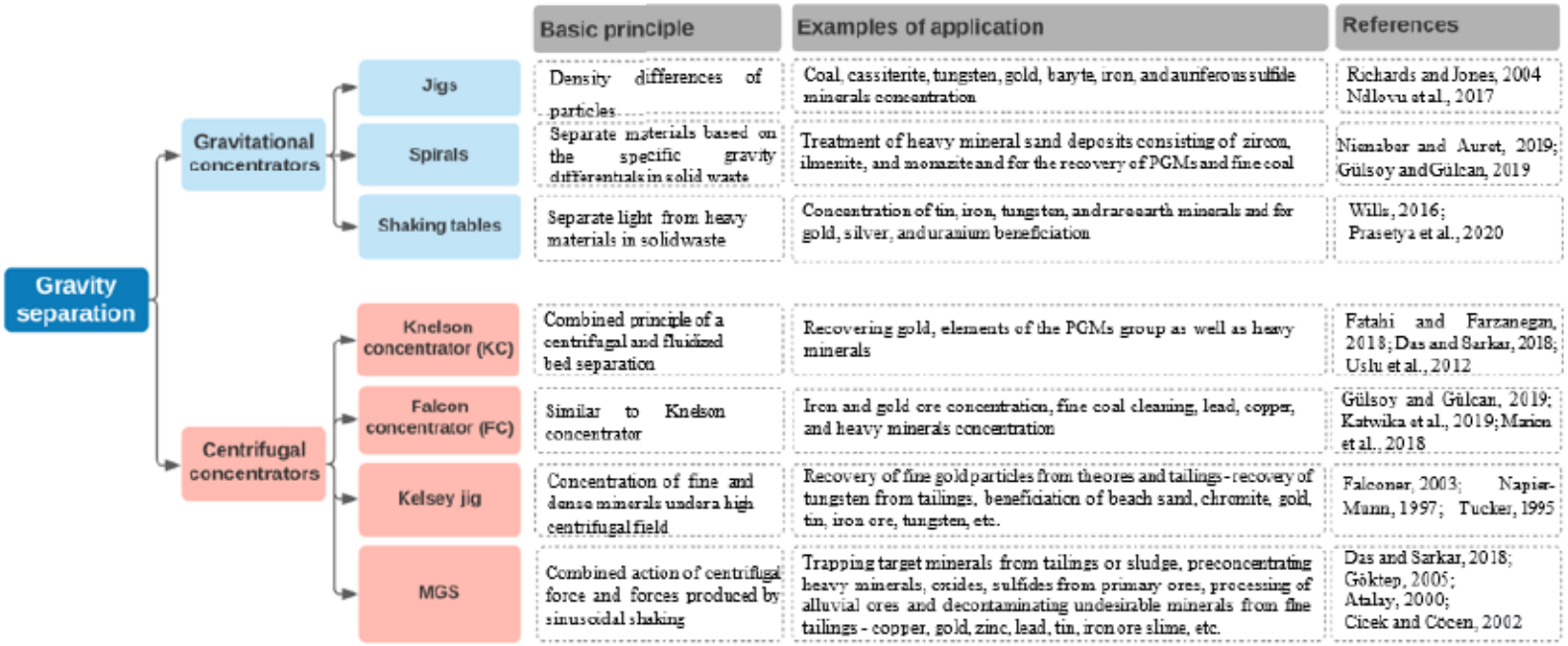

Figure 2.7 Common gravity separation equipment and technologies

To illustrate the importance of this concentration criterion, take the example of the Raglan tailings (Canada). According to Benzaazoua et al. (2017), the tailings contain pyrrhotite as the most abundant sulfide and mainly lizardite as gangue. If pyrrhotite is being separated from quartz using water as the carrier fluid, the C_T is 2.35 (density of pyrrhotite being 4.7; lizardite being 2.57), which is why this separation is quite possible (assuming these minerals are liberated).

Table 2.5 The relative ease of gravimetric separation according to the concentration criterion and particle size

Taggart C_T	Separation	Minimum particle size
> 2.5	Relatively easy	75 µm
2.5 - 1.75	Possible	150 µm
1.75 - 1.5	Possible but difficult	1.7 mm
1.5 - 1.25	Possible but very difficult	6.5 mm
< 1.25	Not possible	-

This concept is effectively used in conventional gravity separation operations such as jigs, spirals and shaking tables. However, the simplistic description of Taggart is not always exact. Indeed, the settling of particles is also dependent on particle size (Ndlovu et al., 2017). When the particle size is too small, settling kinetics are slower because forces linked to the flow of water are more dominant than those of gravity. Consequently, even if the concentration criterion is favorable, target minerals contained in fine particles have proven to be unrecoverable because the time required for an effective separation is impracticably long and challenging to achieve (Das and Sarkar, 2018). Traditional gravimetric techniques are not able to provide such long sedimentation times and are therefore not suitable for fine particles less than 1 mm (Das and Sarkar, 2018). Moreover, the finer the particle size, the higher the specific surface area and mineral liberation. These two parameters become important when dealing with sulfides or sulfosalts, which are very reactive and able to oxidize and generate contaminated rock drainage (Chopard et al., 2017). The work of Benzaazoua et al.

(2017) on the environmental desulfurization of the Raglan mine tailings in Canada confirms these relationships. That study showed that pyrrhotite was mainly present in the fraction below 106 µm and better liberated in the finer fraction (<53 µm). To overcome the technological limitation related to recovery of finer particles, the use of advanced gravity concentrators was highly recommended, whereby the particles would be subjected to a centrifugal force field, thus enhancing the settling kinetics (Majumder and Barnwal, 2006; Marion et al., 2018; Tripathy et al., 2017).

2.5.3 Dense Medium Separation (DMS)

Dense medium separation, also known as heavy medium separation, is a technique of enrichment or physical beneficiation method by which particles are separated based on differences in relative density (Marion et al., 2017). It has been used for more than fifty years as an economical solution to mineral preconcentration when the coarsely liberated particles are of different densities. DMS is commonly used in the coal and diamond industries and the preconcentration of some valuable minerals (e.g., cassiterite) from contaminants and gangues (Grewal et al., 2014; Khalil et al., 2019). The minerals to be separated are immersed in a separation medium that consists of a heavy liquid with a well-defined density or a suspension of ultra-fine and dense particles, resulting in an apparent density between that of heavy and light minerals (Marion et al., 2017). The heavy particles sink into the suspension while light particles float (Fig. 2S) (Annexe A). Ferrosilicium powder (FeSi) and magnetite (Fe_3O4) are the most frequently used materials for the preparation of the suspension (dense medium) (Ndlovu et al., 2017). Given their magnetic properties, these two industrial products can be easily recovered to be recirculated in the same application (Ndlovu et al., 2017).

Compared to other gravimetric techniques, this process offers certain advantages as it can make sharp cuts with a high degree of efficiency, even if the difference between the densities of the particles to be separated is less than 0.1 g/cm^3 (Wills, 2016).

Provided there is a difference in density, there is no upper size limit; this is determined by the plant's ability to handle the material. To improve the efficiency of fine particle separation (<500 µm), it is recommended to use centrifugal (dynamic) separators to enhance their migration through the dense medium (Khalil et al., 2019). Numerous recent studies have proven the efficiency of centrifugal DMS in the treatment of fine minerals (Hirajima et al., 2005; Khalil et al., 2019). Despite the existence of many dense medium centrifugal devices (Table 2.6), the dense medium cyclone (DMC) is most commonly used in the mining industry (Grewal et al., 2014).

Table 2.6 Different devices of dense medium separation

	Device	Particle size	Capacity	Reference
Gravitational separators	Cone Wemco	> 10 cm	500 t/h	Wills, 2016
	Drum	> 30 cm	450 t/h	Wills, 2016
Centrifugal separators	DMC (*)	0.3 - 40 mm	250t/h	Wills, 2016
	WOC (**)	0.2 - 1 mm	High	Luttrell et al., 2014; Majumder and Barnwal, 2011
	CL (***)	6 - 90 mm	800 t/h	Napier-Munn et al., 2014
	Dyna Whirlpool	0.5 - 30 mm	100 t/h	Wills, 2016

(*) Dense medium cyclone

(**) Water-only cyclone

(***) Cyclone Larcodems

DMS has been widely used in the coal, diamond, and iron ore industries. However, other research has demonstrated the success of the separation and upgrading of other base metals and decontaminating of mine wastes (Grewal et al., 2014; Khalil et al., 2019; Marion et al., 2017).

2.5.4 Magnetic Separation

Magnetic separation exploits the susceptibility of materials to magnetism, which reflects the behavior of a mineral or a material when it is subjected to a magnetic field. Magnetic separation is moderately used in the mining industry because of the operating

conditions required. It is used in the processing of iron ore, ilmenite, chromite, silica, kaolin, and others (Ndlovu et al., 2017). Minerals can be classified into two broad groups of magnetic susceptibility (Wills, 2016): i) strongly magnetic minerals classified as ferromagnetic, such as iron and magnetite, which can be easily separated from other minerals by the application of a low-intensity magnetic field (LIMS; <~ 0.3T); and ii) weakly magnetic minerals, generally classified as paramagnetic and diamagnetic. These two types of minerals differ in the way they interact with magnetic fields. Paramagnetic minerals are weakly attracted, while diamagnetic minerals are weakly repelled along the lines of magnetic forces (Rikers et al., 1998). These minerals require a high-intensity magnetic field (HIMS; > ~ 2T) for separation (Mercier et al., 2001; Svoboda, 1994). Typical examples are rutile, ilmenite, and chromite.

The magnetic separation process is generally an inexpensive recovery method with a large capacity despite the use of high-intensity separators. Separation can be accomplished under wet or dry conditions (Wills, 2016). The magnetic field can be produced via a permanent magnet or an electromagnet. The main advances are the introduction of permanent magnets based on rare earth oxides, which allow greater efficiency at a lower cost price, and the development of Cryo magnetism using superconductivity (Wills, 2016). Figure 2.8 shows some magnetic separation equipment that is most commonly used on an industrial scale as well as the particle size conditions for their efficient applications (Gillet, 2004; Wills, 2016). Recent studies at the laboratory and intermediate scale show the potential and the possibility of the use of this technique to desulfurize mine wastes (Rezvanipour et al., 2018; Taskinen et al., 2018).

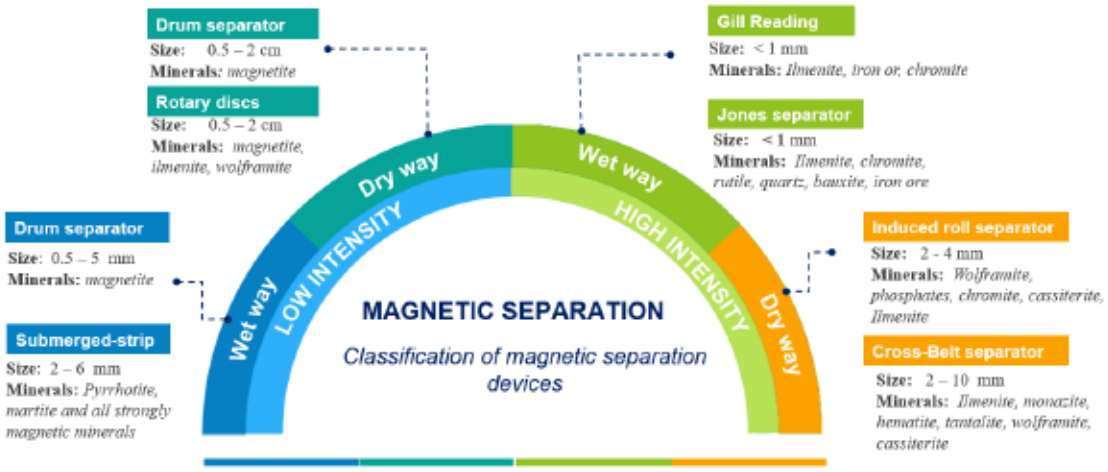

Figure 2.8 Application and particle size limits of magnetic separators

2.5.5 Electrical Separation

Electrical separation exploits the differences in electrical conductivity between the different minerals or various particles to be separated. This method is rarely used due to the required processing conditions (Wills, 2016). The main application of this technique is related to the separation of rutile, ilmenite, and zircon from sand (Dance and Morrison, 1992). It is also applied to other minerals such as phosphates and scheelite to separate them from pyrite and certain salts, as well as to recover metallic particles in sands (Gill, 1991). It should be noted that before starting the electrostatic separation, a step of selective development of the charges on the mineral particles is required. Generally, since electrical conduction occurs on the outer surface layers of atoms (Dance and Morrison, 1992), electrostatic separation can be compared to flotation, in which the separation is based on the state of the mineral surface. There are three main mechanisms by which particles are charged: ion bombardment, conductive induction, and contact electrification (Wills, 2016).

Two main families of electrical separators exist: electrostatic separators and electrodynamic separators (also called high-voltage separators). Although their

separation principles are substantially similar, electrodynamic separators are the most widely used on an industrial scale with better capacities (Gosselin et al., 1999). With this technique, it is possible to separate the different particles into those that are electrically conductive and those that are not. From an environmental standpoint, the separation of metallic particles in sand is probably the most advantageous application of this separation technique. As there is generally a difference in electrical conductivity between the sulfur minerals (electrically conductors) and gangue, the use of electrical separation for the desulfurization of mine wastes is possible.

2.5.6 Sensor-based Sorting Technique

Sensor-based separation, also known as sensor-based sorting, has existed for over 70 years, mainly for the concentration of diamonds (Von Ketelhodt, 2009). However, it still represents an emerging technology with a limited number of industrial applications (Dalm et al., 2014). Automated sorting systems inspect particles in spectral ranges invisible to the naked eye to determine the value of specific properties using non-contact (non-destructive) measurements in real-time. The particles pass through a sensor mechanism, which sends a signal to the processor. The latter decides whether the particle contains target minerals with target grade. This decision is transmitted to the sorting mechanism to create two classes of particles: valuable and gangue (Fig. 3S) (Annexe A). Table 2.7 presents examples of properties that can be exploited using commercially available sensor technologies as well as examples of industrial applications.

This technique is attracting more attention and has a potential advantage for the mining industry because it can be applied to relatively coarse particles (Dalm et al., 2014). Indeed, it can be implemented as a preconcentration step in the ore processing scheme. This technique will remove material of non-economic value (gangue minerals) prior to the concentration methods (Robben and Wotruba, 2019) and send only a reduced

amount of feed material to the high energy-consuming grinding circuit. In addition to decreasing the energy to be consumed during grinding thanks to the sorting of the ore (decreased quantity), capital savings be obtained by decreasing the concentration equipment size and the tailings ponds area. Moreover, the concentrator feed variability is eliminated, resulting in improved control and efficiency of the concentration (Robben and Wotruba, 2019). On an environmental level, this technique ultimately makes it possible to produce minimal quantities of easily manageable fine tailings, given their decreased volume (Robben and Wotruba, 2019).

Table 2.7 Some industrial and automated sensor technologies and applications

Sensor type	Material property	Applications
Radiometric	Natural gamma radiation	Uranium, precious metals
X-ray transmission	X-ray attenuation coefficient, atomic density	Base/precious metals, coal
X-ray fluorescence	Elemental composition	Base/precious metals
X-ray luminescence	Visible luminescence under X-rays	Diamonds
Visual spectrometry	Reflection / absorption	Metals, industrial minerals,
Color	Color, reflectance, brightness, transparency	Base/precious metals
Photometric	Monochromatic reflection/absorption	Industrial minerals, gemstones
NIR spectrometry	Reflectance/ IR radiation absorption	Base and industrial minerals
Thermal infrared	Differential heating conductivity	Base/precious metals

In terms of managing mine wastes, "waste sorting" could be used with the objective of waste desulfurization. With this separation technique, low-sulfur waste rock could be produced without any geochemical risk. A similar principle used in situ, especially for open pit mines, has been developed for the recovery of ore by the Australian CRCore, called Grade Engineering®. This approach is aimed at preconcentrating the ore by defining a cut-off grade before it is directed to the crushing step. It allows the rejection of low-quality non-economic materials (mine waste rock) as early as possible. Grade Engineering® has been identified as an effective operational strategy allowing the productivity of mining industries to be increased considerably.

2.6 Applicability of Physical Separation

To our knowledge, the potentials, limitations, and advantages of physical mineral separation processes have not been sufficiently examined so far in the context of environmental desulfurization of mine wastes. The applicability of physical separation techniques to mine wastes for desulfurization mostly depends on a few parameters, which are presented in Figure 2.9.

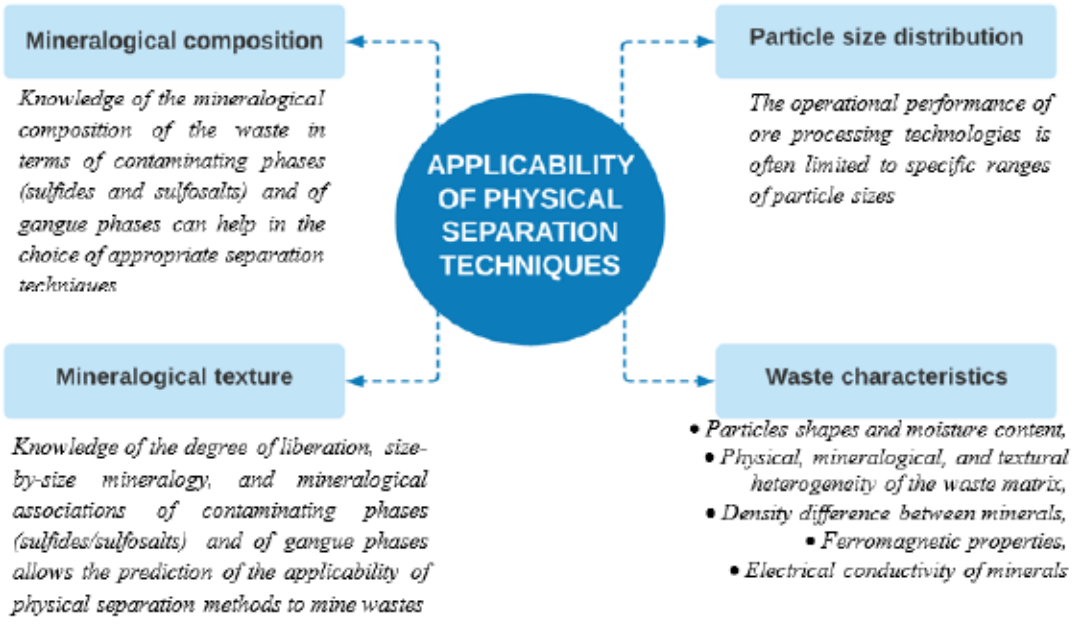

Figure 2.9 The different parameters used for defining the applicability of physical separation techniques to environmental desulfurization of mine wastes.

The modal mineralogical composition of mine wastes is the first information to determine. It is beneficial to anticipate which separation technique could be effectively applied for desulfurization operations. Identification of contaminating and gangue phases will help in the choice of an appropriate method. This information already gives an idea of the physical properties of the different minerals that constitute the waste and, therefore, the various possibilities of separation. However, modal composition is not

enough. The description of the mineralogical textures (e.g., size-by-size mineralogy, liberation degree, and mineralogical associations) is also of great importance.

Gosselin et al. (1999) developed a protocol for evaluating the treatability of soil, sludge, and contaminated sediment by physical separation methods. This protocol considers the exhaustive mineralogical characterization and the particle size analysis of the material to treat. The characterization of mineralogical liberation makes it possible to determine for each mineral phase of interest (sulfide/sulfosalt in our case) its proportion of exposure to the external medium. The liberation degree of the sulfides strictly depends on the mineralogical aspects of the different phases (shape, morphology, and mineralogical association with the carrying phases: carbonates, phyllosilicates, Fe oxides, or others). Figure 2.10 summarizes various and possible degrees of liberation for the mineral phases to separate and the feasibility of applying physical separation.

The effective treatability of mine wastes by physical separation techniques also depends on several other waste characteristics, such as: i) particle size distribution, ii) particle shape, iii) moisture content, iv) heterogeneity of waste matrix, v) difference in density between the sulfurous and gangue minerals, and vi) ferromagnetic properties and the electrical conductivity of contaminants (Dermont et al., 2008). Based on these characteristics, the separation can be determined as difficult, sometimes even impractical, in the following cases (Dermont et al., 2008):

- difference in density between sulfides/sulfosalts and gangue not significant;
- great variability in mineralogical composition;
- contaminant minerals present in all particle size fractions of the solid waste; and
- waste containing clay content above 30% (clay defined from a particle size perspective).

	**(a) Mineral phases included in the matrix** ○ Liberation degree is very low ○ Density depends on the mineral phases and their carrying phase ○ Physical separation is very difficult or impossible ○ Crushing is required
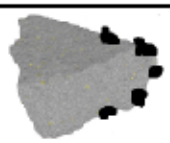	**(b) Mineral phases weakly bounded on surface** ○ Liberation degree is estimated as medium ○ Physical separation is applicable if the mineral phases can be liberated by a simple washing
	**(c) Mineral phase associated** ○ Liberation degree is estimated as medium ○ Density depends on the mineral phase itself and its carrying phase ○ Surface properties are not constant ○ Physical separation can be applicable (e.g., gravity concentration)
	**(d) Mineral phase liberated or free** ○ Liberation degree is very high ○ Density depends on the mineral phase only ○ Surface properties are constant ○ Physical separation is applicable (e.g., gravity concentration, DMS)

Figure 2.10 Feasibility of applying physical separation according to liberation degree of the contaminant particles. Adapted from Dermont et al. (2008).

However, the particle size distribution (PSD) of the mine waste and sulfur minerals remains the main parameter that determines the applicability of physical separation technologies. The case of waste rock is a typical example: it is essential to characterize particle size distribution because this type of mine waste generally contains a wide range of particle sizes (Amar et al., 2020b; Elghali et al., 2019a). Moreover, the operational performance of mineral-based technologies is often limited to a specific

range of particle sizes. Figure 2.11 illustrates the ranges of particle sizes appropriate for each physical separation technique. Usually, most hydro-classifiers and gravimetric concentrators have a good applicability for the fraction ranging from 63 µm to 2000 µm, which is a typical range for tailings (Dermont et al., 2008). Conventional gravity concentrators (jig, shaking table, and spiral) are generally not suitable for fine particles (< 63 µm), while centrifugal concentrators are more suitable for finer particle sizes. The specific requirements for the application of each technology will be detailed in the following sections.

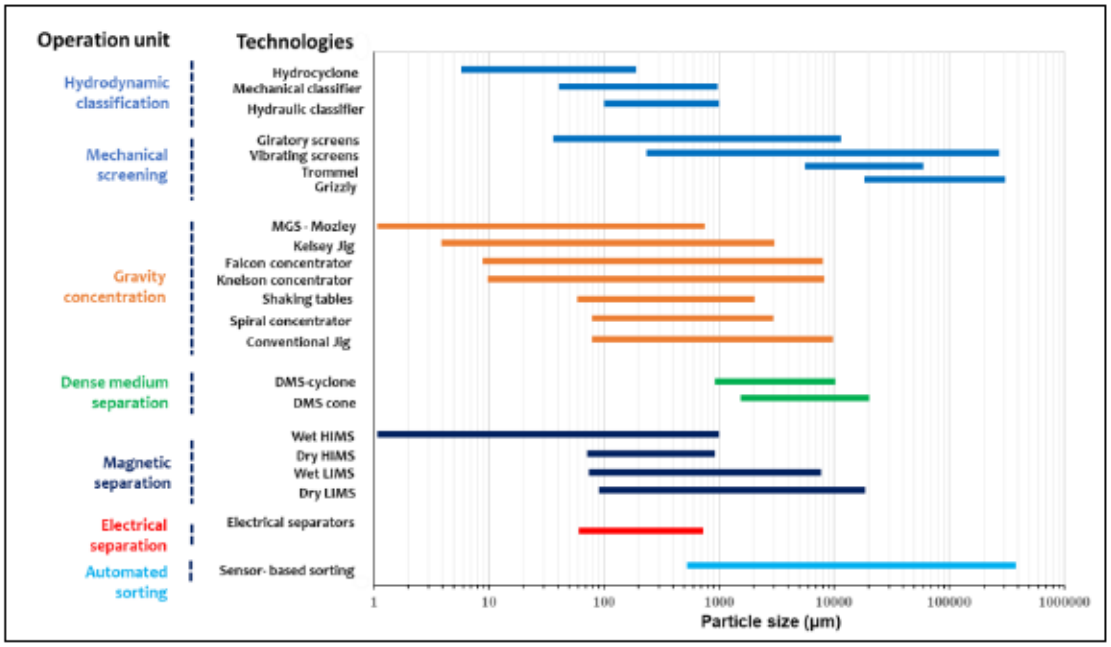

Figure 2.11 Suitable feed particle size ranges for the application of physical separation techniques. Adapted from Abols and Grady. (2006); Chatterjee. (1998); Dermont et al. (2008).

2.7 Special Requirements for Better Performance

Classification Techniques

Hydrodynamic classification and mechanical screening are the main techniques for particle size classification. To guarantee its efficiency, the mineral separation process must be preceded by operations classifying the material into well-defined particle size fractions (Farrokhpay, 2020; Gosselin et al., 1999; Kelly and Spottiswood, 1982). The classification by size is generally conducted under wet or dry processes and requires the use of screens or sieves for the grainy fractions (> 250 µm). For particle dimensions less than 250 µm, the use of hydraulic classifiers such as hydro cyclone is recommended (Tripathy et al., 2015).

Gravity Concentration and Dense Medium Separation (DMS)

Density remains the primary condition on which these processes are based. Gravity separation is inefficient when used to separate particles with a wide particle size distribution and a narrow density distribution (Williford and Bricka, 2000). Gosselin et al. (1999) reported that a density difference of more than 1g/cm^3 must exist between minerals for efficient gravity separation. Ferron et al. (1991) mentioned that rare earth minerals, sulfides, and sulfosalts with relatively high densities (ranging from 4 to 7 as indicated in Table 2.8) will appear as good candidates for separation by gravity when associated with a silicate matrix which is significantly less dense (such as quartz with a density of about 2.7). As this technique also depends on the size of the particles, the dimension of the minerals must be less than 5 cm for an efficient separation (Gosselin et al., 1999). As illustrated in Figure 2.12, the efficiency of the different gravity concentration processes directly depends on the size range of the particles to be separated (Hesford and Wellings, 1988).

As mentioned previously, the most common gravity concentrators used for processing ores are jigs, shaking tables, and spirals. Jigs are usually used to concentrate relatively coarse particles, with sizes varying between 0.5 and 10 mm (Kelly and Spottiswood, 1982). However, the limit can be lowered to 75 µm in some specific applications (Wills, 2016). Shaking tables are used for the processing of particles with diameters varying between 15 µm and 15 mm (Gülsoy and Gülcan, 2019), while spirals are more suitable for handling fine to medium/coarse sand fractions with particle sizes ranging from 75 µm to 3 mm (Marion et al., 2018; Wills, 2016). When the difference between the densities of the materials to be separated is equal to or greater than 1 g/cm^3, the quality of separation increases (Dermont et al., 2008; Gosselin et al., 1999). Notably, it is essential to perform size classification operations prior to concentration. Clay fractions (<75 µm) and very fine sand (75–125 µm) can be processed with advanced centrifugal concentrators such as KC, FC, and MGS Mozley. KC and FC are capable of handling a wide range of particle sizes from 10 µm to 8 mm. The MGS is applied to fine particles with a maximum particle size of approximately 1 mm (Gosselin et al., 1999).

Table 2.8 Classification of the most common sulfides and sulfosalts in mine wastes according to their relative densities, magnetic susceptibilities, and electrical character (Rezvanipour et al., 2018; Wills, 2016)

Mineral		Formula	Density ($g.cm^{-3}$)	Magnetic property; relative susceptibility (ξ $*10^{-6}$ cgs)	Electrical response
Fe Sulfides	Pyrite	FeS_2	4.9 – 5.2	Paramagnetic (*)/diamagnetic ξ ~ 35 to 5000	Conductor
	Marcasite	FeS_2	4.6 – 4.9	Paramagnetic (*); ξ – 18720	Conductor
	Pyrrhotite	$Fe_{1-x}S$	4.6 – 4.7	Ferromagnetic ξ ~ 1200 to 3200000	Conductor
	Troilite	FeS	4.6	Diamagnetic; ξ – 5 187	Conductor
Cu Sulfides	Chalcopyrite	$CuFeS_2$	4.1– 4.3	Paramagnetic ; ξ ~ 23 to 4000	Conductor
	Covellite	CuS	4.6 – 4.7	Diamagnetic; ξ – -55	Conductor
	Chalcocite	Cu_2S	5.5 – 5.8	Diamagnetic	Conductor
As Sulfides/ sulfosalts	Arsenopyrite	FeAsS	5.9 – 6.2	Diamagnetic/paramagnetic (*) ; ξ ~ 240	Conductor
	Realgar	AsS	3.5	Diamagnetic	Conductor
Others	Sphalerite	ZnS	3.9 – 4.1	Diamagnetic; ξ ~ -25 to -60	
	Galena	PbS	7.4 – 7.6	Diamagnetic; ξ ~ -3 to + 84	Conductor
	Stibnite	Sb_2S_3	4.5 – 4.6	Diamagnetic; ξ ~ - 86	Conductor
	Pentlandite	$(Fe,Ni)_9S_8$	4.6 – 5.0	-	
	Molybdenite	MoS_2	4.7 – 4.8	Diamagnetic; ξ ~ -63 to -77	Conductor
	Cobaltite	CoAsS	6.0 – 6.3	Diamagnetic	Conductor
	Gersdorffite	NiAsS	5.9	-	

(*) Variations in the magnetic susceptibilities of minerals can occur mainly in the presence of inclusions.

DMS is more efficient when used to treat coarse grain sizes greater than 1 mm (Figure 2.11 & Figure 2.12). It should also be noted that the efficiency of these separation techniques (gravity and DMS) depends on the mineral liberation degree from the carrying phases (Gosselin et al., 1999; Williford and Bricka, 2000). Thus, the mineral phases to be separated must be liberated as much as possible; otherwise, their densities will be impacted and may not ensure a significant differentiation, leading to poor separation.

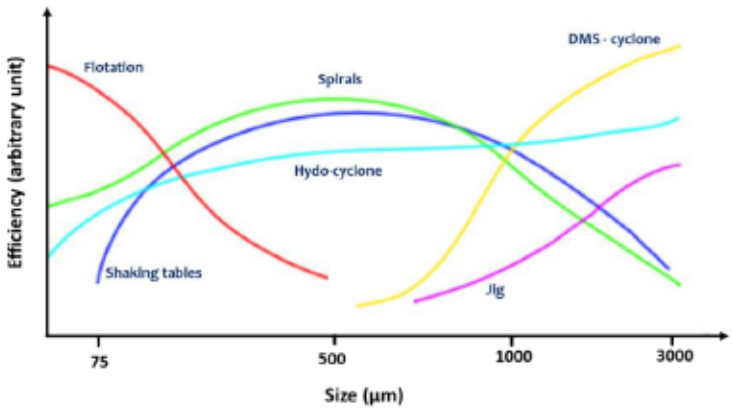

Figure 2.12 Comparison of some separation techniques efficiencies. Adapted from Hesford and Wellings, 1988

Magnetic Separation

As reported in Table 2.8, the sulfides and sulfosalts commonly encountered in mining wastes have low magnetic susceptibilities and are mainly classified as diamagnetic. These can be attracted and separated from other gangue minerals using strong magnetic fields. Therefore, it is challenging to separate them magnetically from gangue minerals. In contrast, pyrrhotite has a ferromagnetic character that is easy to separate through the application of low-intensity separators. In this context, the important parameters to consider are the magnetic properties of the sulfur minerals and gangue, the texture (e.g., liberation degree, associations), and the particle size. Selection of the appropriate class of separation devices (i.e., low or high intensity) depends on an understanding of the presence of target minerals via modal mineralogical characterization of mine wastes and their magnetic properties. As for the liberation degree, it should be maximized. Separation will not occur when the material to be separated consists of particles which have both ferromagnetic phases and non-ferromagnetic species. Indeed, if two minerals have very similar magnetic susceptibilities, the magnetic separation will not be efficient. As mineralogical criteria and magnetic properties of minerals are strongly associated, the particle size must be considered because it informs not only the

treatment mode to be considered (i.e., dry or wet) but also the type of device to be used. Generally, coarse minerals are separated by a dry process while the finer ones (<1 mm) are separated by a wet process. Wet treatment is more selective thanks to the existence of weak inter-particle forces. Thus, magnetic separation is not entirely adequate for fine particles with a particle size of less than 75 µm (Gosselin et al., 1999).

Electrical Separation

Sulfides and sulfosalts, as conductive mineral phases (Table 2.6), must not be completely associated with other phases that are not conductive. The particles to be separated must be perfectly dry because the presence of humidity alters the electrical behavior of the particles (Wills, 2016). This technique is more suitable for mine wastes with a high degree of liberation of the sulfur minerals and gangue (Gosselin et al., 1999). A particle size range between 60 and 500 µm is more suitable for this type of separation (Wills, 2016). For more efficient separation, the preferred particle size is 75 to 250 µm, with a narrow particle size distribution (Haldar, 2018). The weight of the particles limits the upper value, while the minimum value is limited by the electrical behavior of particles smaller than 60 µm. If the small particles are conductive, their behavior will be influenced by the surface charge acquired by non-conductive particles. This influence is reflected in the entrainment of the conductive fines by the insulating particles (Gosselin et al., 1999).

Sensor-based Sorting

Robben and Wotruba (2019) recommend a step to condition the materials before presenting the particles for automated sorting. This step consists of sieving to allow for the particle size to be carefully selected with enough liberation. For most detection technologies, the upper limit of the particle size is technically 350 mm, while the lower limit is technically 0.5 mm (Wills, 2016). However, the ratio of minimum to maximum particle size (size range coefficient) should generally not exceed 1:3 for an efficient

separation (Wills, 2016). Based on this literature review and on the comparison with the typical use of these techniques in ore processing, Table 2.9 summarizes the requirements inherent to the various physical separation techniques as well as their applicability to environmental desulfurization of mine wastes.

Table 2.9 Summary of the specific requirements to the various mineral processing techniques and technologies as well as their applicability to mine wastes for their desulfurization

		Gravity concentration							DMS	Magnetic separation	Electrical separation	Sensor-based sorting
		Gravitational concentrators			Centrifugal concentrators							
Properties		**Jig**	**Spirals**	**Shaking tables**	**Knelson**	**Falcon**	**MGS Mosley**	**Kelsey Jig**				
Particle size		75 μm to 10 mm	75 μm to 3 mm	15 μm to 15 mm	10 μm to 8 mm	9 μm to 8 mm	5 μm to 1 mm	4 μm to 3 mm	0.3 to 40 mm	> 75 μm	75 to 250 μm	0.5 to 350 mm
Density difference		> 1	> 1	> 1	> 1	> 1	> 1	> 1	> 0.1	> 1	> 1	> 1
Liberation degree		High	High	High	High	High	High	High	High	Medium	High	High
Magnetic properties		n.a.	n.a.	n.a.	n.a.	n.a.	n.a.	n.a.	n.a.	High	n.a.	n.a.
Electrical conductivity		n.a.	n.a.	n.a.	n.a.	n.a.	n.a.	n.a.	n.a.	n.a.	High	n.a.
Response to specific sensing		n.a.	n.a.	n.a.	n.a.	n.a.	n.a.	n.a.	n.a.	n.a.	n.a.	Ok
Applicability to environmental desulfurization	Tailings	**Ok**	**Ok**	**Ok**	**Ok**	**Ok**	**Ok**	**Ok**	**Ok**	**Little**	**Little**	**No**
	Waste rock	**Ok**	**Ok**	**Ok**	**Little**	**Little**	**No**	**Ok**	**Ok**	**Ok**	**Little**	**Ok**

n.a.: Not applied

2.8 Successful Applications

Physical separation has been used successfully to remove contaminants and sulfur minerals from mine wastes (tailings and waste rock). Some examples and data demonstrating the successful use of these techniques (on their own or as part of an integrated process) to decontaminate and desulfurize mine waste are described in Table 2.10. A combination of the various mineral processing techniques could ensure better operation efficiency. According to Dermont et al. (2008) a typical flowsheet of the successful physical separation processes generally includes: i) a preliminary size classification step using screening or mechanical sieving to separate target fractions, ii) a hydro classification operation coupled or preceded by washing by attrition to provide a range of particle sizes suitable for other desulfurization techniques, iii) a treatment of the sand fraction (75 µm to 40 mm) by gravity or DMS, and iv) the treatment of the fine fraction (< 75 µm) by centrifugal gravity devices or flotation. Because the fine fraction of mine waste is often considered to be contaminated and geochemically reactive (liberated particles), and the coarse fraction to be less or uncontaminated (Dermont et al., 2008), the physical separation process for desulfurization could be based on simple particle size. Sorting by screening could be an efficient technique for the overall management of waste rock. However, contamination by residual sulfur minerals can be distributed among different size fractions. In this case, separation based solely on particle size cannot ensure efficient separation of contaminants. Separation based on a combination of two or more properties may be considered. Aleksandrova et al. (2019) studied gold and silver ore from the Nezhdaninskoe deposit in the Russian Arctic region. This study included lab-scale testing of an integrated separation method consisting of shaking tables followed by froth flotation. They were able to efficiently separate (yield of 86%) the sulfosalts of tetrahedrite and boulangerite (sulfosalts of Pb and Sn) and some sulfides (galena and arsenopyrite) from other silicate gangue minerals.

Table 2.10 Some successful applications of various physical separation techniques

Technology	Application	Target minerals	Removal efficiency	Comments	References
Spirals	Beneficiation of low-grade PGMs tailings	PGMs	70%	About 70% of PGMs associated with silicates were separated from oxide and sulfide minerals (e.g., chromite, pentlandite, chalcopyrite, pyrrhotite, pyrite, and millerite)	Siame and Kasaini, 2013
Shaking tables	Gold beneficiation from the Nezhdaninskoe gold deposit of the Russian Arctic region	Gold, tetrahedrite, galena and arsenopyrite	86%	The researchers were able to separate tetrahedrite, native gold, galena, and arsenopyrite as well as the sulfosalt known as bakerite (sulfosalt of Pb and Sn) from the other silicate gangue minerals via shaking tables followed by a flotation step	Aleksandrova et al., 2019
Mozley table	Desulfurizing three waste rock lithologies from Canadian Malartic mine	Sulfur minerals	84%	This use of the Mozley table and Knelson concentrator offered a sulfur recovery better than the flotation technique, which prevented the generation of AMD	Amar et al., 2020a
Knelson	Beneficiation of high talc-containing copper-cobalt tailings	Cuprite, chalcopyrite, heterogenite	87%	This enrichment technique has been proven to be profitable and environmentally friendly for low-grade ores and for tailings whose target minerals are too fine and disseminated in complex matrixes	Katwika et al. 2019
	Cleaning oxidized coal with high sulfur content	Pyrite	92%	This technique has the capability of beneficiating fine coal	Uslu et al., 2012
DMS	Reprocessing and cleaning up of two different tailings	Cerussite and smithsonite	88.8% & 91% resp	DMS could be used effectively for decontamination and desulfurization purposes of mine wastes.	Khalil et al., 2019
	Concentration of low-grade nickel sulfides ores	Nickel sulfides	88%	This work demonstrated the success of the separation and upgrading of nickel bearing minerals	Denysschen and Wagner, 2009
Magnetic separation	Desulfurizing Kopsa Au-Cu tailings	Arsenopyrite, and other sulfides	> 60% & 90% resp	Successful removal of As-bearing minerals and sulfides from the tailings was achieved using a combination of high-gradient magnetic separation coupled with sizing and froth flotation	Taskinen et al., 2018
Sorting/ Screening	Waste desulfurization	Sulfides	-	Sorting the waste rock by screening, after blasting, according to the diameter of physical locking of sulfides (DPLS), could be an efficient technique for the overall management of mine waste rock. Low sulfur waste rock could be produced without any geochemical risk.	Amar et al., 2020b; Elghali et al., 2018; Elghali et al., 2019a

Marion et al. (2018) were able to concentrate rare earth elements from rare earth ore sludge using DMS and a modified Falcon concentrator. Nakhaei and Irannajad (2017) worked on the desulfurization of tailings (P80 of 95 µm) rich in iron sulfides (mainly pyrite). An integrated method combining flotation, gravity (spirals), and magnetic separation (HIMS and LIMS) made it possible to desulfurize these tailings and prevent the generation of AMD. The results of this research revealed that the combination of the three techniques decreased the sulfur concentration from an initial value of 1.05 wt. % to a final level of 0.085 wt. %. With this combination of techniques, an iron concentrate was produced and, simultaneously, the reactive fraction of sulfides was separated and could be managed more easily owing to the decrease in volume.

2.9 Desulfurization Effectiveness: Flotation vs Physical Separation Techniques

Very few studies exist that compare the effectiveness of flotation vs physical separation techniques in desulfurizing mine wastes. Recent studies conducted by Amar et al (2020a) and Amar et al (2020b) are the most remarkable in this field, comparing the effectiveness of flotation vs gravity techniques in desulfurizing mine wastes, especially waste rock. The effectiveness of both methods applied to the fraction < 2.4 mm was controlled by sulfur recovery (Amar et al., 2020a). Flotation and gravity methods (Knelson separator and Mozley table) exhibited different efficiencies for cleaning sulfide from feed samples. The sulfur recovery for the studied material by flotation ranged between 54 wt % and 74 wt %. However, the gravity technique resulted in a sulfur recovery greater than 81%. As a result, the use of Knelson separator and Mozley table was determined to be more efficient than flotation. Amar et al. (2020b) examined the feasibility of reprocessing polymetallic waste rock (collected in the waste dump from Langlois mine at Lebel-sur-Quévillon, Quebec, Canada) using a desulfurization process (gravity and flotation). This study focused on the decontamination of the reactive fraction (<2.4 mm). The gravity separation using a Wilfley shaking table showed a sulfur recovery of 61 wt% with a high residual sulfur content that exceeded

1 wt% for the gravity desulfurized material. However, the flotation test results allowed a sulfur recovery of 80 wt %. The low recovery by gravity and by flotation was explained by the large size range of the studied sample (0 –2.4 mm) and the lowest mineral liberation of sulfur minerals. The combined application of both processes in series ensured a high sulfur removal (89 wt %) and generated a final desulfurized material classified as non-acid generating. Generally, the combination of several techniques including flotation can be considered to improve considerably the desulfurization efficiency.

2.10 Knowledge Gap and Future Research Needs/Opportunities

Many research and development related to the beneficiation of fine-grained low-grade ore (as tailings) are made in the field of flotation. For instance, new "green" flotation reagents have been developed based on cellulose to replace the non-biodegradable and sometimes harmful reagents commonly used (Lopéz et al., 2019; Noirant et al., 2019). Furthermore, given the difficulty of efficient ultra-fine particles flotation (Wang et al., 2014), the selective flocculation of desired minerals (e.g., sulfide minerals) to a suitable size for efficient separation during flotation is being developed (Yu et al., 2017). The use of new generation of machines is promising to overcome this challenge; theses later use well calibrated bubble size distribution enabling good adhesion of fine particles (Niedoba et al., 2021). Jameson cells, hydrofloat and column flotation represent typical examples.

Other current and future developments in mineral processing field include innovations in size reduction techniques, classifiers and physical separation techniques (Das and Sarkar, 2018; Farrokhpay, 2020). The digitization of industrial processes is also one of the main developments to be mentioned. Via this development, the ore/ waste sorting using specific sensors allows for mineral sorting according to their chemical and/or mineralogical composition or shape/color (Robben and Wotruba, 2019). In addition,

the implementation of machine learning (McCoy and Auret, 2019) should further improves process performances and allows greater selectivity (sulfide minerals vs gangue). Other developments include gravity concentrators, magnetic separation, superconducting separators, flash flotation and electro-flotation. The implementation of such technologies will minimise consumption of energy, water and reagents, as well as the amount of generated waste without causing any environmental hazards.

2.11 Conclusion

Although the application of environmental desulfurization by flotation has been successfully carried out on several tailings, this technique remains efficient for a size fraction between 20 µm and 1 mm. Moreover, its efficiency depends on the physico-chemical parameters imposed by the previous treatments and the mineralogical properties (modal composition and textures) of the material. To address these gaps, this review provides a basic understanding of the suitability of other mineral processing techniques that could be considered for environmental desulfurization of mine wastes.

Based on this literature review, physical separation techniques known for the enrichment of ore could be used to desulfurize mine wastes. These techniques can be more efficient in some cases, less expensive, and, above all, more environmentally friendly than flotation. The selection of an appropriate physical technique for environmental desulfurization depends on several factors including: i) mineralogy (type of sulfides/sulfosalts), ii) texture (liberation degree and mineralogical associations), and iii) particle size distribution. The size-by-size mineralogical analysis of mine wastes that is often carried out for environmental desulfurization by flotation provides important information to determine the potential and limitations for the use of these techniques for desulfurization. Size-by-size mineralogy makes it possible to identify the sulfides and sulfosalts (with the different mineralogical parameters) in each of the particle size fractions as well as some of their physical properties that mineral

processing techniques can exploit for concentration. For tailings, the use of centrifugal gravimetric concentrators (e.g., Knelson, Falcon) is recommended for improved environmental desulfurization efficiency, especially because they can treat fine particles (< 20 µm). For waste rock, the use of DMS, sensor-base sorting, and magnetic separation (especially in the presence of pyrrhotite) is more promising for desulfurization.

To improve desulfurization efficiency, combinations of several techniques including flotation can be considered. When mine wastes to be desulfurized have a wide particle size distribution, it is often useful to proceed to sieving or classification prior to other separation techniques. Then, the appropriate types of mineral processing equipment could be selected for each fraction. Hydrometallurgical and pyrometallurgical (roasting) technologies have not been described in this report. These technologies could be applied to the desulfurization of mine wastes (Everaert et al., 2020; Tambwe et al., 2020). Moreover, the integrated processes that combine both physical and chemical/pyrometallurgical extraction processes can also be envisaged.

CHAPITRE 3

OBJECTIFS, HYPOTHÈSES ET ORIGINALITÉS

Bien que l'application de la désulfuration environnementale ait été menée avec succès sur plusieurs rejets miniers (et surtout résidus) à travers le monde (Benzaazoua et al., 2000a; Mermillod-Blondin, 2005), il n'en demeure pas moins que son efficacité dépend de plusieurs facteurs tels que les propriétés minéralogiques (composition modale et textures) et granulométriques des rejets en question ainsi que les paramètres physico-chimiques imposés par le traitement antérieur lorsqu'il s'agit de rejet de concentrateur.

La flottation non sélective reste la technique la plus utilisée pour la désulfuration des résidus miniers issus de concentrateurs. Cependant, des études récentes montrent que ce type de procédé pourrait également s'appliquer aux stériles miniers (Amar et al., 2020) et que d'autres techniques utilisant la séparation gravimétrique pourraient être également et efficacement envisagées dans ce cadre (Amar et al., 2020; Atrafi et al., 2012; Falconer, 2003). En revanche, à ce jour, le potentiel de génération de DNC (cas de l'arsenic et de nickel en particulier) des rejets de désulfuration reste encore une préoccupation pour les chercheurs du domaine et les industriels. D'autre part, la présence de certains sulfosels (skutterudite, gersdorffite, nickéline) dans les rejets miniers (résidus et stériles miniers) n'a jamais été abordée dans les études antérieures consacrées à la désulfuration environnementale par flottation et/ou par gravimétrie. Cette dernière problématique trouve à ce jour une application dans le cas des rejets (résidus et stériles miniers) de la mine d'Amaruq (Nunavut, Canada) renfermant la gersdorffite. Ce minéral présente une réactivité très élevée avec un taux d'oxydation important lorsqu'il est soumis aux conditions atmosphériques, comme le montrent les travaux de Chopard et al. (2017).

Dans ce contexte, l'objectif général de ce travail de recherche est d'approfondir davantage le cadre d'application de la désulfuration environnementale, en tant que

technique de gestion intégrée des rejets miniers, pour le contrôle de la génération du DMA à un cadre plus large de contrôle et prévention de la génération du DNC à l'arsenic et au nickel suite à l'oxydation de certains sulfures et sulfosels non conventionnels.

De cela découlent quatre objectifs spécifiques :

i. Caractériser les mécanismes surfaciques fondamentaux inhérents à la flottation de quelques sulfosels (skuttérudite, gersdorffite et nickéline), dans le but de diminuer le potentiel contaminant des rejets miniers porteurs de ces minéraux moins communs;
ii. Optimisation la désulfuration environnementale des résidus miniers renfermant de la gersdorffite pour un meilleur contrôle de la génération de DMC à l'arsenic et au nickel par amélioration des rendements de désulfuration;
iii. Étude du comportement environnemental (réactivité) des rejets désulfurés issus de tests optimaux afin d'évaluer l'efficacité de la désulfuration environnementale à contrôler la génération du DMC;
iv. Détermination du DPLS pour une gestion économique et éfficace du stérile minier avec désulfuration de la fraction fine (retraitement);

Quatre principales hypothèses sont à la base de ce projet :

i. Comme la désulfuration environnementale produit des rejets désulfurés qui respectent les normes environnementales en termes de DMA (directive 019), elle pourra de même être appliquée à des rejets miniers pour le contrôle et l'atténuation du potentiel de génération des contaminants (DNC);
ii. La désulfuration environnementale par flottation non sélective pourra être appliquée à des résidus miniers contenant des sulfosels et des sulfures moins

communs comme la gersdorffite pour le contrôle de la génération du DNC à l'arsenic et au nickel;

iii. Comme le KAX est le collecteur le plus utilisé (et plus performant) dans l'industrie minière pour la flottation des sulfures plus communs, il pourra de même être performant pour la flottation des sulfosels (skuttérudite, gersdorffite et nickeline);

iv. La décontamination/désulfuration de la fraction fine des stériles miniers par des techniques physiques/gravimétriques combinées ou non à la flottation pourra produire des rejets désulfurés qui respectent les normes environnementales en termes de DMA et même de DNC.

Ce projet s'inscrit d'une part dans la continuité d'un ensemble de travaux portant sur la recherche d'outils visant à diminuer le potentiel polluant des rejets miniers, et d'autre part dans la continuité d'études permettant une meilleure compréhension des mécanismes de formation des phases oxydées à la surface de différents types de sulfures/sulfosels lors de leur conditionnement superficiel pendant les étapes du procédé de flottation, ainsi qu'à une meilleure connaissance au sujet des mécanismes d'adsorption des xanthates sur ces derniers.

Ce projet de doctorat est original et novateur. La nouveauté de l'étude se justifie en partie par la caractérisation surfacique de la gersdorffite, le skuttérudite et la nickéline (arséniures porteurs de contaminants) pour définir et comprendre les mécanismes surfaciques inhérents à leur flottation dans le contexte de désulfuration environnementale. En effet, les interactions xanthates/skuttérudite, xanthates/gersdorffite et xanthates/nickéline n'ont pas reçu autant d'attention que le système pyrite/xanthate ou pyrrhotite/xanthate dans la littérature. Ainsi, la technique DRIFTS n'est pas été utilisée pour cette caractérisation surfacique fondamentale ainsi que les phases xanthate adsorbées à la surface de ces arséniures. L'originalité de cette thèse repose aussi sur l'utilisation de la séparation gravimétrique par DMS (séparation

en milieu dense) et par spirale/table à secousses pour désulfurer les stériles miniers. L'application de cette technique sur des produits miniers porteurs d'arséniures (e.g., gersdorffite) fait aussi l'originalité de ce travail. À noter aussi que l'utilisation des plans d'expériences (méthodologie de surface de réponses : RSM) pour l'optimisation du procédé de désulfuration des résidus miniers porteurs de la gersdorffite afin de prévenir la génération du DNC, rajoute plus d'originalité à ce projet. En résumé, la principale originalité de ce projet est désormais d'ouvrir le champ d'utilisation de la désulfuration environnementale en tant que gestion intégrée des rejets miniers pour la prévention de la génération du DMA à un champ plus global de diminution du potentiel contaminant des rejets miniers.

CHAPITRE 4

SURFACE PHYSICO-CHEMICAL CHARACTERIZATION OF ARSENIDE MINERALS BEFORE AND AFTER XANTHATES ADSORPTION FOR FLOTATION PURPOSES: CASE OF SKUTTERUDITE ($(Co,Ni,Fe)AS_3$), GERSDORFFITE (NiAsS), AND NICKELINE (NiAs)

Préambule : cet article est accépté pour publication potentielle dans la revue *Minerals Engeneering* après des corrections mineures

Y. Ait-khouia[1], A. El-bouazzaoui[1], Y. Taha[2], I. Demers[1], M. Benzaazoua[1,2,*]

[1] Research Institute on Mines and Environment (RIME), University of Quebec in Abitibi Témiscamingue, 445, boul. de l'université, Rouyn-Noranda J9X 5E4, Quebec, Canada

[2] Mohammed VI Polytechnic University (UM6P) - Mining Environment & Circular Economy, Ben Guerir 43150, Morocco

* Corresponding author. E-mail address: mostafa.benzaazoua@uqat.ca

4.1 Abstract

Skutterudite ($(Co,Ni,Fe)As_3$), gersdorffite (NiAsS), and nickeline (NiAs) are common arsenic- and nickel-bearing minerals often encountered worldwide in mine ores and mine wastes. These arsenides can be the source of arsenic- and nickel-contaminated neutral drainage (CND) when subjected to atmospheric conditions. CND effluent is often characterized by circumneutral pH and metals/metalloids release (e.g., Ni, As) at concentrations that exceed the existing regulatory limits or biological tolerances. Environmental desulphurization by froth flotation is a promising technique to control and prevent environmental risks (CND generation) and has already been applied to tailings to prevent acid mine drainage (AMD). This technique concentrates

sulphides/sulphosalts by froth flotation to produce a desulphurized product that can be managed safely and at a lower cost. This study fills a knowledge gap in the evolution of the surface physicochemistry of these arsenides under different conditions. This data is required to determine the best conditions for arsenide flotation and successful environmental desulphurization. This work aims to evaluate the impact of grinding, air-oxidation (aging), and conditioning at natural pH values and alkaline pH values (10.5 using caustic soda (NaOH) and limewater (CaO)) on skutterudite, gersdorffite, and nickeline surfaces, as well as their interaction with potassium amyl xanthate (PAX) as a flotation collector under the same conditions. The effect of activation by copper sulphate ($CuSO_4$) was also studied. The adsorption of amyl xanthate was analyzed through ultraviolet–visible (UV–Vis) spectrophotometry and zeta potential measurements, and the surface was characterized using the DRIFTS technique (diffuse reflectance infrared fourier transform spectroscopy) that allowed the speciation of the oxidation layer across the different mineral surfaces to be evaluated. Dry grinding and aging of the arsenides produced thin heterogenous oxide and hydroxide layers mainly enriched in arsenic oxides, especially in the form of arsenate (as an oxidation product of arsenite), and arsenic, cobalt, and nickel sulphates and hydroxides. Moreover, the skutterudite grinding and aging study confirmed the formation of Ni and Co hydroxides and arsenic oxides; arsenite (AsO_3^{3-}) appeared after 12 h and disappeared after 48 h, whereupon arsenate (AsO_4^{3-}) started forming, which suggests that arsenate was the oxidation product of arsenite. Gersdorffite and nickeline showed similar behavior, but with even higher oxidation rates, where the surface showed the presence of arsenite after only 4 h , followed by arsenate after only 6 h. Nickel hydroxides were also observed on the nickeline surface. Arsenide conditioning under alkaline conditions enhanced the oxidation effect on the mineral surfaces compared to natural conditions. Adsorption isotherms and zeta potential measurements demonstrated that copper sulphate activation was effective on the arsenides and was shown to improve the adsorption of xanthate on the oxidized arsenide surfaces (including gersdorffite),

especially under alkaline conditions. The results of this study led to a better understanding of the surface chemistry of these arsenides before and after the collector adsorption, which should impact their flotation behavior.

Key words: skutterudite, gersdorffite, nickeline, environmental desulphurization, flotation, amyl xanthate, surface characterization, DRIFT spectroscopy, UV–Visible.

Résumé

La skutterudite ($(Co,Ni,Fe)As_3$), la gersdorffite (NiAsS) et la nickeline (NiAs) sont des minéraux communs contenant de l'arsenic et du nickel et souvent rencontrés dans les minerais et les rejets miniers. Ces arséniures peuvent être la source d'un drainage neutre contaminé par l'arsenic et le nickel (CND) lorsqu'ils sont soumis aux conditions atmosphériques. Les effluents de CND sont souvent caractérisés par un pH neutre et des métaux/métalloïdes en solution (par exemple, Ni, As) présents à des concentrations qui dépassent les limites réglementaires ou les tolérances biologiques existantes. La désulfuration environnementale par flottation est une technique prometteuse pour contrôler et prévenir les risques environnementaux (génération de CND) et a déjà été appliquée aux résidus pour prévenir la génération du drainage minier acide (DMA). Cette technique concentre les sulfures/sulfosels par flottation pour produire un rejet désulfuré qui peut être géré en toute sécurité et à moindre coût. Cette étude comble un manque de connaissances sur l'évolution de la physicochimie de surface de ces arséniures dans différentes conditions. Ces données sont nécessaires pour déterminer les meilleures conditions pour leur flottation et la réussite de la désulfuration environnementale. Ce travail vise à évaluer l'impact du broyage, de l'oxydation à l'air (vieillissement) et du conditionnement à des valeurs de pH naturelles et alcalines (10,5 en utilisant de la soude caustique (NaOH) et du lait de chaux (CaO)) sur les surfaces minérales de la skutterudite, de la gersdorffite et de la nickeline, ainsi que leurs interactions avec l'amylxanthate de potassium (PAX) comme collecteur de flottation dans les mêmes conditions. L'effet de l'activation par le sulfate de cuivre ($CuSO_4$) a

également été étudié. L'adsorption du xanthate a été analysée par spectrophotométrie ultraviolet-visible (UV-Vis) et par mesures de potentiel zêta, et la surface minérale a été caractérisée à l'aide de la technique DRIFTS (diffuse reflectance infrared fourier transform spectroscopy) qui a permis la spéciation de la couche d'oxydation à travers les différentes surfaces minérales à évaluer. Le broyage à sec et le vieillissement des arséniures ont produit de fines couches superficielles hétérogènes d'oxydes et d'hydroxydes principalement enrichies en oxydes d'arsenic, et plus particulièrement sous forme d'arséniate (en tant que produit d'oxydation de l'arsénite), et de sulfates et hydroxydes d'arsenic, de cobalt et de nickel. De plus, l'étude de broyage et de vieillissement de la skutterudite a confirmé la formation des hydroxydes de Ni et de Co ainsi que d'oxydes d'arsenic ; l'arsénite (AsO_3^{3-}) est apparu après 12 h et a disparu après 48 h, après quoi l'arséniate (AsO_4^{3-}) a commencé à se former, ce qui suggère que l'arséniate était le produit d'oxydation de l'arsénite. La gersdorffite et la nickeline ont montré un comportement similaire, mais avec des taux d'oxydation encore plus élevés, où la surface a montré la présence d'arsénite après seulement 4 h , suivie d'arséniate après seulement 6 h. Des hydroxydes de nickel ont également été observés à la surface de la nickeline. Le conditionnement des arséniures dans des conditions alcalines a amélioré l'effet d'oxydation sur les surfaces minérales par rapport aux conditions naturelles. Les isothermes d'adsorption et les mesures du potentiel zêta ont démontré que l'activation du sulfate de cuivre est efficace sur les arséniures et améliore l'adsorption du xanthate sur les surfaces d'arséniures oxydés (y compris la gersdorffite), en particulier dans des conditions alcalines. Les résultats de cette étude ont permis de mieux comprendre la chimie de surface de ces arséniures avant et après l'adsorption du collecteur, ce qui devrait impacter leur comportement à la flottation.

Mots clés : skutterudite, gersdorffite, nickeline, désulfuration environnementale, flottation, amyl-xanthate, caractérisation de surface, spectroscopie DRIFT, UV–Visible.

4.2 Introduction

Arsenic is a common metalloid associated with many types of ore deposits and mine wastes worldwide. Arsenic is rarely recovered as a by-product in mining practices; as such, it is often discarded in mine tailings (Craw and Bowell, 2014). The weathering of these tailings can increase the exposure of As-bearing minerals, resulting in surficial oxidation that promotes arsenic release (in acid and/or neutral media) and mobilization to the local surface environment. The behavior and release of arsenic from mine tailings is dependent on the As-bearing minerals present, which are a function of the geological context of the deposit (polymetallic or precious metals) (Chopard et al., 2017). The common As-bearing minerals include sulpharsenides and arsenides such as gersdorffite (NiAsS), skutterudite ($(Co,Ni,Fe)As_3$), and nickeline (NiAs).

Due to the strict environmental regulations and the geochemical risks that mine tailings can create, sustainable management of mine tailings has become a global environmental concern. Furthermore, the recent exploitation of low-grade, large-scale deposits of sulphide, arsenide, and sulpharsenide minerals is set to further aggravate this problem (Avarmaa et al., 2018; Elghali et al., 2019). Consequently, mining companies are required to adequately manage their mine tailings to prevent contaminated mine drainage (CMD). Indeed, mining companies must integrate and develop sustainable strategies as a part of the final closure plan to ensure that contamination does not adversely affect the environment. Different approaches have been proposed and developed by many researchers from around the world. Environmental desulphurization using froth flotation as an integrated tailings management technique is one approach that has gained much popularity in the last two decades (Ait-Khouia et al., 2021; Amar et al., 2021; Benzaazoua et al., 2017; Demers et al., 2009). This promising technique aims to limit and control AMD/CND by separating sulphides/sulphosalts (acid/contamination generating) and gangue minerals (desulphurized fraction that does not generate CMD) and managing both fractions

accordingly (Benzaazoua et al., 2000a; Derycke, 2012; Hesketh et al., 2010; Mermillod-Blondin et al., 2005b). This strategy has already been applied to numerous mine tailings around the world, from small to industrial scales, and has been proven successful in preventing AMD (Benzaazoua et al., 2000b; Bois et al., 2005; Broadhurst and Harrison, 2015; Bruckard and McCallum, 2007; Demers et al., 2008; 2018; Kongolo et al., 2004; Nadeif et al., 2019; Nakhaei and Irannajad, 2017). Nevertheless, its application to prevent CND from unconventional arsenides has received minimal attention and has not yet been sufficiently addressed (Benzaazoua et al., 2017; Derycke, 2012; El-bouazzaoui et al., 2022). To concentrate sulphides and sulphosalts, the mineral surfaces often need to be modified by organic collectors such as potassium amyl xanthate (PAX). These chemical compounds adsorb on the surface of target particles and cover them with a hydrophobic layer (Wills and Finch, 2016). The study of the evolution of the surface chemistry of minerals is essential for a better understanding of the mechanisms involved in the froth flotation process and, by extension, environmental desulphurization. The collector adsorption mechanism (through various physicochemical conditions) is also an important aspect of the flotation process that needs to be deeply studied and investigated.

Although floatability of the most common sulphide minerals (e.g., pyrite, pyrrhotite, and arsenopyrite) has been deeply studied and documented in the literature for desulphurization purposes, its worth mentioning that few studies deal with the floatability of arsenides as unconventional minerals (e.g., skutterudite, gersdorffite, and nickeline) that can generate arsenic- and nickel-CMD (Craw and Bowell, 2014; El-bouazzaoui et al., 2022; Iwasaki et al., 1988; Nakazawa and Iwasaki, 1986; Qun and Heiskanen, 1990; Smith et al., 2011). Indeed, the study of surface chemistry by identifying and understanding the fundamental surface mechanisms inherent to the flotation of these arsenides was developed in the current study. The overall goal is to address skutterudite, gersdorffite, and nickeline flotation challenges for environmental purposes, especially for controlling the generation of As- and Ni-CMD. To meet these

objectives, this research focused on characterizing the surface evolution of skutterudite, gersdorffite, and nickeline of a standard size (32–63 µm). Different spectroscopic techniques were jointly used for the quantitative and qualitative characterization of the surface chemistry, electrochemistry, and the interaction with the well-known PAX collector.

4.3 Research Materials and Methods

4.3.1 Methodology

Figure 4.1 displays the steps and the operations followed to conduct this research. Skutterudite, gersdorffite, and nickeline were subjected to fundamental studies/characterizations before and after PAX adsorption. These studies included surface state chemical characterization (under different conditions), adsorption isotherm construction, and zeta potential measurements. Specifically, the general methodology was essentially divided into the following objectives:

- characterization of the surface state of the pure minerals after dry grinding and conditioning in ultra-pure water;
- characterization of the surface (in an aqueous medium): effect of pH, pH regulator type, and activation with copper sulphate;
- physicochemical characterization of aqueous solutions by UV–Vis spectrophotometry: construction of adsorption isotherms;
- study of the influence of surface species on xanthate/mineral interaction mechanisms and therefore on adsorption efficiency; and
- characterization of the surface: tracking the superficial electrical potential of the arsenides before and after xanthate adsorption (with and without surface activation).

The surface evolution was characterized through different conditioning steps using DRIFTS (diffuse reflectance infrared fourier transform spectroscopy) analyses: grinding, conditioning with water and at different pH values (natural and alkaline) using different reagents (soda ash (NaOH) and lime (CaO)), activation with copper sulphate ($CuSO_4$), and PAX adsorption. The impact of air-oxidation (aging) on the mineral surface was also evaluated. The main objective of using DRIFTS was to provide further insight into the surface chemical composition and speciation of the arsenide minerals, especially before the PAX adsorption. It seems interesting to mention that interactions of PAX with skutterudite, gersdorffite, and nickeline have not yet been addressed compared to the pyrite/pyrrhotite and arsenopyrite/xanthate system in the literature. Furthermore, DRIFT spectroscopy has not been employed to qualitatively characterize the surface chemical evolution of these arsenides and the xanthate phases adsorbed at their surface. The affinity of xanthates to the surface of different arsenides was studied using ultraviolet–visible (UV–Vis) spectroscopy under different physicochemical conditions by plotting adsorption isotherms and calculating the statistical surface coverage values. This affinity/interaction was also explored using zeta potential measurements that play a basic role in determining the electrical charge of the studied minerals and defining the flotation conditions (Derhy et al., 2022).

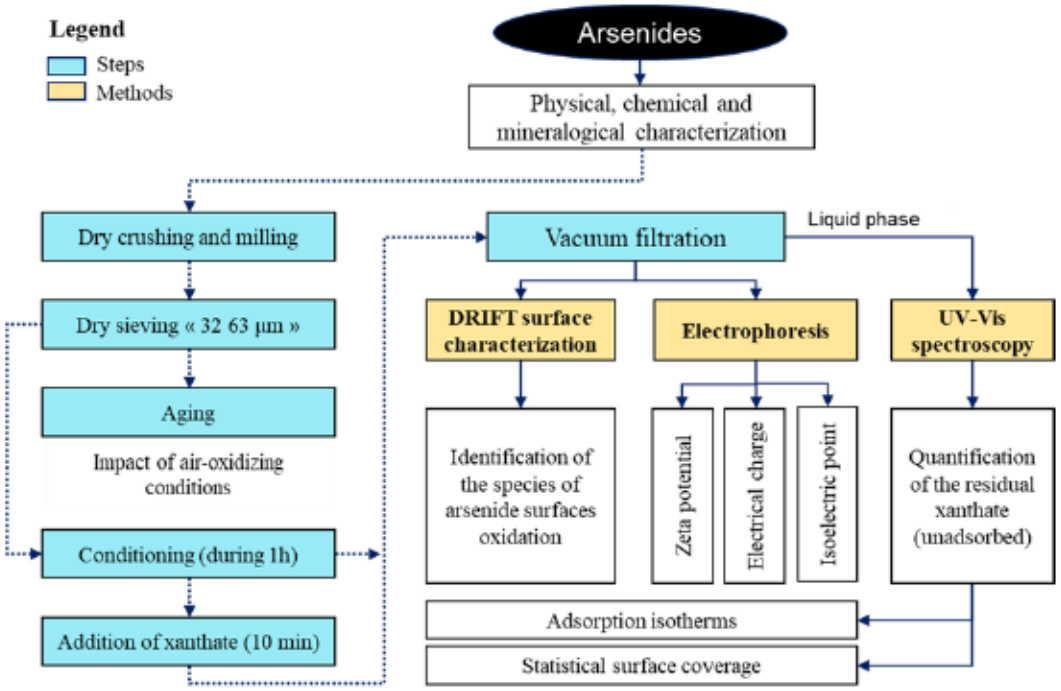

Figure 4.1 Methodology illustrating the experimental work followed to investigate the surface physicochemistry of the studied arsenide minerals.

Adsorption of PAX on the studied arsenide surfaces was performed at i) natural pH, and at alkaline conditions (pH 10.5) using ii) NaOH and iii) CaO as regulating agents. This adsorption of the xanthate collector on the arsenide surfaces was also carried out with different concentrations allowing testing of a wide-range of xanthate surface coverage. By increasing the concentration of the xanthate collector, a saturation plateau was formed where the collector no longer adsorbed on to the arsenide surface and the Q_{ads} stayed at a constant value. The modelling of adsorption isotherms, also known as sorption isotherms, can help to interpret the adsorption phenomena (Ayawei et al., 2017). A mixed model of the commonly used Langmuir and Freundlich adsorption models was used to fit the data, as done elsewhere (Álvarez et al., 2004; Umpleby et al., 2001a). This model had been used for mineral surfaces that are homogeneous and

heterogeneous and for different concentrations of sorbent (low to high) (Umpleby et al., 2001b). This mixed model formula is expressed as:

$$Q_{ads} = \frac{N * K^m * C_{eq}^m}{1 + K^m * C_{eq}} \qquad \text{With : } K = a^{1/m} \qquad (4)$$

where Q_{ads} represents the amount of adsorbed xanthate (mol/m^2), C_{eq} is the equilibrium concentration of amyl-xanthate in mol/L, N is the number of binding sites, m is a fitting parameter related to the Freundlich model that corresponds to the surface site energy heterogeneity, K is the median binding activity, and a is a fitting parameter related to K and m.

The statistical surface coverage, θ, was used instead of the adsorbed quantity (Q_{ads}) to interpret the data, as it considers the total surface sites available for adsorption in addition to the adsorbed quantity. To maximize the correlation coefficient (R^2) and minimize the squared sum of the residuals (the difference between data and model), the solver function in Microsoft Excel was used by iteratively modifying the parameters N, m, and a.

4.3.2 Chemicals and Reagents

Flotation requires different types of reagents to create the proper surface conditions for mineral concentration. The pH regulator reagents used in this study were solutions of NaOH and CaO. Copper sulphate pentahydrate ($CuSO_4.5H_2O$) was used as an activator. PAX from Univar Canada Ltd was used as a collector; it is the most widely used PAX in the mining industry and its properties and adsorption mechanisms are well documented in the literature. For better characterization of the adsorption on the arsenide surfaces, the PAX was purified by dilution in acetone and precipitation in diethyl ether according to the procedure described by Rao. (1971) to avoid unwanted interference from impurities (Kongolo, 1991; Kongolo et al., 2004).

4.3.3 Arsenides: Origin and Conditioning

Skutterudite, gersdorffite, and nickeline minerals were selected for this study based on their occurrence in some typical polymetallic sulphide-rich deposits and mine wastes. The arsenide samples investigated in this study were obtained from the Bouazzer mine (Morocco). As they were not completely pure, they were hand-sorted to remove macroscopic impurities under a binocular lens. For the experiments, the high-quality samples of gersdorffite, skutterudite, and nickeline were dry ground with a steel laboratory mortar, then milled using a FRITSCH Planetary Ball Mill Pulverisette 5. Dry sieving was used to isolate the fraction between 32–63 µm for each mineral, a fraction proven to lead to high quality spectra with DRIFTS (Derycke et al., 2013; Mermillod-Blondin et al., 2005a). To prevent surface oxidation, the fractions were stored in a freezer in airtight bags and used within two days. However, some samples were stored at room temperature to assess the effects of air-oxidizing conditions (aging) on the arsenide surface.

Aqueous conditioning of the arsenides was carried out by the addition of 3 g of mineral into 40 mL of deionized water (18.2 MΩ.cm at 25 °C) in a rotary shaker. One hour of conditioning was sufficient to bring the mineral surface in equilibrium with the solution, as previously demonstrated by several studies (Caldeira et al., 2008; De Donato et al., 1999; De Donato et al., 1993). The pH of the suspension was adjusted to 10.5 using a solution of NaOH or CaO. Copper sulphate was added as a surface activator at a concentration of 2.10^{-4} mol/L (equivalent to around 25 g/t collector concentration with 1% arsenide slurry), with an additional 10 min of conditioning. A prepared PAX solution (10 v%/v) was added to the suspension at different concentrations and conditioned for another 10 min at 25°C in a rotary shaker. The resulting pulp was then filtered by vacuum filtration to separate the liquid and solid phases. The equilibrium solution was analyzed by UV–Vis spectroscopy to measure the amount of unadsorbed PAX (residual collector) and therefore construct the adsorption diagrams. The filtered

solid was dried on a filter paper for a short time, sampled, and immediately analyzed by DRIFTS to avoid any surface state evolution.

4.3.4 Physical, Chemical, and Mineralogical Characterization Methods

4.3.4.1 Physical and Chemical Characterization

The particle size distribution of the sieved fraction of the arsenides was determined using a laser grain size analyzer (Malvern Mastersizer S). The specific gravity (Gs) of each arsenide specimen was measured with a micromeritics helium pycnometer (Micromeretics, Accupyc 1330), and the specific surface area (SSA) was analyzed with a micromeritics surface area analyzer using the Brunauer-Emmett-Teller (BET) method (based on nitrogen adsorption for the 32–63 µm fraction) (Brunauer et al., 1938). The bulk chemical composition of the high-grade minerals was performed at Activation Laboratories (Actlabs) in Ancaster, Ontario, Canada using peroxide fusion inductively coupled plasma mass spectrometry/optical emission spectrometry (ICP-MS/OES).

4.3.4.2 Mineralogical Investigation

Mineralogical investigations of pure minerals (polished sections) were conducted through quantitative and automated mineralogy. Indeed, QEMSCAN® (quantitative evaluation of materials by scanning electron microscopy) and electron probe microanalysis (EPMA) were used to characterize the mineralogy of the samples. QEMSCAN® is an automated mineralogy system that produces particle maps (color-coded by mineral) using rapidly acquired X-rays. The corresponding data files allow quantification of various mineralogical parameters such as modal mineralogy and texture (mineral liberation degree and mineralogical associations). QEMSCAN®

analyses were performed at XPS (Expert Process Solutions) laboratories in Sudbury, Ontario, Canada.

A more precise quantification of the chemical composition of pure arsenides and trace elements was achieved using EPMA at the XPS laboratory. The instrument used for the EPMA analysis was a Castaing Cameca SX-100 coupled with a WDS (wavelength-dispersive X-ray spectrometer). Operating conditions included a focused beam (spot size of < 1 μm), an accelerating voltage of 20 kV, and a constant beam current of 20 nA. This instrument had lower detection limits than other scanning electron microscopy systems (e.g., scanning electron microscopy with energy dispersive X-ray spectroscopy; SEM-EDS) and it allowed for more efficient data analysis and linking with QEMSCAN® measurements. This quantitative investigation was carried out by analyzing approximately 10 particles from each sample (six spots on average for each mineral). A set of calibration standards (pyrite, chalcopyrite, InAs, Co, Ni, etc.) was used to improve the quality of the quantitative analysis of the arsenides, allowing for accurate microanalysis across a wide range of concentrations.

4.3.4.3 Spectroscopic Methods

In this study, different spectroscopic methods were jointly used for qualitative and quantitative characterization of the surface chemistry and electrochemistry of the pure arsenides and their interaction with the xanthate collector.

Surface Characterization: Diffuse Reflectance Infrared Fourier Transform Spectroscopy (DRIFTS)

DRIFTS was used to identify/characterize superficial phases (oxidation products) present at the arsenide surface at the molecular scale. It uses a penetration depth of the infrared radiation (IR) that covers the first 25,000 Å (De Donato et al., 1993; Derycke et al., 2013). For this analysis, the arsenide samples must be in the form of a 32–63μm

powder. To avoid a very high absorbance (high intensity of the peaks), the sample powder was mixed with 85% potassium bromide (KBr) (15% of material) because this inert matrix does not absorb medium IR (De Donato et al., 1999). A Fourier transform infrared (FTIR) spectrometer (Shimadzu IRTracer100) equipped with a diffuse reflectance module (PIKE EasiDiff) was used to record the infrared spectra. The optical line was adjusted to avoid the contribution of specular reflection. All diffuse infrared spectra in the range 4,000–600 cm^{-1} were plotted in absorbance units (log of the intensity ratio RKBr/Rsample with RKBr and Rsample representing the diffused beam intensities of the reference and the sample, respectively) (De Donato et al., 1999; De Donato et al., 1993; El-bouazzaoui et al., 2022). The spectral resolution was set to 4 cm^{-1}, with 200 point scans. To validate the DRIFTS results, repeatability and reproducibility analyses were carried out for the different study conditions. For each parameter, the spectra showed very similar characteristic peaks located approximately at the same wavenumbers as those reported in the literature. However, the amplitude of the peaks was slightly varied for the same parameter, indicating that certain chemical species formed more abundantly during the advancement of conditioning, but that the effective reproducibility of the analyses was confirmed.

Quantification of Residual Xanthate Collector Using Ultraviolet–Visible (UV–Vis) Spectroscopy

After each conditioning step the liquid and solid phases were separated. The residual unadsorbed xanthate in the liquid (filtrate) was quantified using a UV–Vis spectrophotometer (Ultrospec 2100 pro). The amount of xanthate adsorbed was then determined from the difference between the initial concentration of the collector added during conditioning (Ci) and the residual concentration (equilibrium concentration) in the filtrate (Ce). The method involved measuring the intensity of light passing through the filtrate and comparing it to the intensity of light passing through a reference solution.

The Beer–Lambert law was used for calculating the residual concentration according to equation (1) (El-bouazzaoui et al., 2022; Kongolo et al., 2004):

$$A = C_e \times \varepsilon \times L \quad (1)$$

where A is absorbance, Ce is the equilibrium (residual) concentration of the collector (mol/ L), ε is the molar extinction coefficient (L/mol/cm), and L is the cell thickness (1 cm).

UV–Vis spectra were plotted and expressed as absorbance (U.A.) versus wavelength (nm) (190–400 nm). For the PAX collector, the absorbance peak is located at 301 nm. This absorbance is proportional to the concentration according to the Beer–Lambert law with a molar extinction coefficient of ε = 17,660 L/mol/cm for the xanthate in ultra-pure water, regardless of the chain length (Chang et al., 1999; Kongolo et al., 2004). The real molar extinction coefficient was calculated from the slope of the calibration curve generated by plotting absorbance intensity at 301 nm versus the PAX concentrations (mol/L) of standard solutions. The calculated molar extinction coefficient was compared to the pure molar extinction coefficient of xanthate (17,660 L/mol/cm). Knowing this calculated molar extinction coefficient, it was possible to construct the adsorption isotherms, which are expressed in the C_e–Q_{ads} plan. These adsorption isotherms show the affinity of the xanthate collector to the mineral surface under different physicochemical conditions. To do this, the rest method was used (difference between initial and residual concentrations) following equation (2) (Derycke, 2012; Kongolo et al., 2004):

$$Q_{ads} = \frac{(C_i - C_e) \times V}{m} \quad (2)$$

where Qads is the quantity of collector adsorbed on the mineral surfaces (expressed in mol/g), Ci is the initial concentration of the collector (mol/L), V is the volume of the solution (L), and m is the solid mass (g) of the mineral.

The statistical surface coverage, θ, was used instead of the adsorbed quantity Q_{ads} to interpret the data, as it considers the total surface sites available for adsorption in addition to the adsorbed quantity. It is calculated using the equation (3):

$$\theta = \frac{Q_{ads} E_x N_a}{S_s} \quad (3)$$

where E_x is the specific surface coverage area of the collector ($Å^2$), Na is the Avogadro number (Na = 6.022 * 10^{23} /mol), and S_s represents the specific surface area (m^2/g) of the mineral. The specific coverage area for xanthate is equivalent to its cross-sectional area on closest packing bases. According to the literature, this specific coverage area of xanthate is equal to 29 Å (Cases et al., 1989; Kongolo et al., 2004; Tukel and Kelebek, 2010).

4.3.5 Zeta Potential Determination

The zeta potential (ZP) of the prepared suspensions was determined by measuring the electrical potential difference between the ionic layer adsorbed, on the arsenide surfaces, and the bulk solution. Assessing the ZP of the mineral particles before and after the addition of xanthate would be helpful to predict whether PAX will bind to the surface of the arsenides. A Zeta sizer Nano ZS90 (Malvern Panalytical) was used; 0.1% solid content suspensions were prepared by mixing 30 mg of mineral powder with 30 mL of 1 mM KCl as the background electrolyte solution (indifferent electrolyte). After pH adjustment using NaOH and HCl, the suspension was stirred for 5 min. The mixture was left to naturally decant for 10 min before analyzing the supernatant. The same protocol was followed to conduct the zeta potential measurement in the presence of 10^{-4} M PAX prepared with a 1 mM KCl solution (the optimum dosage found based on the isotherm adsorption). When testing the effect of $CuSO_4$, 10^{-3} M $CuSO_4$ solution was prepared with a 1 mM KCl solution. The mineral and the prepared solution were mixed, and the pH was adjusted to the desired values. Afterwards, the suspension was stirred

for 3 min, and PAX was added and conditioned for 2 min. Finally, the suspension was left to precipitate for 10 min before analysis. To ensure the accuracy and reproducibility of the results, all tests were performed in triplicate for each pH value; the experimental values were then averaged.

4.4 Results and Discussion

Section 4.4.1 briefly characterizes the arsenide samples as pure minerals. Section 4.4.2 provides DRIFTS surface characterization of the studied minerals under different conditions prior to xanthate adsorption. The xanthate adsorption ability is directly affected by the sulphide/arsenide surface chemistry (Cases and De Donato, 1991; De Donato et al., 1999; Mermillod-Blondin, 2005), so this section outlines the speciation of the oxide layers in the context of xanthate adsorption. Section 4.4.3 describes and discusses the interaction of PAX with the arsenide surfaces under different physicochemical conditions. DRIFTS and UV–Vis spectroscopy were used jointly as complementary tools for characterizing the evolution of the xanthate both in solution and at the arsenide surfaces in the presence/absence of copper sulphate (activator). Section 4.4.4 sheds light on the evolution of the ZP of skutterudite, gersdorffite, and nickeline as a function of pH before and after interaction with copper sulphate (10^{-3} mol/L) and potassium amyl xanthate (10^{-4} mol/L). This aspect play an important role in defining the adsorption (floatability) conditions.

4.4.1 Physical, Chemical, and Mineralogical Characterization

Results of the chemical and physical characterizations of the studied arsenide samples are summarized in Table 4.1. The specific surface areas of the studied minerals were 0.98 m^2/g, 0.86 m^2/g, and 0.49 m^2/g (sieved fraction: 32–63 μm) for skutterudite, gersdorffite, and nickeline, respectively. The specific gravities were about 6.05, 5.44, and 6.94 g/cm^3 for skutterudite, gersdorffite, and nickeline, respectively; this

demonstrates that the studied minerals are almost pure (as compared to the standard pure skutterudite, gersdorffite, and nickeline with specific gravities of 6.5 g/cm^3, 5.9 g/cm^3, and 7.8 g/cm^3; mineral average densities sourced from web minerals).

Table 4.1 Physical properties and chemical composition (ICP-MS/OES) of the studied arsenide minerals (element grades in wt%).

	Element (wt%)	LOD (%)	Gersdorffite	Skutterudite	Nickeline
Arsenides	**Fe**	0.05	**0.59**	**2.16**	**10.1**
	Ni	0.001	**29.5**	**4.6**	**35.3**
	As	0.001	**51.5**	**76.6**	**44.3**
	S	0.01	**13.9**	**1.2**	**6.3**
	Co	0.001	**3.3**	**14.3**	**0.5**
Impurities	Al	0.01	0.03	0.03	< 0.01
	K	0.1	< 0.1	< 0.1	< 0.1
	Ca	0.01	0.48	< 0.01	0.39
	Si	0.01	0.1	0.11	0.22
	Cr	0.01	0.01	< 0.01	< 0.01
	Cu	0.001	0.002	0.009	0.16
Gs	(g/cm^3)	-	5.44	6.05	6.94
SSA	(m^2/g)	-	0.86	0.98	0.49

LOD: limit of detection

A combination of QEMSCAN® and EPMA were used to characterize the mineralogy of the arsenide samples. The QEMSCAN® mineralogy for the samples is illustrated in Figure 4.2 Quantitatively, the skutterudite sample was 92.4 wt% pure and contained low concentrations of other sulphosalts (gersdorffite = 6.33 wt %) and traces of loellingite Co (1.01 wt%) and nickeline (0.09 wt%). The gersdorffite sample was also pure (93.3 wt%) with some contamination by nickeline (5.13 wt%) and cobaltite (0.52 wt%). The nickeline sample was about 84 wt% pure; it was contaminated with about 9 wt% sulphides, 0.84 wt% loellingite Co, 0.27 wt% gersdorffite, and 5.8 wt% other phases.

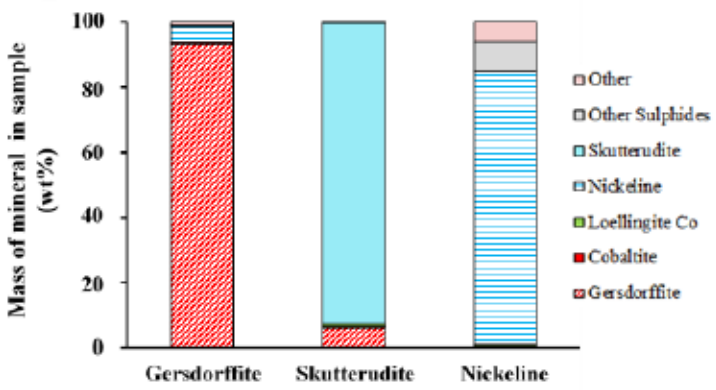

Figure 4.2 Mineralogical composition of the studied arsenide minerals.

The EPMA analyses performed on the studied arsenide samples are illustrated in Table 4.2. The skutterudite contained 2.19 wt% Fe and 1.53 wt% S, and showed a substantial replacement of Co and Ni by Fe and S (Fanlo et al., 2004). The skutterudite sample contained 78.6 wt% As, 16.7 wt% Co, 2.26 wt% Ni, 2.19 wt% Fe, and 1.53 wt% S. This sample contained less Co and Ni and more As than the standard composition, which contains 76.09 wt% As, 17.95 wt% Co, and 5.96 wt% Ni. The gersdorffite sample was a solid solution between NiAsS and CoAsS (Ahmed et al., 2009; Chopard et al., 2017; Fanlo et al., 2004), which contained Co and more As than standard gersdorffite. Ten grains from a prepared polished section were analyzed and the stoichiometry of the studied gersdorffite was 11.62 wt% S, 0.62 wt% Fe, 55.80 wt% As, 26.83 wt% Ni, and 5.13 wt% Co. This sample of gersdorffite contained more arsenic and cobalt and less nickel and sulphur than the standard composition of gersdorffite (theoretically pure gersdorffite contains 19.35 wt% S, 45.22 wt% As, and 35.42 wt% Ni). The nickeline sample had a composition of 56.7 wt% As and 42.83 wt% Ni (Table 4.2), which is similar to the standard composition. Some impurities of Fe, Co, and S were also detected, with concentrations of 0.67 wt%, 0.1 wt%, and 0.07 wt%, respectively.

Table 4.2 EPMA microanalysis of the studied arsenide grains (skutterudite, gersdorffite, and nickeline).

Element (LOD)	Skutterudite			Gersdorffite			Nickeline		
	Analysis (%)		TC (%)	Analysis (%)		TC (%)	Analysis (%)		TC (%)
	Mean value	Range		Mean value	Range		Mean value	Range	
S (0.01)	1.53	0.84–2.25	-	**15.42**	11.85–17.29	**19.4**	0.07	0.02–0.15	-
As (0.06)	**78.60**	77.49–79.43	**76.09**	**51.42**	48.76–56.35	**45.2**	**56.70**	56.46–56.92	**56.07**
Fe (0.04)	2.19	1.23–3.44	-	0.57	0.22–1.08	-	0.67	0.49–0.84	-
Co (0.05)	**16.66**	13.59–18.35	**17.95**	3.36	1.20–6.99	-	0.10	0.05–0.15	-
Ni (0.06)	**2.26**	0.78–4.00	**5.96**	**29.90**	24.83–32.96	**35.4**	**42.83**	41.74–43.36	**43.93**
Cu (0.07	<0.07	<0.07	-	<0.07	<0.07	-	<0.07	<0.07	-
Total	100	-	100	100	-	100	100	-	100

LOD: limit of detection

TC: theoretical composition based on mineral formula

4.4.2 DRIFTS Analyses: Arsenide Surface Product Characterization

The DRIFTS analysis allowed for the surface oxidation products on the mineral surface to be characterized in the spectral range of 4,000–600 cm^{-1}. This analysis was carried out on the studied arsenides after grinding, after aging for two months, and after conditioning at natural and alkaline pH (pH = 10.5). DRIFTS peaks were assigned according to literature data summarized in Table 4.3.

Table 4.3 Peak positions and their species assignment from arsenide IR spectra.

Peak position (cm^{-1})	Band assignment	References
619	Stretching vibration of Ni-OH	Budipramana et al., 2014; Deane et al., 2003; Yuvakkumar and Hong, 2015
649	Co-O stretching vibrations	Muhammad et al., 2020; Tannenbaum et al., 2006; Zhang et al., 2012
640	Ni-O-H stretching bond	Deane et al., 2003
720–750	Antisymmetric elongation vibrations of arsenite (AsO_3^{3-})	Deane et al., 2003) (Nesbitt et al., 2003
840, 865, 940, 963	Antisymmetric elongation of arsenate (AsO_4^{3-}) species	Deane et al., 2003) (Monte et al., 2002
1,050	C=S double bond vibration in xanthate	Wiles et al., 1967; Zhang et al., 2013
1,110	Sulphite (SO_4^{2-}) ionic group vibrations ($NiSO_4$, $CoSO_4$)	Goel et al., 2018; Secco, 1988; Jackson et al., 2003
1,136	C-O-C group: arsenous xanthate	Cases et al., 1995; Leppinen, 1990; Valli et al., 1994
1,191–1,195–1,038	Cuprous xanthate	Cases et al., 1995; Leppinen, 1990
1,075	Amylxanthate	Cases and De Donato, 1991; Cases et al., 1989; Leppinen, 1990
1,038	Cuprous xanthate/ Ferric sulphate	Boily et al., 2010; Leppinen, 1990
1,025	-CS group: dixanthogen/ iron xanthate	Cases and De Donato, 1991; Cases et al., 1989; Cases et al., 1995; Leppinen, 1990
1,800–1,650	Stretching vibration of C=O bond	Jung et al., 1996
1,600, 1,550 and 1,400–1,470	Adsorbed water	Mermillod-Blondin et al., 2005b; Salazar et al., 2015; Soria et al., 2007

4.4.2.1 Characterization of the Ground and Conditioned Arsenide Surfaces

The surface of the 32–63 µm fraction of each arsenide was characterized using DRIFTS after dry grinding and conditioning. Figure 4.3 exhibits the DRIFTS spectra from 2,000

cm^{-1} to 600 cm^{-1} of the fresh surface of the studied arsenides and the evolution after conditioning at natural pH and at pH 10.5 using NaOH and CaO.

The DRIFT spectra of the ground skutterudite (Figure 4.3.**A**) did not show any major peaks. However, a small peak at 940 cm^{-1} related to the arsenic oxides (Deane et al., 2003; Monte et al., 2002) was present. The conditioned skutterudite spectra at natural pH (pH = 6.9) and alkaline pH (pH = 10.5) show that some arsenic oxidation peaks started to clearly appear, mainly at 840 cm^{-1} and 940 cm^{-1}, which are assigned to the stretching vibration of As-O bond (Monte et al., 2002). These peaks correspond to arsenate (AsO_4^{3-}) and arsenite (AsO_3^{3-}) species (Table 4.3). The predominance (high peaks) of the arsenic oxides may indicate that conditioning increased the arsenic oxidation rate (Derycke, 2012; Nesbitt et al., 1995). The absorption band at 619 cm^{-1} appeared after conditioning; this is assigned to the stretching vibration of the Ni-OH bond (Deane et al., 2003; Yuvakkumar and Hong, 2015). Similarly, the peak at 1,110 cm^{-1} appeared on the freshly ground skutterudite but became more apparent after natural conditioning. This absorption band is the typical signature of $NiSO_4$ or $CoSO_4$ group vibration (Jackson et al., 2003). The peaks at 1,570–1,600 cm^{-1} are mainly attributed to the O-H bond and are typically a signature of adsorbed water molecules. Conditioning with NaOH slightly affected the kinetics of arsenic oxidation as compared to conditioning with CaO; indeed, the peak at 840 cm^{-1} that is attributed to the formation of arsenate increased in magnitude in comparison to the conditioning with CaO. The peak around 1,800 cm^{-1} is attributed to the stretching vibration of the C=O bond and is the signature of the adsorption of dissolved CO_2 molecules on the surface of the mineral.

After dry grinding and conditioning the gersdorffite at natural pH (pH = 7.2) and at pH 10.5, DRIFTS analyses were also performed (Figure 4.3.B). Conditioning the gersdorffite caused the formation of more superficial oxide layers (oxidized species) compared to the freshly ground gersdorffite.

The peak at 750 cm^{-1}, which is assigned to the AsO_3^{3-} species was absent in the spectra of the mineral surface after dry grinding but began to appear (small peaks) as soon as the surface was conditioned in aqueous media and at a higher pH (10.5); this suggests the formation of AsO_3^{3-} oxidation products. The low-intensity peak at 1,110 cm^{-1} assigned to Ni sulphates also formed just after grinding. Moreover, the surface characterization showed intense peaks at 865 cm^{-1} and 963 cm^{-1} that are the signature of the antisymmetric elongation vibrations of the AsO_4^{3-} groups, which suggests the oxidation of arsenic into arsenite and then into arsenate. These peaks were also present on the gersdorffite surface after dry grinding, although at low intensities (Figure 4.3.B). This further proved that arsenate ($As^{5+)}$ was the dominant oxidation product as compared to arsenite (As^{3+}), which represents an intermediate oxidation state. Indeed, the surface arsenic atoms were oxidized by reaction with air (after grinding) and continued to oxidize with conditioning. The formation of arsenic oxides outlined in this work is in accordance with the previous studies conducted on gersdorffite by El-bouazzaoui et al. (2022) and Jackson et al. (2003) using X-ray photoemission spectroscopy (XPS). Furthermore, the XPS study conducted by Nesbitt et al. (2003) demonstrated that the reaction of gersdorffite with air (after grinding) is initiated by oxidation of surface As species, which is rapid compared to the oxidation of sulphur species. The study conducted by Jackson et al. (2003) also supported this result; it demonstrated that the gersdorffite reaction rate after conditioning with water is greater than in air, with arsenic being the most reactive element and sulphur being the least reactive. Oxidation of both As and S proceeds through the production of numerous intermediate reaction products in which As and S display intermediate oxidation states. These results are also similar to those obtained for arsenopyrite and niccolite (Jackson et al., 2003; Nesbitt and Muir, 1998; Nesbitt et al., 1995; Schaufuss et al., 2000). The same oxidized As species were, however, produced under alkaline conditions using NaOH and CaO. Moreover, the peak at 1,110 cm^{-1}, which is the typical signature of

$NiSO_4$ group vibration, also formed after conditioning at natural pH and alkaline pH using NaOH and CaO (Figure 4.3.B).

The peak at 1,650 cm^{-1} is typically attributed to the stretching vibration of the C=O bond in adsorbed CO_2. After conditioning, the absorption band at 619 cm^{-1} appeared; it is assigned to the Ni-O-H stretching bond for hydroxylated Ni species (Deane et al., 2003; Yuvakkumar and Hong, 2015). This peak was intense when conditioned under alkaline conditions and less intense when conditioned under natural conditions (Figure 4.3.B). These results suggest that surface Ni atoms were more hydroxylated when conditioned under alkaline conditions, thus quenching the surface peak and intensifying the Ni-OH signal. The Ni-OH species were also observed on oxidized millerite and niccolite surfaces (Legrand et al., 1998; Nesbitt and Reinke, 1999).

The DRIFT spectra of nickeline after grinding and after conditioning at natural (pH = 7.8) and alkaline pH (pH = 10.5) are presented in Figure 4.3.C. The spectra for the fresh surface did not show significant characteristic peaks, but conditioning at natural pH produced well-formed peaks at 1,550 cm^{-1} and 1,400 cm^{-1}. These peaks are characteristic of adsorbed water (O-H stretching and bending, respectively). Moreover, these peaks were well formed when conditioned at natural pH compared to the conditioning at alkaline pH using NaOH and CaO. The peaks at 1,180 cm^{-1} and 940 cm^{-1} were also well formed and are typically assigned to adsorbed CO_2 (Table 4.3) and the stretching vibration of the As-O bond (Monte et al., 2002), respectively. At alkaline pH values, intense peaks formed at 940 cm^{-1} and 840 cm^{-1}, which are the signature of arsenic oxides in the form of arsenate (Table 4.3). The peak at 640 cm^{-1} can be attributed to the Ni-O-H stretching bond (Deane et al., 2003). These results were also supported by the study conducted by Nesbitt and Reinke (1999) using XPS that outlines that the reaction of nickeline with air and distilled water yields a thin oxidized overlayer containing Ni-hydroxide $Ni(OH)_2$, arsenite (AsO_3^{3-}), and arsenate (AsO_4^{3-}). This same study also revealed that the accumulation of arsenite and arsenate salts at the nickeline

surface distinguishes it from millerite and pyrrhotite surfaces that were conditioned and reacted with aerated water. Indeed, nickel and iron sulphate salts produced from these latter two sulphides are highly soluble, and hence do not accumulate at the mineral surface. However, Ni-arsenate and Ni-arsenite salts accumulate on the oxidized nickeline surface along with $Ni(OH)_2$, as they are less soluble compared to Ni- and Fe-sulphate (Nesbitt and Reinke, 1999).

In summary, DRIFTS characterization on the skutterudite, gersdorffite, and nickeline samples revealed the presence of a variety of alteration products that had a wide range of oxidation degrees. For all tested arsenides, the surface mineral lattice and alteration layer were enriched in arsenic phases, especially in in the form of arsenate (As^{5+}) and arsenic and nickel/cobalt sulphates and hydroxides. Arsenic(V) oxides were more abundant than As(III) oxides. Adsorbed water was present on all surfaces, with a greater proportion in the case of the conditioned arsenides. Furthermore, conditioning skutterudite and nickeline under alkaline conditions enhanced the oxidation effect on the mineral surface.

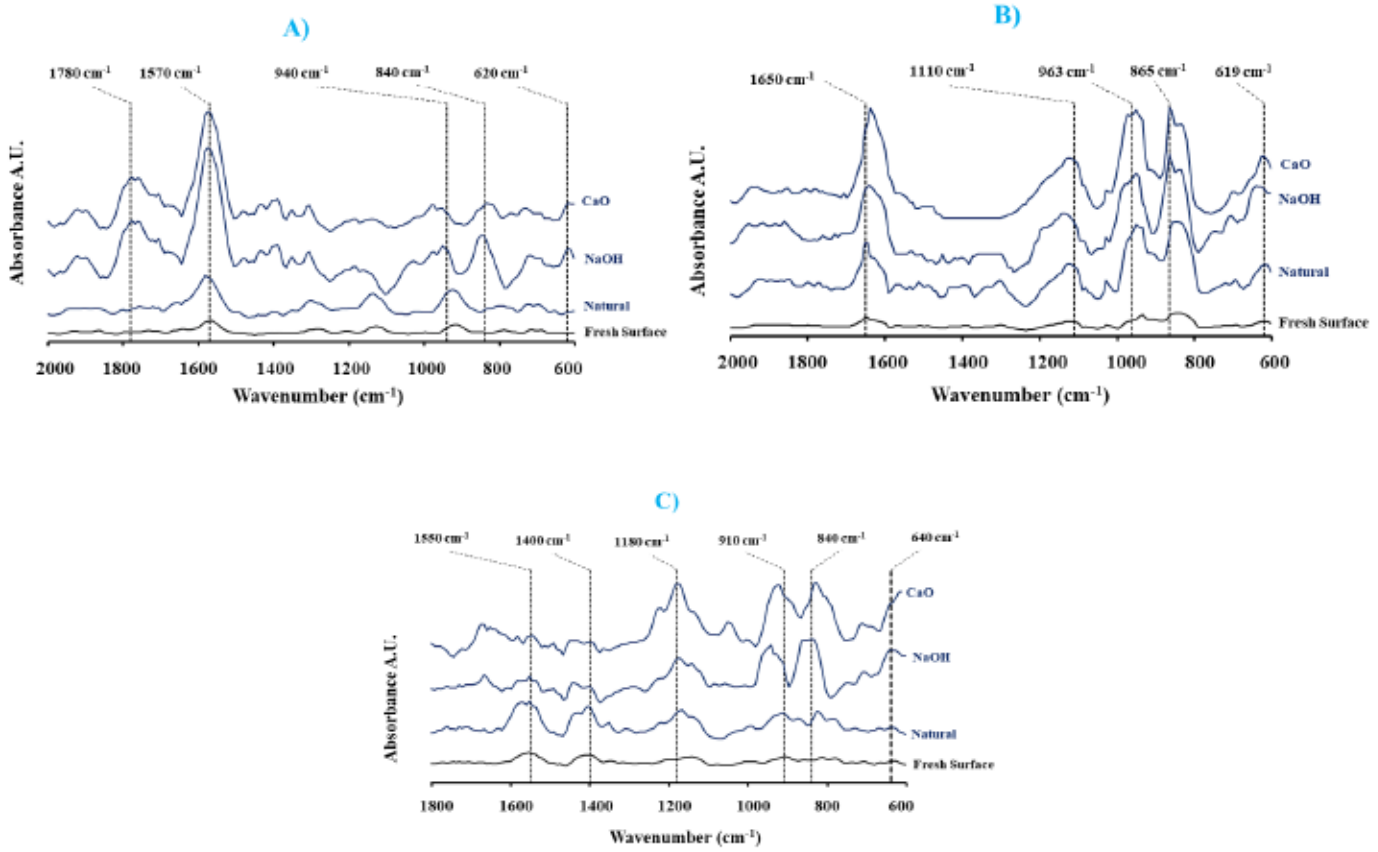

Figure 4.3 DRIFTS spectra from 2,000 cm^{-1} to 600 cm^{-1} of arsenide surfaces under different conditions: fresh surface, conditioning at pH 10.5 with NaOH, and conditioning at pH 10.5 with CaO: A) skutterudite, B) gersdorffite, and C) nickeline

4.4.2.2 Aging and Oxidation Products of the Arsenide Surfaces

DRIFTS analyses ranging from 2,000 to 600 cm^{-1} were conducted to obtain complementary characterization of the oxidized layer. DRIFTS analyses were performed on the three studied minerals (skutterudite, gersdorffite, and nickeline) following fresh grinding and after aging for 1 h, 4 h, 6 h, 12 h, 48 h, 7 d, 1 month, and 2 months (Figure 4.4). The objective was to highlight the state of the surface oxidation after different intervals of time and therefore characterize the altered surface species formed at ambient temperature.

The DRIFT spectra of the skutterudite after grinding and aging (Figure 4.4.A) showed the apparition of bands at 649 cm^{-1} and 750 cm^{-1}, which are characteristic of the Co-O stretching vibrations and antisymmetric elongation vibrations of the arsenite, respectively (Zhang et al., 2012). Furthermore, arsenic oxide peaks at 970 cm^{-1}, 910 cm^{-1}, and 835 cm^{-1} assigned to the stretching vibration of the As-O bond (arsenate groups) (Monte et al., 2002; Nesbitt et al., 2003) appeared clearly after 12 h of aging. This confirms the formation of CoO and AsO bonds on the surface of the mineral, which continued to grow as oxidation time increased. These peaks increased in intensity as the aging time increased (Figure 4.4.A). The predominance (high peaks) of arsenic oxides may indicate that aging increased the arsenic oxidation rate (Jackson et al., 2003; Nesbitt et al., 1995). Indeed, the study conducted by Nesbitt et al. (2003) on an arsenic mineral surface using synchrotron radiation X-ray photoelectron spectroscopy (SRXPS) supported these findings. The authors found that the formation of arsenite increased to a maximum after about 30 min exposure and diminished with increased exposure to the air. In the current study, these species diminished in abundance (low intensities of characteristic peaks) after 48 h of aging as the intensity of the arsenate peaks increased (Figure 4.4.A). The characteristic peaks for the arsenate group were unchanged after 1 h, 4 h, 6 h 12 h, and 24 h of exposure to the atmosphere, but increased appreciably after 48 h (Figure 4.4.A). Indeed, successively longer

exposure resulted in an increase in arsenate, which confirms the result from the skutterudite and gersdorffite conditioning demonstrating the oxidation of arsenic into arsenite and then into arsenate. This altered species is the thermodynamically stable form under ambient conditions and is the penultimate oxidation product of arsenic (Nesbitt et al., 2003).

The growth of the peak at 1,600 cm^{-1}, which is characterestic of the O-H band vibration, confirms the formation of cobalt hydroxides (Table 4.3) along with adsorbed water on the surface. The adsorbed water reached a maximum after 7 d, then decreased. This could be explained by the increase in humidity of the room. The peaks at 1,185 cm^{-1} and 1,260 cm^{-1} are typically attributed to the stretching vibration of the C-O band (Jung et al., 1996), which indicates the adsorption of CO_2 on the surface.

The DRIFT spectra from 1,800 to 600 cm^{-1} for the gersdorffite after grinding and aging is illustrated in Figure 4.4.B, highlighting the main altered surface species produced. After four hours of reaction with air, the gersdorffite spectrum (Figure 4.4.B) showed the formation of a peak at 720 cm^{-1} corresponding to the antisymmetric elongation vibrations of the arsenite (Table 4.3). The major peaks observed are related to arsenic oxides and nickel sulphates. With aging time (exposure to open air), there was a noticeable increase in the peak intensities for arsenic oxides (960 cm^{-1}, 880 cm^{-1}, and 835 cm^{-1}) and Ni-sulphates (1,100 cm-1). The peak at 1,600 cm^{-1} is related to the stretching vibration of O-H bonds; it is largely associated with adsorbed water. This peak decreased in intensity after 30 d of aging, which could be due to the changed room humidity. The 1,200 cm^{-1} peak is assigned to the stretching vibration of the C-O band in CO_2 (Table 4.3). On the other hand, the peak at 1,100 cm^{-1} is assigned to S-O vibrations in the sulphite ion (SO_4^{2-}) (Table 4.3). The peak at 750 cm^{-1}, typically attributed to arsenite group vibration, appeared after only 4 h and remained with a low peak intensity as the exposure times increased; this indicates the continuous oxidation reaction of arsenic to arsenite. Furthermore, the arsenic oxide peaks at 960 cm^{-1}, 880

cm^{-1}, and 835 cm^{-1} assigned to the stretching vibration of the As–O bond (arsenate group) (Table 4.3) and the nickel sulphate peak at 1,110 cm^{-1} (Figure 4.4.B) became more apparent with aging after one month of exposure. After four hours of exposure to air, As^{3+} (arsenite) appeared in the spectrum, followed by arsenate (As^{5+}), indicating progressive oxidation of arsenic. These results support the results of the DRIFT spectroscopy measurements and optical microscopy characterization of the evolution of surface species conducted by El-bouazzaoui et al. (2022). This latest study demonstrated that dry grinding and aging of gersdorffite generates a thin and heterogeneous layer coating mainly composed of arsenic oxides (arsenite and arsenate) and nickel sulphates ($NiSO_4$).

Arsenic is progressively oxidized in a stepwise fashion at the gersdorffite surface by reacting with oxygen, as observed and demonstrated by Nesbitt et al. (2003) for gersdorffite (NiAsS) and by Schaufuss et al. (2000), Nesbitt and Muir, (1998), and Derycke, (2012) for arsenopyrite (FeAsS). Indeed, the results of this DRIFTS study of gersdorffite is consistent with those of arsenopyrite with regard to the formation of oxidized species and with those of gersdorffite conducted using synchroton XPS by Jackson et al. (2003).

Figure 4.4.C provides results on the evolution of the nickeline oxidation products after grinding and aging. The peak at 740 cm^{-1} is typically attributed to the arsenite group vibration; it appeared after only 6 h and disappeared after 24 h. The peaks at 963, 890, and 839 cm^{-1} are the vibration frequencies of As-O bonds in the arsenate group that started forming after arsenite disappeared (i.e., after 24 h of aging), which suggests that it is the oxidation product of AsO_3^{3-}. These peaks became stronger after 7 d of air oxidation (aging). The shoulder at 1,190 cm^{-1} is typically attributed to the stretching vibration of the C-O band in the CO_2 group (Jung et al., 1996). The 1,110 cm^{-1} peak, however, is attributed to sulphite ionic group vibrations. The peak at 1,470 cm^{-1} is typically attributed to the OH bond stretching vibration in adsorbed water (Table 4.3).

Aging of nickeline at 2 months showed an increase in the peaks at 3,800 cm^{-1} and 1,600 cm^{-1} that are attributed to the strengthening of the O-H bonds in the $Ni(OH)_2$ group; this confirms the formation of nickel hydroxides on the surface of the mineral (Jackson et al., 2003). The Nesbitt and Reinke (1999) study using XPS supports these findings. Indeed, it showed that the reaction of nickeline with air over 30 h yields a thin (~10 Å) oxidized overlayer containing $Ni(OH)_2$, arsenite, and arsenate. Furthermore, a thicker oxidized overlayer (~120 Å) containing the same secondary products as the air-oxidized surface was produced on the nickeline after 7 d of reaction time with oxygen. Nesbitt and Reinke (1999) study also indicated that arsenic is more reactive than Ni, as it was demonstrated in the case of skutterudite and gersdorffite. Indeed, after achieving a maximum after 24 h of exposure, arsenite declined and arsenate increased. This suggests that arsenate is an oxidation product of arsenite.

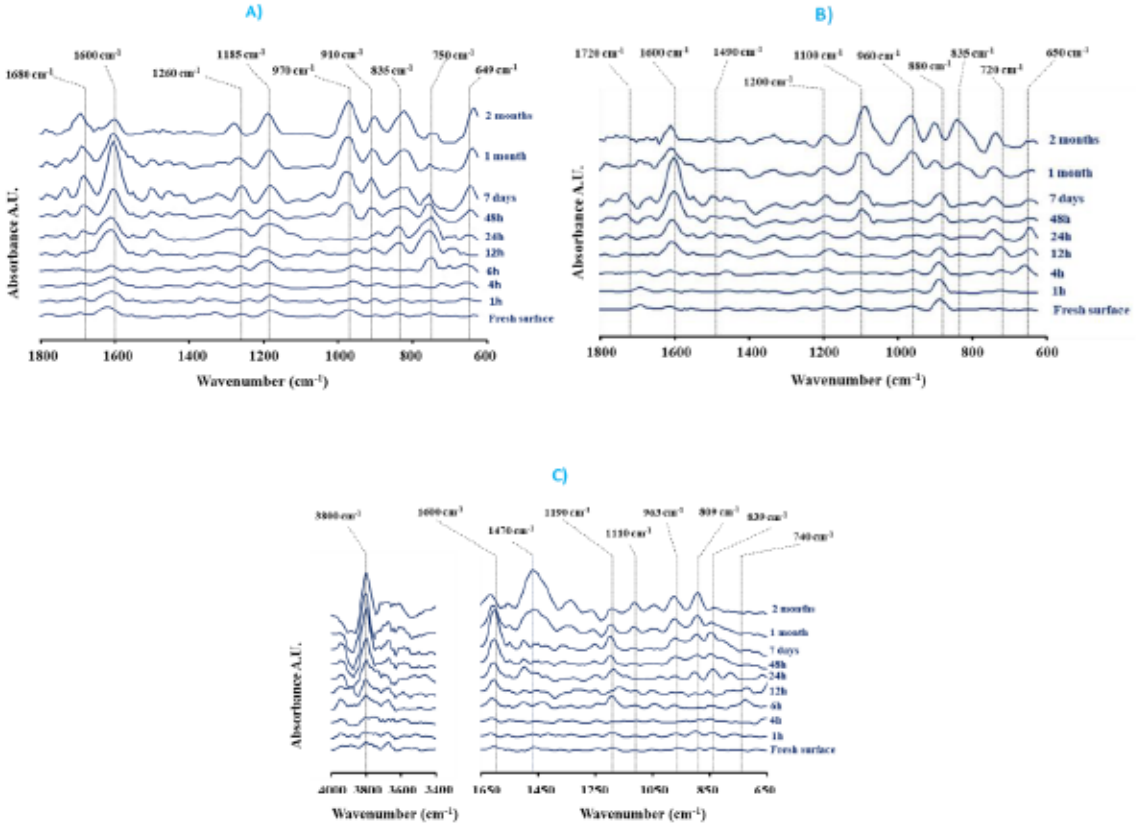

Figure 4.4 Narrow DRIFT aging spectra of arsenides for the 32 to 63 µm fraction at different time intervals: A) skutterudite, B) gersdorffite, and C) nickeline

.

4.4.3 Xanthate Collector Adsorption on the Arsenide Surfaces

4.4.3.1 Absorbance Peaks and Molar Extinction Coefficient Determination

The absorbance peak for the pure xanthate collector is located at 301 nm (Agorhom et al., 2014). This absorbance is proportional to the concentration according to the Beer–Lambert law with a molar extinction coefficient of ε = 17,550 L/mol/cm in ultra-pure water (Kongolo, 1991). Figure 4.5.A shows the absorption curves of the purified xanthate collector at different concentrations in the region between 190–400 nm. These concentrations were specifically chosen to ensure that the detection limit of 3 (absorbance) was not exceeded. Figure 4.5.B shows the absorbance vs concentration curve at the 301 nm wavelength. The results were similar to those obtained from previous works (Kongolo, 1991; Kongolo et al., 2004).

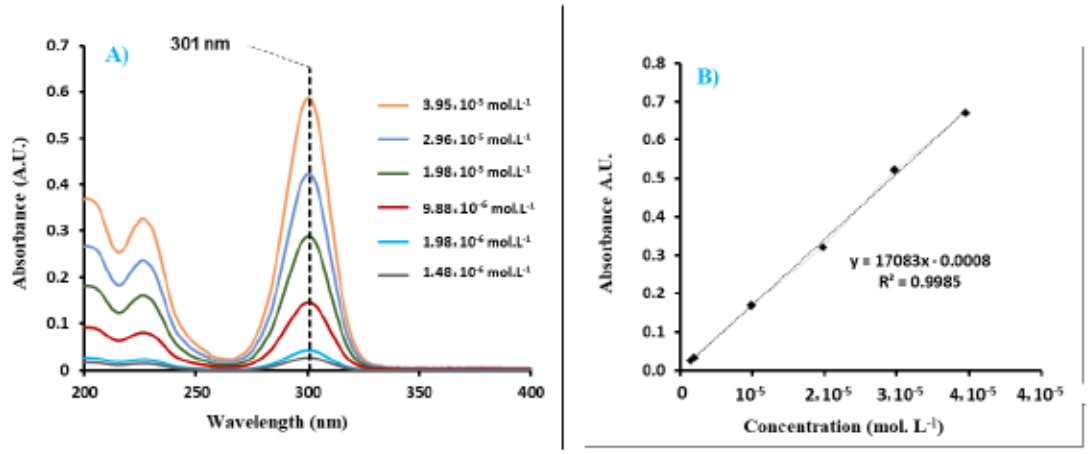

Figure 4.5 Absorbance of xanthate collector in UV–Vis A) as a function of wavelength (λ) and B) as a function of collector concentration (mol. L^{-1}) at 301 nm.

The obtained coefficient of molecular extinction ε_{exp} = 17,083 $L.mol^{-1}.cm^{-1}$ was close to the theoretical one for pure xanthate (ε_{thr} = 17,550 L/mol/cm), and the collector was 97.62% pure.

4.4.3.2 Adsorption Isotherms

Under natural pH conditions, the skutterudite showed a xanthate adsorption isotherm with a plateau (no more xanthate adsorption with increasing amount of xanthate) at a statistical coverage of 25, which corresponds to a total amount of 1.4×10^{-4} mol of xanthate per gram of skutterudite. This adsorption isotherm (Figure 4.6.A) showed a correlation coefficient (R^2) of 0.99. At high xanthate concentrations, dixanthogen was the main adsorbed phase on the skutterudite surface (see following sections). This means that at high concentrations (more than 25 equivalent xanthate monolayers) the skutterudite surface did not allow further oxidation of xanthate into dixanthogen. Under alkaline conditions, the amount of adsorbed collector was significantly reduced to 0.5×10^{-4} mol/g, which corresponds to a statistical coverage of about 10. However, the adsorption slightly diminished while using NaOH as a regulating agent as compared to CaO.

Xanthate showed more affinity towards the gersdorffite surface. Indeed, 4.5×10^{-4} mol/g was fully adsorbed before any residual collector concentration was detected when the mineral was conditioned at natural pH. This total adsorption corresponds to a statistical coverage of 85. This adsorption isotherm (Figure 4.6.B) showed a correlation coefficient (R^2) of 0.96. Conditioning at alkaline pH showed approximately the same behavior for both NaOH and CaO conditions. Less of the collector was adsorbed on the gersdorffite surface under alkaline pH (10^{-4} mol/g of xanthate, corresponding to a statistical coverage area of about 65–70) compared to natural conditions. This phenomenon could be explained by the alteration species (oxidized layer) that formed on the gersdorffite surface under these conditions; the presence of arsenic oxides (especially arsenate) and hydroxylated nickel sulphates under alkaline conditions hindered and reduced the xanthate affinity for the gersdorffite superficial surface. This result was supported by the study conducted by El-bouazzaoui et al. (2022), which demonstrated this same effect on the affinity of some dithiophosphates (DTP) and

mercaptobenzothiazole (MBT) based collectors as alternative sulphide collectors to xanthates for gersdorffite.

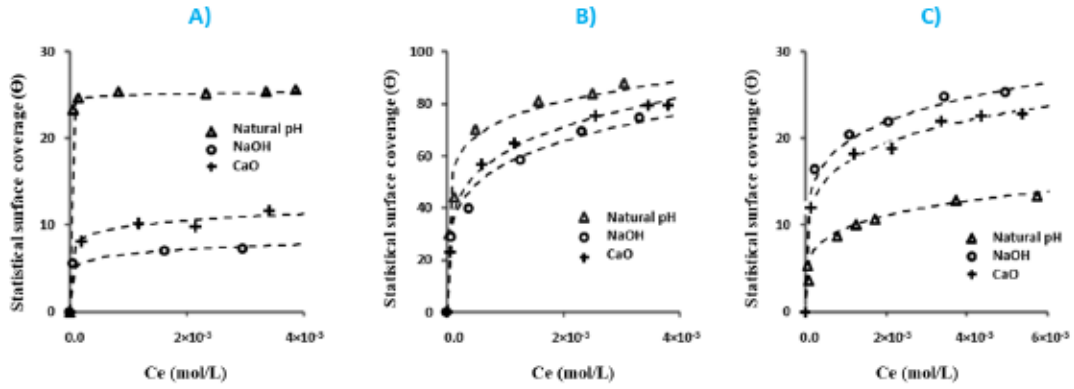

Figure 4.6 Xanthate adsorption isotherms on surfaces of A) skutterudite, B) gersdorffite, C) nickeline (under different pH value using NaOH and CaO regulator), and the corresponding Langmuir-Freundlich model fit.

The effect of pH was less significant in the case of nickeline, where about 0.5×10^{-4} mol/g was adsorbed under alkaline conditions, versus 0.35×10^{-4} mol/g under natural conditions; this corresponds to a statistical coverage of about 25 under alkaline conditions and about 10 under natural conditions (Figure 4.6.**C**). The activation effect was also studied under the same experimental conditions (under natural and alkaline conditions). However, only NaOH was tested as a regulating agent due the similarities between the effects of NaOH and CaO. The results are presented in Fig. 4.7. Activation with copper sulphate significantly affected the adsorption of xanthate on the skutterudite and nickeline surfaces (Fig. 4.7.E-F). Indeed, skutterudite surface activation enhanced the xanthate adsorption from 1.5×10^{-4} mol/g to 3.5×10^{-4} mol/g under natural conditions, and from 0.5×10^{-4} mol/g to 2.6×10^{-4} mol/g under alkaline conditions. Similarly, nickeline surface activation enhanced the xanthate adsorption under both natural and alkaline conditions from approximately 0.5×10^{-4} mol/g (maximum statistical coverage area of about 25) to 2×10^{-4} mol/g (statistical coverage

area of about 90) (Fig. 4.7.F). However, adding the activator slightly negatively affected the adsorption of xanthate on the gersdorffite surface under natural conditions, where it decreased from 4.5×10^{-4} mol/g to approximately 3.8×10^{-4} mol/g; this corresponds to a surface coverage of about 85 and 75, respectively (Fig. 4.7.E). On the other hand, the gersdorffite activation under alkaline conditions enhanced the xanthate adsorption from 10^{-4} mol/g ($\Theta = 70$) to approximately 3.5×10^{-3} mol/g ($\Theta = 90$) (Fig. 4.7.E).

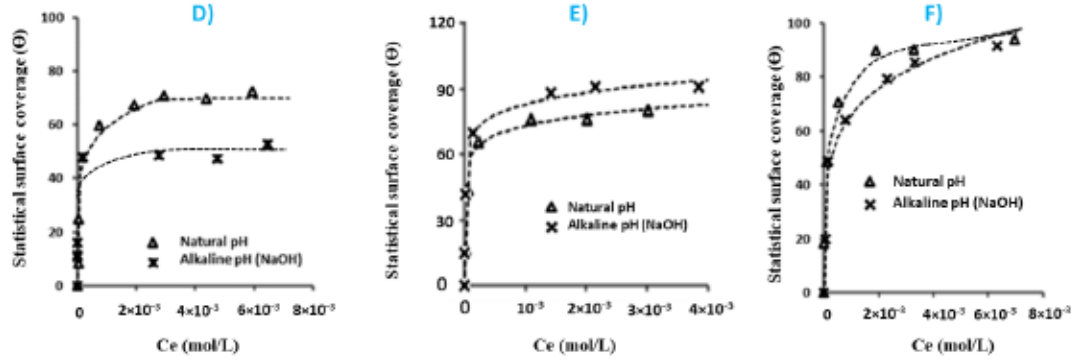

Fig. 4.7 Adsorption isotherms for the xanthate collector on different mineral surfaces after activation with $CuSO_4$ and under natural and alkaline conditions: D) skutterudite, E) gersdorffite, and F) nickeline.

4.4.3.3 Xanthate Collector Adsorption: Nature of the Adsorbed Layers

DRIFT spectroscopy analysis was used to characterize the superficial mineral species following xanthate adsorption on the 32–63 µm fraction for each arsenide. The adsorption was conducted using the optimal conditions determined from the adsorption isotherm study, i.e., the optimal dosage to reach a maximum saturation plateau at which no additional collector could adsorb (d1), along with an optimal pH and optimal activator ($CuSO_4$) dosage. A second slightly higher dosage (d2) was also tested to ensure the availability of the collector for adsorption in each case. These conditions are presented in Table 4.4. The use of the optimal PAX dosage was closely linked to the

fact that high collector concentrations are not very efficient for mineral flotation as only a monolayer of xanthate is sufficient (Mermillod-Blondin et al., 2005a). The remaining xanthate will oxidize to dixanthogen at the mineral surface (Derycke et al., 2013).

Table 4.4 Optimum adsorption conditions determined from the adsorption isotherm spectra for the 32–63 µm size fraction for each mineral using PAX as a collector, NaOH as a pH modifier, and $CuSO_4$ as an activator.

Mineral type	PAX dosage (mol/L)		pH	Activation
	dosage 1	dosage 2		
Skutterudite	7.4×10^{-3}	8×10^{-3}	Natural	Yes
Gersdorffite	4.9×10^{-3}	6×10^{-3}	Natural	No
Nickeline	3.7×10^{-3}	5×10^{-3}	Natural	Yes

The DRIFT spectra for PAX adsorption onto arsenide surfaces under optimal conditions are presented in Figure 4.8 The spectra are enlarged to reveal the details of the characteristic peaks of xanthate in the range of 600 cm^{-1} to 3,100 cm^{-1}.

Spectra show a major peak at 2,960 cm^{-1} assigned to the xanthate alkyl chain (Kongolo et al., 2004). This peak first appeared at the previously determined surface coverage (adsorption isotherms) and increased progressively with increasing surface coverage. The peak situated at 1,050 cm^{-1} is assigned to asymmetric stretching of xanthate (Cases and De Donato, 1991) and the dixanthogen C-S group, and the peak at 1,270 cm^{-1} is assigned to asymmetric stretching of the dixanthogen C-O-C group (Cases et al., 1989; Derycke et al., 2013). These two peaks started growing after the addition of sufficient amounts of the collector (increased surface coverage). The presence of the shoulder at 1,050 cm^{-1} in the case of the three studied minerals demonstrated that amyl xanthate was effectively adsorbed on the mineral surface.

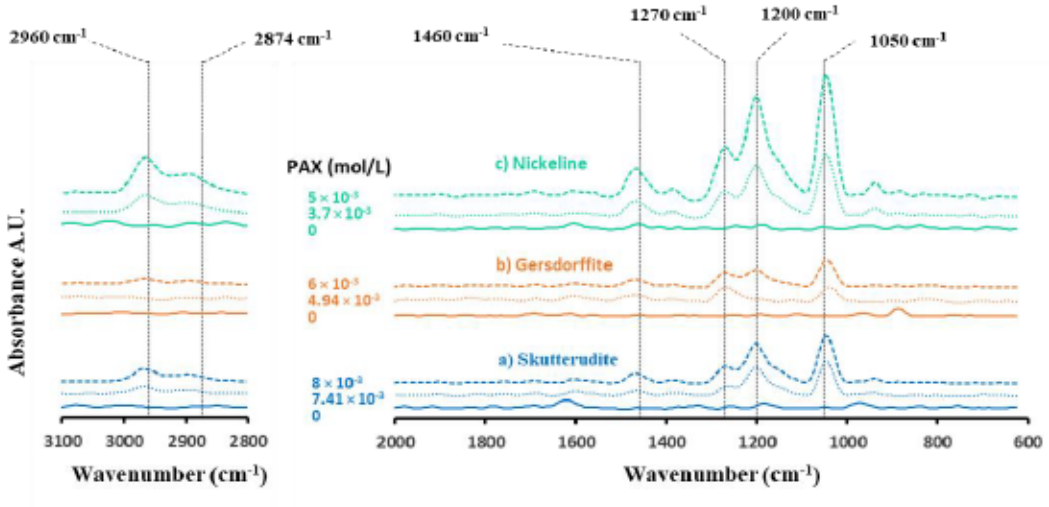

Figure 4.8 Diffuse infrared spectra from 2,000 to 600 cm^{-1} and 3,100 to 2,800 cm^{-1} for the studied arsenides under optimal adsorption conditions and with various xanthate concentrations: a) skutterudite, b) gersdorffite, and c) nickeline.

The peak at 1,200 cm^{-1}, characteristic of the nickel-, cobalt-, or arsenic-xanthate complex, grew with increasing collector dosage in the case of nickeline and skutterudite (Cases et al., 1995; Valli et al., 1994). This reveals that the formation of these metal/metalloid-xanthate complexes at the nickeline and skutterudite surface occurred through reduction of nickel/cobalt and arsenic ions, as observed on pyrite and arsenopyrite with iron oxides (Cases et al., 1989; Derycke, 2012). However, gersdorffite did not show significant growth in the 1,200 cm^{-1} peak characteristic of xanthate complexes and showed increased growth of the 1,270 cm^{-1} and 1,050 cm^{-1} peaks characteristics of dixanthogen. This suggests that nickel- or arsenic-xanthate complexes may present as a quasi-monolayer but are masked in the spectra by the overlying dixanthogen formation due to the high surface coverage (Section 4.4.3.2). Increasing the initial concentration of xanthate increased the quantity of hydrocarbon chains (xanthate alkyl chain) and dixanthogen on the surface, as demonstrated by an increase in the intensities of the peaks at 2,960 cm^{-1}, 1,270 cm^{-1}, and 1,050 cm^{-1} in each mineral spectra, especially for skutterudite and nickeline (Figure 4.8). Likewise,

the other peaks characteristic of the observed oxidation products (e.g., Ni sulphate and hydroxides) were absent in the spectra after xanthate adsorption on the arsenide surfaces. This may be due to high coverage of the surface with xanthate complexes and dixanthogen, masking any signals from oxidation products. Indeed, the flotation of skutterudite, gersdorffite, and nickeline could be effective with a statistical monolayer of xanthate that could be adsorbed as dixanthogen in the case of gersdorffite and as a mixture of dixanthogen and a metal-xanthate complex, especially as an arsenic-xanthate complex, in the case of skutterudite and nickeline.

4.4.4 Zeta Potential (ZP) Analysis

Due to its significant impact/role in mineral separation by flotation, ZP has always been an essential parameter that allows an understanding and the prediction of the physicochemical phenomena occurring at the solid/liquid interface (Derhy et al., 2022). Figure 4.9 shows the ZP of skutterudite, gersdorffite, and nickeline as a function of pH before and after interaction with copper sulphate (10^{-3} mol/L) and potassium amyl xanthate (10^{-4} mol/L). The appearance of the curves for all arsenides was approximately identical before and after adding the PAX; they were, however, shifted in a negative direction throughout the pH range, which indicates the adsorption of the negatively charged xanthate anions onto the surface of the arsenides. These shifts were greater for skutterudite and gersdorffite at pH values greater than 8 and 10, respectively, but less so for nickeline at pH > 9 and for gersdorffite at pH < 7 (Figure 4.9).

Figure 4.9.A-B shows that skutterudite and gersdorffite did not exhibit any isoelectric point (pH value corresponding to a zero ZP). However, nickeline had an isoelectric point of about pH 3 (Figure 4.9.C). At pH > 3, the surface zeta potential of nickeline was negative, while at pH < 3 it was positive. When the PAX was added and compared to the arsenide curves (initial state), the ZP shifted to slightly negative values throughout the tested pH range, indicating the presence of xanthate anions (X^-) on the

mineral surfaces. However, these curves in the presence of PAX tended to join the curve in its absence, especially at pH values greater than 9 for nickeline, implying that the PAX did not effectively adsorb on the studied arsenide surfaces (Figure 4.9). As previously indicated (Section 4.4.2.1), these arsenides were extremely susceptible to oxidation. DRIFTS results showed that a surface coating containing arsenite/arsenate and nickel hydroxide was formed on the oxidized arsenides when conditioning under both natural and alkaline conditions. Furthermore, the conditioning of skutterudite and nickeline, especially under alkaline conditions, promoted the oxidation effect on the mineral surface. These oxidation products (arsenite/arsenate and nickel hydroxide coating) could hinder the adsorption of xanthate onto the mineral surface, decreasing the floatability (xanthate adsorption). These results suggest that the oxidation products interfered with PAX adsorption and thereby require an excessive dosage of PAX to render the arsenide surfaces more hydrophobic. Indeed, Nakazawa and Iwasaki (1986) reported that during aeration for flotation, oxidation products (e.g., $Ni(OH)_2$ and As_2O_3) were formed on the surface of nickel arsenide and inhibited the flotation (depression effect). In fact, the arsenide floatability could be improved so long as the surface was unoxidized (Nakazawa and Iwasaki, 1986).

The ZP analysis also demonstrated that copper activation improved the floatability (adsorption capacity) of the studied arsenides, especially under alkaline conditions. After adding copper sulphate and xanthate, the ZP shifted more negatively for skutterudite and gersdorffite at pH > 7 and for nickeline at pH > 6, modifying the surface properties of the minerals. This ZP on the arsenide surface decreased significantly with increasing pH (under alkaline conditions), and the absolute value of the ZP gradually increased. This indicates the presence of a negatively charged species on the copper activated mineral surface. These results suggest that copper sulphate activation was effective on arsenides and was shown to improve the adsorption of xanthate on oxidized arsenide surfaces, especially under alkaline conditions.

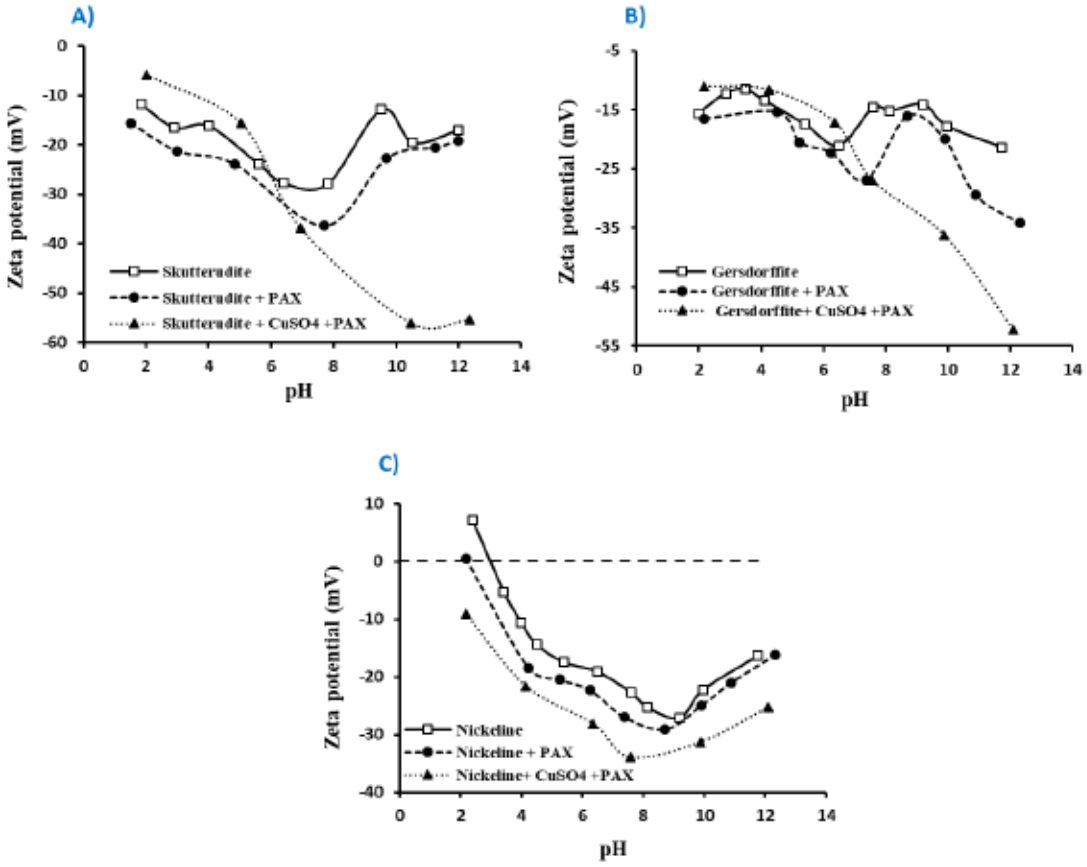

Figure 4.9 Zeta potential of A) skutterudite, B) gersdorffite, and C) nickeline as a function of pH in the presence/absence of the activator (10^{-3} mol/L $CuSO_4$) and collector (10^{-4} mol/L PAX).

It has been reported that copper sulphate activation was effective on cobalt arsenide and arsenopyrite (Abeidu and Almahdy, 1980). Indeed, Nakazawa and Iwasaki (1986) pointed out the ability of Cu(I) and Cu(II) to precipitate As(III) in the form of copper arsenide. Furthermore, XPS surface analysis of activated nickel arsenide (as oxidation product) showed that cuprous arsenide, arsenite, and arsenate might be present on the surface (Nakazawa and Iwasaki, 1986). Since xanthate will adsorb on cuprous arsenide, surface activation might improve the floatability of the studied arsenides. For pH < 7, the ZP shifts were smaller in magnitude than those at pH > 7, regardless the arsenide

surface activation. This result confirms that copper activation was not successful under acidic conditions regarding adsorption of PAX, which may be attributed to the thermodynamic considerations (oxidation and reduction state of copper). Derycke (2012) and Leppinen (1990) also demonstrated that copper activation led to lower xanthate adsorption on arsenopyrite under acidic conditions.

4.5 Conclusion

This work provides results on the evolution of skutterudite, gersdorffite, and nickeline oxidation products through grinding, air oxidation (aging), conditioning, and collector (PAX) adsorption. The characterization of these arsenide surfaces allowed the following conclusions to be drawn:

- dry-ground arsenides produced a variety of alteration products on the mineral surface that had a wide range of oxidation degrees. For all tested arsenides, the surface mineral lattice and alteration layer were enriched in arsenic phases, especially in the form of arsenite (As(III)), arsenate (As(V)), and arsenic and nickel/cobalt sulphates and hydroxides;
- conditioning skutterudite and nickeline under alkaline conditions enhanced the oxidation effect on the mineral surfaces. The gersdorffite surface showed oxidation products in the form of arsenate, and changing pH value and/or pH regulator type did not have any significant effect;
- conditioning gersdorffite (either under natural or alkaline conditions) caused the formation of more superficial oxide layers (oxidized species) compared to freshly ground gersdorffite;
- the aging study identified the formation of cobalt hydroxides on the surface of skutterudite. Arsenite, on the other hand, appeared after 12 h and disappeared

after 48 h, whereupon arsenate started forming, which suggests that arsenate is the oxidation product of arsenite;

- aging of gersdorffite generated a thin and heterogeneous layer coating mainly composed of arsenic oxides (arsenite and arsenate) and nickel sulphates (only after 4 h);
- nickeline showed a similar behavior, but with even higher oxidation rates compared to the skutterudite, where after only 6 h the surface showed the signature of arsenite, followed by arsenate. Nickel hydroxides were also observed on the nickeline surface;
- nickel-, cobalt-, and arsenic-xanthate complexes were detected after conditioning nickeline and skutterudite with xanthate under natural pH conditions. Increasing the initial concentration of xanthate increased the quantity of hydrocarbon chains and dixanthogen on the surface. Gersdorffite, however, showed only the formation of dixanthogen;
- nickel- or arsenic-xanthate complexes may have been present as a quasi-monolayer on the gersdorffite surface but were masked in the DRIFTS spectra by the overlying dixanthogen formation due to the high surface coverage;
- activation with copper sulphate improved the adsorption of xanthate onto the mineral surfaces, except for gersdorffite where it relatively hindered the adsorption at natural pH; and
- ZP measurements demonstrated that copper sulphate activation was effective on arsenides and was shown to improve the adsorption of xanthate on the oxidized arsenide surfaces (including gersdorffite), especially under alkaline conditions.

Some valuable original data were determined in this study, including the ZP of the arsenide surfaces with or without flotation reagents (copper sulphate as activator and amyl xanthate as collector). These data can provide a reference for future studies.

CRediT authorship contribution statement

Ait-khouia Yassine: Conceptualization, Formal analysis, Investigation, Methodology, Writing - original draft, Writing – review and editing. **Abdelilah Elbouazzaoui**: Investigation, Writing - original draft, Writing – review and editing. **Yassine TAHA**: Investigation, Writing - original draft, Writing – review and editing. **Isabelle Demers**: Supervision, Writing - review & editing. Funding acquisition. **Benzaazoua Mostafa**: Conceptualization, Methodology, Supervision, Validation, Writing – original draft, Writing – review & editing,

Declaration of competing Interest

The authors declare that they have no known competing financial interests or personal relationships that could have appeared to influence the work reported in this paper.

Acknowledgements

The authors would like to acknowledge the project funded by Collaborative Research and Development granted to I. Demers by NSERC and industrial partners. The authors thank URSTM staff for their support with materials testing and analyses. Finally, many thanks must go to the XPS laboratory in Sudbury (Canada) for their help in achieving QEMSCAN and EPMA analysis.

CHAPITRE 5

FEASIBILITY OF REPROCESSING GOLD TAILINGS: INTEGRATED MANAGEMENT APPROACH FOR THE CONTROL OF CONTAMINATED NEUTRAL MINE DRAINAGE

Préambule : Cet article a été publié dans la revue Minerals Engineering. Volume 187, septembre 2022, 107821. https://doi.org/10.1016/j.mineng.2022.107821

Ait khouia Yassine [a], Benzaazoua Mostafa [a, b, *], Elghali Abdellatif [c], Chopard Aurélie [d], Demers Isabelle [a]

[a] Research Institute on Mines and Environment, University of Quebec in Abitibi Témiscamingue, 445, boul. de l'université, Rouyn-Noranda J9X 5E4, Quebec, Canada

[b] Mining environment and circular economy, Mohammed VI Polytechnic University, Lot 660. Hay Moulay Rachid, 43150, Ben Guerir, Morocco

[c] Geology and sustainable mining department, Mohammed VI Polytechnic University, Lot 660, Hay Moulay Rachid, Ben Guerir 43150, Morocco

[d] Agnico Eagle Mines Ltd, 10 200 route de Preissac, Rouyn-Noranda, QC J0Y 1C0, Canada

Corresponding author. E-mail address: mostafa.benzaazoua@uqat.ca

5.1 Abstract

Sulfide ore processing generates finely ground mine tailings that often contain sulfide minerals such as pyrite, pyrrhotite, arsenopyrite, and gersdorffite. These minerals can generate acid mine drainage or contaminated neutral drainage (CND) due to weathering (aqueous oxidation by oxygen, and bacterial activity). Contaminated neutral mine

drainage affects the surrounding environment by contaminant release (e.g., As, Ni, Fe, Cu, and Zn), which is one of the most challenging environmental issues for the mining industry. This paper examines the feasibility of desulfurization by flotation at the laboratory scale as a sustainable tailings management approach to prevent CND generation from tailings produced by the Amaruq mine (Nunavut, Canada). The flotation tests were conducted using a five-level statistical experimental design (DOE) using five parameters that include: collector dosage (PAX), activator dosage ($CuSO_4$), frother dosage (MIBC), pH, and solid content (Cs). The response surface methodology (RSM) was used to predict sulfur recovery and to choose the optimal conditions of flotation. The mineralogical properties of the samples before and after reprocessing were investigated by combining optical microscopy, X-ray diffraction spectroscopy (XRD), and the quantitative evaluation of materials by scanning electron microscopy (QEMSCAN®). The trace element (As, Co, Ni, etc.) microanalysis of the identified minerals was quantified using electron probe micro-analyser (EPMA), and the bulk chemical composition was analyzed using induction furnace, X-ray fluorescence, and ICP-AES/MS. Finally, the geochemical behavior of the initial (WTT) and desulfurized (DWT) tailings was evaluated using kinetic weathering cells. The main results demonstrated that sulfur recovery can reach up to 97% using the following optimal conditions: pH of 11.5, PAX dosage of 158 g/t, $CuSO_4$ dosage of 300 g/t, MIBC dosage of 55 g/t, and Cs of 29.3%. Moreover, the residual sulfides within the desulfurized tailings were completely locked within the non-sulfide gangue minerals as analyzed by QEMSCAN® and optical microscopy. Kinetic testing was performed on WTT and DWT to assess their contaminant release rates (especially As, Ni, Cu, Fe, and Zn). The desulfurized material is unlikely to cause significant risk of contaminated mine drainage generation. All released contaminants were below the limits of Quebec provincial legislation under laboratory conditions.

Keywords: Contaminated mine drainage, Environmental desulfurization, Froth flotation, Sulfides and Sulfosalts, statistical experimental design, Integrated waste management, geochemical behavior.

Résumé

Le traitement du minerai sulfuré génère des résidus miniers finement broyés qui contiennent le plus souvent des minéraux sulfurés tels que la pyrite, la pyrrhotite, l'arsénopyrite et la gersdorffite. Ces minéraux peuvent générer un drainage minier acide ou un drainage neutre contaminé (CND) quand soumis aux conditions atmosphériques (oxydation aqueuse par l'oxygène et activité bactérienne). Le drainage neutre contaminé affecte le milieu environnant par la libération de contaminants (par exemple, As, Ni, Fe, Cu et Zn), qui est l'un des problèmes environnementaux les plus difficiles pour l'industrie minière. Cet article examine la faisabilité de la désulfuration par flottation à l'échelle du laboratoire comme approche de gestion durable des résidus pour prévenir la génération de CND à partir des résidus produits par la mine Amaruq (Nunavut, Canada). Les tests de flottation ont été effectués à l'aide d'une conception expérimentale statistique (DOE) à cinq niveaux utilisant cinq paramètres, notamment : le dosage du collecteur (PAX), le dosage de l'activant ($CuSO_4$), le dosage du moussant (MIBC), le pH et la concentration solide (C_s). La méthodologie de surface de réponse (RSM) a été utilisée pour prédire la récupération en soufre et pour choisir les conditions optimales de flottation. Les propriétés minéralogiques des échantillons avant et après retraitement ont été étudiées en combinant la microscopie optique, la diffraction des rayons X (DRX) et l'évaluation quantitative des matériaux par microscopie électronique à balayage (QEMSCAN®). La microanalyse des éléments traces (As, Co, Ni, etc.) des minéraux identifiés a été quantifiée à l'aide d'un micro-analyseur à sonde électronique (EPMA) et la composition chimique globale a été analysée à l'aide d'un four à induction, d'une fluorescence X et d'un ICP-AES /MS. Enfin, le comportement géochimique des résidus initiaux (WTT) et désulfurés (DWT) a été évalué à l'aide des

mini-cellules d'altération. Les principaux résultats ont démontré que la récupération en soufre peut atteindre jusqu'à 97 % en utilisant les conditions optimales suivantes : pH de 11,5, dosage de PAX de 158 g/t, dosage de $CuSO_4$ de 300 g/t, dosage de MIBC de 55 g/t, et C_s de 29,3 %. De plus, les sulfures résiduels dans les résidus désulfurés étaient complètement enfermés dans les minéraux de gangue non sulfurés, tels qu'analysés par QEMSCAN® et la microscopie optique. Des tests cinétiques ont été effectués sur WTT et DWT pour évaluer leurs taux de lixiviation de contaminants (en particulier As, Ni, Cu, Fe et Zn). Il est un peu probable que le matériau désulfuré entraîne un risque significatif de génération de drainage minier contaminé. Les concentrations de tous les contaminants lixiviés (dans des conditions de laboratoire) étaient inférieures aux limites dictées par la législation provinciale du Québec.

Mots-clés : drainage minier contaminé, désulfuration environnementale, flottation, sulfures et sulfosels, conception expérimentale statistique, gestion intégrée des rejets miniers, comportement géochimique.

5.2 Introduction

Throughout the world, mining activities extract both base and precious metals from sulfide ores and provide high economic benefits for many countries. However, with the recent exploitation of high-tonnage/low-grade ores, the mining process gives rise to substantial tonnages of finely ground tailings, which are conventionally disposed of in saturated surface impoundments (Elghali et al., 2019a). Depending on the geological context of the orebody, the tailings frequently contain a non-negligible content of residual sulfides (e.g., pyrite, pyrrhotite, and arsenopyrite) and/or sulfosalts (e.g., gersdorffite, cobaltite) considered as gangue during mineral processing. Exposure of sulfides and sulfosalts to atmospheric conditions (water, oxygen) accelerates their oxidation, which represents a source of contamination for the surrounding environment (Benzaazoua et al., 2008; Brown Jr and Calas, 2011; Chopard et al., 2017). Sulfide and

sulfosalt oxidation can result in either: i) acid mine drainage (AMD), if the neutralization potential is insufficient to buffer the produced acid (Amar et al., 2020a; Elghali et al., 2019a; Elghali et al., 2019c); or ii) contaminated neutral drainage (CND), where the leachates are characterized by neutral pH values and significant amounts of contaminants such as heavy metals, metalloids (e.g., Fe, As, Ni, Sb, Cu, Pb, Zn), and sulfates (Amos et al., 2015; Benzaazoua et al., 2004; Blowes et al., 2014; Dold, 2017; Elghali et al., 2019b; Nordstrom, 2000). Contrary to AMD, CND occurs when neutralizing minerals are present in sufficient amounts to counterbalance the acidity produced by sulfide/sulfosalt oxidation. However, the chemical quality of this type of effluent does not meet the existing environmental criteria even at neutral pH: concentrations of metals and metalloids are above the environmental regulation criteria (Ait-Khouia et al., 2021; Heikkinen et al., 2009; Nordstrom et al., 2015; Plante et al., 2011). The formation of AMD and/or CND presents a serious environmental issue for the mining industry (Ait-Khouia et al., 2021; Benzaazoua et al., 2004; Broadhurst et al., 2015; Elghali et al., 2019a; Lemos et al., 2021; Nordstrom, 2000; Plante et al., 2010; Simate and Ndlovu, 2014). Furthermore, the recent increasing legislative and social awareness has prompted a growing trend towards the development of several strategies to prevent and contaminated mine drainage (AMD/CND). Consequently, numerous strategies have been developed to manage the contaminated tailings by acting on one or more of the components of sulfide/sulfosalt oxidation. These strategies include: water exclusion (Williams et al., 2006; Zhan et al., 2006), oxygen exclusion (Demers et al., 2008; Lessard et al., 2018), sulfide/sulfosalt removal through environmental desulfurization (Benzaazoua et al., 2000; Benzaazoua and Kongolo, 2003; Bois et al., 2005; Broadhurst and Harrison, 2015), and acidity buffering through alkaline and cementitious amendments (Duchesne and Laforest, 2006; Elghali et al., 2021b; Elghali et al., 2019b).

Environmental desulfurization has gained much popularity in the last two decades to sustainably manage contaminated mine tailings (Benzaazoua et al., 2017; Broadhurst

and Harrison, 2015; Kongolo et al., 2004; Nadeif et al., 2019; Rezvanipour et al., 2018). Environmental desulfurization consists of sulfide/sulfosalt removal from the tailings, which decreases the acid generation potential of the mine tailings. This technique produces a sulfide/sulfosalt concentrate, which can be reintroduced into the processing plant for metal recovery or be stored underground as a cemented paste backfill (Benzaazoua et al., 2008; Benzaazoua et al., 1999), and non-problematic tailings, which can be safely disposed of in surface storage facilities (Ait-Khouia et al., 2021; Broadhurst and Harrison, 2015). Flotation is the most widely used mineral processing technique in this field (Broadhurst and Harrison, 2015; Lamia, 2017; Nadeif et al., 2019). Previous laboratory- and intermediate-scale studies have shown that froth flotation is a feasible and cost-effective process for removing contaminant-bearing sulfur minerals from mine waste (Amar et al., 2020b; Benzaazoua et al., 2017; Bois et al., 2005; Drif et al., 2018; Noirant et al., 2019). Nonetheless, its effectiveness depends on various physicochemical (e.g., reagent type and concentration, mineral surface state, conditioning pH) and hydrodynamic parameters (e.g., rotation speed, air flow).

In order to accentuate the differences in surface features of sulfur minerals (hydrophobic state) and non-sulfide gangue minerals (NSG), particular reagents (e.g., collectors, frothers, and activators) are added to the slurry prior to the flotation process (Adkins and Pearse, 1992; Uçurum and Bayat, 2007; Wills and Finch, 2016). The reagent types and quantities are the key parameters that greatly influence the separation performance during the flotation process (Drif et al., 2018; Ghodrati et al., 2020; Mehrabani et al., 2010). In this context, the optimization of the process parameters is important to develop a process flowsheet for successful desulfurization of mine tailings to prevent CND generation. An efficient option is to adopt a modeling technique to predict desulfurization performance and to solve for maximum sulfur mineral recovery. A combined approach of an experimental design technique (e.g., central composite design: CCD) and response surface methodology (RSM) was found to be a suitable method to predict flotation performances (Aksoy and Sagol, 2016; Ghodrati et al., 2020;

Mehrabani et al., 2010). RSM is a set of mathematical and statistical techniques that can be used to model and analyze a phenomenon (i.e., flotation performance) in which the response of interest to be optimized (i.e., recovery) is affected by multiple parameters. The CCD approach was broadly used to design an experimental program to determine the significance of operating factors (including their interactions) that affect the flotation performances (response), and to develop mathematical models for the optimization of the process. CCD is one of the most widely used experimental designs in process optimization studies (Ghodrati et al., 2020; Mehrabani et al., 2010). Recently, statistical optimization and modeling techniques (e.g., RSM) have been successfully used for the optimization of flotation reagents to maximize flotation efficiency. For instance, Aslan and Fidan (2008) employed RSM combined with three-level Box–Behnken factorial design for modeling and optimizing physicochemical parameters of lead flotation at the laboratory scale. Asadi et al. (2019) have used RSM based on CCD to optimize various factors for the concentration of silicate-carbonate ore containing malachite at the laboratory scale.

This study investigates the feasibility and optimization of environmental desulfurization by bulk sulfide flotation on the Whale Tail tailings from the Amaruq mine, located in Nunavut, Canada, to prevent CND generation (especially As–Ni-CND). Therefore, this study aims to establish a relationship between flotation parameters (slurry pH, collector dosage, activator dosage, solid concentration, and frother dosage) and the efficiency of desulfurization of the Whale Tail tailings (recovery of sulfur minerals). Laboratory-scale flotation tests were used to determine the conditions (optimum variables) that maximize sulfide minerals removal using RSM along with CCD as a statistical tool. An automated QEMSCAN® mineralogy analysis was used to determine the available reactivity of the initial and desulfurized final tailings. Static and kinetic tests were conducted to evaluate the environmental behavior of the initial Whale Tail tailings and desulfurized tailings and to determine the effectiveness of the desulfurization process. The instantaneous concentrations of

leached contaminants (metals and metalloids: As, Ni, Cu, and Fe) from weathering cells (kinetic testing) were compared to the criteria set by Directive 019.

5.3 Material and Methods

5.3.1 Materials

5.3.1.1 Amaruq Mine and Ore Processing Description

The Amaruq gold deposit, owned by Agnico Eagle Mines Ltd. (AEM), is located approximately 50 km northwest of the Meadowbank gold mine in the Kivalliq District of Nunavut in northern Canada. The main mineralized zones in this deposit are hosted in a volcano-sedimentary sequence made of: i) chert ± graphitic, ii) silicate ± sulfide iron formation, iii) mafic to ultramafic volcanic (komatiite), and iv) greywackes (de Vazelhes et al., 2021). The Amaruq mineral deposit is divided into three significant sectors: Whale Tail, IVR, and Mammoth. In these sectors, three main styles of gold mineralization coexist. The gold is predominantly hosted by: i) silica flooding with disseminated arsenopyrite-pyrrhotite in chert and graphitic chert, ii) pyrrhotite disseminations and quartz veins crosscutting iron formation, and iii) quartz veins crosscutting various type of hosting rocks (De Vazelhes et al., 2021). The tailings used in this study are from the Whale Tail sector.

During production, Amaruq ore is transported using long haul off-road type trucks to the Meadowbank gold processing plant, which is expected to process 9,000 to 10,000 tonnes/day. After two stages of crushing and grinding in the mill circuit (open circuit SAG mill and closed-circuit ball mill with six hydrocyclones), any "free gold" is then removed by a Falcon gravity concentrator. A gravity preconcentration process followed by a regrind mill is added to the already existing circuit to treat the Amaruq ore. The remainder is sent to the gold recovery circuit where it is leached using cyanide, with

the gold captured using carbon-in-pulp (CIP) and electrowinning. Gold-plated cathodes and Falcon concentrate (free gold) are smelted in an induction furnace and poured as "Dore bars" (Figure 5.1). To ensure that no cyanide escapes into the environment, the plant includes both a sulfur dioxide–air cyanide destruction circuit and a cyanide recycling thickener. Tailings (slurry) are placed in the permanent tailings facility and water is pumped back to the plant for reuse (Kojovic et al., 2019).

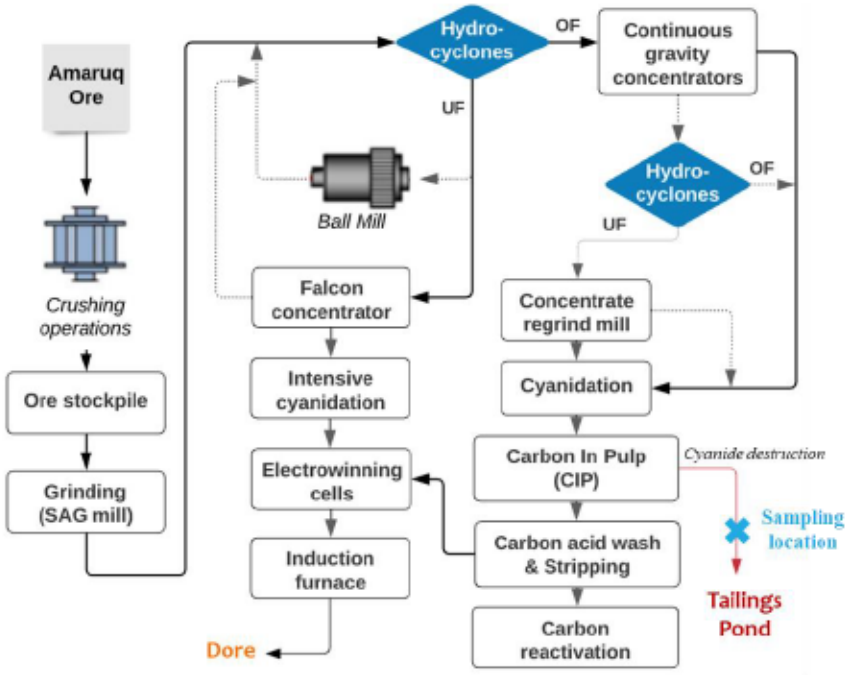

Figure 5.1 Simplified Amaruq processing flowsheet and sampling location.

5.3.1.2 Sampling and Sample Preparation

For the laboratory testing, the Whale Tail tailings (WTT) were sampled from the spigot at the outlet of the processing plant (at Meadowbank) as a slurry with approximately 30% solid content. Figure 5.1 shows the position of the sampling point. The homogeneous sampled tailings were stored in sealed bottles under process water for transportation to the URSTM-IRME UQAT laboratory in Quebec, in order to ensure

minimal contact with air and to preserve as much as possible the physicochemical slurry properties (pH, Eh, etc.).

5.3.1.3 Reagents

Flotation requires various types of reagents to accentuate the differences in surface features of the target minerals (sulfides and sulfosalts, in our case) and gangue. Adding the reagents favours the proper chemical condition for the slurry and then for the collection mechanisms. The type and the quantity of these reagents are the most important parts of the flotation process.

The reagents tested in the flotation experiments in this study and their technical specifications are as follows:

- collector: potassium amyl xanthate (PAX-51 diluted at 10%; technical purity of 86 wt%; molecular weight 202.3 g). All xanthate concentrations presented in this paper were adjusted according to the purity of the real xanthate concentration based on analyses done with UV-visible spectrophotometry (Kongolo et al., 2004);
- frother: methyl isobutyl carbinol (MIBC);
- activator: hydrated copper sulfate ($CuSO_4$) diluted at 10% (technical purity of 98%); and
- pH modifiers: diluted solutions of NaOH and H_2SO_4. They were ACS quality.

5.3.2 Methodology

The methodology followed in this study is highlighted in Figure 5.2.

i) preparation of samples using homogenisation and division;
ii) physical, chemical, and mineralogical characterization of the fresh tailings sample;

iii) environmental desulfurization of tailings by froth flotation using optimal parameters for a maximum sulfur recovery; and

iv) acid and contamination generation potential assessment using acid-base accounting (ABA), net acid generation (NAG) tests, and kinetic tests for the initial tailings and desulfurized material.

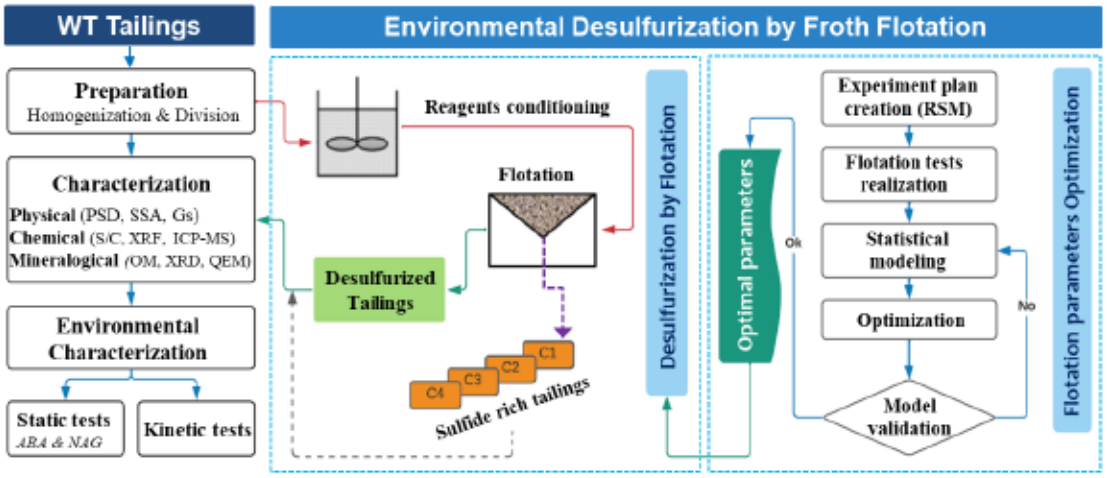

Figure 5.2 Methodology applied in this study.

5.3.3 Methods

5.3.3.1 Physical and Chemical Characterization

Particle size distribution (PSD) of the studied tailings was determined using a laser grain size analyser (Malvern Mastersizer S). The specific gravity (Gs) measurement was performed using a helium gas pycnometer (Micromeritics Accupyc 1330) in the URSTM-IRME UQAT laboratory in Quebec, Canada (Allen, 2013). The specific surface area (SSA) was analyzed with a Micromeritics surface area analyzer implementing the Brunauer–Emmett–Teller (BET) method (Brunauer et al., 1938).

Samples were homogenized and pulverized prior to performing all chemical analyses. The bulk chemical composition was carried out using inductively coupled plasma atomic emission spectroscopy (ICP-AES) after a total acidic digestion using $HNO_3/Br_2/HF/HCl$ (HNO_3 and Br_2 are used to oxidize sulfur, and HCl with HF to dissolve silicates) (Potts, 1987). The ICP-AES analysis was done in the SGS Laboratory in Ontario, Canada. The trace elements were analyzed at Activation Laboratories (Actlabs) in Ancaster, Ontario, Canada using peroxide fusion inductively coupled plasma mass spectrometry/optical emission spectrometry (ICP-MS/OES). Total sulfur (wt% S ± 0.1 to 0.5) and total carbon (wt% TC ± 0.6 to 1.1) contents were analyzed in the URSTM-IRME UQAT laboratory using an induction furnace (ELTRA CS-2000) with a detection limit of 0.09%. Four standards (low carbon (0.5 wt.%), high carbon (11.97 wt.%), low sulfur (0.28 wt%), and high sulfur (18.03 wt%) were used to calibrate the induction furnace. One duplicate was introduced for each 10 analyzed samples.

The chemical composition of the minor and major elements (SiO_2, Al_2O_3, Fe_2O_3, MgO, CaO, Na_2O, K_2O, TiO_2, P_2O_5, MnO, and LOI) was also analyzed by X-ray fluorescence (XRF) (Thermo Scientific NITON 2008 at the SGS Laboratory in Ontario, Canada). The chemical composition of the weathering cell leachates was analyzed by ICP-AES on samples acidified with 2% HNO_3. The pH, redox potential (Eh), and electrical conductivity (EC) of the leachates were analyzed using pH/Eh/conductivity meters.

5.3.3.2 Mineralogical Characterization

The mineralogical composition in terms of crystalline minerals of the initial tailings was determined by X-ray diffraction spectroscopy (XRD) in the URSTM-IRME laboratory. The diffractometer used was an AXS Advance D8 system (Bruker) equipped with a copper anticathode (XRD, Bruker Ltd., Canada), scanning over a diffraction angle (2θ) ranging from 5° to 70°. The DiffracPlus EVA (version 9.0) and

TOPAS (version 2.1) software were used respectively to identify and to quantify the abundance of all identified mineral species implementing Rietveld refinement (Rietveld, 1969; Young, 1993). The absolute precision of this quantification method is about ±0.5 to 1 wt% (Raudsepp and Pani, 2003). The identification of the mineral species and the texture observations were performed in reflected light mode using an AxioImager M2m optical microscope (OM) (Zeiss, Oberkochen, Germany) equipped with the AxioVision software V4.8.

The mineralogical composition and texture of the Whale Tail tailings and desulfurized tailings were characterized using Quantitative Evaluation of Materials by Scanning Electron Microscopy (QEMSCAN®, FEI, Quanta 650 platform with Field Emission Gun) in the XPS laboratory in Sudbury (Ontario, Canada). This instrument is fitted with Bruker SDD energy dispersive spectrometers (EDS). It is an automated mineralogy system that produces particle maps (colour coded by mineral) through the collection of rapidly acquired X-rays. The maps and corresponding data files allow the quantification of modal mineralogy, texture, mineral size, elemental deportment, and liberation (Benzaazoua et al., 2017; Pirrie et al., 2004). Polished sections were analyzed in particle mineralogy analysis (PMA) mode generating full X-ray maps. Measurement resolution ranged between 0.5 µm and 7 µm depending on particle size and mineral texture. Uncertainty for analyses is based on reconciling calculated assays from the mineralogy and the measured elemental assays.

Electron probe micro-analysis (EPMA) was also performed at the XPS laboratory to confirm the mineral identification and to quantify the chemical composition of the minerals of interest (Benzaazoua et al., 2003). In this study, the minerals of interest were pyrite, pyrrhotite, arsenopyrite, gersdorffite, and other NSG minerals. A minimum of six particles were analyzed with a minimum of six counts for each identified mineral using a Cameca SX-100 Electron Probe Micro - Analyzer. This

instrument is coupled with four high resolution wavelength - dispersive X - ray spectrometers (WDS). All quantitative analyses (EPMA) were done using a focused beam with an accelerating voltage of 20 kV and a constant beam current of 20 nA. To better perform quantitative analysis of the materials, a set of calibration standards (e.g., pyrite, InAs, Co, Ni, chalcopyrite, orthoclase, Cr2O3, wollastonite, etc.) was used, allowing accurate microanalysis over a wide range of concentrations.

5.3.3.3 Size-by-Size Analysis

The purpose of the size-by-size analysis was to investigate the sulfur and carbon content and their distribution in different particle size fractions. Therefore, the Whale Tail sample was sieved using a specific combination of ASTM series sieves. The following sieves were used: 125 µm, 80 µm, 63 µm, 45 µm, 32 µm, and 20 µm (ASTM, 2014). The choice of sieves was based on preliminary results of grain size distribution obtained from the Malvern Mastersizer S laser analyzer. After wet sieving, the corresponding size fractions of all batches were first dried for 24 h in an oven at 60 °C, then weighed using a laboratory balance. Finally, each sieved sample was ground (<75 µm) and sent for total sulfur and carbon analysis using an induction furnace (ELTRA CS-2000).

5.3.3.4 Flotation Experimental Design

Slurries were sampled at the mine concentrator at the Meadowbank site in a way that all the initial physicochemical characteristics of the pulp (e.g. residual reagents, pH, Eh) were preserved as much as possible. Figure 5.3 presents the flotation setup used to recover sulfur minerals. All flotation tests were performed in a 1.2 liters Denver D-12 lab sub-aeration flotation machine. The pH was measured and adjusted by adding a diluted NaOH solution for pH increase and diluted H_2SO_4 solution for acidification, depending on the tests. At the end of the 9 min conditioning (2 min for the pH, 3 min

for the activator, 3 min for the collector, and 1 min for the frother), air was fed, and the flotation was conducted for 5 min. The rotor-stator was adjusted to an impeller speed of 1,000 rpm and airflow was set at 3 L/min. To obtain consistent results, the froths were mechanically removed with a spatula by the same operator for all the flotation tests. For each flotation test, five concentrates and the final desulfurized tailings were recovered separately and analyzed for sulfur and carbon grade to study the kinetics and rate of sulfur mineral recovery.

The flotation tests were carried out at different reagent dosages and different pH and solid concentrations according to the experimental design, while the other operational variables such as hydrodynamic parameters were kept constant.

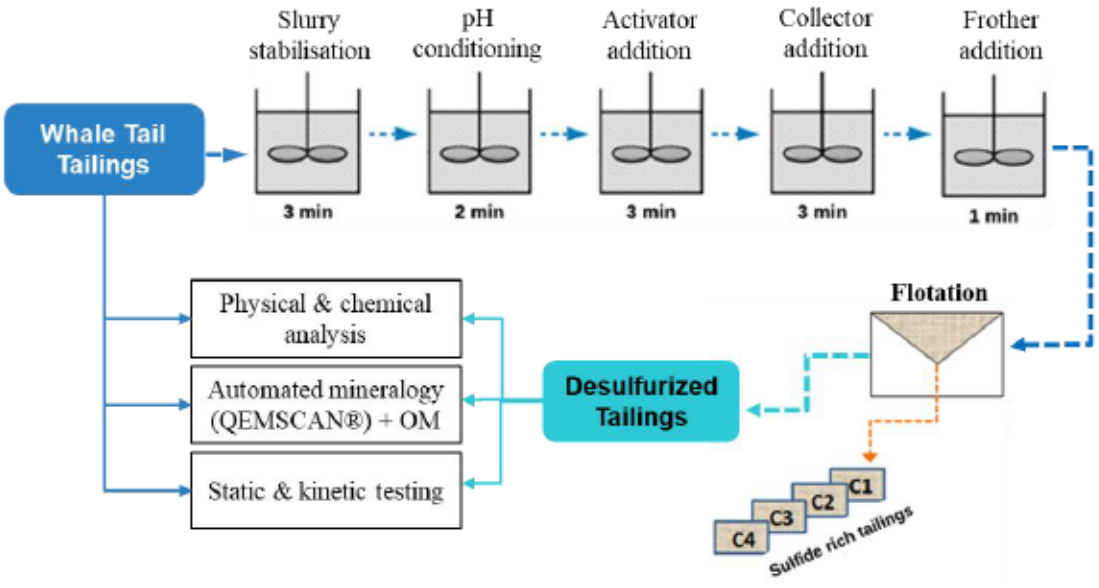

Figure 5.3 Flotation tests scheme.

Many flotation tests under different flotation conditions are required to determine the optimal flotation variables that allow the best total sulfides recovery. The vast range of possible flotation conditions (pH, collector dosage, activator dosage, frother dosage, solid concentration, and others) imply a large number of tests. This problem can be

overcome by using a reliable modeling technique to predict flotation performance while minimizing the number of experimental tests.

The CCD technique uses a full-factorial second level experimental design in addition to a point at the center (coded 0) and two additional points for each factor (called starpoints) at a distance -α and +α from the center. This yields a total of five levels for each factor. Low and high factors were coded as −1 and +1.

The DX 13 version of the Design Expert® software was used for statistical design. The value of α used in the calculation of axial points was taken as 2.36 as proposed by the software for quadratic design. Table 5.1 shows the design values, the units for each factor, and their coded values. Preliminary tests were performed to choose the ranges of the various parameters. In the context of environmental desulfurization, flotation tests at alkaline pH are more promising to avoid dissolving carbonates by adding acid. Overall, 50 runs were designed to be performed based on the CCD to investigate the relationship between the independent variables (physico-chemical parameters) and the response (recovery of sulfur minerals), possible interactions between the independent variables, and their effects on the desulfurization performance using flotation processes (Kökkılıç et al., 2015; Kwak, 2005). The final objective was to specify the optimized dosages of reagents and parameters allowing the optimal total sulfur mineral recovery.

Table 5.1 Independent variables and their levels (process parameters)

Variable	Name	Unit	Coded low (-α)	Min (-1)	Mean (0)	Max (+1)	Coded high (+α)
A	pH	-	6.03	8.25	9.87	11.5	13.71
B	PAX	g/t	23.53	85	130	175	236.46
C	$CuSO_4$	g/t	0	121.75	210.87	300	421.73
D	MIBC	g/t	16.34	30	40	50	63.65
E	Cs	g/t	18.17	25	30	35	41.83

* α = 2.36

The mathematical relationship between the variables and the response can be approximated by a second order model (equation 1) using a variance analysis (ANOVA) on the chosen experimental points:

$$R = R_0 + c_1A + c_2B + c_3C + c_4D + c_5E + c_{11}A^2 + c_{22}B^2 + c_{33}C^2 + c_{44}D^2 + c_{55}E^2 + c_{12}AB + c_{13}AC + c_{14}AD + c_{15}AE + c_{23}BC + c_{24}BD + c_{25}BE + c_{34}CD + c_{35}CE + c_{45}DE \quad (1)$$

where R is the predicted response (sulfur recovery); R0 is the model constant; A, B, C, D, and E are the pH, PAX dosage, $CuSO_4$ dosage, MIBC dosage, and solid concentration (Cs), respectively; the coefficients c1 to c5 are the linear constants; the coefficients c11 to c55 are the quadratic constants; and c12, c13, c14, c15, c23, c24, c25, c34, c35, and c45 are the interactive coefficients. The statistical software package Design Expert® (DX13) from Stat-Ease was used for regression analysis and optimization of the parameters. The regression coefficients, i.e., the main effect (ci), the quadratic effect (cii), and the two-factor interactions (cij) from the experimental results, were determined. The significance of the model was also statistically analyzed by analysis of variance (ANOVA). The proposed model was analyzed using RSM. Optimization was achieved by using a response surface for different interactions between any two independent variables and keeping the value of the third variable constant at the central (0) level (Kökkılıç et al., 2015).

5.3.3.5 Acid Generation Potential Assessment

Static tests

The static tests were performed on the initial tailings and desulfurized material using the ABA test according to Sobek method (Sobek, 1978) to evaluate their acid generation potentials. The AGP was calculated assuming the sulfide was only pyrite, using sulfur-sulfide (Ssulfide) (AP = 31.25 × Ssulfides wt.% (kg $CaCO_3$/t)), and calculating the carbonate neutralization potential (CNP) based on the total inorganic carbon, assuming the carbonate was only calcite (NP = 83.3 × TIC wt.% (kg $CaCO_3$/t)). If the NNP (NNP = NP-AP) value is lower than −20 kg $CaCO_3$/t, the material is

classified as acid generating, whereas material with NNP higher than 20 kg $CaCO_3$/t is considered as non-acid generating. An uncertainty zone is determined by NNP values between – 20 and 20 kg $CaCO_3$/t (Bouzahzah et al., 2015; Miller et al., 1991; Sobek et al., 1978). The AGP was also assessed using the neutralization potential ratio (NPR = NP/AP); a material is considered non-acid generating if NPR > 2.5, uncertain if 1 < NPR< 2.5, and acid generating if the NPR < 1 (Benzaazoua et al., 2004; Miller et al., 1991).

According to Elghali et al. (2018), the NP and AP tests were corrected based on the carbonate and sulfide liberation using Eqs. (2) and (3):

$$\text{Available AP} = 31.25 \times S_{sulfides}\ \text{wt\%}\ (\text{kg } CaCO_3/\text{t}) * L_s \qquad (2)$$

$$\text{Available NP} = 83.3 \times \text{TIC wt\%}\ (\text{kg } CaCO_3/\text{t}) * L_c \qquad (3)$$

where L_s and L_c are the liberation degree of sulfide and carbonate, respectively, as analyzed by QEMSCAN®.

The acid generation potential of the studied samples was also assessed using the NAG test to support the ABA tests. The NAG test with single addition consists of the addition of 250 ml of 15% H_2O_2 to 2.5 g of pulverised material (< 75 µm) (Sapsford et al., 2008; Stewart et al., 2006). The final pH of the leachate is recorded after 24 h reaction as NAG pH (Parbhakar-Fox et al., 2011). If the NAG pH is > 4.5, the sample is considered non-acid forming (NAF); if the NAG pH is < 4.5, the sample is considered acid forming (AF). The combination of NAG tests and ABA results allowed an improved classification of the AGP of the studied materials (Whale Tail tailings and desulfurized material).

Weathering cells

The geochemistry of the Whale Tail tailings and the resulting desulfurized tailings from flotation was evaluated using weathering cell tests. The weathering cells consist of

accelerating the oxidation of mine tailings (Cruz et al., 2001). Dry samples weighing 67 g were flushed twice a week using 50 mL of deionized water. The samples were allowed to react with deionized water for 4 hours. After that, the leachates were collected, filtered to 0.45 µm, and then analyzed for their chemical composition using ICP-AES (PerkinElmer OPTIMA 3100 RL, relative precision of 5%) on an aliquot acidified to 2% HNO_3 for preservation. The collected leachates were also analyzed using pH/Eh/EC meters, and alkalinity/acidity using an automatic titrator. In this study, the weathering cells were placed in a controlled ‑ weather box to maintain the samples under optimal saturation conditions and to avoid extreme drying (Chopard et al., 2017). The weathering cells were monitored for 157 days.

5.4 Results and Discussion

5.4.1 Whale Tail Tailings (WTT) Characterization

The physical and chemical properties of the studied samples as well as the results of the AGP assessment using static tests are summarized in Table 5.2. The particle size distribution results showed fine-grained materials with D_{10} = 3.28 µm, D_{60} = 35 µm, and D_{80} = 79.9 µm. The G_s of the WTT was 2.81 g/cm^3 and the specific surface area was 3.14 m^2/g.

The WTT comprises the following major elements, according to the decreasing order of their average concentrations: Si> Fe > Ca > Al > Mg > K > Mn. Silicon and iron contents exceeded 26 wt% and 13 wt%, respectively. Aluminum, calcium, and magnesium contents were 3.27, 2.00, and 2.68 wt%, respectively. The major oxides analysis using XRF showed that SiO_2, Fe_2O_3, and Al_2O_3 contents were respectively 59.6, 18.0, and 6.18 wt% (Table 5.2). The total sulfur content was 3.03 wt%. Sulfur-sulfate content ($S_{sulfate}$), which indicates sulfide oxidation/ subsequent sulfate precipitation, was approximately 0.05%. Therefore, S_{total} is considered to be $S_{sulfide}$.

Arsenic, nickel, and copper, as examples of the harmful metals (contaminants) for the environment, were detected in concentrations of 0.24, 0.04, and 0.01 wt%, respectively. As also highlighted in Table 5.2, other elements were detected in various concentrations, such as K, Mn, Ti, Zn, Pb, and Co.

Table 5.2 Primary characteristics of the Whale Tail tailings (WTT) and desulfurized material (DWT)

		Detection limit	WTT	DWT
Physical Properties	D_{10} (µm)	-	3.28	3.89
	D_{80} (µm)	-	79.9	96.4
	Gs (g/cm^3)	-	2.84	2.78
	SSA (m^2/g)	-	3.14	2.32
Chemical Analysis	Si	0.01%	26.8	32.8
	Fe	0.05%	13.1	9.3
using ICP-MS/AES	Al	0.01%	3.27	3.33
	Ca	0.01%	2.00	2.06
(%wt/wt)	Mg	0.01%	2.68	2.42
	Mn	0.001%	0.33	0.34
	K	0.1%	1.2	1.2
	Ti	0.001%	0.13	0.13
	As	0.001%	0.24	0.03
	Ni	0.001%	0.036	0.014
	Cu	0.001%	0.009	0.005
	Zn	0.001%	0.008	0.009
	Pb	0.001%	0.006	0.003
	Co	0.001%	0.003	<0.001
	Cr	0.01%	0.06	0.05
	Sb	0.002%	< 0.002	<0.002
S/C Analysis, Static	S_{total} (%)	0.09	3.03	0.11
	C_{total} (%)	0.09	0.58	0.65
& NAG tests	AP ($CaCO_3$/t)	-	94.69	3.44
	NP ($CaCO_3$/t)	-	48.31	54.15
	Net NNP	-	-46.37	50.71
	($CaCO_3$/t)	-	AG*	Non-
	AGP		2.43	AG
	NAG pH			8.12

*Acid generating according to Quebec Directive-019

The ABA results show that the NP value was lower (NP = 55.81 kg $CaCO_3$/t) than the AP value (AP= 92.5 kg $CaCO_3$/t), leading to an NNP value undoubtedly within the acid

generating zone (< -20 kg $CaCO_3$/t). Based on the NP/AP ratio, the studied material is classified as acid generating, as this ratio is under 1. Similarly, the NAG pH was <4.5, confirming the same conclusion as the NNP.

5.4.2 Mineralogical Characterization

5.4.2.1 Bulk Mineralogy

As shown in Table 1S (Annexe B), the mineralogy determined by XRD analysis is dominated by quartz (~ 39%), stilpnomelane (10.2%), amphibole (9.2%), mica (9.8%), feldspar (8.3%), chlorite (8.4%), calcite (1.2%), and sulfide/sulfosalt minerals (i.e., pyrite, 2.2%; pyrrhotite, 0.4%; cobaltite/gersdorffite, 0.5%; and chalcopyrite, 0.3%). The polished sections were observed under the optical microscope in reflected light mode to confirm the identified acid-generating minerals by XRD. The observations showed that the main sulfides in the studied sample were pyrite and pyrrhotite. Arsenopyrite and chalcopyrite were also present in trace amounts (Figure. 5.4). These sulfides displayed different textures that could be classified as three exposure states: i) totally liberated sulfides (e.g., pyrite) with no common boundaries with other NSG minerals (Figure. 5.4.A-B- C); ii) mid-liberated sulfides with boundaries partially shared with NSG minerals (Figure. 5.4.D-E-F); and iii) fully encapsulated sulfides that are entirely locked within NSG minerals, such as chlorite, quartz, and micas (Figure. 5.4.E-F).

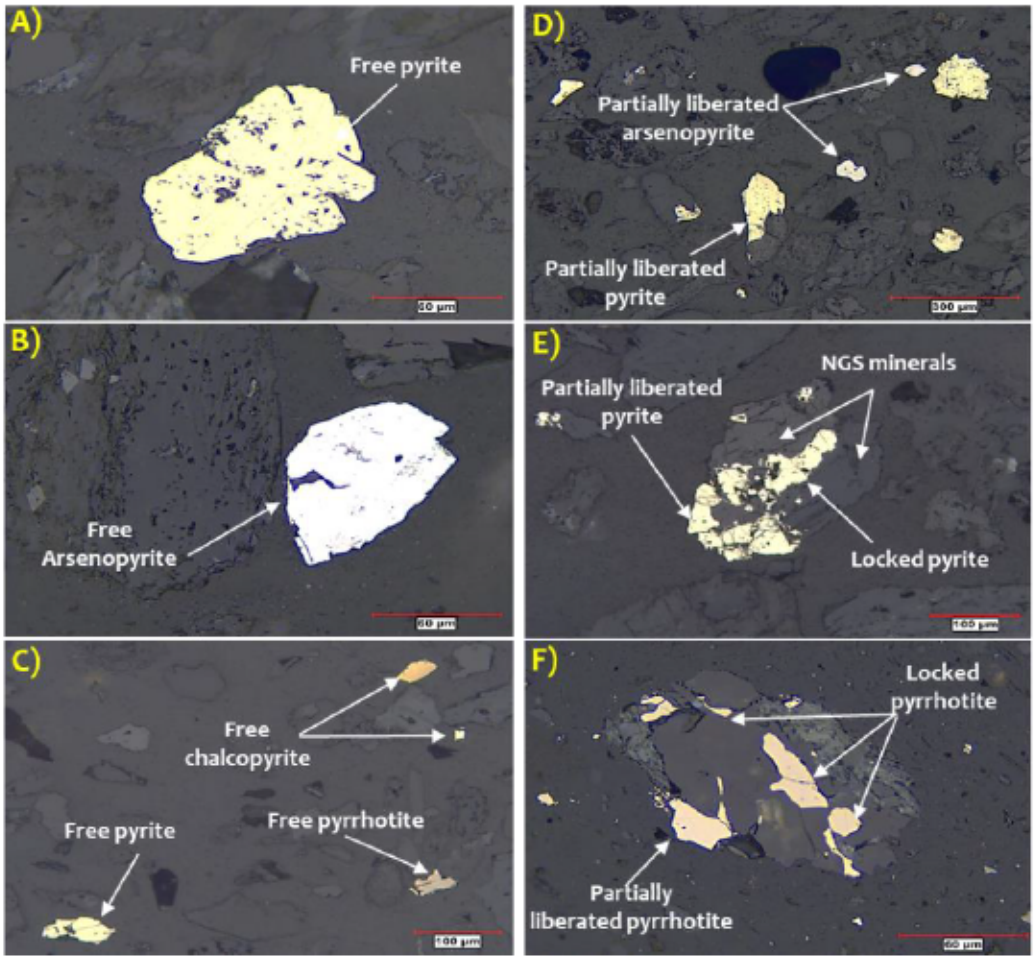

Figure. 5.4 Optical microscopy (reflected light mode) photomicrographs of the studied tailings highlighting the textures and mineralogical associations of sulfides and gangue minerals.

To investigate other mineralogical characteristics of the WTT, the sample was submitted for mineralogical assessment using QEMSCAN®; the results are summarized in Figure 5.5.A. Sulfides were mainly pyrite and pyrrhotite, as well as arsenopyrite, chalcopyrite, gersdorffite, and pentlandite in trace amounts. Carbonates occurred mainly as calcite. The bulk mineralogical composition was dominated by non-sulfide gangue minerals, particularly quartz, chlorite, micas, amphibole, and Fe-silicate. Quantitatively, sulfide contents were ~3.03 wt% pyrite, 2.72 wt% pyrrhotite, 0.15 wt%

arsenopyrite, 0.08 wt% chalcopyrite, and 0.04 wt% gersdorffite. Carbonate content was 1.42 wt%. Furthermore, quartz and chlorite contents were 39.5 wt% and 12.5 wt%, respectively. Micas, amphibole, and Fe-silicate contents were 12.0 wt%, 12.0 wt%, and 5.2 wt%, respectively. Other identified minerals, with contents lower than 5 wt%, included: plagioclase (2.93 wt%), orthoclase (1.80 wt%), Fe oxide (2.43 wt%), siderite (1.59 wt%), and Fe and Mg serpentine (1.15 wt%).

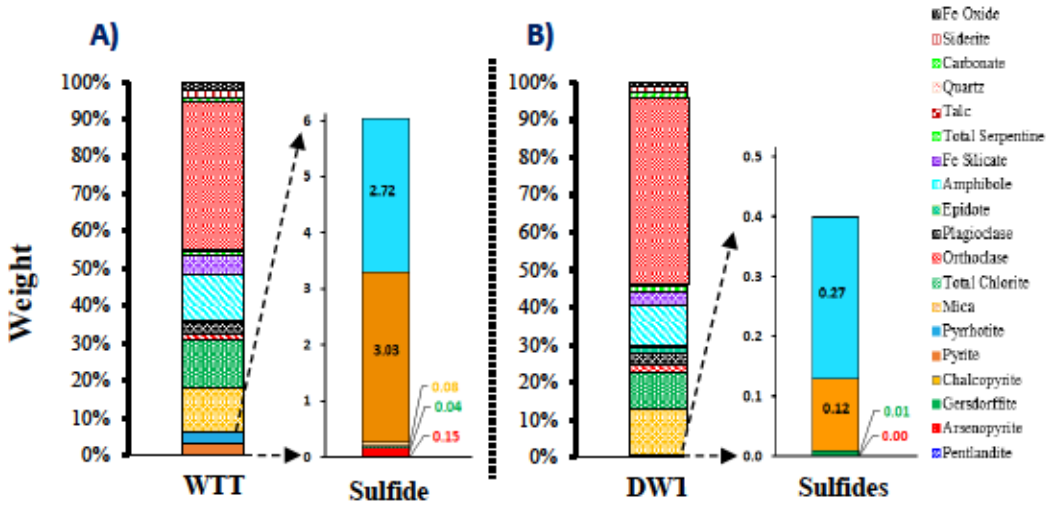

Figure 5.5 Modal mineralogy of A) WTT and B) DWT.

5.4.2.2 Textural Analysis and Mineral Liberation Quantification

Mineral liberation and associations

Sulfides and carbonates liberation degrees and their mineralogical associations are shown in Figure 5.6, which describes the exposure and the relationship of these minerals with surrounding minerals (Elghali et al., 2018). The more liberated the sulfides and carbonates, the higher their reactivity (Blowes et al., 2003; Paktunc and Davé, 2000). In this study, a mineral is considered free when its liberation degree is higher than 95%, and it is considered totally locked when its liberation is lower than

10%. Finally, a mineral is considered mid-liberated when more than 90% of the particle area is composed of the mineral of interest and the associated minerals. In this study, pyrrhotite and pyrite were combined as Fe sulfides in the liberation data. As shown in Figure 5.6.A, sulfides were more liberated (90 wt%) than carbonates (61.3 wt%). Sulfide and carbonate mineralogical associations are shown in Figure 5.6.A. Sulfide and carbonate minerals were associated with non-sulfide gangue minerals (e.g., silicates and others) as binary associations. Arsenic/nickel and iron sulfides were associated with NSG minerals in proportions of 5 wt% and 9 wt%, respectively. Carbonates were associated with silicates and others NSG minerals with about 32 wt% and 6 wt%, respectively (Figure 5.6.A).

Sulfur, cobalt, arsenic, and nickel deportment

Elemental deportment of chemical species of interest (S, Co, As, and Ni) was calculated based on the bulk chemical composition and mineralogical composition of the solid samples and the elemental composition of the identified minerals as analyzed by EPMA. Sulfur within the Whale Tail tailings was attributed to pyrite, pyrrhotite, arsenopyrite, chalcopyrite, gersdorffite, and pentlandite. These minerals have a different reactivity within AMD generation. Figure 5.6.B shows S, Co, As, and Ni deportment within the studied sample. The results showed that 62.07%, 35.34%, 1.14%, 1.00%, 0.22%, and 0.11% of S was associated with pyrite, pyrrhotite, arsenopyrite, chalcopyrite, gersdorffite, and pentlandite, respectively. Cobalt within the studied sample was attributed to gersdorffite (100%), while 46.58%, 41.68%, and 11.74% of the Ni was attributed to gersdorffite, pyrrhotite, and pentlandite, respectively. For arsenic, it was attributed to arsenopyrite (77%), gersdorffite (21.33%), and pyrrhotite (1.69%).

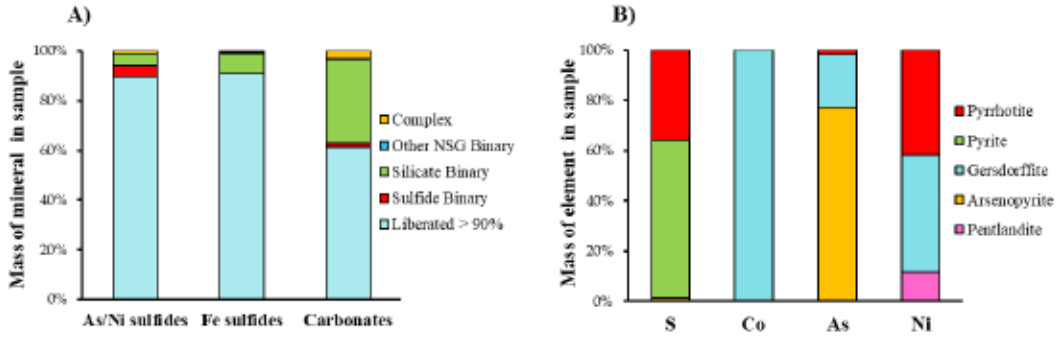

Figure 5.6 A) Mineralogical associations and B) Sulfur, cobalt, arsenic, and nickel deportments for the studied WTT

EPMA results

Elemental analyses of individual minerals grains (sulfides and NSG minerals) as determined by electron probe micro-analyzer (EPMA) are presented in Table 5.3 and Table 2S (Annexe B. The pyrrhotite and arsenopyrite grains were nickeliferous (Ni at 0.36 ± 0.06 wt% and 0.11 ± 0.06 wt%). All the analyzed gersdorffite grains were Fe gersdorffite. The gersdorffite grains contain Fe and Co at 9.05 ± 0.04 and 1.64 ± 0.05 wt%, respectively. Pyrite exhibited a composition close to its theoretical stoichiometry. The deleterious elements (i.e., As, Ni, Cu, and Co) were not deported by the NSG minerals.

Table 5.3 EPMA analysis of grains sulfides observed within the WTT.

Element (LOD)*	Pyrite			Pyrrhotite			Arsenopyrite			Gersdorffite		
	Analysis (%)		TC (wt%)**	Analysis (%)		TC (wt%)**	Analysis (%)		TC (wt%)**	Analysis (%)		TC (wt%)**
	Mean value	Range		Mean value	Range		Mean value	Range		Mean value	Range	
S *(0.01)*	**53.38**	53.18 - 53.85	**53.45**	**38.90**	38.00 - 39.38	**37.67**	**18.54**	17.81-19.74	**19.69**	**19.19**	18.89 – 19.48	**19.4**
As *(0.06)*	<0.06	<0.06	-	<0.06	<0.06	-	**46.66**	46.04-47.55	**46.01**	**47.47**	47.02 – 47.78	**45.2**
Fe *(0.04)*	**46.14**	45.98 - 46.46	**46.55**	**57.51**	54.89 - 58.93	**62.33**	**34.77**	33.59-35.96	**34.30**	9.05	8.70 – 9.27	-
Co *(0.05)*	<0.05	<0.05	-	0.05	0.05 - 0.06	-	<0.05	<0.05	-	1.64	0.69 – 2.72	-
Ni *(0.06)*	<0.06	<0.06	-	0.36	0.30 - 0.47	-	0.11	0.10-0.13	-	**24.48**	23.38 – 25.41	**35.4**
Cu *(0.07)*	<0.07	<0.07	-	<0.07	<0.07	-	<0.07	<0.07	-	<0.07	<0.07	-
Total	100.00	-	**100.00**	100.00	-	**100.00**	100.00	-	**100.00**	100.00	-	**100.00**

* LOD: limit of detection** TC: theoretical composition based on mineral formula

5.4.3 Size-by-size Chemical Analysis

The distributions of sulfur and carbon in these fractions were determined and are presented in Fig. 1S (Annexe B). The sulfur analysis on a size-by-size basis indicated that sulfur varied between 0.56 and 1.30 wt% in the coarse and intermediate size fractions (80-125 µm), while the fine fractions (0-63 µm) recorded the highest sulfur content (3.12 to 4.36 wt%) (Fig. 1S-A) (Annexe B). The carbon grade, as is shown also in Fig. 1S-A (Annexe B), was distributed in an almost homogeneous way over all the particle size fractions. The distribution of sulfur and carbon by size fractions is shown in Fig. 1S-B (Annexe B). The results show that about 80% and 90% of carbon and sulfur, respectively, were contained in fine fractions (<45 µm).

5.4.4 Central Composite Design (CCD)

CCD was used to determine the optimal parameter combination and show the effects of each parameter on flotation performance. Fifty flotation experiments were conducted using the chosen experimental conditions given by the CCD. The detailed experimental design and random order adopted to execute the experiments as well as the flotation results can be found in Table 5.4. Results show that the highest sulfur recovery (96.8%) was achieved on the 4^{th} run while the 35^{th} run saw the lowest (61.7%). Due to the limited supply of tailings, it was decided to conduct one run seven times to evaluate reproducibility, instead of duplicating each run. The results had a standard deviation of 0.4, which was deemed acceptable. A variance analysis was then applied on the experimental results, which allowed us to evaluate the interactions between different variables in the experimental design.

Table 5.4 Experimental design conditions and responses.

Run	A	B	C	D	E	Recovery (%)
1	8.25	85	121.75	30	25	83.9
2	11.5	85	121.75	30	25	84.1
3	8.25	175	121.75	30	25	92.6
4	11.5	175	121.75	30	25	96.8
5	8.25	85	300	30	25	83.7
6	11.5	85	300	30	25	80.8
7	8.25	175	300	30	25	91.5
8	11.5	175	300	30	25	96.7
9	8.25	85	121.75	50	25	84.7
10	11.5	85	121.75	50	25	86.2
11	8.25	175	121.75	50	25	95.3
12	11.5	175	121.75	50	25	92.4
13	8.25	85	300	50	25	84.9
14	11.5	85	300	50	25	83.5
15	8.25	175	300	50	25	95.3
16	11.5	175	300	50	25	96.4
17	8.25	85	121.75	30	35	83.8
18	11.5	85	121.75	30	35	79.5
19	8.25	175	121.75	30	35	91.9
20	11.5	175	121.75	30	35	95.1
21	8.25	85	300	30	35	78.5
22	11.5	85	300	30	35	82.3
23	8.25	175	300	30	35	90.1
24	11.5	175	300	30	35	92.3
25	8.25	85	121.75	50	35	78.9

Run	A	B	C	D	E	Recovery (%)
26	11.5	85	121.75	50	35	80.0
27	8.25	175	121.75	50	35	93.5
28	11.5	175	121.75	50	35	96.1
29	8.25	85	300	50	35	84.5
30	11.5	85	300	50	35	84.9
31	8.25	175	300	50	35	95.8
32	11.5	175	300	50	35	93.0
33	6.03	130	210.88	40	30	89.9
34	13.72	130	210.88	40	30	94.4
35	9.88	23.53	210.88	*40*	*30*	61.7
36	9.88	236.47	210.88	40	30	75.9
37	9.88	130	0.00	40	30	89.2
38	9.88	130	421.74	40	30	95.2
39	9.88	130	210.88	16.34	30	89.1
40	9.88	130	210.88	63.66	30	93.9
41	9.88	130	210.88	40	18.17	89.7
42	9.88	130	210.88	40	41.83	87.3
43	9.88	130	210.88	40	30	94.9
44	9.88	130	210.88	40	30	90.0
45	9.88	130	210.88	40	30	90.0
46	9.88	130	210.88	40	30	91.8
47	9.88	130	210.88	40	30	95.2
48	9.88	130	210.88	40	30	93.4
49	9.88	130	210.88	40	30	93.7
50	9.88	130	210.88	40	30	94.2

5.4.4.1 Establishment of Model for Sulfur Mineral Recovery and Variance Analysis

The experimental results shown in Table 5.4 were fitted to a quadratic second order model equation using multiple regression analysis for sulfur recovery. The p-value for the quadratic model is less than 0.05. This means that the quadratic equation can be used to fit the experimental data. After discarding insignificant effects, the quadratic model for sulfur recovery can be expressed as follows:

$$\text{Recovery (\%)} = 33.76 + 0.31\ pH + 0.54\ PAX + 0.15\ MIBC + 0.97\ Cs + 0.006\ pH * PAX + 0.001\ pH^2 - 0.002\ PAX^2 - 0.001\ MIBC^2 - 0.025\ Cs^2 \quad (4)$$

To assess the variables and their possible interactions, an ANOVA was performed. Table 3S (Annexe B) lists the results of variance analysis at 95% confidence intervals regarding sulfur recovery. Although the quadratic model has a p-value of less than 0.01, its error p-value (or p-value for lack of fit) is much higher than 0.05. The lack of fit is the opposite of the whole-model test, which indicates that all the terms in the model are significant. However, the lack of fit tests determines if any term left out is significant. The results of the lack of fit F-value of 1.85 implies that the lack of fit is not significant relative to the pure error. PAX dosage, pH, MIBC, and Cs had positive coefficients that indicated a positive effect on the recovery values. PAX was the most significant factor with a p-value <0.001. The $CuSO_4$ value was not significant. The quadratic term for PAX dosage (B^2) was found to be the only significant quadratic term with a p-value <0.001.

The value of R^2 in this study was 0.91. This indicates that the model could account for 91% of the changes in sulfur recovery using the four significant parameters. Pred-R^2 was 0.69 and adj-R^2 was 0.85. Adj-R^2 was acceptably close to R^2. Adeq-Precision measures signal-to-noise ratio. A ratio greater than 4 is desirable. This study showed an acceptable signal with a ratio of 22.16. The coefficient of variation (CV=2.97%) was low, which is a sign of both precision and reliability of the experiments. The model

was statistically significant and powerful.This model can be used to calculate and estimate flotation recovery for different reagent dosages. Figure 5.7 shows the observed and predicted values from the model equation. This figure also shows that the main effects of variables on recovery were significant at 95% confidence intervals. Based on the quadratic model for sulfur recovery, three-dimensional response surfaces were created using Design-Expert® version 13 software. The objective was to understand the interactions between variables and how they affect the response values.

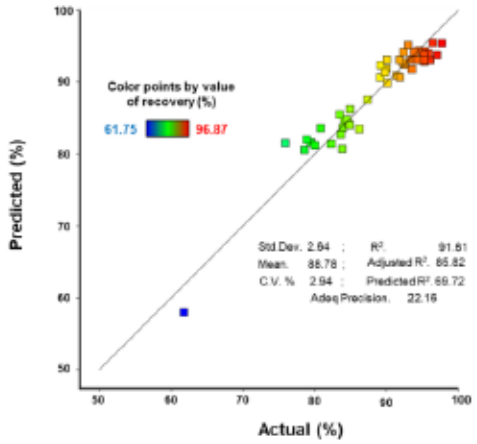

Figure 5.7 Actual vs. predicted sulfur recoveries.

Figure 5.8 illustrates the 3D response surface relationship between the different parameters of the experimental design. The PAX dosage significantly affected the response surfaces as shown in Figure 5.8. A-B-C, where the PAX dosage is plotted against pH, $CuSO_4$, and Cs, respectively. The PAX dosage is a significant variable: this translates to a curved surface around PAX values in the response surface plot. Less curvature was noticed for the other variables. An increase in the PAX dosage was generally followed by a steady increase in recovery until a maximum value was reached around 160 g/t of PAX. The recovery decreased to lower values after 160 g/t. This behavior can be interpreted as the covering of the monolayer around the mineral surface until a maximum is reached. Any added collector dosage was then responsible for exceeding this monolayer and by consequence causing a decrease in recovery (Wills,

2016). No noticeable improvement was observed in the recovery after a high $CuSO_4$ dosage, which translates to a plane surface in response surface of $CuSO_4$ vs pH (Figure 5.8.D) with no curvature or inclination. MIBC positively affected the recovery at lower pH values judging from the slight inclination of the response surface towards lower values of recovery at lower values of pH (i.e., recovery passed linearly from 90% to 95%) (Figure 5.8.E). Cs showed similar behavior (Figure 5.8.F).

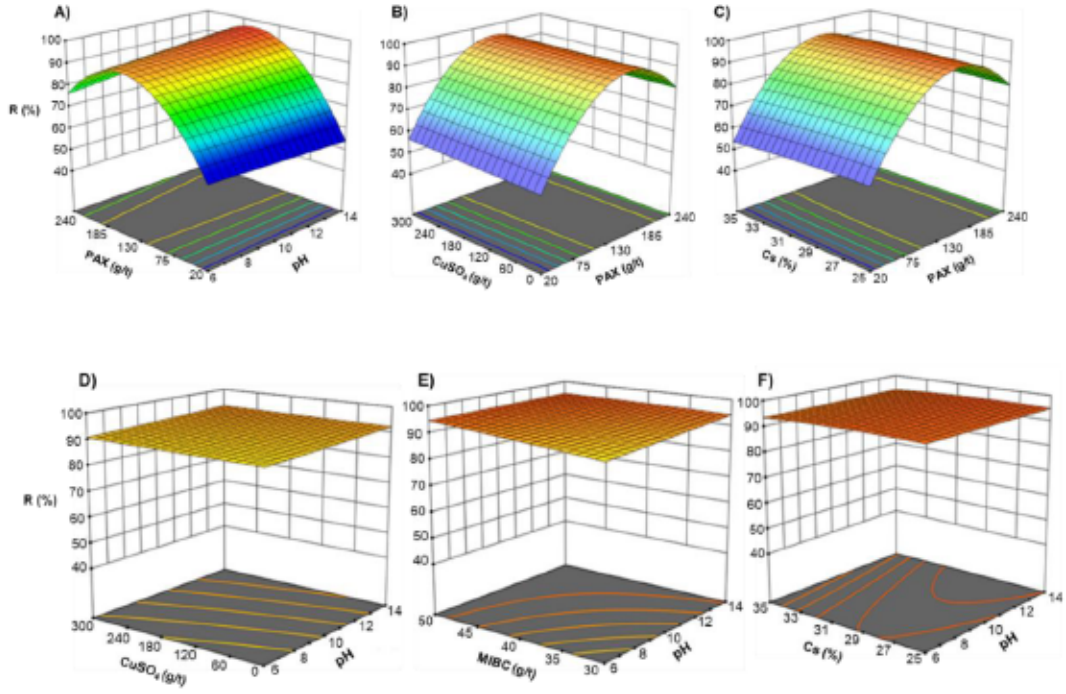

Figure 5.8 The three-dimensional quadratic response surfaces for total sulfur recovery with A) PAX vs pH with $CuSO_4$=200 (g/t), and MIBC=40 (g/t); B) $CuSO_4$ vs PAX for pH=10 & MIBC=50 (g/t); C) Cs vs PAX for pH=10, $CuSO_4$=210 (g/t), and MIBC=40(g/t); D) $CuSO_4$ vs pH for PAX=120 (g/t) and MIBC=40 (g/t); E) MIBC vs pH for PAX=130 (g/t) and $CuSO_4$=300 (g/t); F) Cs vs pH for PAX=130 (g/t), $CuSO_4$=300 (g/t), and MIBC=50 (g/t).

5.4.4.2 Optimization and Validation

The flotation optimization process was designed to determine the optimal operational conditions that would maximize the sulfur recovery. The optimum values of response variables were predicted from the regression models by using a numerical optimization algorithm in the Design-Expert® 13 (DX13) software. To ensure maximum desirability, all factors were kept within the initial range of the study, while the sulfur recovery was set to maximum. Table 5.5 shows the optimization scheme for maximum sulfur recovery. This design is suitable for use because the desirability value (0.99) indicates that data fitting was extremely reliable. Maximum sulfur recovery of 96.94% could be achieved when pH, PAX, $CuSO_4$, MIBC, and solid content were, respectively, set at 11.5, 158 g/t, 300 g/t, 55 g/t, and 29.3%.

Table 5.5 Optimum level of each parameter for a 0.99 desirability and maximum recovery.

Solution	pH	PAX	$CuSO_4$	MIBC	Cs	Recovery (%)	Desirability
	11.5	158 g/t	300 g/t	55 g/t	29.3%	96.94	0.99

Experiments were repeated three times (triplicates), and their average value was considered as the outcome (recovery). Under these optimal flotation conditions, it was experimentally possible to desulfurize tailings (WTT) and to achieve a sulfur recovery yield of 96.80% (maximum). Sulfur recovery and residual sulfur evolutions as a function of flotation time are presented in Fig. 5.9. This desulfurization experiment showed that the residual sulfur content in the tailings was <0.8% after 1 min and 0.11% after 6 min, which corresponds to a recovery of approximately 75% after 1 min and 96.8% after 6 min. The sulfur recovery reached a plateau after a flotation duration of around 4 min, which corresponds to a recovery of 95.3% and a residual sulfur of 0.15 wt%.

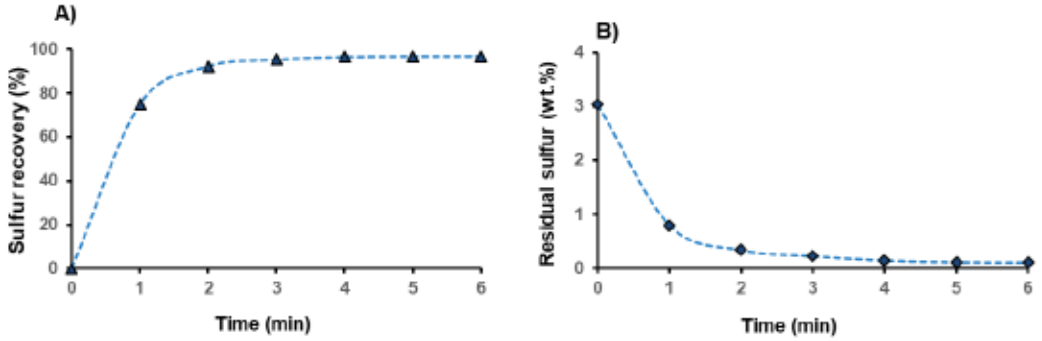

Fig. 5.9 Sulfur flotation kinetic of the Whale Tail tailings (desulfurization): A) Sulfur recovery vs. time; B) Residual sulfur vs. time.

5.4.5 Desulfurized Whale Tailings (DWT) Characterization

The results of physical and chemical analyses of the desulfurized tailings are illustrated in Table 5.2. These results show that it is characterized by lower metal concentrations than the feed sample. Silicon, Fe, Al, Ca, K, and Mg are the main elements of the chemical composition of the DWT, with concentrations of 32.8%, 9.33%, 3.33%, 2.06%, 1.20%, and 2.42%, respectively. The high presence of Si can be explained by the abundance of silicate minerals according to the mineralogical composition and whole rock analysis by XRF (Table 5.2). Sulfur and carbon were found at concentrations of 0.11 wt% and 0.65 wt%, respectively.

Figure 5.5.B shows a summary of the mineralogical composition of the desulfurized tailings. It was mainly composed of quartz (49.38 wt%), mica (12.30 wt%), amphibole (10.54 wt%), and chlorite (9.87% wt), in accordance with higher Si, Fe, Al, Ca, K, and Mg concentrations. Other non-sulfidic minerals were identified with contents less than 5%, including Fe silicates (3.77 wt%), plagioclases (2.94 wt%), orthoclase (2.03 wt%), epidote (1.80 wt%), carbonates (1.74 wt%), serpentine (1.43 wt%), and Fe-oxides (1.22 wt%). The sulfide mineral content was reduced to less than 0.41 wt% versus 6.03 wt% in the feed sample. The small amounts of remaining sulfides were mainly in the form of pyrrhotite (0.27 wt%) and pyrite (0.13 wt%). Some traces of gersdorffite were also

detected (0.01 wt%). Mineral liberation and mineralogical associations are recognized to be an important parameter influencing a mineral's reactivity. The investigation of these parameters showed that the remaining sulfides and carbonates in fresh and desulfurized tailings displayed different liberation degrees (Figure 5.10.A-B). The carbonates (neutralizing minerals) within the DWT were more liberated than the sulfide minerals (acid- and contamination-generating minerals). Quantitatively, about 60% of the carbonates had a liberation degree of more than 80%, and about 98% of the sulfides had a liberation degree of less than 30%. This proves that most of the remaining sulfides were not liberated, and that the liberated sulfide particles were efficiently recovered by the flotation process.

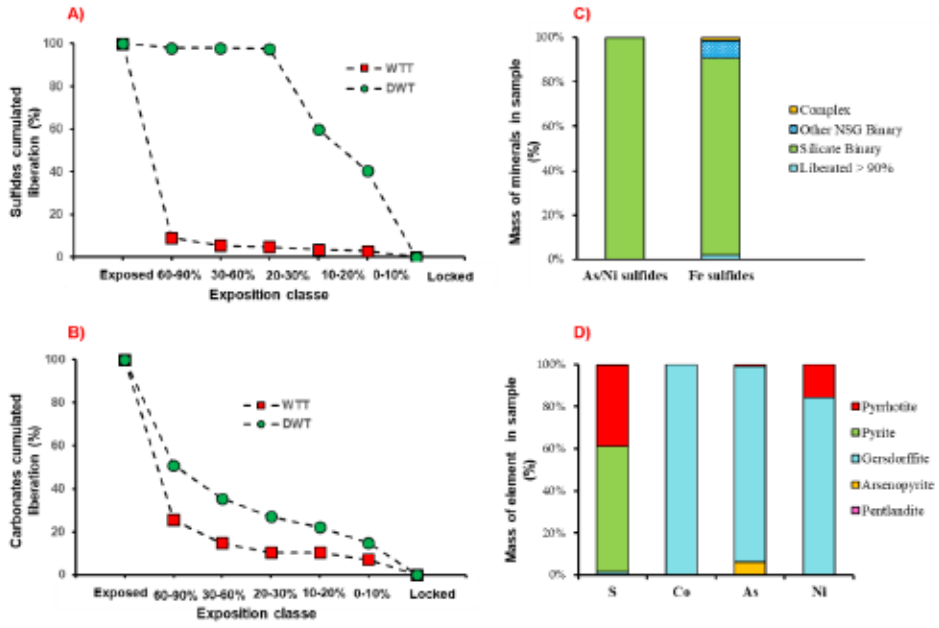

Figure 5.10 Mineral liberation of (A) sulfide and (B) carbonate minerals within the WTT and DWT samples. C) Mineralogical associations of sulfide minerals within the DWT. D) Sulfur, cobalt, arsenic, and nickel deportments for DWT.

The desulfurization process was unable to remove residual sulfides that were locked within NSG minerals; as such, they were considered unavailable for flotation. As shown in Figure 5.10.D, the residual sulfur was predominantly attributed to pyrite (59.50%) and pyrrhotite (38.75%). It also occurred in gersdorffite (1.20%) and in arsenopyrite (0.20%). Arsenic mainly occurred in gersdorffite (93%) and arsenopyrite (6%). About 1% of the arsenic was included in pyrrhotite, and Co occurred only in gersdorffite, as demonstrated by the EPMA results (Table 5.3). The majority of the Ni occurred in gersdorffite (84.41%) and pyrrhotite (15.59%) as inclusions (Table 5.3).

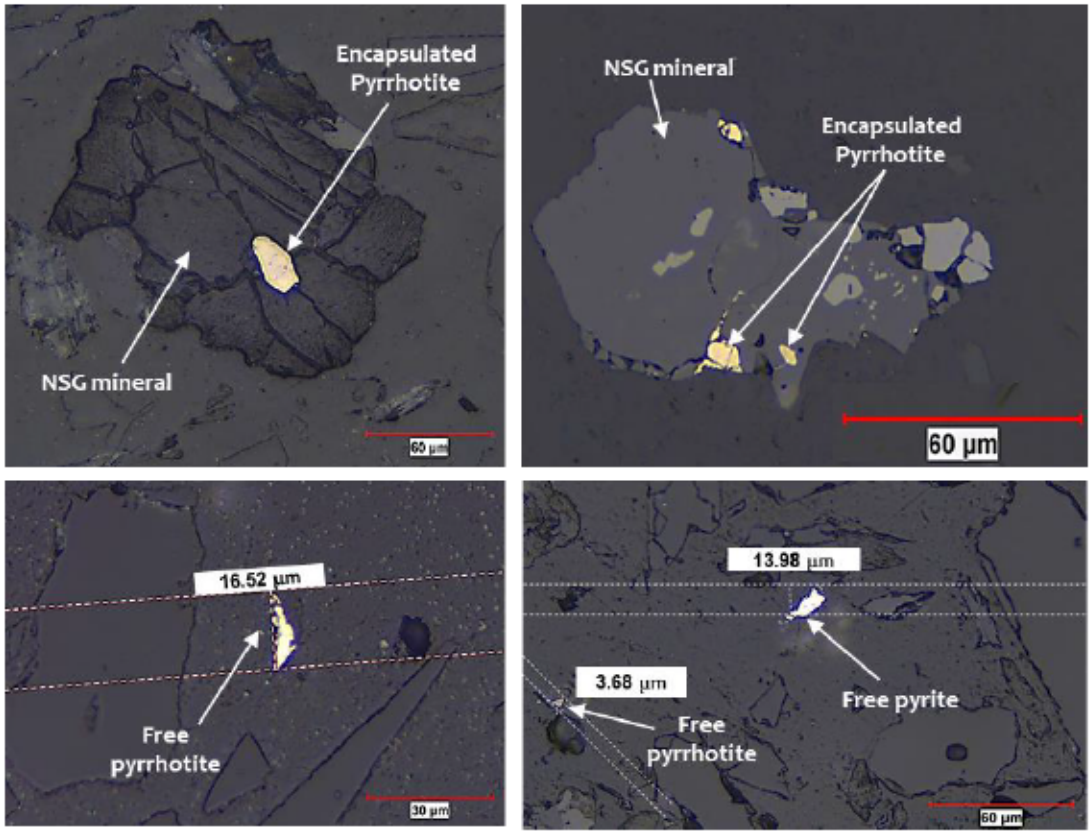

Figure 5.11 Optical microscopy of the polished section of desulfurized tailings.

As demonstrated by automated microscopy, the tailings sample from the flotation test contained traces of pyrite (0.13 wt%), pyrrhotite (0.27 wt%), and gersdorffite (0.01

wt%). About 98% of these minerals were encapsulated or attached to the NSG minerals (e.g., silicates); the remaining 2% of these sulfides were free. Optical microscopy demonstrated that the unrecovered free portion was in the form of very small particles (<20 µm) (Figure 5.11). The flotation process was unable to remove these residual minerals, as they were finer than the optimal size range (between 20 µm and 1 mm) for flotation (Ait-Khouia et al., 2021; Derycke et al., 2013).

5.4.6 Environmental Behavior of the Whale Tail and Desulfurized Tailings

5.4.6.1 Acid Generation Potential Assessment by Static Tests

Compared to the initial tailings, sulfide removal by flotation decreased the AP of the desulfurized materials; subsequently, the NP and NNP were increased due to the increase in the relative content of neutralizing minerals (e.g., carbonates, silicates) (Table 5.2). Quantitatively, the AP of the tailings was reduced from 94.7 to 3.4 kg $CaCO_3$/t, and the NP was slightly increased from 48.3 to 54.2 kg $CaCO_3$/t. Thus, the NNP was increased from -46.4 to 50.7 $CaCO_3$/t. According to the classification criteria proposed by Miller et al. (1991), the WTT tailings are potentially acid generating (i.e., NNP < −20 kg $CaCO_3$/t), and the DWT are non-acid generating (i.e., NNP > 20 kg $CaCO_3$/t). These results are confirmed by the NP/AP ratio criteria. The classification results are plotted in the NP vs AP graphs (Figure 5.12).

As shown in Figure 5.10.A-B-C, sulfides and carbonates were not completely liberated. The AP and NP are corrected considering sulfide and carbonate liberation degrees as analyzed by QEMSCAN® to consider the differences in terms of particle size distribution (Elghali et al., 2018; Elghali et al., 2019a). The sulfide and carbonate liberation degrees (% L) were recalculated considering all liberation classes and using the equation 5 (Elghali et al., 2018):

$$\%L = \sum_{c=0}^{100} Ci * Fi/100 \qquad (5)$$

where C_i is the average liberation class as determined by QEMSCAN®, and F_i is the class C_i average frequency. For example, the value used for the class 20 – 30% is 25%.

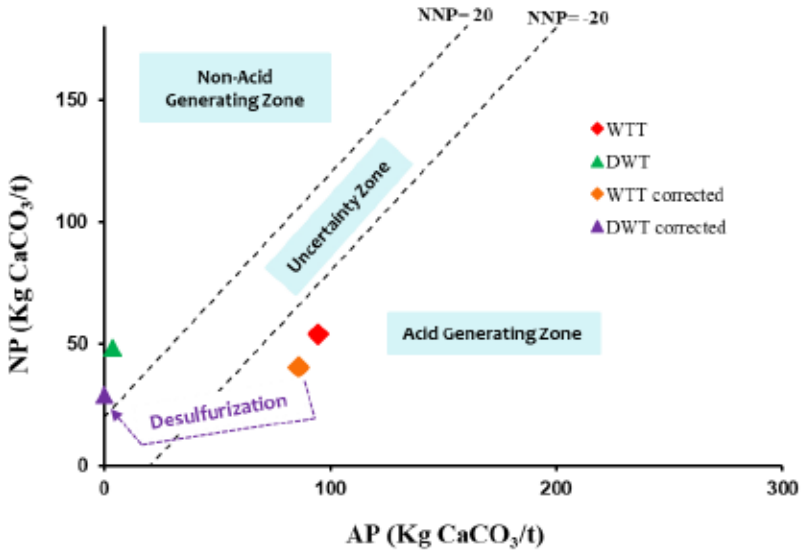

Figure 5.12 WTT and DWT classification in terms of absolute AP and NP and available AP and NP after correcting for the sulfide and carbonate liberation degrees.

Results for the recalculated sulfide and carbonate liberations are presented in Fig. 2S-A-B (Annexe B).

The difference between the absolute and available NP and AP depends on the mineralogical textures. This figure compares the results of absolute and available AP, NP, and NNP for initial and desulfurized samples (WTT and DWT, respectively). As can be seen, the NNP of WTT and DWT were, respectively, increased slightly from -46.4 to -45.7 kg $CaCO_3$/t and reduced from 50.7 to 34.8 kg $CaCO_3$/t. Thus, the correction of AP and NP by sulfide and carbonate liberation did not change the AGP statement for WTT and DWT.

Concerning the NAG tests, the NAG pH of WTT and DWT were 2.43 and 8.12, respectively. For a better AGP classification as suggested by Parbhakar-Fox et al. (2018), the NAG pH values were interpreted using the NPR as shown in Fig. 2S-C (Annexe B). Thus, the WTT was classified as potentially acid forming (PAF), while the DWT was classified as non-acid forming (NAF). This classification remained the same even after the correction of NPR using sulfide and carbonate liberation degrees. Finally, regarding the conclusions drawn from the ABA tests and NAG pH vs NPR, it can be concluded that the desulfurization reduced the AGP of the mine tailings. The initial sample was potentially acid generating, and the desulfurized sample was non-acid generating. The static tests used in this study allowed a rapid and low-cost classification of the AGP of the studied samples. However, this classification remains incomplete in terms of contaminant neutral drainage potential, mineral reactivity, and long-term prediction of the AGP of the studied samples. For this reason, kinetic tests were carried out. The next section describes the kinetic tests conducted on the studied samples using weathering cells.

5.4.6.2 Acid Generation Potential by Kinetic Tests

The geochemical behavior of the WTT and DWT was evaluated under accelerated weathering conditions using weathering test cells (Cruz et al., 2001). These tests were mainly used to evaluate the effectiveness of environmental desulfurization to limit contamination generation by quantifying: i) the sulfide oxidation rate, ii) the contaminant release rate, and iii) the environmental long-term behavior of sulfidic and desulfurized tailings. The chemical quality of the leachates from the WTT and DWT over 157 days is presented in Figure 5.13 and Figure 5.14. The chemical quality of the leachates was analyzed in terms of pH (Figure 5.13.A), EC (Figure 5.13.B), acidity/alkalinity (Figure 5.13.C-D), and chemical composition (Figure 5.14). Qualitatively, the two samples showed a similar behavior in terms of pH and acidity/alkalinity, and a different behavior in terms of EC and chemical species release

rates. The pH of the leachates was circumneutral, ranging between 7.3 and 7.9 for WTT and between 7.8 and 8.7 for DWT. The electrical conductivity (EC) showed high values for both samples at the beginning of the kinetic tests (2940 µS/cm for WTT and 1273 µS/cm for DWT) and tended to stabilize at average values of 547 µS/cm for WTT and 166 µS/cm for DWT. The high values of EC at the earlier stage of the kinetic tests correspond to the release of weakly-bonded soluble and pre-oxidized elements (Elghali et al., 2021a; Mayer et al., 2002).

The WTT and DWT samples did not show acidification during the 157 days of leaching; as expected, the pH remained circumneutral (i.e., between 7 and 8.5). The acidity evolution of the leachates from the weathering cells for both samples is shown in Figure 5.13.C. The acidity and the elements released by the samples during the first three cycles were relatively high mainly due to the leaching of elements initially present in the samples and can be related to previous oxidation. The acidity generated by the WTT was slightly higher than that generated by the DWT. Average acidity was respectively about 20 and 7 mg $CaCO_3$/L for WTT and DWT. The alkalinity of the leachates was around 58 mg $CaCO_3$/L for DWT and around 82 mg $CaCO_3$/L for WTT (Figure 5.13.D).

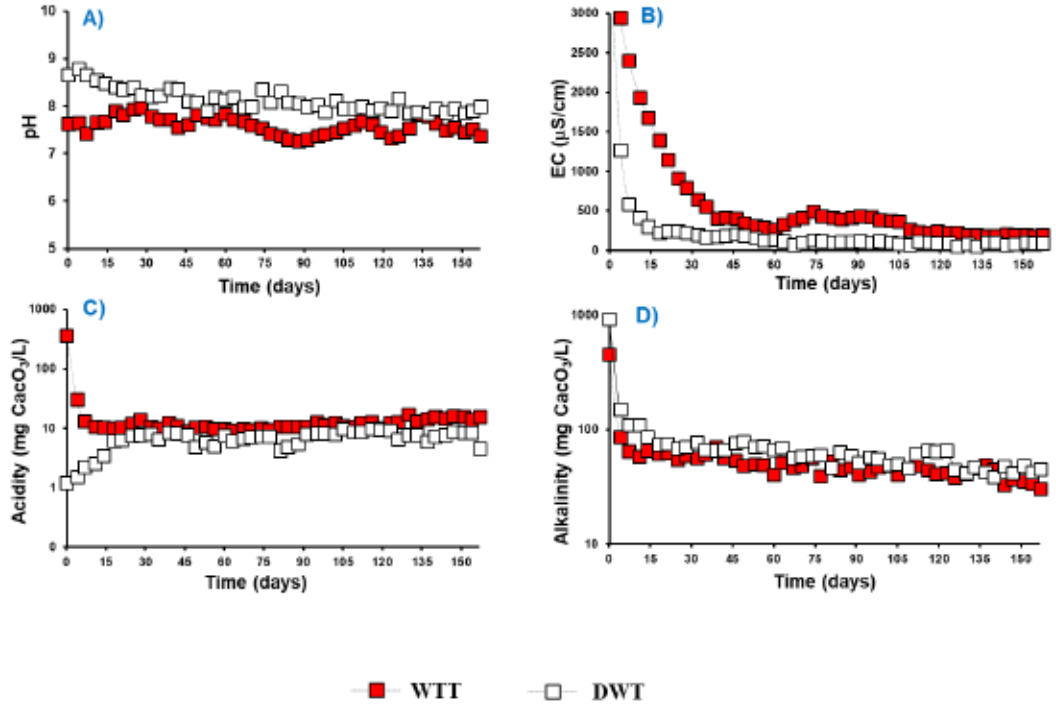

Figure 5.13 (A) pH, (B) electrical conductivity, (C) acidity, and (D) alkalinity evolution within the leachates from the WTT and DWT tailings.

Figure 5.14 shows the chemical quality of the leachates in cumulative and mass-normalized concentrations (mg/kg). Sulfate was selected as a tracer for sulfide oxidation, while Si and Al were selected to indicate aluminosilicate dissolution and [Ca+Mg] was selected to indicate carbonate dissolution (Benzaazoua et al., 2004). Fe, As, Ni, and Cu were chosen as examples of contaminants. Cumulative sulfate leaching over 157 days was substantially different for the two studied samples, with about 6358 mg/kg for WTT and 1391 mg/kg for DWT. More sulfate was leached from WTT compared to DWT due to the high content and high liberation degree of sulfur minerals within WTT (Figure 5.14.A). Moreover, the small amounts of remaining S-bearing minerals in the DWT tailings were mostly in the form of pyrite and pyrrhotite, while the S-bearing minerals in WTT were essentially pyrite, pyrrhotite, arsenopyrite, and gersdorffite. Arsenopyrite and gersdorffite exhibit very high reactivity with a high

oxidation rate when subjected to atmospheric conditions, as demonstrated by the study of Chopard et al. (2017). Calculated sulfide mineral oxidation rates for the studied samples were 40.5 mg/kg/day and 8.8 mg/kg/day for the WTT and DWT samples, respectively.

Figure 5.14.D shows that the cumulative aluminum release was approximately similar in both tailings: approximately 1.5 mg/kg for WTT and 1.2 mg/kg for DWT. However, more Si was released by the DWT sample compared to the WTT (Figure 5.14.E). Silicon release was about 936 mg/kg for DWT and 677 mg/kg for WTT. Thus, the Si-bearing minerals were enriched DWT by bulk sulfide flotation and then the release rate was higher within this sample.

As shown in Figure 5.14.B-C, Ca and Mg releases were higher in WTT compared to DWT. Cumulative Ca and Mg concentrations over 157 days were approximately 1975 and 882 mg/kg for WTT and DWT, respectively. This behaviour is closely related to the WTT oxidizing geochemical environment. Indeed, this result follows the expected behavior of the both samples during weathering tests: sulfides oxidize and carbonates dissolve, buffering the acid being produced (Dold, 2017; Rimstidt and Vaughan, 2003). This result also justifies the neutral values of the pH over the 157 days of reaction. Less Ca and Mg was released from DWT due to its low reactivity. The DWT released more Fe than the WTT samples (Figure 5.14.F). Iron release was approximately 1.07 mg/kg for DWT and 0.56 mg/kg for WTT. Moroever, the change in geochemical conditions (e.g., pH, Eh, iron concentrations) may have led to iron hydroxide precipitation. Indeed, leachates from the WTT were characterized by circumneutral pH values (7.3–7.9) and oxidation-reduction potential ranged between 0.4 and 0.7 V, which are more favorable for iron hydroxide precipitation (Cravotta III, 2008; Elghali et al., 2021a).

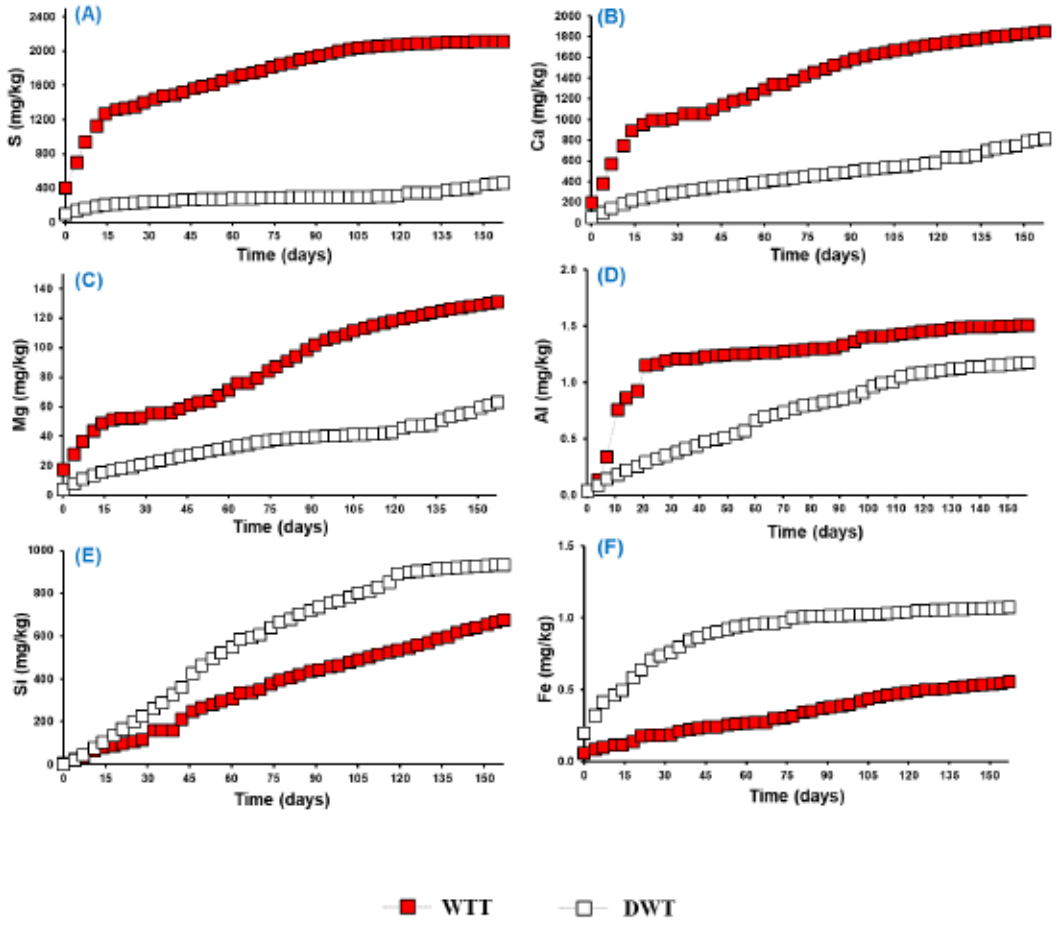

Figure 5.14 Evolution of the chemical quality of the leachates from WTT and DWT: (A) S, (B) Ca, (C) Mg, (D) Al, (E) Si, and (F) Fe. Concentrations are presented as cumulative, and mass normalized.

A significant difference was observed in terms of the concentration of some leached metals from WTT and DWT. As expected, the WTT sample was characterized by a non-negligible contamination potential. Concentrations of Ni and As collected immediately after each leaching cycle exceeded the maximal accepted concentrations fixed by Quebec provincial legislation (Directive 019, 2012). However, Fe and Cu never exceeded environmental criteria (Figure 5.15). DWT leachates present very low concentrations of contaminants (i.e., As, Ni, Fe, and Cu). Thus, this desulfurized

material showed a low risk potential in weathering cell test conditions. Since the weathering cells are not recognized as representative of field conditions, and their leachates cannot be directly compared to environmental criteria, it is suggested to confirm the results with larger scale tests, such as column tests, to better define the risk.

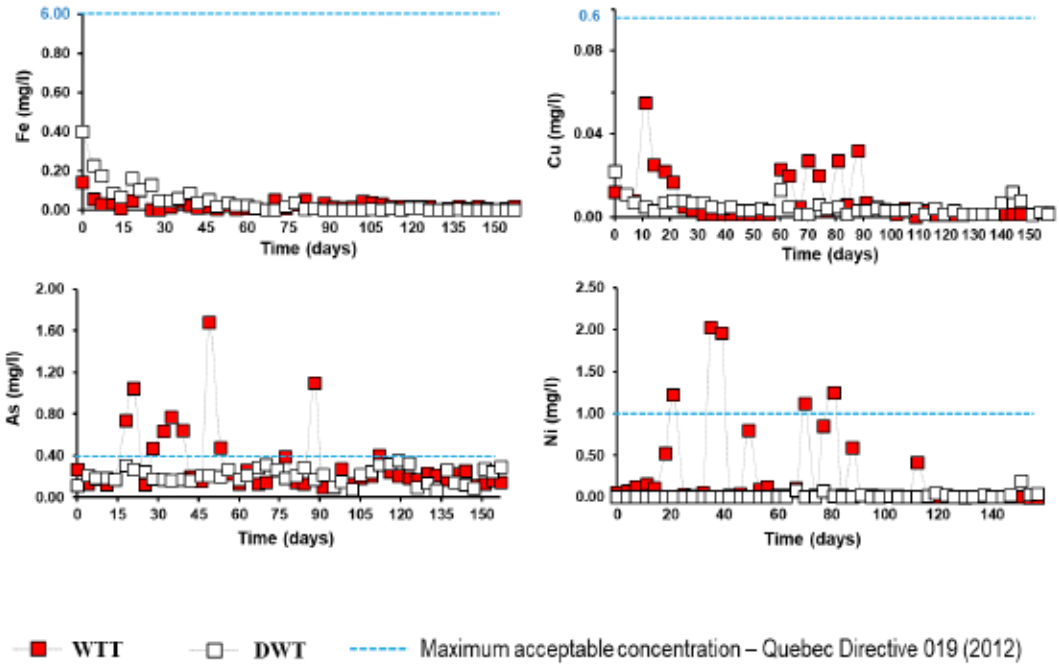

Figure 5.15 Contaminants (Fe, Cu, As, and Ni) leaching within WTT and DWT.

Long-term assessment of the AMD generation potential

As demonstrated previously using static and NAG tests, WTT would be acid generating. However, the kinetic test results do not support this conclusion. The pH values ranged between 7.3 and 7.9 over the 157 days of testing. This can be explained by the texture of the material and the relatively short testing time. Moreover, the lag time for acid generation is an important consideration in AMD control. Early results of geochemical testing may not reflect long-term behavior (Chopard et al., 2019). Thus, long-term

predictions of geochemical behavior for the studied samples were performed using oxidation–neutralization curves (Benzaazoua et al., 2004), which use Ca+Mg+Mn releases as a tracer of neutralizing mineral dissolution and sulfate release as a tracer of sulfide oxidation. This involves comparing the initial solid concentrations of Ca+Mg+Mn and S with the collected concentrations of the same elements within the leachates. In this study, only [Ca+Mg] were used and Mn was excluded because of its capacity to hydrolise and generate acidity, similar to Fe (Jambor et al., 2003). The oxidation-neutralization curves are plotted to compare the cumulative amount of the dissolved sulfide oxidation products (sulfate: SO_4^{2-}) from each cycle and the acid neutralization products (Ca, Mg) (Benzaazoua et al., 2004). These curves showed a linear relationship. Correlation coefficients (R^2) for the linear regression were higher than 0.9 and are presented in Fig. 3S-A and 3S-B (Annexe B).

Extrapolating the oxidation–neutralization curves over a longer time and projecting the initial sulfur and [Ca+Mg] contents of the solid materials (Fig. 3S-C) (Annexe B), the acid generating potential of the studied samples was assessed and derived. The results revealed that the WTT could generate AMD in the long-term. However, the DWT is not likely too. It is important to mention that this extrapolation relies on three hypotheses: i) the linear relationship will not be affected by the mineralogical composition of the solid samples over the long-term, ii) the geochemical environment is constant with time, and iii) the ratio between neutralization products and oxidation products remains linear (Benzaazoua et al., 2004).

The WTT sample was located under the oxidation–neutralization curve, which means that this material would be acid generating in the long term. Contrariwise, the DWT was located above the oxidation–neutralization curve. This means that the DWT would not be acid generating in the long-term. In other terms, the desulfurized material contains less sulfides/sulfosalts and sufficient neutralizing minerals to neutralize the

acidity generated by sulfide/sulfosalt oxidation. Thus, the kinetic tests (long-term) predicted results agree with the conclusions drawn from static and NAG tests.

5.5 Conclusion

This study was structured around two main goals: i) modeling and optimization of environmental desulfurization of the Whale Tail tailings (Amaruq mine) using flotation to prevent CMD generation (especially As/Ni-CND), and ii) studying the effectiveness of the desulfurization process by assessing the environmental behavior of the desulfurized tailings. Modeling and optimization of the bulk sulfide flotation process of the Whale Tail tailings containing 3% S and 0.24% As was performed using response surface methodology along with central composite design as a statistical tool. pH, collector (PAX) dosage, activator ($CuSO_4$) dosage, MIBC dosage, and solid concentration were the control factors in this study.

The main findings and conclusions drawn from this study are as follows:

- the Whale Tail tailings (WTT) consist of fine-grained particles with a high sulfur content, mostly in the form of pyrrhotite, pyrite, and gersdorffite;
- WTT was classified as acid generating using the ABA test according to the Sobek and NAG tests;
- collector dosage was the factor with the most statistically significant effect on sulfur recovery;
- environmental desulfurization using non-selective flotation process under optimal conditions allowed for the removal of more than >96% of the sulfides occurring within the tailings;
- the best performance of WTT desulfurization test reached 0.11% of residual sulfur and 0.03% of residual arsenic in the desulfurized material, for a flotation

conducted at pH=11.5, PAX= 158 g/t, $CuSO_4$= 300 g/t, MIBC= 55 g/t, and Cs= 29.3%;

- remaining sulfides (pyrrhotite, pyrite, gersdorffite) within the desulfurized tailings (DWT) were mainly associated or locked in gangue grains;
- remaining sulfide minerals in the desulfurized Whale tailings (DWT) were considered to be non-reactive due to their association with gangue minerals (mainly silicates);
- DWT did not present a significant risk of acid generation, as confirmed by the ABA and NAG tests;
- kinetic tests, at laboratory scale, proved that leached metals (As, Ni, Cu, and Fe) were below the criteria set by Directive 019; and
- environmental desulfurization by froth flotation is considered an integrated approach to sustainably manage mine tailings by preventing the generation of contaminated mine drainage.

Acknowledgements

The authors thank URSTM staff for their support with materials testing and analyses. Funding for this study was provided by a Collaborative Research and Development granted to I. Demers by NSERC and industrial partners. Finally, many thanks must go to the XPS laboratory in Sudbury for their help in achieving QEMSCAN analysis.

CHAPITRE 6

ENVIRONMENTAL DESULPHURIZATION OF WASTE ROCK TO PREVENT CONTAMINATED NEUTRAL DRAINAGE GENERATION, PART I: MINERALOGICAL FEATURES AND PROSPECTS OF INTEGRATED WASTE MANAGEMENT

Préambule : Cet artcile a été accepté pour publication dans la revue *Journal of Geochemical Exploration*, après des corrections mineures.

Ait-khouia Yassine[a], Benzaazoua Mostafa[a,b,*], Morozova Ievgeniia[c] ,Demers Isabelle [b]

[a] Research Institute on Mines and Environment, University of Quebec in Abitibi Témiscamingue, 445, boul. de l'université, Rouyn-Noranda J9X 5E4, Quebec, Canada

[b] Mining environment and circular economy, Mohammed VI Polytechnic University, Lot 660. Hay Moulay Rachid, 43150, Ben Guerir, Morocco

[c] Nikon Metrology, 12701 Grand River Ave, Brighton, MI, 48116, USA

Corresponding author. E-mail address: mostafa.benzaazoua@uqat.ca

6.1 Abstract

Mining activities generate vast amounts of waste rock (WR); if this waste is sulphide- and sulphosalt-bearing, it can pose a risk to ecosystems due to contaminated mine drainage. Strategic long-term planning is necessary to prevent and mitigate adverse environmental impacts. This study includes a detailed characterization of WR from a mine in northern Canada and defines the diameter of physical locking of sulphides and sulphosalts (DPLS) that can be used to separate the WR into two fractions according

to the geochemical reactivity. An automated mineralogy system (QEMSCAN®) and computed tomography were used to quantify the liberation degrees of acid-generating (sulphides) and neutralizing minerals (carbonates). Chemical and mineralogical characterization indicated that sulphides, mostly pyrite (FeS_2) and gersdorffite (NiAsS) (dominant sulphides), were enriched in the fine- to mid-sized fractions compared to the coarse fractions. These minerals were more liberated within the fine fractions and their liberation degree was considered negligible at sizes > 2.5 mm. Consequently, 2.5 mm was defined as the critical diameter of sulphide reactivity (DPLS) for the studied WR. Furthermore, kinetic tests using humidity cells were conducted to confirm this result and to assess the geochemical behaviour of the total fraction (< 10 mm), the coarse fraction (> 2.5 mm) and the fine fraction (< 2.5 mm). Sulphides associated with the coarse fraction were not significantly exposed to weathering conditions; sulphides were associated with non-sulphide gangue minerals, which was confirmed by QEMSCAN® and computed tomography. Moreover, mineral weathering occurred primarily in the fine fraction (< 2.5 mm) due to the higher available exposed surface area of the minerals. The geochemical analysis of the leachate from the humidity cells revealed that the pH values remained between 7.07 and 8.61 and that the instantaneous metal concentrations (Fe, Cu, and Ni) were below the environmental limits for the duration of the test (154 days). However, As concentrations from fine and total fractions exceeded environmental criteria. Sample reactivity showed that the fine fraction controlled the geochemical behaviour of the studied WR, where the fine fraction was 1.5 times more reactive than the total fraction and 10 times more reactive than the coarse fraction which represents about 60 wt% of the total sample. Consequently, screening waste rock in accordance with the DPLS could prove to be an effective method for managing WR to prevent contaminated drainage. This approach may allow a reduction in the amount of WR to be stored in surface piles (which need to be managed) and will reduce the costs associated with the reclamation of waste rock piles.

Keywords: contaminated mine drainage, waste rock management, mineral liberation degree, diameter of physical locking of sulphides, humidity cells.

Résumé

Les activités minières génèrent de grandes quantités de stériles miniers (WR); si ces rejets contiennent des sulfures et des sulfosels, ils peuvent présenter un risque pour les écosystèmes en raison du drainage minier contaminé. Une planification stratégique à long terme est nécessaire pour prévenir et atténuer les impacts environnementaux négatifs. Cette étude comprend une caractérisation détaillée des WR issus d'une mine au nord du Canada et définit le diamètre d'encapsulation physique des sulfures et des sulfosels (DPLS) qui pourra être utilisé pour séparer les WR en deux fractions selon leurs réactivités géochimiques. Un système de minéralogie automatisé (QEMSCAN®) et la tomographie 3D (CT) ont été utilisés pour quantifier les degrés de libération des minéraux générateurs d'acide (sulfures) et neutralisants (carbonates). La caractérisation chimique et minéralogique ont indiqué que les sulfures, principalement la pyrite (FeS_2) et la gersdorffite (NiAsS) (sulfures dominants), sont enrichis en fractions fines à moyennes par rapport aux fractions grossières. Ces minéraux sont plus libérés dans les fractions fines et leur degré de libération est considéré comme négligeable à des tailles > 2,5 mm. Par conséquent, 2,5 mm a été défini comme le diamètre critique d'encapsulation physique des sulfures (DPLS) pour le WR étudié. De plus, des essais cinétiques en cellules humides ont été réalisés pour confirmer ce résultat et évaluer le comportement géochimique de la fraction totale (< 10 mm), de la fraction grossière (> 2,5 mm) et de la fraction fine (< 2,5 mm). Les sulfures associés à la fraction grossière n'ont pas été significativement exposés aux conditions atmosphériques; les sulfures sont associés à des minéraux de gangue non sulfurés, ce qui a été confirmé par QEMSCAN® et la CT. De plus, l'altération des minéraux s'est produite principalement dans la fraction fine (< 2,5 mm) en raison de la plus grande surface exposée des minéraux sulfureux. L'analyse géochimique des lixiviats issus des cellules humides a

révélé que les valeurs de pH restent comprises entre 7,07 et 8,61 et que les concentrations instantanées en métaux (Fe, Cu et Ni) sont inférieures aux limites environnementales pendant la durée de l'essai (154 jours). Cependant, les concentrations d'As provenant des fractions fines et totales dépassent les critères environnementaux. La réactivité de l'échantillon a montré que la fraction fine contrôle le comportement géochimique global du WR étudié, où la fraction fine était 1,5 fois plus réactive que la fraction totale et 10 fois plus réactive que la fraction grossière qui représente environ 60 % en poids de l'échantillon total. Par conséquent, le criblage des stériles miniers selon le DPLS pourrait s'avérer une méthode efficace de gestion des WR pour prévenir le drainage minier contaminé. Cette approche peut permettre une réduction de la quantité de WR à stocker dans des tas de surface (qui doivent être gérés) ainsi que les coûts associés à la remise en état des tas de stériles.

Mots-clés : drainage minier contaminé, gestion des stériles miniers, degré de libération minérale, diamètre d'encapsulation physique des sulfures, cellules humides.

6.2 Introduction

Mining extraction and ore processing activities worldwide produce large amounts of WR and tailings. They are the most common solid waste categories at a mine site, regardless of the deposit type, and/or extraction method. Although recent technical and technological advances in mining have made extraction more efficient, most of the raw material (low-grade bedrock) moved to access profitable ore bodies is still discarded as waste (Vriens et al., 2020). Gigatons of waste are generated by the mine activity each year worldwide (Hudson-Edwards et al., 2011). As lower-grade/higher tonnage mineral deposits are mined to meet growing global demand for mineral resources, this amount is expected to grow (Elghali et al., 2018).

Waste rock (WR) is often kept on-site indefinitely if there is no technical and economic ability for reuse or valorization (Ait-Khouia et al., 2021; Dino et al., 2020; Lottermoser, 2011). It is commonly deposited in unsaturated piles, usually reaching large dimensions, and can cause a significant threat to the environment (Ait-Khouia et al., 2021; Elghali et al., 2019a). WR is composed of coarse materials that are highly heterogeneous, especially in terms of particle size distribution (PSD), as opposed to tailings, which are more homogeneous (Vriens et al., 2020). Depending on the geological context of the deposit, WR can contain residual sulphide minerals (e.g., pyrite, pyrrhotite, arsenopyrite) with different reactivities under atmospheric conditions. The weathering of sulphidic WR when exposed to water and oxygen triggers acidic drainage generation with high metal/metalloid and sulphate concentrations above the regulatory criteria (Blowes et al., 2014; Dold, 2017; Paktunc and Davé, 2000). This phenomenon is known as acid mine drainage (AMD) and is considered an environmental problem on a global scale. AMD causes water quality problems that persist for many decades or even millennia (Förstner and Wittmann, 2012; Vriens et al., 2020). Oxidation of sulphidic WR can generate circumneutral drainage effluent if there is a sufficient amount of neutralizing minerals (e.g., carbonates and silicates). However, the effluent quality in terms of harmful metal(oids) release may not meet the environmental criteria even at neutral pH. This could lead to environmental problems such as contaminated neutral drainage (CND) (Ait-Khouia et al., 2021; Mayes et al., 2009; Plante et al., 2011).

The geochemistry of mine drainage (AMD and CND) is dependent on the mineralogy of the WR in terms of sulphide and carbonate types, their content, and their dissolution rates (acidifiers and neutralizers), which can be variable (Blowes et al., 2014; Charuseiam et al., 2021; Paktunc and Davé, 2000; Parbhakar-Fox et al., 2018). Contaminated mine drainage prediction is essential for assessing the environmental impact of mine waste and designing an appropriate convenient reclamation scheme (Demers et al., 2017). The WR geochemical behaviour assessment is generally performed at a laboratory scale using static and kinetic tests (Amar et al., 2021; Dold,

2017; Jambor et al., 2007). For short-term, low-cost, and rapid prediction of AMD formation, acid-base accounting (ABA), and net acid generating (NAG) test are the most commonly used static tests (Sapsford et al., 2008; Sobek, 1978; Stewart et al., 2006). Kinetic tests are designed to assess the minerals reactivity and leaching rates for various chemical species (Erguler and Erguler, 2015; Paktunc and Davé, 2000).

Previous studies have also demonstrated that the tree main factors controlling the geochemical reactivity of mine waste (including WR) were particle size, specific surface area, and mineral liberation degrees (Amar et al., 2020; Elghali et al., 2021; Mafra et al., 2020). The particle size is directly related to the specific area (Mbonimpa et al., 2009) and subsequently to the mineral liberation degree. Based on recent findings on the effect of the PSD and mineral liberation on the geochemical behaviour, Erguler and Erguler (2015) demonstrated that the geochemical behaviour of mine waste was positively correlated to the particle size. It was found that when the particle size of a material is finer, its specific surface area increases, and its geochemical reactivity becomes higher. This can be explained by the higher percentage of sulphides exposed to the weathering (liberation degree) in fine samples. These findings were confirmed by Amar et al. (2020) and Elghali et al. (2018), who studied the effect of particle size and the liberation degree of sulphides and carbonates on WR geochemistry. In this context, the study conducted by Elghali et al. (2018) defined the parameter called "diameter of physical locking of sulphides (DPLS)" to manage WR. The DPLS is the size of particles above which sulphides liberation is negligible. Using this parameter, WR could be separated upstream into two fractions to improve waste management: i) a fraction above the DPLS, considered coarser and unreactive, in which the sulphide minerals are negligibly liberated (locked inside gangue minerals) - generally, this fraction could be valorized in the field of civil engineering (Taha et al., 2021); and ii) a fraction below the DPLS, considered the fine and reactive fraction (sulphides mostly liberated), that could be desulphurized, valorized, or managed as tailings (Ait-Khouia et al., 2021; Amar et al., 2020). The definition of the DPLS is based on advanced

automated mineralogical analysis coupled with kinetic testing (Elghali et al., 2019a). The screening of WR material according to the DPLS parameter could prove to be an effective technique in global mine WR management. This approach may allow a reduction in the amount of problematic WR to be stored in surface piles (which need to be managed) and consequently a decrease in the economic cost of WR pile reclamation.

This study aimed to tackle challenges related to sustainable WR management. It was focused on developing practices that allow decontamination, stabilization, and safe storage of mine WR containing contaminant-bearing sulphide minerals. More specifically, this work involved advanced characterization techniques with an evaluation of the environmental behaviour and prediction of contaminated mine drainage generation (AMD and CND) of WR sampled from an open-pit mine in northern Canada. Indeed, the influence of the particle size and liberation degree of sulphides and carbonates on the geochemistry of mine drainage were carefully examined. The main objectives of this paper were to: i) characterize the WR, ii) determine the DPLS and confirm it using humidity cell kinetic tests, and iii) predict the long-term oxidation/neutralization potential of the WR considering sulphide and carbonate mineral liberation.

6.3 Materials and Methods

This section details the sampling methods, material preparation, characterization, and static testing using acid-base accounting (ABA) tests as well as kinetic testing using humidity cells.

6.3.1 Sampling and Material Preparation

According to the preliminary tests conducted in situ by the mining company, it was demonstrated that a material crushing and screening step at 10 mm (as critical size particles) was to be implemented for successful upgrading by sensor-based ore sorting (SBS). As shown in **Figure 6.1**, the material used in this study is the fraction below 10 mm, which was marginalized because it could not be sorted efficiently due to its size. This material was received from an operating gold mine in northern Canada.

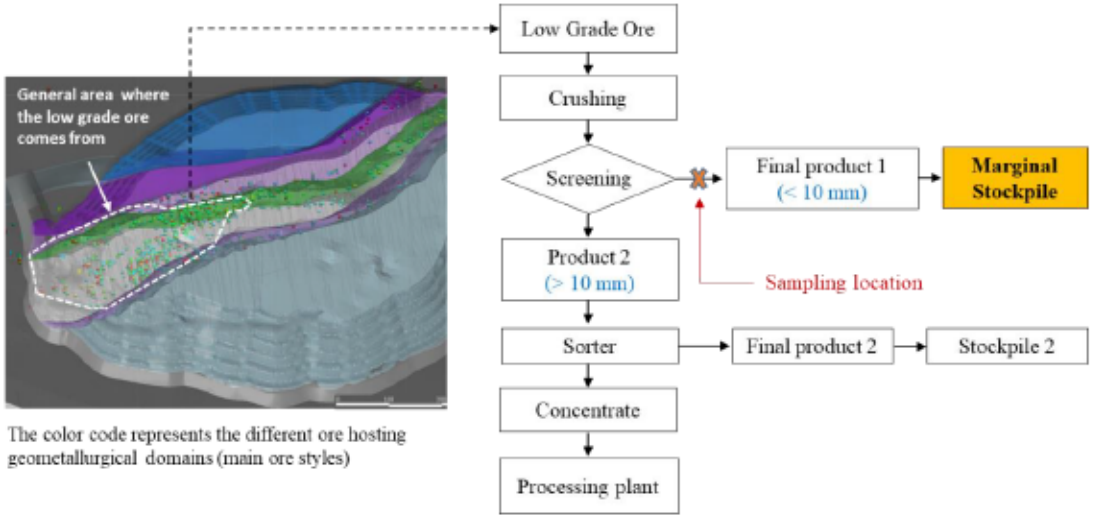

Figure 6.1 Sampling and simplified sorting plant concept.

To ensure objectivity in sampling, a small-scale pile of material (approximately 3.5 tone) was built during the operation. This approach allowed samples to be obtained with a representative particle size distribution as compared to other widely used approaches such as grab sampling in the WR dump. This small stockpile came from various areas peripheral to the mineralized zones, as shown in Figure 6.1. The 3.5 t was then prepared by coarse crushing (100 mm) and sieving (10 mm and 25 mm). Three particle size fractions were then produced: –10 mm, (+10 mm / –25 mm) and (+25 mm / –100 mm). All fractions were sampled regularly during production to obtain

approximately 20–25 kg for detailed characterization. The –10 mm sample was then transported to the IRME-UQAT laboratory for further preparation steps and experiments. This fraction could not be sorted out because it was too fine. To ensure that the sample was representative and homogeneous, manual quartering was completed. The sample was then divided into seven grain-size fractions: –53 µm (F1); –300 µm / +53 µm (F2); –850 µm / +300 µm (F3); –1.4 mm / +850 µm (F4); –2.5 mm / +1.4 mm (F5); –5 mm / +2.5 mm (F6); and –10 mm / +5 mm (F7). The wet sieving of this WR allowed the removal of any fine particles that were attached to larger particles by cleaning their surfaces. All fractions were characterized to study their mineralogy as well as their geochemical behaviour.

6.3.2 Methodology

To better estimate the acid generation potential (AGP) of the studied WR, a rigorous methodology was used, starting by material sampling, followed by a multi-technique laboratory characterization. The sample was divided into seven grain-size fractions to take into account sulphide and carbonate distributions among particle sizes and to target the most environmentally problematic fraction. The coarse fractions (i.e., F4, F5, F6 and F7) were washed to remove fine particles attached to the particle surface due to the intrinsic humidity of the material. The methodology used in this project is summarized in Figure 6.2.

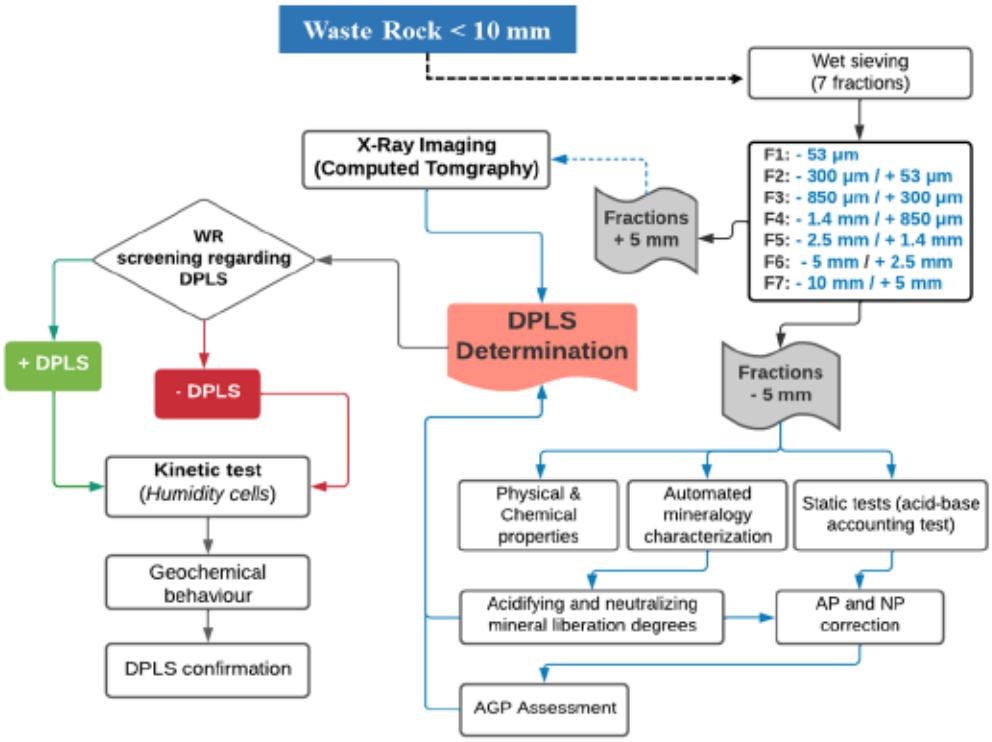

Figure 6.2 Methodology used in this study.

6.3.3 Material Characterization

6.3.3.1 Physical and Chemical Properties

Particle size distribution was determined by sieving materials at the following sieve sizes: 0.053 mm, 0.3 mm, 0.85 mm, 1.4 mm, 2.5 mm, 5 mm, and 10 mm (ASTM, 2014). Specific gravity (Gs) was determined using a helium gas pycnometer with Micromeritics Accupyc 1330 in the URSTM-IRME UQAT laboratory in Quebec, Canada (Allen, 2013), and specific surface area (SSA) was determined by a Micromeritics surface area analyzer implementing the B.E.T. method (Brunauer et al., 1938). Chemical assays were performed at Activation Laboratories (Actlabs) in

Ontario, Canada using peroxide fusion inductively coupled plasma mass spectrometry/optical emission spectrometry (ICP-MS/OES). These chemical analyses were performed on the samples after they had been homogenized and pulverized.

Total sulphur (wt% S ± 0.1 to 0.5) and total inorganic carbon (wt% TC ± 0.5 to 1) contents were analyzed by induction furnace (ELTRA CS-2000 with a detection limit of 0.09%). The chemical composition of the major and minor elements (Al_2O_3, Cr_2O_3, K_2O, MnO_5, Na_2O_5, F_2O_3, SiO_2, MgO, and LOI) was determined by X-ray fluorescence (XRF) (Thermo Scientific, SGS Laboratory in Ontario, Canada) with a detection limit of 0.01 wt%.

6.3.3.2 Mineralogical Investigations

The mineralogical composition of the WR was determined by optical microscopy (OM) in the URSTM-IRME UQAT laboratory. The identification of mineral species and texture observations were carried out in reflected light mode using an AxioImager M2m optical microscope (Zeiss, Oberkochen, Germany) equipped with the AxioVision (Version 4.8) software. Depending on the particle size fraction, the number of polished section was determined carefully to make a good statistical representation (e.g., more than 10,000 grains were analyzed in the fine fractions) (Benzaazoua et al., 2017a). The number of polished sections analysed were 1, 2, 2, 3, 4, and 4 for F1, F2, F3, F4, F5, and F6, respectively.

The mineralogical composition and texture of the different fractions were further characterized using Quantitative Evaluation of Materials by Scanning Electron Microscopy (QEMSCAN®, FEI, Quanta 650 platform with Field Emission Gun) in the XPS laboratory in Sudbury, Ontario, Canada. This instrument was fitted with Bruker SDD energy dispersive spectrometers (EDS). QEMSCAN® is an automated mineralogy tool able to analyze the mineralogical composition of samples based upon their chemical composition at a micrometer scale. Using fast X-ray spectra acquisition,

it generates particle maps that are colour-coded by mineral. Interpretation of the corresponding data files enables quantification of modal mineralogy, grain size, mineral texture, elemental deportment, and mineral liberation of samples (Benzaazoua et al., 2017b; Butcher et al., 2000; Pirrie et al., 2004). The polished sections were analyzed in PMA mode (particle mineralogy analysis), generating full X-ray maps at the set measurement resolution. The measurement resolution ranged from 0.5 to 7 µm depending on sample particle size and mineral texture. Uncertainty for analyses was based on reconciling calculated assays from the mineralogy and the measured elemental assay. To confirm the mineral identification and chemical composition, electron probe micro-analysis (EPMA) was also conducted on the samples. A Cameca SX-100 electron probe micro-analyzer was used to analyze at least ten particles of each mineral. This provided a more accurate and precise composition of the minerals and quantification of trace elements. This instrument was coupled with four high-resolution wavelength-dispersive X-ray spectrometers (WDS). All quantitative analyses (EPMA) were performed using a focused beam at 20 kV accelerating voltage and 20 nA constant beam current. A set of calibration standards (e.g., InAs, Co, Ni, chalcopyrite, orthoclase, pyrite, etc.), was used to better perform quantitative analysis of the materials and allow accurate microanalysis at a wide range of concentrations.

6.3.3.3 X-Ray Computed Tomography: Characterization of Sulphide Distribution

The fraction size greater than 5 mm (F7) was scanned by the X-ray computed tomography (X-ray CT) technique using an XTH 225 ST system (Nikon Metrology). X-ray CT, a non-destructive imaging device, can be used for many purposes in materials sciences and geological applications (Maire and Withers, 2014; Stock, 2008). It is a powerful tool in geosciences for characterizing the spatial distribution of minerals in three dimensions (3D) (Kahl et al., 2017), as well as fractures and pores (Latief et al., 2017). X-ray CT can also be used to qualitatively and quantitatively analyze the internal structures of geological materials as long as they are sufficiently distinguished

by differences in atomic composition and material density. This tool has the main advantage of being able to analyze the 3D interior of samples. This eliminates the stereological error that is present in conventional two-dimensional (2D) microscopy analysis (Guntoro et al., 2019). A set of projection images taken from various angles of the specimen are used to reconstruct tomographic images (tomograms). After the 3D image reconstruction, data could be used to conduct qualitative and quantitative specimen analyses, including the porosity distribution and localization of structural material inclusions (spatial mineral distribution). A rotary rifle divider was used to select the > 5 mm fraction for this analysis. This fraction sample was placed in a cylindrical polystyrene mold (120 x 200 mm) and scanned using CT. Some selected grains from this fraction were also scanned separately. Over 360° rotation, the number of projections taken per CT was about 2500 (minimum). The 3D reconstruction was made from all 2500 radiographs and the voxel size resolution was about 70 µm.

6.3.4 Acid Generation Potential (AGP) Assessment

6.3.4.1 Static Tests

Static tests were performed on the WR materials (different fractions) using the acid-base accounting (ABA) test according to the original Sobek method (Sobek, 1978), modified by (Miller et al. (1991b) to evaluate the acid generation potential. The acid potential (AP) was calculated considering pyrite as the only sulphide using $S_{sulphide}$ (AP = 31.25 × $S_{sulphide}$ wt% (kg $CaCO_3$/t)). The carbonate neutralization potential (NP) was calculated using total carbon (Tc) considering calcite as the only the carbonate (NP = 83.3 × Tc wt% (kg $CaCO_3$/t)). The net neutralization potential (NNP) was calculated by subtraction of the AP from the NP (Miller et al., 1991a; Weber et al., 2004). An NNP value greater than 20 kg $CaCO_3$/t classifies the material as non-acid forming, whereas a material with NNP less than -20 kg $CaCO_3$/t is considered as acid generating. NNP values between –20 and 20 kg $CaCO_3$/t defines the uncertainty (Bouzahzah et al.,

2015;Miller et al., 1991; Sobek, 1978). The NPR indicator (neutralization potential ratio; NP/AP) can also be used to assess AGP; typically, a sample is classified as non-acid forming if NPR > 2.5, uncertain if 1 < NPR < 2.5, and acid generating if NPR < 1. The AP and NP tests were corrected to account for sulphide and carbonate liberation considering the initial texture of the studied fractions (Erguler and Erguler, 2015; Mafra et al., 2020). To do so, Eqs. (1) and (2) were used, as suggested by Elghali et al. (2018):

$$\text{Available AP} = 31.25 \times S_{sulphide}\ \text{wt\%}\ (\text{kg } CaCO_3/\text{t}) * L_s \quad (1)$$

$$\text{Available NP} = 83.3 \times T_C\ \text{wt\%}\ (\text{kg } CaCO_3/\text{t}) * L_c \quad (2)$$

where L_s and L_c are the liberation degree of sulphide and carbonate, respectively. Their values were obtained by recalculating considering all liberation classes and using Eq (3) (Elghali et al., 2018):

$$\%L = \sum_{c=0}^{100} Ci * Fi/100 \quad (3)$$

where Ci is the average liberation class as determined by QEMSCAN®, and Fi is the class Ci average frequency. For instance, 55% is the value used for the class 50–60%.

6.3.4.2 Kinetic Tests: Humidity Cells

The diameter of the physical locking of sulphides (DPLS) parameter was defined based on the automated mineralogy system. This diameter separates the WR into two fractions according to the geochemical reactivity. To confirm the DPLS and to assess the geochemical behaviour, three fractions were prepared for use in humidity cell testing (HC): a fraction with all grains < 10 mm, hereafter referred to as the total fraction; ii) a fraction above the DPLS, called the coarse fraction; and iii) a fraction below the DPLS, called the fine fraction. The HC are mid-term leach tests standardized by ASTM standard D5744 (ASTM, 2014), and that are considered to be the most reliable geochemical characterization method for estimating the leachate quality of

mined materials (Maest and Nordstrom, 2017). HC are designed to accelerate the oxidation rate of sulphide minerals, the dissolution of carbonates, and the release of chemicals (Lapakko and Antonson, 2006).

This procedure consists of using a Plexiglas® cell with a 10.2 cm inner diameter and a 20.3 cm height holding 750 g of waste rock (dry mass). A geotextile layer is placed at the cell base to prevent loss of fine particles and simultaneously allow air to flow upward and leachate to drain downward. Each weathering cycle in the HC lasts for seven days and involves three steps: i) aeration of each cell with dry air for three days; (2) circulation of humid air (humidity index ranging between 90 and 100%) for the following three days; and (3) flushing the cells on the last day with 1 L of deionized water. After 4h of contact with the different tested fractions, the leachates from the humidity cells were collected and then analysed for pH, electrical conductivity (EC), redox potential (Eh), alkalinity, acidity, sulphur, and elemental concentrations. The elemental concentrations were analyzed using ICP-AES (PerkinElmer OPTIMA 3100 RL relative precision of 5%) on an aliquot acidified to 2% HNO_3 for preservation. The HC were run for 22 weekly cycles with no changes in the parameters.

6.4 Results

6.4.1 Physical and Chemical Characterization

Table 6.1 summarizes some properties of the studied WR (total fraction). Results from the particle size distribution showed coarse-grained materials with D_{10} = 0.18 mm, D_{30} = 1.4 mm, and D_{80} = 7.6 mm. The specific surface area of the WR was around 0.52 m^2/g and the specific gravity was 2.82 g/cm^3.

Table 6.1 Primary characteristics of the studied WR.

	Physical characteristics				
	D10(mm)	**D30 (mm)**	**D80 (mm)**	**SSA (m^2/g)**	**Gs**
Waste Rock	0.18	1.4	7.6	0.52	2.82

	S (%)	**C (%)**	**NNP ($CaCO_3/t$)**	**Acid generation**	**NPR**
Waste Rock	1.43	1.66	93.82	Non-Acid Generating	3.09

Whole rock analysis using XRF (wt%)		
Element	DL (%)	(%)
SiO_2	0.01	48.2
Al_2O_3	0.01	7.82
Fe_2O_3	0.01	16.5
MgO	0.01	11.7
CaO	0.01	6.08
Na_2O	0.01	0.46
K_2O	0.01	1.44
TiO2	0.01	0.34
P_2O_6	0.01	0.08
MnO	0.01	0.33
Cr_2O_3	0.01	0.25
LOI	0.01	5.20

Chemical analysis (%) using ICP-MS		
Element	DL (%)	%
Al	0.01	4.20
Ca	0.01	3.60
Fe	0.05	11.7
K	0.1	1.41
Mg	0.01	5.64
Mn	0.001	0.24
Si	0.01	23.7
As	0.001	0.06
Co	0.001	0.00
Ni	0.001	0.09
Cr	0.01	0.13
Ti	0.01	0.18
Zn	0.001	0.01

DL: detection limit

Chemical analyses of the total sample as well as its corresponding fractions revealed that Si, Fe, Mg, Al, Ca, and K dominated the chemical composition (Table 6.1) and are closely related to non-sulphide gangue (NSG) minerals. The contents of Mn, Cr, and Ti in all fractions did not exceed 0.26, 0.2, and 0.28 wt%, respectively (Table 6.2). Sulphur and C contents did not exceed 2.2 wt% and 2 wt%, respectively. Iron-, arsenic-, cobalt-, nickel-, and zinc-bearing minerals (contaminant-bearing minerals) were primarily sulphides but occurred in small quantities. Average As, Co, Ni, and Zn concentrations were 0.064%, 0.006%, 0.09%, and 0.011% for all fractions, respectively. Results showed that the sulphur content was higher in the fine fractions (F2: 2.55 wt%; F3: 2.32 wt%) compared to other fractions (F1: 1.30 wt%; F4: 1.49 wt%; F5: 1.39 wt%; F6: 1.27 wt%; and F7: 1.14 wt%) (Table 6.2). The carbon content was high in the coarse fractions F4 (1.65 wt. %), F5 (1.84 wt.%), F6 (1.79 wt.%), and F7 (1.83 wt.%). The

whole rock using XRF analysis revealed the presence of major elements in oxide form. These included silicon (SiO_2) with 48.2 wt%, iron (Fe_2O_3) with 16.5 wt%, and magnesium (MgO) with 11.7 wt%. Other elements such as aluminium (Al_2O_3) and Ca, were also present in relatively high proportions. These results were consistent with previous ICP analyses (Table 6.1).

6.4.2 Mineralogical Characterization

A mineralogical study of the WR sample (smaller than 5 mm) and the corresponding fractions (F1 to F6) was performed using complementary techniques (OM, QEMSCAN®, and EPMA). Thus, modal mineralogy, mineral compositions, mineral liberation degrees, mineralogical associations, and S, Co, As, Ni, Ca, and Mg deportments were provided for all samples. Sample larger than 5 mm were characterized using X-ray CT to calculate the sulphide liberation degree.

Table 6.2 ICP-MS/induction furnace chemical analyses and static tests of the total sample and its corresponding fractions.

	Al	Ca	Fe	K	Mg	Mn	Si	As	Co	Ni	Cr	Ti	Zn	S	C	NNP	NP/AP	Fraction
	%	%	%	%	%	%	%	%	%	%	%	%	%	%	%	kg $CaCO_3$/t		wt%
Detection Limit	0.01	0.01	0.05	0.1	0.01	0.001	0.01	0.001	0.001	0.001	0.01	0.01	0.001	0.09	0.09			
F1 : –53 µm	5.14	3.82	13.1	1.7	7.38	0.26	20.3	0.08	0.012	0.15	0.2	0.28	0.015	1.30	0.68	16.01	1.39	7.12
F2 : –300µm / +53µm	4.31	4.50	12.6	1.4	5.26	0.24	21.9	0.08	0.009	0.09	0.14	0.21	0.014	2.55	1.48	43.56	1.55	5.97
F3 : –850µm / +300µm	4.37	3.66	12.2	1.4	5.29	0.22	23.1	0.05	0.006	0.08	0.14	0.20	0.012	2.32	1.38	42.38	1.59	9.47
F4 : –1.4mm / +850µm	4.35	3.51	11.9	1.4	5.41	0.23	23.8	0.05	0.005	0.07	0.12	0.19	0.012	1.49	1.65	90.83	2.95	8.42
F5 : –2.5mm / +1.4mm	4.21	3.68	12.1	1.4	5.38	0.23	23.5	0.05	0.005	0.07	0.12	0.18	0.011	1.39	1.84	109.81	3.52	9.88
F6 : –5mm / +2.5mm	4.21	3.45	11.5	1.5	5.28	0.23	24.4	0.05	0.005	0.08	0.13	0.18	0.01	1.27	1.79	109.52	3.77	23.24
F7 : –10mm / +5mm	3.92	3.48	11.3	1.3	5.81	0.24	24.6	0.07	0.006	0.09	0.13	0.16	0.01	1.14	1.83	116.67	4.26	35.90
Total sample	4.20	3.59	11.8	1.4	5.64	0.24	23.8	0.06	0.006	0.09	0.13	0.18	0.01	**1.43**	**1.66**	93.82	3.09	100

Table 6.3 EPMA analysis of observed sulphide grains.

Element	**Pyrite**			**Gersdorffite**			**Pyrrhotite**		
(LOD)	Analysis (%)		TC (%)	Analysis (%)		TC (%)	Analysis (%)		TC (%)
	Mean value	Range		Mean value	Range		Mean value	Range	
S (0.01)	53.27	52.44–55.44	46.55	19.25	18.89–19.48	19.4	38.70	38.05–39.28	37.67
As (0.06)	< 0.06	0–0.09	-	47.22	47.02–47.78	45.2	<0.06	< 0.06	-
Fe (0.04)	46.29	45.03–46.80	46.55	7.66	7.25–8.27	-	57.69	54.88–58.95	62.33
Co (0.05)	0.05	0–0.05	-	1.42	0.69–2.72	-	0.06	0.05–0.08	-
Ni (0.06)	< 0.06	< 0.06	-	24.46	23.38–25.41	35.4	0.38	0.30–0.49	-
Cu (0.07)	< 0.07	< 0.07	-	< 0.07	< 0.07	-	<0.07	< 0.07	-
Total	100.00	-	100.00	100.00	-	100.00	100.00	-	100.00

LOD: limit of detection; TC: theoretical composition based on mineral formula

6.4.2.1 Bulk mineralogy

Observations under OM indicated that pyrite was the major sulphide present in the WR, with trace amounts of arsenopyrite, pyrrhotite, and chalcopyrite (Fig. 6.3**A**). Different textures were displayed by sulphide minerals, which could be classified into three states: i) totally liberated sulphides (Fig. 6.3B), ii) moderately liberated sulphides with boundaries partially shared with other non-sulphide gangue minerals (NSG) (Fig. 6.3**C**), and iii) totally locked sulphides that were entirely encapsulated within NSG minerals (Fig. 6.3D). Qualitative OM observations revealed that the sulphide liberation degree depended on the grain-size fraction. Thus, sulphide minerals in coarser fractions (> 1.4 mm) were less liberated than those found in finer fractions. For the coarser fractions (> 2.5 mm), sulphide minerals became more encapsulated, with boundaries partially or fully shared with NSG minerals.

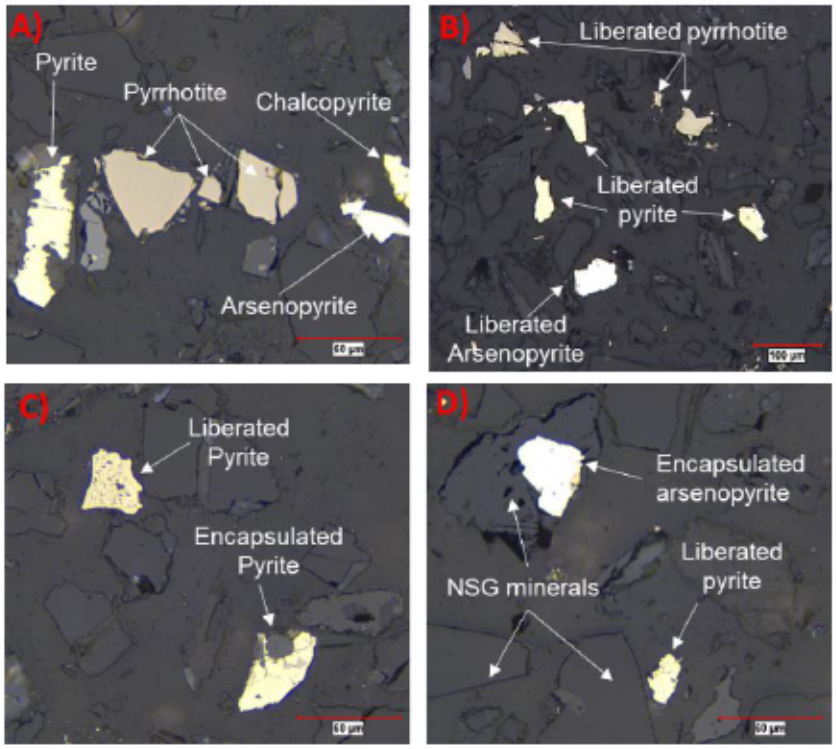

Fig. 6.3 Optical microscopy images illustrating sulphides and their liberation states: A) sulphide mineral observation, B) liberated sulphides, C) and D) sulphides partially liberated and/or totally encapsulated within NSG minerals.

The studied WR and its corresponding grain-size fractions were also analyzed by QEMSCAN® to determine the mineralogy, texture, and element deportments. Mineralogical results are provided in Figure 6.4, which shows the size-by-size mineralogy for the WR and all fractions as mineral mass wt% in the fraction (using size distribution for weighting). The mineral distribution for key minerals (sulphides and carbonates) in each fraction is also shown and compared to the size distribution to observe any preferential partitioning to particular particle size class. Electron probe microanalysis (EPMA) was performed on each sample to confirm the chemical composition of the minerals of interest (especially sulphides and carbonates).

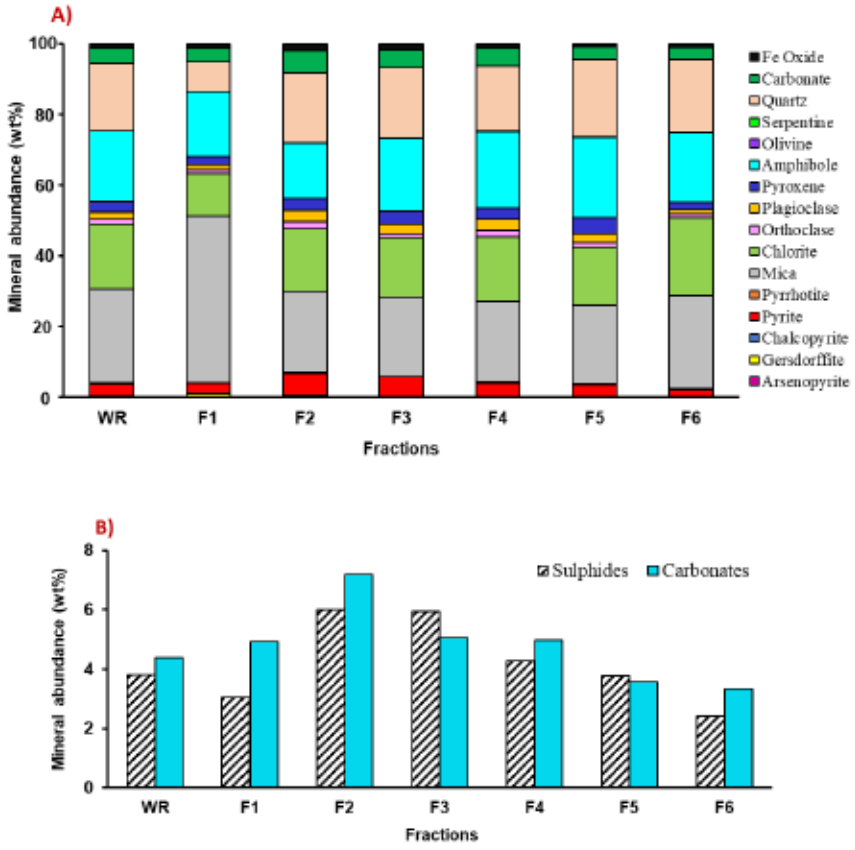

Figure 6.4 A) Mineralogical compositions of the studied WR (total sample) and its corresponding grain-size fractions using QEMSCAN® analysis, and B) carbonates and sulphides distributions within the studied WR and grain-size fractions.

The assay reconciliation is provided and the relationship between chemical assays and chemical compositions calculated using modal mineralogy is illustrated in Fig. S1.1 (Annexe C). This process involved the calculation of the mineralogical composition that corresponded with the ICP-MS and XRF chemical analyses. The coefficient of determination between the mineralogical composition and the chemical assay was approximately 0.99 (Fig. S1.1) (Annexe C).

The results of the QEMSCAN® modal analyses showed that silicates (mica, amphibole, quartz, chlorite, pyroxene, plagioclase, and orthoclase) constituted approximately 90 wt% of the studied WR (fraction < 5 mm) and all grain-size fractions (Figure 6.4A).

The principal sulphide phases detected were pyrite, pyrrhotite, and gersdorffite, with some traces of arsenopyrite and chalcopyrite (Figure 6.4A). Sulphide contents ranged from 2.43 to 5.99 wt% in different fraction samples. The F2 and F3 fractions contained the most sulphide-rich minerals with proportions of 5.99 and 5.94 wt%, respectively (Figure 6.4B). The studied WR contained more carbonates than sulphides, expect for F5 and F3, which contained slightly more sulphides than carbonates. Carbonates ranged from 3.34 to 7.20 wt% in the different fractions. The F2, F3, and F4 fractions were the richest with proportions of 7.20, 5.05, and 4.97 wt%, respectively (Figure 6.4B). Arsenopyrite and chalcopyrite occurred as trace minerals (< 0.1 wt%). These minerals ranged from 0.01 to 0.09 wt% and from 0.01 to 0.04 wt%, respectively, in all fractions. Pyrite was the dominant sulphide in the analyzed samples; its modal abundance was 3.49 wt% in the WR and ranged from 2.02 to 6.08 wt%. High pyrite abundances were noted in F2 and F3 with proportions of 6.08 and 5.58 wt%, respectively. In general, pyrrhotite was present in trace amounts (< 0.2 wt%) in most of these samples. High pyrrhotite (0.35 wt%) was noted in the F2 fraction. Arsenopyrite and gersdorffite were the main arsenic-bearing minerals. Generally, trace amounts of arsenopyrite (< 0.1%) were noted in all samples, while the amount of gersdorffite was higher and ranged from 0.15 wt% in F6 to about 1 wt% in F1. The total fraction (WR) contained about 0.3 wt% of gersdorffite. Chalcopyrite occurred as a trace mineral and did not exceed 0.05 wt%.

Elemental analyses of individual minerals grain (sulphides and NSG minerals) as determined by EPMA are presented in Table 6.3 and Table S1 (Annexe C). EPMA was used to determine the exact concentration of trace elements in the identified minerals and the exact stoichiometry of some minerals like pyrite, pyrrhotite, and gersdorffite.

Micro-analysis allowed the main contaminant-bearing minerals to be identified. This study revealed that the major sulphides and sulphosalts (cited below) were the main contaminant-bearing minerals (As, Ni, Fe, and Cu). Subsequently, grains of pyrite, pyrrhotite, and gersdorffite were analyzed. Pyrrhotite grains were nickeliferous (Ni at 0.38 ± 0.06 wt%). All the analyzed gersdorffite grains contained Fe and Co at 7.66 ± 0.04 and 1.42 ± 0.05 wt%, respectively. However, pyrite exhibited a composition close to its theoretical stoichiometry but contained traces of Co (0.05 wt%). The harmful elements (i.e., As, Ni, Cu, and Co) were not deported by the NSG minerals except some amphibole with which some nickel was associated (0.09 wt% ± 0.03) (Table S1) (Annexe C).

6.4.2.2 Textural and Mineral Liberation Analyses

6.4.2.2.1 Element Deportment and Mineralogical Associations

Sulphur within the studied WR was mainly associated with pyrite, gersdorffite, pyrrhotite, arsenopyrite, and chalcopyrite. These contaminant-bearing sulphides differ in their involvement in mine drainage processes. Figure 6.5A shows S, Co, As, Ni, Ca, and Mg deportment within the studied waste rock. The results show that 93.33 wt%, 3.33 wt%, 2.66 wt%, 0.33 wt%, 0.29 wt%, and 0.06 wt% of the S was associated with pyrite, pyrrhotite, gersdorffite, arsenopyrite, chalcopyrite, and pentlandite, respectively. Cobalt within the studied sample was totally associated with gersdorffite (100 wt%), while 90.33 wt% and 9.67 wt% of the As was associated with gersdorffite and arsenopyrite, respectively. For Ni, it was associated with gersdorffite (76.3 wt%), pentlandite (1.43 wt%), and pyrrhotite (0.98 wt%). However, a large proportion of the Ni was associated with amphibole (21.30 wt%), as also confirmed by EPMA analysis. Calcite, amphibole, and plagioclase were the main Ca-bearing minerals with proportions of about 66 wt%, 23 wt%, and 7 wt%, respectively. Magnesium within the

studied sample was associated mainly with mica (33.18 wt%), chlorite (26.06 wt%), and amphibole (13.75 wt%).

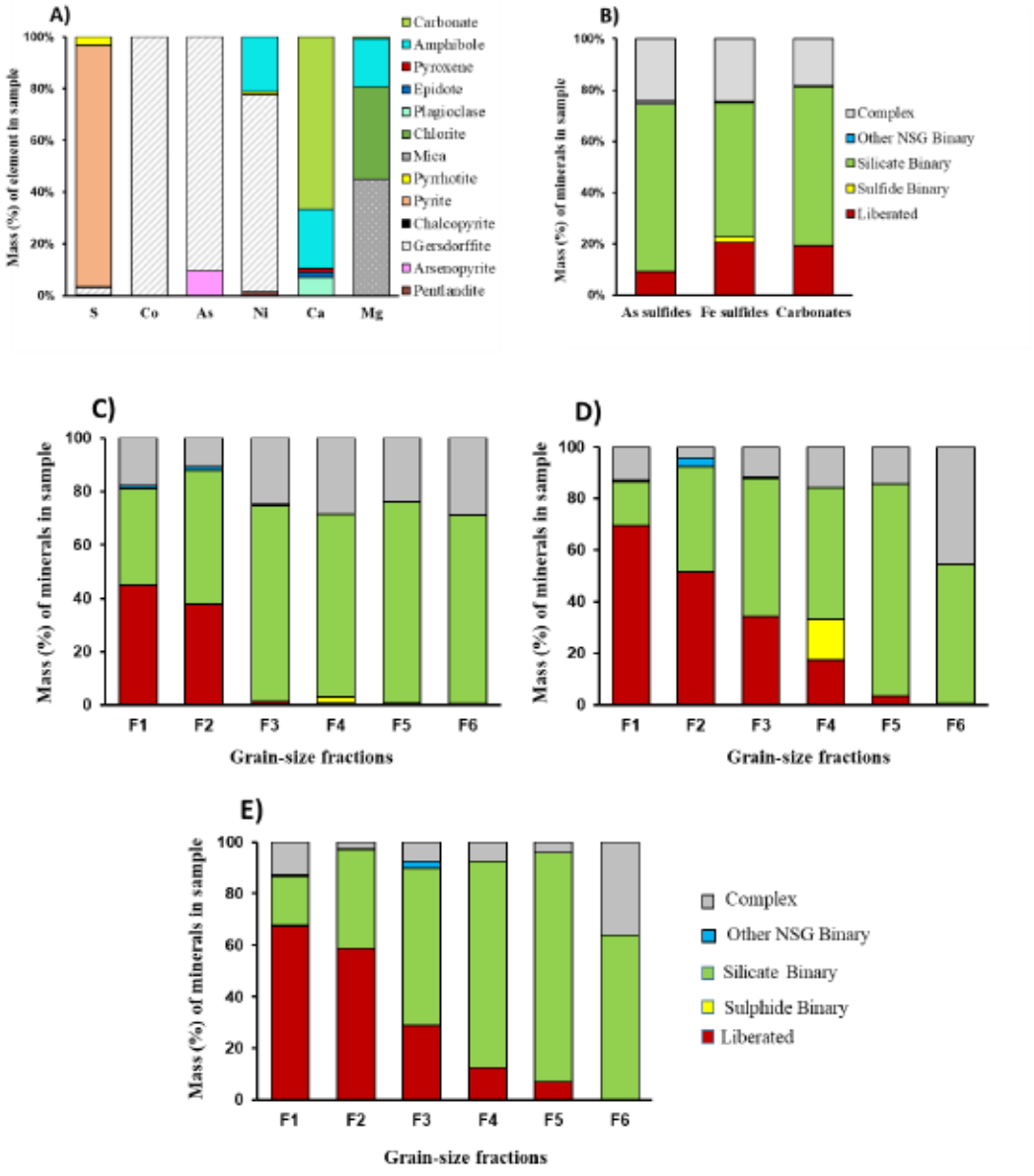

Figure 6.5 Element deportment and mineralogical associations of the studied WR and corresponding fractions: A) S, Co, As, Ni, Ca, and Mg deportment; B) mineralogical associations for carbonates and sulphides within the WR; and C) mineralogical

associations for As-sulphides, D) Fe-sulphides, and E) carbonates within different grain-size fractions (F1 to F6).

Mineralogical associations of sulphides and carbonates within the studied WR are illustrated in Figure 6.5B. Pyrrhotite and pyrite have been combined as Fe-sulphide, and gersdorffite and arsenopyrite as As-sulphides in the liberation data. Furthermore, free is defined as > 95 wt% of the particle is composed of the mineral of interest. A binary is defined as > 95 wt% of the particle area is composed of the mineral of interest and one of the associative minerals. Sulphides were mostly associated with NSG minerals (especially silicates) as binary associations (65.74 wt% and 52.55 wt%, for As-sulphides and Fe-sulphides, respectively), and were less present as free sulphide particles (9.11 wt% and 20.47 wt%, respectively). Carbonates were mostly linked with silicates (61.05 wt%) and were free in a proportion of 19.23 wt% (Figure 6.5B). Furthermore, for coarser grain-size distributions, the proportion of free sulphides (Figure 6.5C-D) and carbonate minerals (Figure 6.5E) decreased. Thus, the fine fractions (F1 and F2) showed the highest proportions of free sulphides and free carbonates (69.38 wt%, 44.92 wt%, and 67.37 wt% for Fe-sulphides, As-sulphides, and carbonates, respectively, for F1; 51.43 wt%, 37.58 wt%, and 58.62 wt%, respectively, for F2). The other proportion of these minerals was mainly associated with NSG minerals as binary associations. As shown in Figure 6.5C-D-E, As-sulphides, Fe-sulphides, and carbonates were associated with NSG minerals in proportions of 37.28 wt%, 17.62 wt%, and 19.40 wt%, respectively, for F1, and in proportions of 51.35 wt%, 44.14 wt%, and 38.58 wt%, respectively, for F2. Contrary to the fine fractions, the coarse fractions (F5 and F6) had lower proportions of free sulphides (3.36 wt% and 0.32 wt% for Fe-sulphides, 0.76 wt% and 0.59 wt% for As-sulphides) and carbonates (7.93 wt% and 1.23 wt% for carbonates in F5 and F6, respectively).

6.4.2.2.2 Mineral Liberation Degree

Mineral liberation and mineralogical associations of the acid-forming and neutralizing minerals are recognized to be important parameters influencing the reactivity of a mineral (Erguler and Erguler, 2015; Parbhakar-Fox et al., 2011). An examination of these parameters showed that the remaining sulphides and carbonates in the WR (fraction < 5 mm) and the corresponding grain-size fractions displayed different liberation degrees with respect to the particle size fractions (Figure 6.6). QEMSCAN® analysis of the total WR sample (< 5 mm) showed that the liberation degree for total sulphides and carbonates is respectively 21.24 wt% and 19.23 wt%. Furthermore, sulphide and carbonate liberation degrees were significantly different for all samples, decreasing with increasing grain size (Fig. S2.2) (Annexe C). Quantitatively, the highest sulphide (around 61.89–50.93 wt%) and carbonate (around 67.37–58.62 wt%) liberation degrees were analyzed in the fine fractions F1 (– 53 µm) and F2 (–300 / +53 µm), respectively. These minerals (i.e., sulphides and carbonates) became increasingly unliberated as the particle size increased (Fig. S2.2, Figure 6.6). More specifically, Fe-sulphides were more liberated than As-sulphides; their liberation degrees ranged from 69.38 wt% (F1) to 3.36 wt% (F5) for Fe-sulphides, and from 44.92 wt% (F1) to 0.76 wt% (F5) for As-sulphides. Carbonates were more liberated than As-sulphides for all fractions, and more liberated than Fe-sulphides for F2, F5, and F6 (Figure 6.6).

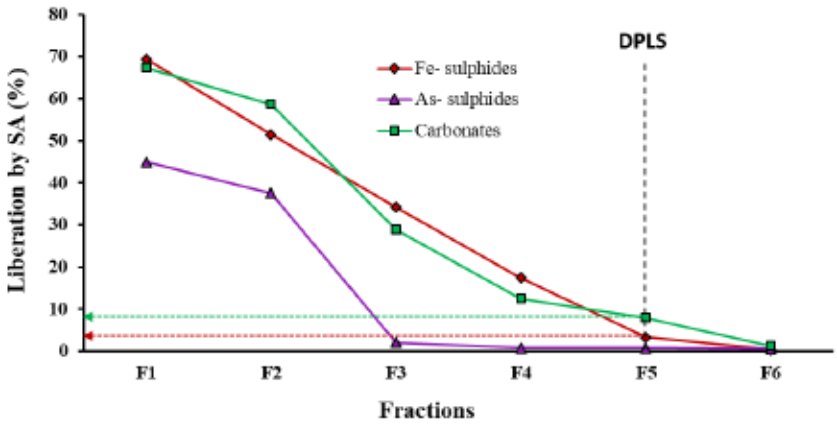

Figure 6.6 Free sulphide and free carbonate liberation degrees versus grain-size fractions.

As the particle size increased, carbonate and sulphide liberation degrees decreased. However, at 2.5 mm, which corresponds to F5, the sulphide liberation degree became negligible (< 5 wt%) compared to that of the carbonates, which was about 8 wt% (Figure 6.6). The liberation degree was 3.4 wt% and 0.8 wt% for Fe-sulphides and As-sulphides, respectively. Thus, 2.5 mm could be considered the DPLS as defined by Elghali et al. (2018). Therefore, the studied WR (< 5 mm) could be split into two fractions of different reactivities at 2.5 mm (DPLS).

For automated mineralogy analysis purposes, fractions larger than 5 mm can't be mounted in polished sections due to limitations in the preparation. The mold for the polished sections had a diameter of 3 cm; consequently, in order to get statistically acceptable results for larger fractions, it would be necessary to analyze a large number of polished sections. Therefore, the coarser fractions were characterised with computed tomography to estimate: i) the sulphide liberation degree, ii) the sulphide volume distribution, and iii) the sulphide content within the material. Figure 6.7 shows the spatial distribution of sulphides within the coarser fraction (> 5 mm). CT data revealed that the amount of sulphide minerals found on the surface of the particles was very low (considered as negligible) compared to the amount of sulphide minerals locked within

the grains. In this instance, the liberation degree of the sulphides was defined as the ratio between the amount of sulphides on the surface of the particle and the total amount of sulphides within the whole particle. These obtained results were expected given that the automated mineralogy (QEMSCAN®) results indicated that the sulphide liberation degree decreased as the grain size increased (Figure 6.6). The obtained results showed that sulphide minerals in the coarse fraction were tightly encapsulated within NSG minerals. The sample volume analyzed was about 260,000 mm^3 and the total sulphide volume distribution was about 3.75%. However, 0.84% of the volume corresponded to the sulphides appearing at the surface of the grain (liberation degree).

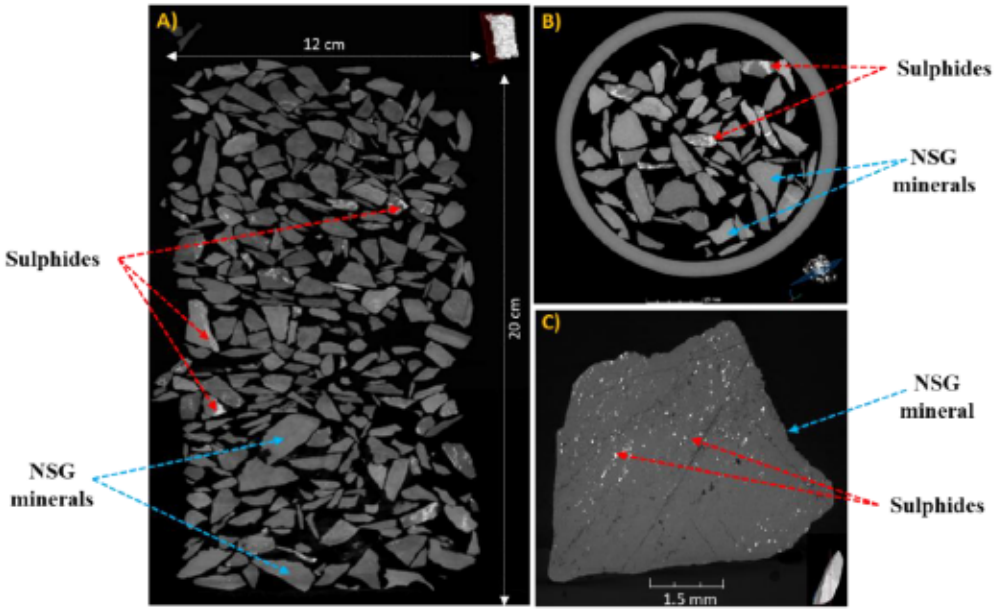

Figure 6.7 Mapping of sulphide minerals within the coarser specimen sample (WR > 5mm) using CT. Spatial distributions of sulphides in A) vertical and B) horizontal sections (X-slice) from the tomogram of the scanned specimen sample. C) Grain showing sulphide distribution at its surface. The light grey to white areas of the images represent sulphide minerals, and the grey areas are non-sulphide gangue (NSG).

Based on obtained results, the sulphide liberation degree was estimated to be approximately 5 wt%. To better illustrate this result, various scans were also carried out on multiple specimens providing a calculation of sulphide distribution and liberation degree. Figure 6.8 illustrates some examples of pieces scanned using CT and results are summarized in Table S2 (Annexe C).

Quantitatively, the volumes of the pieces analyzed were 3,216.15 mm^3, 650.57 mm^3, 240.61 mm^3, and 88.42 mm^3. The volume distribution of total sulphides was 0.74%, 1.45%, 0.68%, and 0.70%, respectively. However, 5.23%, 3.38%, 4.90%, and 4.84% of the volume corresponded to the sulphides appearing at the surface grains. These ratios represent the sulphide liberation degrees. According to the CT investigation results for the coarse fraction (> 5 mm), the liberation degree of sulphide minerals was considered to be negligible (average < 5%) (Table S2) (Annexe C).

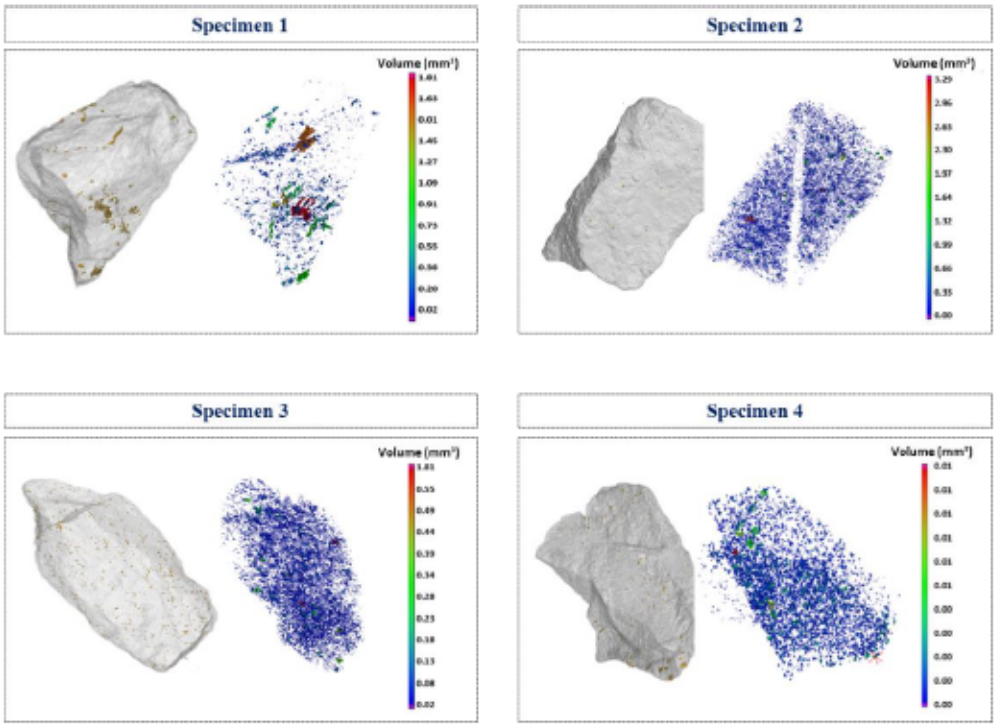

Figure 6.8 Volume distribution of sulphide minerals within some analyzed specimens.

6.4.3 Acid Generation Potential Assessment

6.4.3.1 Acid Base Accounting (ABA)

The ABA test was used to predict the AGP for each fraction and the total sample (WR < 5 mm). Neutralizing potentials (NPs) were calculated using the total carbon analysis. The results of the ABA test are presented in Table 6.2 and in Figure 6.9. The studied fractions had a high NP (56.64–153.27 kg $CaCO_3$/t) and an AP of 39.58–79.72 kg $CaCO_3$/t (Figure 6.9A). The F2 and F3 fractions showed the highest AP (79.72 and 72.57 kg $CaCO_3$/t, respectively) due to their high sulphur content (2.55 and 2.32 wt%, respectively). The net neutralization potential (NNP) was calculated to be between 16.01 and 109.81 kg $CaCO_3$/t. Based on the classification criteria proposed by Miller

et al. (1991b), the F1 fraction was considered as uncertain (i.e., –20 < NNP < 20 kg $CaCO_3$/t), while the total sample and other fractions were non-acid generating. Considering the NPR, the fine fractions (F1 to F3) were classified as uncertain, while the total sample and the F4 to F6 fractions were non-acid generating (Figure 6.9A).

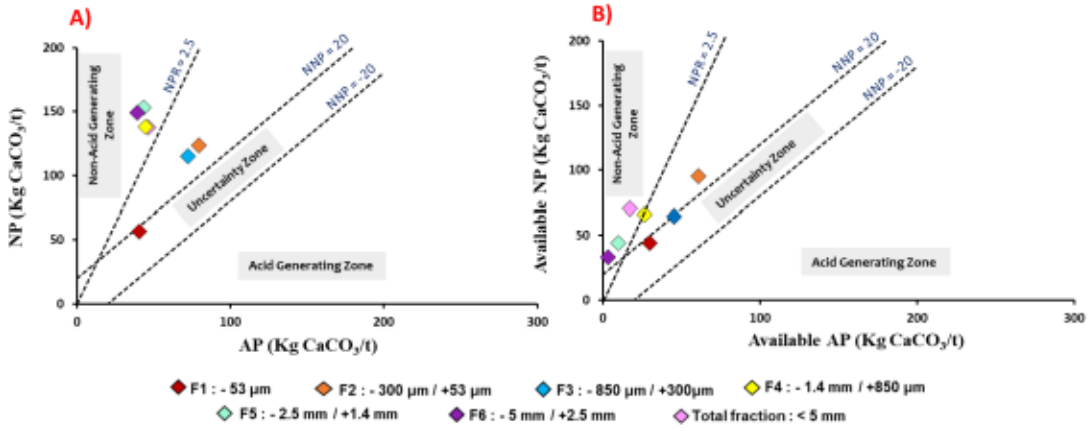

Figure 6.9 Graph illustrating results of acid generation potential through ABA tests with: A) absolute AP and NP, and B) available NP and AP (after correction with carbonate and sulphide liberation degrees).

The calculation of the effective (available) AP and NP using the liberation degree within the total sample and different fractions allowed the initial particle size distribution to be considered. The F3 fraction was initially classified as non-acid forming, but became uncertain after correction with the carbonate and sulphide liberation degrees (Figure 6.9B). Based on the effective NPR (NRP = 2.5), F2 and F4 also became uncertain before they were non-acid forming. According to the results of these static tests, and in order to ascertain the AGP of some fractions (F1, F2, F3, and F4) and confirm that 2.5 mm was the DPLS, it was essential to evaluate the geochemical behaviour (especially CND generation) of the different fractions (i.e., above and under the defined DPLS, and for the total sample (< 5mm)). This reactivity

evaluation can be obtained by simulating field conditions at the laboratory scale. Kinetic leaching tests using humidity cells were performed. Thus, the results from automated mineralogical analyses and computed tomography could be confirmed and a suitable management plan could be developed for the studied WR.

6.4.3.2 Kinetic Tests: Geochemistry of the Leachates from the Humidity Cells

Chemical results from the humidity cell tests over 154 days are presented in Figure 6.10, Figure 6.11 & Figure 6.12. The chemical composition of the leachates is presented as cumulative and mass-normalized releases (mg/kg). Calcium and magnesium were selected to indicate the neutralizing phase dissolution (mainly carbonates) and sulphate was chosen as a tracer for sulphide oxidation (Benzaazoua et al., 2004). Aluminum and silicon were selected to indicate the alumino-silicate mineral dissolution.

The geochemical responses within the humidity cell tests revealed that the studied fractions (fine, coarse, and total) were non-acid forming as the leachates were characterized by circumneutral pH values. The evolution of pH values (Figure 6.10A) showed an similar behaviour for the three fractions with circumneutral values (between 7.07 and 8.61).

Electrical conductivity (Figure 6.10B) varied considerably depending on the grain-size of sample. The fine fraction had the highest EC values, while the total fraction had medium values. The coarser fraction showed the lowest values. Average EC values were approximately 459 µS/cm for the fine fraction, 293 µS/cm for the total sample, and 61 µS/cm for the coarse fraction. EC showed high values for the three samples at the beginning of the kinetic tests (2,040 µS/cm for the fine fraction, 1,650 µS/cm for total fraction, and 428 µS/cm for the coarse fraction) and tended to stabilize at average values of 370 µS/cm, 221 µS/cm and 44 µS/cm for the fine, total and coarse fractions, respectively. The release of weakly-bonded soluble and pre-oxidized components is

reflected in the high EC levels at the earlier stages of the kinetic testing (Elghali et al., 2021; Mayer et al., 2002). For all samples tested, the acidity of the leachates was below 20 mg $CaCO_3$/L (Figure 6.10C). Alkalinity results showed a similar tendency to the EC values (Figure 6.10D). The leachates derived from the fine sample had the highest alkalinity and averaged about 60 mg $CaCO_3$/L. For the coarse and total samples, the average alkalinity was around 20 and 40 mg $CaCO_3$/L, respectively. All samples showed a high redox potential of more than 200 mV, which suggests oxidizing conditions.

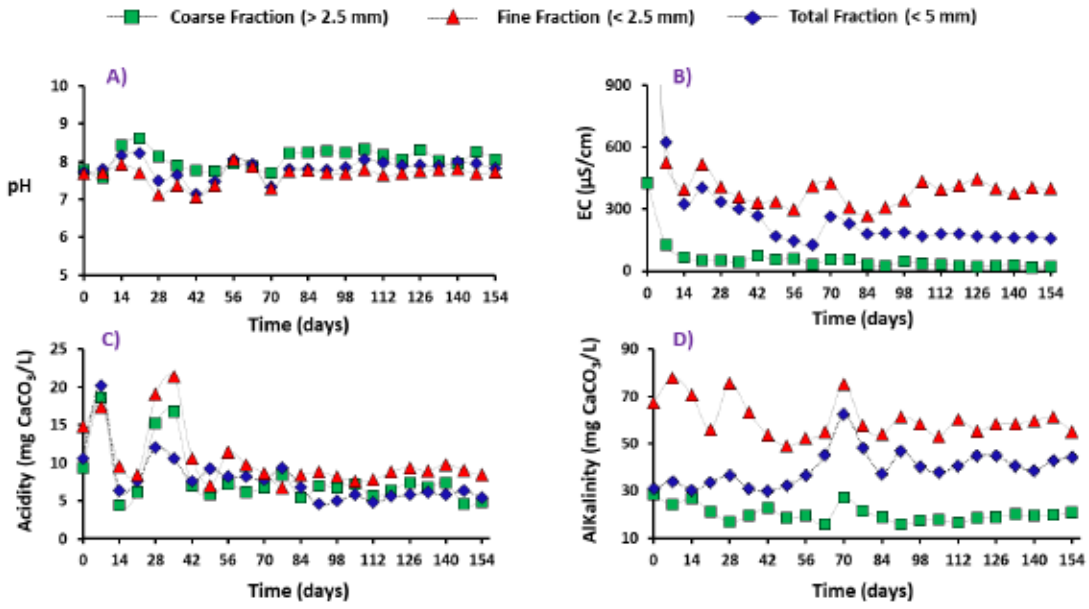

Figure 6.10 Evolution of pH, electrical conductivity, acidity, and alkalinity within the humidity cells.

Calcium was the most leachable element within the three fractions as compared to Al, Si and Mg. As shown in Figure 6.11A-B, cumulative Ca and Mg concentrations over 154 days of leaching tests were approximately 897 and 60.74 mg/kg for the fine fraction, 738 and 78 mg/kg for the total fraction, and 116 and 23 mg/kg for the coarse fraction, respectively. The lower concentrations of Mg were related to the lower

reactivity of silicates, with which all the Mg was associated, compared to the carbonates (calcite). These differences are closely linked to an oxidizing geochemical environment. This is consistent with the expected behaviour of the studied fractions during kinetic testing: sulphides oxidize, carbonates dissolve, and any acidity is neutralized (Dold, 2017; Rimstidt and Vaughan, 2003). This also justifies the neutral pH values observed over the 154 days of testing. Less Ca and Mg were released from the coarse fraction due to its low reactivity. Silicon leaching was low compared to Ca and Mg (Figure 6.11**C**); it was less than 346 mg/kg for the fine fraction and less than 339 mg/kg for the total fraction. However, more Si was leached from the coarse fraction (271 mg/kg) compared to Ca and Mg leaching. Figure 6.11D shows that the cumulative aluminum release was approximately similar in the coarse and total fractions but was lower in the fine fraction; it was approximately 0.71 mg/kg for the coarse fraction, 0.76 mg/kg for the total fraction, and 0.4 mg/kg for the fine fraction.

Sulphates were leached in high concentrations from the fine fraction compared to the coarse and total fractions. After 154 days of leaching, total sulphate loading was about 185 mg/kg for the coarse sample, 1,271 mg/kg for the total sample, and 1,878 mg/kg for the fine sample (Figure 6.11**E**). Iron was leached in small concentrations (Figure 6.11**F**): about 0.5 mg/kg cumulative concentration was noted in all samples. The neutral to alkaline pH (7.07–8.61) was due to the calcite content, availability (liberation), and reactivity, which ensured neutralization of the acidity produced by sulphide oxidation. Thus, low Cu, Ni, Fe, and high As within the leachate from the total fraction (studied WR) will result in the formation of As-contaminated neutral mine drainage (CND).

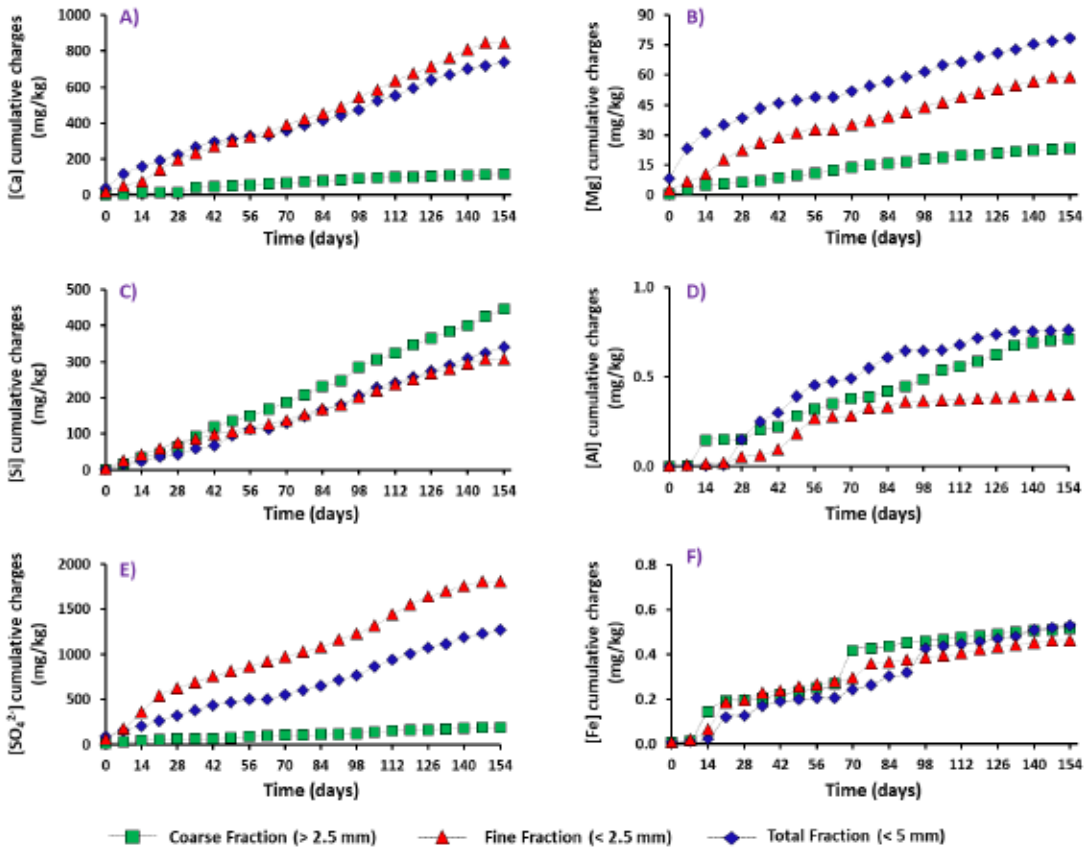

Figure 6.11 Calcium, magnesium, silicon, aluminum, sulphate, and iron load in the studied fractions.

For indication, the instantaneous Cu, Ni, and Fe concentrations collected immediately after each leaching cycle met environmental laws and regulations for all fractions (Directive 019, provincial legislation in Quebec) (Figure 6.12). However, As concentrations from the fine and total fractions exceeded D019 environmental criteria (0.4 mg/L). The coarse fraction did not present a significant risk for acid and contamination generation as confirmed by static and kinetic tests. However, the fine and total fractions had the potential to generate As-bearing CND, contrary to the coarser fraction. Thus, the concentration of As after each leaching cycle for the fine and total fractions exceeded the environmental criteria (Directive 019 in Québec)

(Figure 6.12). As shown in Figure 6.12, the As released by the coarse fraction during the first three cycles slightly exceeded legislative criteria due to previous oxidation. However, larger scale testing is needed to better define the risk.

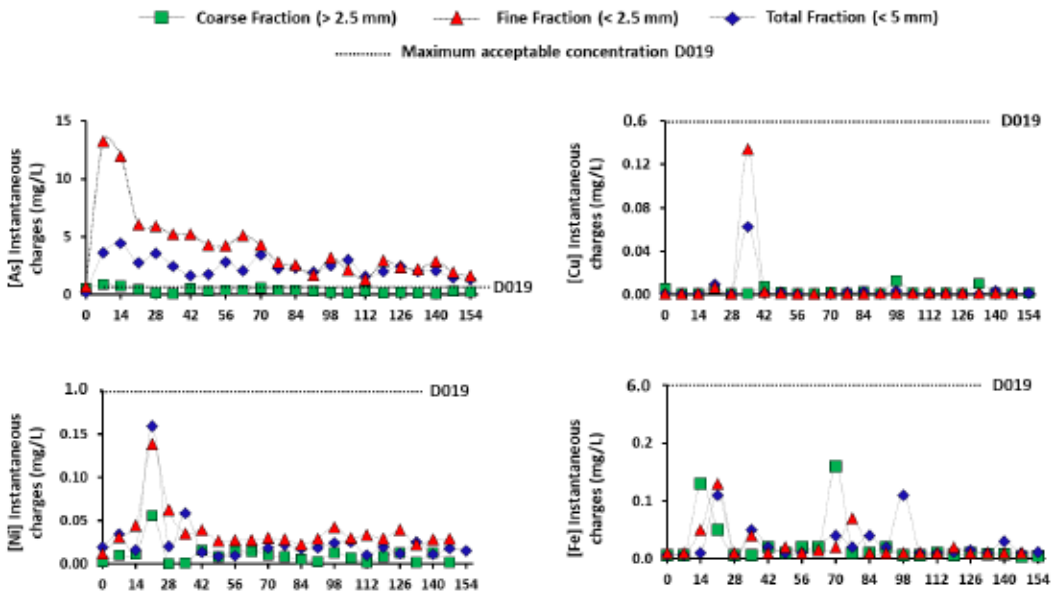

Figure 6.12 Instantaneous As, Cu, Ni, and Fe concentrations within the studied fractions (D019 corresponds to directive 019 which is environmental standard used in Quebec (Canada) for mining projects).

6.5 Discussion

6.5.1 Interest of Characterization to Study the Environmental Behaviour

This study consisted of the use of automated mineralogy and kinetic tests to characterize WR reactivity for the purposes of WR management and evaluation of environmental behaviour. As recommended by various researchers, the ABA testing was done on pulverized samples (Bouzahzah et al., 2015; Sobek, 1978). These tests revealed that some fractions were not acid-forming and some were uncertain. These tests required sample pulverization that significantly destroyed the initial texture of the

samples. The AP and NP determination based on pulverized samples considered that sulphides and carbonates are fully free (liberated). However, this is not the case with WR which has a heterogeneous and wide particle size distribution. Therefore, the environmental behaviour of waste rock should be assessed based on the initial texture (initial liberation degree of sulphides or carbonates). Paktunc and Davé (2000) highlighted this issue by performing kinetic leaching studies on encapsulated and liberated pyrite and calcite. Calculation of the effective AP and NP based upon carbonate and sulphide liberation degrees revealed another classification for the studied fractions in terms of their acid generation potential (Figure 6.9). This means that only the exposed carbonates and sulphides were considered (Blowes et al., 2003; Erguler and Erguler, 2015; Paktunc and Davé, 2000). QEMSCAN® analyses also revealed that the carbonate and sulphide liberation degrees decreased as the particle size increased.

Considering the results from the mineralogical analyses on the samples and the results of the humidity cell tests, the studied waste rock could be divided into two fractions at 2.5 mm (DPLS). According to the particle grain-size distribution (Table 6.2), the fraction below 2.5 mm represented approximately 40% of the studied waste rock mass (i.e., fraction below 10 mm); this was the most reactive fraction and controlled the overall geochemical behaviour of the studied waste rock.

This study revealed that the DPLS can be used to separate waste rock following extraction. This contrasts with the conventional bulk disposal of WR on unsaturated surface piles (Elghali et al., 2019a).

6.5.2 Sulphate–Carbonate Depletion and Oxidation/Neutralization Curves

Early results of geochemical testing may not reflect long-term behaviour (Chopard et al., 2019). Thus, long-term predictions of environmental behaviour for the studied fractions were carried out using the oxidation/neutralization curves (Benzaazoua et al., 2004), which use sulphate release as a tracer of sulphide oxidation and Ca+Mg+Mn

releases as a tracer of neutralizing mineral dissolution (Fig. S2.3)(Annexe C). The initial solid concentrations were projected onto the graph Ca+Mg+Mn vs SO_4^{2-}. If the sample is located on the sulphate side, it is considered to be acid-generating; if it is located on the Ca+Mg+Mn side, it is non-acid forming (Villeneuve et al., 2009). In this study, only [Ca+Mg] were used and Mn was excluded because of its capacity to hydrolize and generate acidity (Benzaazoua et al., 2004; Lapakko, 1994). Results showed that the three fractions (fine, coarse, and total) were located above the oxidation/neutralization curve, which indicates that these samples were classified as non-acid forming over the long-term. The kinetic tests revealed that the finer fraction was the most reactive and primarily responsible for the overall geochemical behaviour of the studied WR. The coarse fraction (2.5–10 mm) exhibited low reactivity (1.21 mg/kg/day) due to the lower sulphur content (1.19 wt%) and encapsulated sulphides within the non sulphide gangue minerals, compared to the total fraction (8.26 mg/kg/day for reactivity and 1.43 wt% for sulphur content) and the fine fraction (12.19 mg/kg/day for reactivity and 1.78 wt% for sulphur content). Based on these sulphide oxidation rates, the fine fraction was 1.5 times more reactive than the total fraction and 10 times more reactive than the coarse fraction. The results support and complement previous findings from various studies that examined the overall effect of PSD on material reactivity (Amos et al., 2015; Brough et al., 2017; Lapakko et al., 2006). However, this study highlights the importance of quantifying the impact of carbonate and sulphide liberation on the geochemical behaviour of WR. This is a key factor in controlling mineral reactivity.

6.5.3 Decisional Guide for Waste Rock Management

According to these results, which support the findings of Amar et al. (2020) and Elghali et al. (2018), a new approach for WR management is proposed: the separation of waste rock into two different fractions with completely different geochemical reactivities.

This separation could be achieved by defining the critical DPLS, which is the particle size that defines the reactive fraction of a given sulphide-bearing WR (Elghali et al., 2018; Elghali et al., 2019a).

The reactivity of the whole sample (i.e., WR) is globally affected by the fraction smaller than the DPLS. The fraction larger than the DPLS, however, has a minimal environmental effect due to the unavailability of the sulphides and sulphosalts for oxidation. Thus, DPLS can be used to divide WR before construction of the conventional WR piles. This could significantly reduce the cost related to the WR pile management and reclamation. The proposed methodology for integrated WR management is illustrated in Figure 6.13. This methodology involves sampling waste rock (< 10 mm) following crushing and screening operations to assess the particle size distribution. The representative sample will be divided into multiple fractions. These fractions will then be subjected to chemical assays and static tests (ABA) to determine their acid formation potential. The fine fractions (< 5 mm) should first be characterized using an automated mineralogy system (e.g., QEMSCAN®) to define the DPLS, while the coarse fraction (> 5 mm) should then be characterized using CT to assess sulphide liberation degrees. Based on the DPLS, kinetic testing could be done to assess the reactivity for samples below and above the defined DPLS as well as for the total sample. Therefore, initial results from automated mineralogical analysis and computed tomography could be confirmed and an effective approach for sustainable WR management could be proposed and studied.

The coarse and unreactive fraction (>DPLS) could be valorized in civil engineering field or be stored in the form of WR dumps. However, the fine fraction could be desulphurized (decontaminated), valorized, or deposited in an appropriate tailings storage facility.

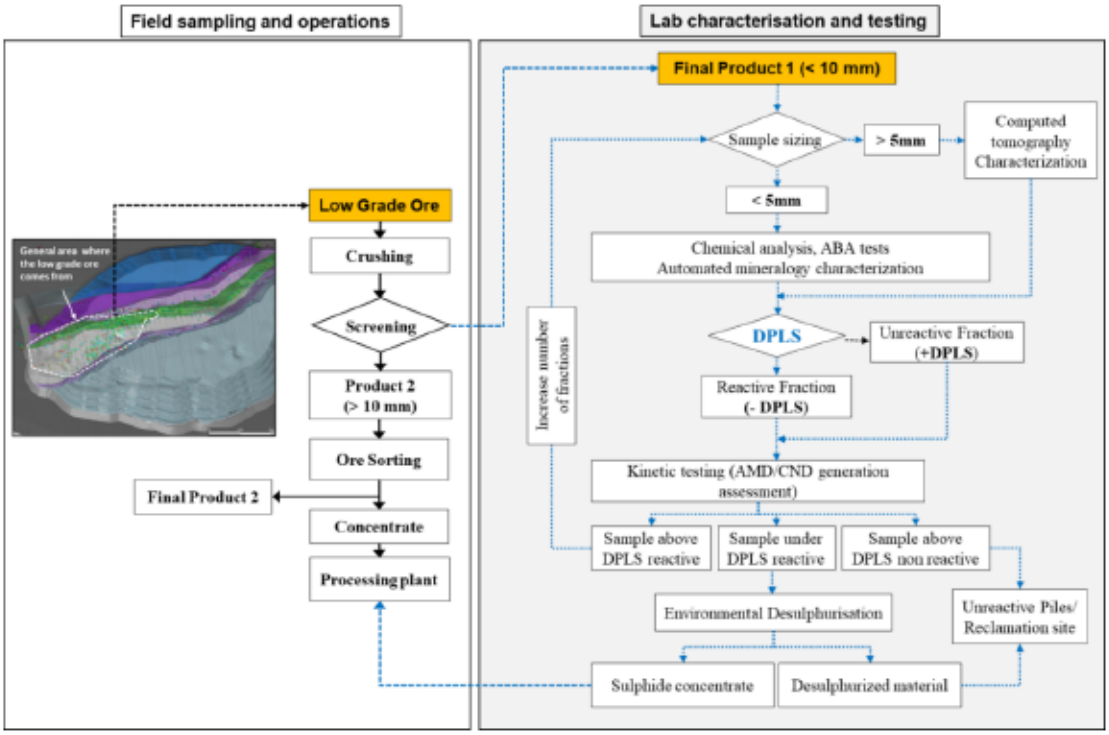

Figure 6.13 Suggested integrated and sustainable WR management methodology.

6.6 Conclusion

The main objectives of this study were to determine the diameter of physical locking of sulphides and sulphosalts (DPLS) within the studied waste rock and to confirm it by evaluating the geochemical behaviour of the three produced fractions through kinetic testing using humidity cells. More specifically, the goal was to examine the influence of particle grain-size and carbonate/sulphide liberation degree on the geochemistry of mine drainage. Advanced automated mineralogical analysis techniques (QEMSCAN® and CT) combined with kinetic testing were used. Based on mineralogical and kinetic test results, the DPLS for the studied WR was determined to be 2.5 mm. These results showed that the fine fraction was the most sulphidic, and the sulphide and carbonate liberation degrees were higher relative to the coarse and total fractions. The determined DPLS was kinetically confirmed using humidity cell tests monitored over 154 days.

Within the three fractions, carbonates were available in sufficient amounts and with sufficient liberation degrees to produce the neutral behaviour observed during the 154-day kinetic tests for the three fractions. Depending on the fraction (fine, coarse, or total), the sulphide oxidation and species release rates were totally different. The fine fraction (< 2.5 mm) had a high oxidation rate compared to the coarse fraction (> 2.5 mm) and the total sample (< 10 mm) due to different degrees of sulphide mineral liberation. The fine fraction was characterized by high sulphide mineral liberation compared to the total sample. The coarse fraction had very low oxidation rate and species release rates due to the low sulphide mineral liberation; this is also due to the initial sulphide and carbonate contents. Leachates obtained during the kinetic tests were compared to estimate likelihood of As generation. The coarse fraction produced leachates with As concentrations below the directive 019 limit, while the fine and total fractions had leachates that exceeded that limit. The coarse fraction is therefore less likely to produce As-contaminated neutral drainage, but more specific tests for CND are required to better assess the risk.

The DPLS parameter could be integrated in waste rock pile management. WR could be divided into two fractions, leading to the construction of two waste rock piles: i) a pile containing only material +DPLS, which is non-reactive due to the encapsulation of sulphides into NSG minerals; and ii) a pile containing the fraction –DPLS, which is more reactive and generates CND. The non-reactive fraction (coarse fraction) constituted about 60% of the total sample (WR) and could potentially become valorized in the field of civil engineering or ceramics or be stored in a waste rock dump. However, the fine fraction could be managed differently: it could be desulphurized (decontaminated), valorized, or deposited in an appropriate tailings storage facility. Based on the results of this study, screening of WR according to the DPLS parameter can provide an effective approach for sustainable WR management. It may minimize the amount of problematic WR to be managed and, consequently, minimize the costs

related to pile reclamation. However, WR size fractions must be better characterized and analyzed to accurately determine this key DPLS value.

Acknowledgements

The authors are grateful to the URSTM staff for their support with materials testing and analyses, Ievgeniia Morozova and NIKON METROLOGY staff for their collaboration and their help with CT analysis. Funding for this study was provided by a Collaborative Research and Development granted to I. Demers by NSERC and industrial partners. Finally, many thanks must go to the XPS laboratory in Sudbury (Canada) for their help in achieving QEMSCAN analysis.

CHAPITRE 7

ENVIRONMENTAL DESULPHURIZATION OF WASTE ROCK TO PREVENT CONTAMINATED NEUTRAL DRAINAGE GENERATION, PART II: WASTE ROCK DECONTAMINATION FOR SUSTAINABLE MANAGEMENT

Préambule : Ce chapitre a été soumis pour publication potentielle dans la revue *Journal of Geochemical Exploration*.

Ait-khouia Yassine [a], Benzaazoua Mostafa [a,b,*], Yassine Taha [b] , Demers Isabelle [a]

[a] Research Institute on Mines and Environment (RIME), University of Quebec in Abitibi Témiscamingue, 445, boul. de l' université, Rouyn-Noranda J9X 5E4, Quebec, Canada

[b] Mohammed VI Polytechnic University (UM6P), Mining Environment & Circular Economy, Ben Guerir 43150, Morocco

Corresponding author. E-mail address: mostafa.benzaazoua@uqat.ca

7.1 Abstract

The mining industry produces large quantities of waste rock (WR), which is characterised by a wide particle size distribution (PSD). The mineralogical and textural characteristics of the WR are influenced by their PSD. Thus, mineralogical investigations have defined the diameter of physical locking of sulphides (DPLS), allowing the WR to be split into two separate fractions according to geochemical reactivity: i) a reactive fine fraction (< DPLS), and ii) an inert coarse fraction (> DPLS). The critical DPLS for the studied WR was 2.5 mm. According to this parameter, the

current study was carried out to evaluate the acid- and contamination-generating potential of the fine fraction (feed sample), determine the reprocessing feasibility using desulphurization processes (i.e., gravity separation and flotation), and study the geochemical behaviour of the desulphurized materials. Chemical and mineralogical characterisation revealed that the studied feed sample was enriched in contaminant-bearing sulphides (i.e., 4 wt% pyrite, 0.33 wt% gersdorffite, 0.15 wt% pyrrhotite, etc.) and carbonates (i.e., 4.47 wt% calcite). This paper examined the use of centrifugal dense medium separation (DMS), spiral/shaking table, and combined gravity and flotation techniques as decontamination processes for the studied material. The geochemical properties of the studied sample and the desulphurized materials were evaluated using kinetic weathering cells (WCs). DMS and a combined gravity-flotation process yielded better results for decontaminating the studied WR, with a desulphurized material achieving a low sulphur content (0.28 wt%) and high sulphur recovery compared to the concentrate (88 wt%). The final concentrates from the DMS and combined gravity-flotation approaches showed an interesting gold content (> 1.8 g/t). Kinetic tests revealed that the materials desulphurized using DMS and the combined approach had the lowest As concentration in their leachates. The leachates from the material desulphurized using the spiral/shaking table were slightly above environmental limits (D019, Quebec, Canada) for As concentration. Upstream environmental desulphurization has been confirmed as an effective strategy for WR management and valorization.

Keywords: contaminated neutral drainage, sulphides/sulphosalts, environmental desulphurization, dense medium separation, spirals, shaking tables, flotation.

Résumé

L'industrie minière produit de grandes quantités de stériles miniers (WR), qui se caractérisent par une large distribution granulométrique (PSD). Les caractéristiques

minéralogiques et texturales des WR sont influencées par leur PSD. Ainsi, les investigations minéralogiques ont défini le diamètre d'encapsulation physique des sulfures (DPLS), permettant de séparer le WR en deux fractions distinctes selon leurs réactivités géochimiques : i) une fraction fine réactive (< DPLS), et ii) une fraction grossière inerte (> DPLS). Le DPLS critique pour le WR étudié est de 2,5 mm. Selon ce paramètre, la présente étude a été menée pour évaluer le potentiel de génération d'acide et de contamination de la fraction fine (échantillon d'alimentation), déterminer la faisabilité du retraitement de ce matériel à l'aide de procédés de désulfuration (séparation gravimétrique et flottation), et d'étudier le comportement géochimique des matériaux désulfurés. La caractérisation chimique et minéralogique a révélé que l'échantillon d'alimentation étudié est enrichi en sulfures porteurs de contaminants (4 % en poids de pyrite, 0,33 % en poids de gersdorffite, 0,15 % en poids de pyrrhotite, etc.) et en carbonates (4,47 % en poids de calcite). Cet article examine l'utilisation de la séparation centrifuge en milieu dense (DMS), de la spirale/table à secousses et des techniques combinées de gravimétrie et de flottation comme procédés de décontamination pour le matériel étudié. Les propriétés géochimiques de l'échantillon étudié et des matériaux désulfurés ont été évaluées à l'aide des tests cinétiques en mini-cellules d'altération (WCs). Le DMS et le procédé combinant la flottation et gravimétrie ont montré de meilleurs résultats pour la décontamination du WR étudié. Ainsi, le produit désulfuré titre 0,28 % S (en poids), ce qui correspond à une récupération élevée du soufre de 88 % (en poids). Les concentrés finaux issus de l'approche DMS et celle combinant gravimétrie-flottation ont montré une teneur en or intéressante (> 1,8 g/t). Les tests cinétiques ont révélé que les matériaux désulfurés via DMS et la combinaison gravimétrie-flottation présentent la plus faible concentration d'As dans leurs lixiviats. Cependant, la concentration en As dans les lixiviats issus du produit désulfuré à l'aide de la spirale/table à secousse est légèrement supérieure à la limite environnementale (D019, Québec, Canada). La désulfuration environnementale a été confirmée comme une stratégie efficace pour la gestion et la valorisation des WR.

Mots-clés : drainage neutre contaminé, sulfures/sulfosels, désulfuration environnementale, séparation en milieu dense, spirales, tables à secousse, flottation.

7.2 Introduction

During the past decades, the development of underground and open pit mining worldwide has been impacted by a difficult economic context and high prices for some critical, strategic, and precious metals. This has resulted in a growing interest in low-grade and high-tonnage deposits, including in Canada. This type of operation creates a large footprint on the landscape and requires that significant volumes of blasted and non-economic material called waste rock (WR) be stored at the surface (Amos et al., 2015; Elghali et al., 2018; Jamieson et al., 2015; José Neto et al., 2019; Taskinen et al., 2018). WR is the part of the orebody with a metal value below the operation cut-off grade. This material is commonly stored at the surface in unsaturated piles that can reach tens to hundreds of meters in height and cover hundreds of hectares (Aubertin et al., 2008; Blowes et al., 2003). Once deposited in storage facilities, WR piles are highly anisotropic in terms of chemical, physical, mineralogical, and hydrogeological properties (Jamieson et al., 2015). These heterogeneities can be attributed to the construction techniques of the piles and the segregation that can occur due to water infiltration. Because this material is often sulphide- and sulphosalt-bearing, if not properly managed it may generate a serious threat to the environment, such as acid mine drainage (AMD) or contaminated neutral drainage (CND), soil pollution, or water contamination (Ait-Khouia et al., 2021; Dold, 2017; Hakkou et al., 2008). Indeed, sulphides and sulphosalts exposed to atmospheric oxygen and water can be oxidized, leading to acidic or neutral drainage water frequently loaded with high concentrations of metals/metalloids, such as arsenic, nickel, iron, copper, and zinc, that do not adhere to the existing regulatory criteria (Blowes et al., 2014; Mayes et al., 2009).

The environmental behaviour of WR is generally controlled by its chemical, mineralogical, and physical properties (Aubertin et al., 2008; Jamieson et al., 2015; Nordstrom, 2000), as well as by biological processes and other external factors (Parbhakar-Fox and Lottermoser, 2015). Particle size is acknowledged as one of the most significant factors controlling the reactivity and geochemical behaviour of WR (Amar et al., 2020b; Elghali et al., 2018; Erguler and Erguler, 2015). Indeed, it influences the degree of liberation of acid-generating and acid-neutralising minerals and consequently determines the reactivity of the WR. According to recent studies, WR can be divided into two distinct fractions with highly different reactivities using a multi-disciplinary characterization approach coupled with geochemical kinetic tests. The diameter of physical locking of sulphides and sulphosalts (DPLS) is a new parameter used to determine the critical particle size at which the degree of liberation of sulphides/sulphosalts becomes negligible (Elghali et al., 2018). WR from an operational mine in northern Canada was sampled and characterised using advanced techniques (QEMSCAN® and computed tomography), including evaluation of the environmental behaviour and prediction of acid and contaminated neutral mine drainage generation. These characterisations revealed that at a particle size greater than 2.5 mm, the degree of liberation of the sulphides/sulphosalts becomes negligible (< 5%). Thus, the studied WR was divided into two fractions: i) a coarse fraction (>DPLS) considered as non-reactive due to the encapsulation of sulphides into non-sulphide gangue minerals (NSG), and ii) a fine fraction (< DPLS) that was more reactive and prone to generating arsenic-rich CND (Ait-khouia et al., 2022a). This fine and reactive fraction, representing about 40% of the total studied WR, must be safely managed.

To reduce the severity and extent of the effects of CND on the surrounding environment, significant efforts are needed to raise awareness amongst stakeholders (citizens, government, and industry) to establish effective controls and sustainable management techniques. During the last decades, environmental desulphurization using flotation has gained much popularity to control AMD generation in several mine tailings by

decreasing the sulphide and sulphosalt content (Amar et al., 2020a; Benzaazoua and Kongolo, 2003; Rezvanipour et al., 2018). However, this technique is limited by the particle size distribution and remains efficient only for the tailings fraction between 20 µm and 1 mm (Ait-Khouia et al., 2021; Derycke et al., 2013), whereas DPLS is expected to be in the vicinity of 2.5 mm. In this context, beneficiation techniques commonly used in ore enrichment (e.g., gravity) could address this gap. Gravity separation is a method of concentrating mineral particles by separating them from a fluid (water or air). The main benefits of this operation include ease-of-use, low operating costs (no reagent costs), processing of coarse grain sizes at a high flow rate, and ecofriendly aspects (Ait-Khouia et al., 2021; Amar et al., 2020b). This technique can be considered when target minerals have densities that are sufficiently different from those of gangue minerals (Ait-Khouia et al., 2021; Gülsoy and Gülcan, 2019). Dense medium separators (DMS) (Marion et al., 2018), spirals (Gülsoy and Gülcan, 2019), shaking tables (Aleksandrova et al., 2019; Bergmann et al., 2016), and centrifugal gravity concentrators such as Knelson (Gülsoy and Gülcan, 2019; Katwika et al., 2019; Uslu et al., 2012) are some best known gravity methods. The desulphurization of WR applied in this study, combined with DPLS assessment, is an original idea proposed for prevention of AMD and CND from WR. Desulphurization of WR has benefitted from few studies due to the large grain size distribution and the difficulty to obtain liberated sulphides and sulphosalts.

This study focused on the use of environmental desulphurization as an integrated mine waste management approach. The development of novel practices that allow reactive WR to be decontaminated, stabilized, and stored more safely were studied. More specifically, this paper focused on: i) environmental desulphurization (decontamination) of the reactive fraction of WR by using novel techniques (i.e., DMS, Knelson, spirals, shaking tables, and flotation processes), ii) evaluation of the geochemical behaviour of the studied WR (reactive fraction) and its desulphurized fractions (prediction of acid

and contaminated neutral mine drainage generation), and iii) evaluation of the feasibility of gold concentration using the desulphurization process.

7.3 Materials and Methods

7.3.1 Sampling, Material Preparation, and Methodology

The WR (feed sample) used in this study was received from an operating gold mine in northern Canada. The studied material was sampled from a small-scale pile of material (approximately 3.5 tonnes) built during mine operation. The WR feed was homogenized using a quartering technique and a portion was sampled for testing and studying. This sample was then wet sieved with an aperture of 2.5 mm (DPLS) following the conclusions of the study by Ait-khouia et al. (2022a) (chapitre 6), where additional details about sampling, sample preparation, and characterisations can be found. After the WR feed sample was screened based upon the DPLS parameter, the fine fraction (< 2.5 mm) underwent processing tests using flotation and gravity techniques to efficiently remove sulphides and sulphosalts. The methodology followed in this study is highlighted in Figure 7.1:

i) physical, chemical, and mineralogical characterisation of the feed sample (fresh reactive fraction, < 2.5 mm);
ii) environmental desulphurization of the feed sample by DMS, spiral/shaking table, and combined techniques, including DMS, Knelson concentrator, and flotation;
iii) acid- and contamination-generation potential assessment using acid-base accounting (ABA), net acid generation (NAG) tests, and kinetic tests for the feed sample and desulphurized materials; and
iv) evaluation of gold content.

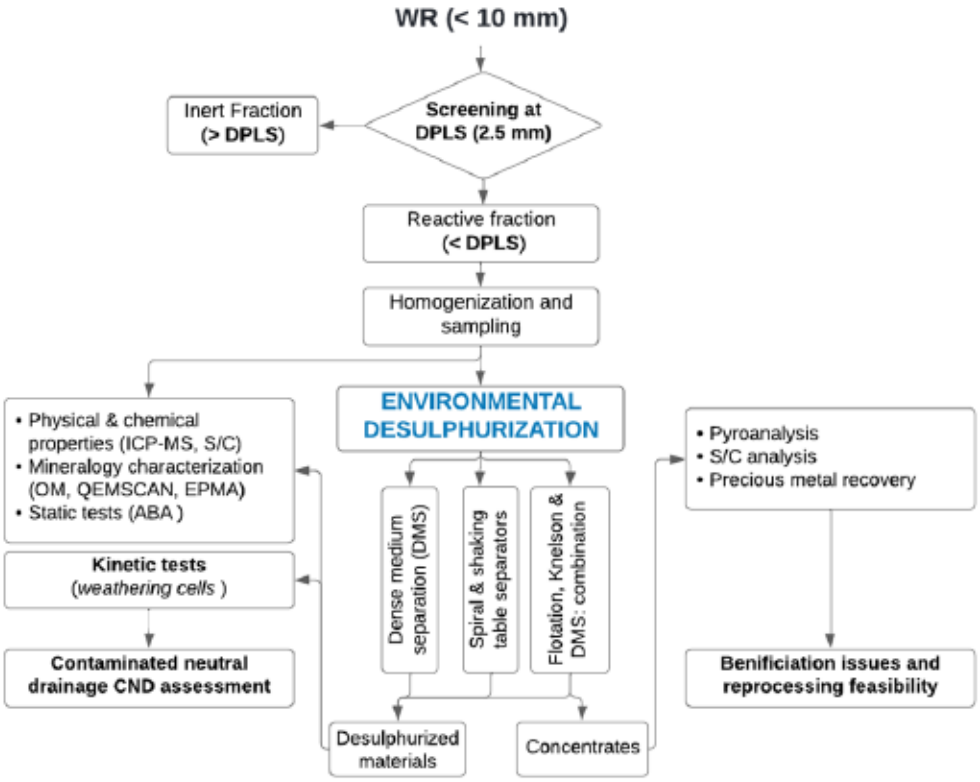

Figure 7.1 Methodology followed for WR characterisation and desulphurization to assess contaminated mine drainage generation and the recovery of precious metals.

Decontamination studies (desulphurization) were carried out on DMS (Figure 7.3A), spiral/shaking table (Figure 7.3B), and combined concentrators (DMS, Knelson, and flotation) (Figure 7.3C), with the objective to pre-concentrate the sulphides and sulphosalts. A combination of multiple techniques was used to improve desulphurization (decontamination) efficiency. As the studied WR had a relatively wide particle size distribution, it was useful to proceed to sieving prior to other separation techniques. Gravity separation is inefficient when used to separate particles with a wide particle size distribution and a narrow density distribution (Williford and Bricka, 2000). Thus, the test sample material with a particle size < 2.5 mm was

screened at 850 µm (Figure 7.3C). DMS is more effective when used to treat coarse grains larger than 850 µm (Ait-Khouia et al., 2021). The fine fraction (< 850 µm) is processed with Knelson as an advanced centrifugal concentrator and bulk flotation. Thus, for fine particles smaller than 63 µm, conventional gravity concentrators (e.g., shaking tables and spirals) and flotation are less effective, while centrifugal concentrators (e.g., Knelson) are more suitable for these finer particle sizes (Ait-Khouia et al., 2021).

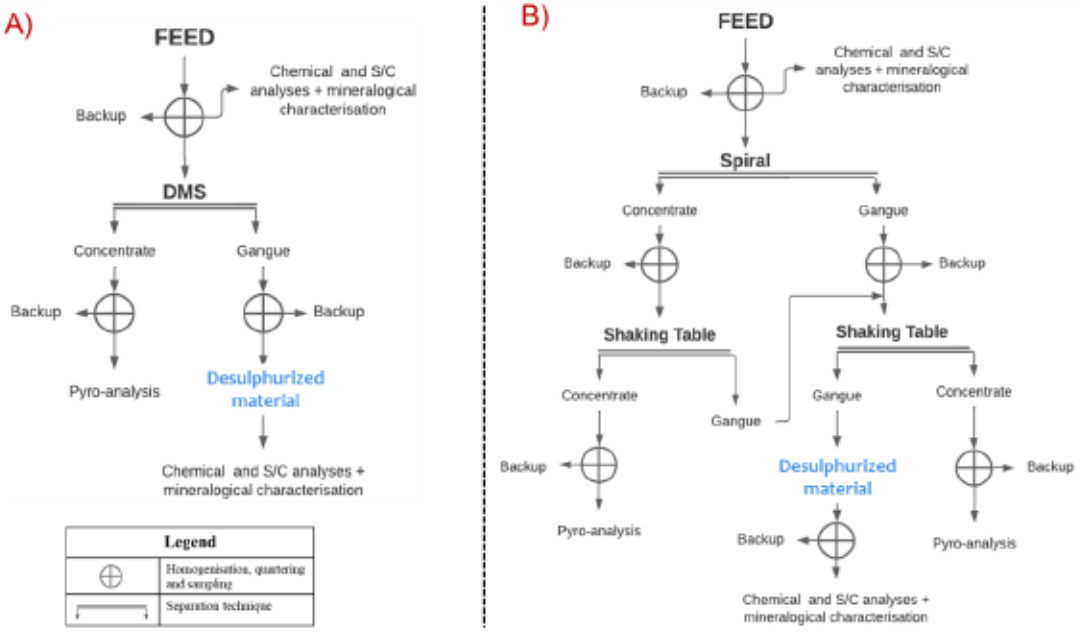

Figure 7.2 A process flow chart of the different decontamination techniques used: A) DMS approach, B) spiral/shaking table approach, and C) combination gravity and flotation approach.

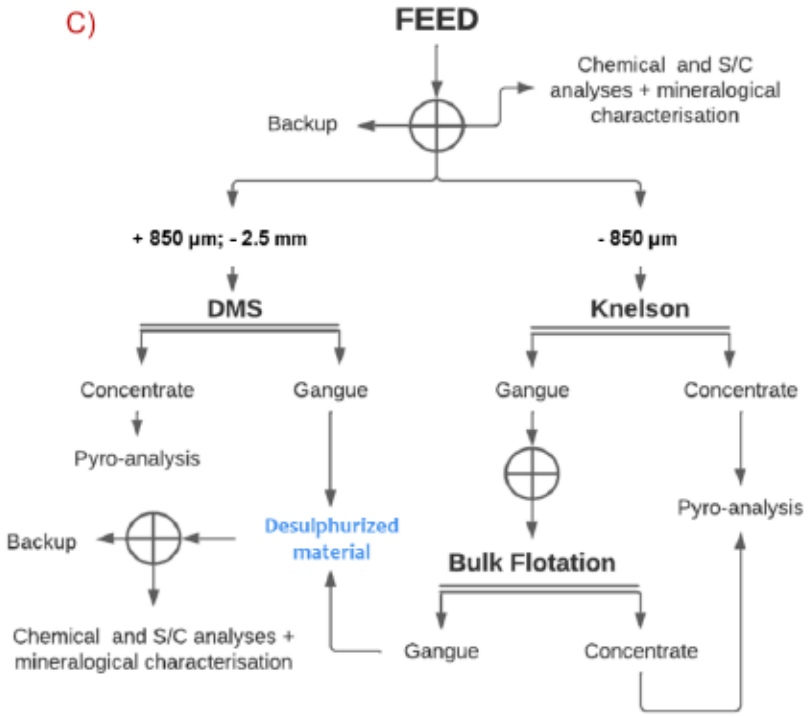

Figure 7.3 A process flow chart of the different decontamination techniques used: A) DMS approach, B) spiral/shaking table approach, and C) combination gravity and flotation approach (suite).

7.3.2 Physical, Chemical, and Mineralogical Properties

The specific surface area (SSA) was determined with a Micromeritics surface area analyser implementing the Brunauer-Emmet-Teller (BET) method (Brunauer et al., 1938). The specific gravity (S_G) was determined using a helium gas pycnometer with Micromeritics Accupyc 1330 in the URSTM-IRME UQAT laboratory in Quebec, Canada (Allen, 2013). Total sulphur (wt% S ± 0.1 to 0.5) and inorganic carbon (wt% C ± 0.6 to 1.1) contents were analysed by induction furnace (ELTRA CS-2000 with a detection limit of 0.09%). The bulk chemical composition of the solid samples was determined at Activation Laboratories (Actlabs), Ontario, Canada using peroxide fusion inductively coupled plasma mass spectrometry/optical emission spectrometry

(ICP-MS/OES). The chemical composition of the weathering cell (WC) leachates was analysed with inductively coupled plasma atomic emission spectroscopy (ICP-AES) on samples acidified with 2% HNO_3.

Polished sections of the studied WR and desulphurized materials were prepared and observed using optical microscopy in reflected light mode (AxioImager M2m optical microscope, Zeiss, Oberkochen, Germany, equipped with the AxioVision software V4.8) to identify the mineral species and observe the texture. The mineralogical composition and texture of the studied WR (reactive fraction) and the desulphurized materials from the various processing techniques were also characterised using Quantitative Evaluation of Materials by Scanning Electron Microscopy (QEMSCAN®, FEI, Quanta 650 platform with Field Emission Gun) at the XPS laboratory in Sudbury (Ontario, Canada). QEMSCAN® is an automated mineralogy system that produces particle maps (colour coded by mineral) through rapid acquisition of X-ray spectra. The maps and corresponding data files allow the quantification of modal mineralogy, texture, elemental deportment, and mineral liberation (Benzaazoua et al., 2017; Pirrie et al., 2004). Measurement resolution ranged between 0.5 µm and 2.5 µm depending on particle size and mineral texture. The samples were also subjected to electron probe micro-analysis (EPMA), which confirmed the mineral identification and the chemical composition. A Cameca SX-100 EPMA was used to analyse at least ten particles of each mineral. This provided more precise and accurate compositions of minerals as well as quantification of trace elements within minerals. This instrument was coupled with four high-resolution wavelength-dispersive X-ray spectrometers (WDS). All quantitative analyses (EPMA) were conducted using a focused beam at a 20kV accelerating potential and a 20nA constant beam current. Mineralogical reconciliation was achieved by setting the wt% of identified minerals (QEMSCAN®) to obtain the minimum difference between the chemical analysis (ICP-MS) and the calculated chemical composition using mineral stoichiometry (EPMA results).

7.3.3 Desulphurization/Decontaminating Techniques

Gravity and flotation separations were pre-selected as feasible techniques based on the knowledge from the literature and the WR characteristics (Ait-khouia et al. 2021). The experiments were performed at the URSTM laboratory at UQAT (Quebec, Canada).

7.3.3.1 Dense Medium Separation in Lab Centrifuge

A non-toxic heavy liquid, lithium heteropolytungstate (LST), was used to conduct centrifugal DMS tests. It has a density of 2.85 and 20% water. This liquid is distinguished by its high thermal stability, which allows it to easily be recycled through a heating procedure that allows for its original density to be regained. Furthermore, it requires shorter centrifuge times during the separation process. The separating density (2.9) was carefully determined based on the specific gravity and proportion of all the gangue mineral occurrences (Table 7.1). Thus, this separation produced a light mineral fraction (SG < 2.9), which corresponds to NSG minerals, and a heavy mineral fraction (SG > 2.9; lower mass recovery) consisting of sulphides and sulphosalts.

Table 7.1 Average densities of the minerals in the studied sample

Fraction	Mineral	Proportion (%)	Average density *	Targeted cut-density
Reactive (< 2.5 mm)	Mica	26.75	2.82	**2.9**
	Fe chlorite	10.76	2.82	
	Clinochlore	5.36	2.65	
	Amphibole	20.15	2.84	
	Calcite	4.97	2.71	
	Quartz	17.96	2.62	
	Pyroxene	3.45	2.8	
	Pyrite	4.06	5.1	
	Pyrrhotite	0.15	4.6	
	Gersdorffite	0.33	5.9	
	Arsenopyrite	0.02	6.1	

*minerals average densities sourced from web minerals.

To achieve a solid content of 20% wt/wt, the representative samples were added (about 23g) to 40 mL LST (with a S_G of 2.9) in 50 mL centrifuge tubes. The tubes were then thoroughly stirred to mix the LST with the material and then centrifuged at 2,000 rpm for ten minutes using a MSE mistral 2000R centrifuge (Mistral 2000R, MSE, UK). The heavy and light portions were then extracted, washed with distilled water, filtered, dried, mass balanced, and analysed.

7.3.3.2 Spiral and Shaking Table

The spiral separator used in this work was a Humphrey-24A model from Humphreys Engineering (Canada). The material was fed as a slurry of about 25% w/w solids. Slurry is introduced from the top and circulates downward in the conduit describing a helix.

The shaking table used in this study was a 13B Wilfley (laboratory) table model from Outokumpu Technology, Inc. (Canada). The feed, at about 25% solids by weight, is introduced and distributed across the deck. As the suspension of particle moves across the table, it is caught and forms pools behind the longitudinal riffles. The double action of differential shaking and wash water cause specific gravity stratification as well as reverse size classification. Three separate layers of particles are formed: the table concentrate (high density), the low-density rejects, and the mixed particles with intermediate density. The parameters of the shaking table were optimized to achieve good gravity separation efficiency: i) 6° slope, ii) 5.6 L/min water flow rate, and iii) 250 g/min feed rate. A total weight of 7 kg of the feed was passed on the table for sulphide and sulphosalt preconcentration.

7.3.3.3 Knelson Concentrator

The Knelson Concentrator (KC) used in this study was a KC-MD3 model (FLSmidth Knelson, Canada). The parameters of the KC were optimized to obtain good sulphide and sulphosalt separation efficiency. Thus, it was operated with a bowl speed of 1,200

rpm and a fluidizing water rate of 2.8 L/min. The material was fed at a 30% solid concentration with a flow rate of 250 g/min and a centrifugal force exceeding the gravitational force by 90 g.

7.3.3.4 Flotation

Flotation tests were conducted by using a Denver D-12 lab flotation machine (1.2 L cell volume, 1,100 rpm rotor stator, and 3 L/min airflow) that supports 357 g of solid. The reagents tested for flotation experiments and their technical specifications were as follows:

- collector: potassium amyl xanthate (PAX-51) diluted at 10% (technical purity of 86 wt%; molecular weight 202.3 g);
- activator: hydrated copper sulphate ($CuSO_4$) diluted at 10% (technical purity of 98%); and
- frother: methyl isobutyl carbinol (MIBC).

The conditioning times for the activator (150 g/t), the collector (100 g/t), and the frother (50 g/t) were 3 min, 2 min, and 1 min, respectively.

7.3.4 Acid Generation Potential Assessment

7.3.4.1 Static Tests

Static tests were conducted on the head sample (reactive fraction) and the desulphurized materials using the ABA test according to the Sobek method (Sobek, 1978) modified by Bouzahzah et al. (2015) to evaluate their acid generation potentials (AGP). The acidification potential (AP) was calculated using S sulphide (AP = 31.25 x S sulphide (kg $CaCO_3$/t)), while the neutralization potential (NP) was calculated using total inorganic carbon (TIC; NP = 83.3 x TIC (kg $CaCO_3$/t)). The materials were classified as acid generating if the net neutralisation potential (NNP) value (NNP = NP – AP) was less than −20 kg $CaCO_3$/t; material with a NNP value greater than 20 kg

$CaCO_3$/t was considered as non-acid generating and uncertain if the NNP value was between −20 and 20 kg $CaCO_3$/t (Bouzahzah et al., 2015; Miller et al., 1991). The AGP was also assessed using the neutralization potential ratio (NPR = NP/AP); typically, a material is considered as acid generating if the NPR < 1, non-acid generating if the NPR > 2.5, and uncertain if 1 < NPR < 2.5 (Adam et al., 1997; Benzaazoua et al., 2004; Bouzahzah et al., 2014). To support the ABA calculation, the NAG test was performed on the feed sample and the corresponding desulphurized materials. This test involved mixing a 15% H_2O_2 solution with 2 g of comminuted sample (< 75 µm) over 24 h (Devin et al., 2008; Stewart, 2020). The final pH (NAG pH) of the leachate was then measured. If the NAG-pH is > 4.5, the sample is considered non-acid forming (NAF); if the NAG pH is < 4.5, the sample is considered acid forming (AF) (Stewart, 2020). Comparing the results of the AGP assessment with the NAG tests provided an improved classification.

7.3.4.2 Kinetic Leaching Tests: Weathering Cells

The geochemistry of the feed sample and the desulphurized materials from the different techniques was evaluated using weathering cell tests. The weathering cells accelerate the oxidation of the studied materials (Cruz et al., 2001). Twice a week, 50 mL deionized water was used to flush 67 grams of dry sample. The samples were left to react for four hours with deionized water. The leachates were then collected, filtered at 0.45 µm, and analysed for their chemical composition using ICP-AES (PerkinElmer OPTIMA 3100 RL, relative precision of 5%) on an aliquot acidified to 2% HNO_3 for preservation. The leachates were also analysed for pH, Eh, and electrical conductivity (EC) using pH-Eh-conductivity meters, and acidity and alkalinity using automated titration. To maintain optimal saturation conditions for the tested samples and to prevent extreme drying, the weathering cells were placed into a controlled-weather box (Chopard et al., 2017). The weathering cells were monitored over 80 consecutive days.

7.4 Results

7.4.1 Physical and Chemical Characteristics

The physical and chemical properties of the studied WR and the results of the AGP assessment using static tests are summarized in Table 7.2. The specific gravity of the WR was 2.88 g/cm^3 and the SSA was 1.38 m^2/g. Sulphur and carbon analysis revealed that the sulphur content was approximately 1.78 wt%. The high silicon and iron contents (22.68 and 12.33 wt%, respectively) were related to the presence of silicon- and iron-bearing minerals such as oxy-hydroxide minerals (i.e., hematite, magnetite, etc.) and iron-bearing sulphides (pyrite and pyrrhotite). Aluminum, calcium, and magnesium contents were 4.5, 3.8, and 5.7 wt%, respectively. Arsenic, nickel, cobalt, and copper, as examples of environmentally deleterious elements (contaminants), were detected in concentrations of 0.07, 0.095, 0.007, and 0.008 wt%, respectively. Table 7.2 also highlights other elements detected, such as K, Mn, Ti, Zn, and Pb.

Table 7.2 Physical properties, chemical properties, and static test results of the feed sample and its corresponding desulphurized materials (SSA: specific surface area; S_G: specific gravity)

		DL[a]	Feed	DDMS[b]	DST[c]	DC[d]
Physical Properties	S_G (g/cm^3)	-	2.88	2.68	2.78	2.66
	SSA (m^2/g)	-	1.38	1.22	1.34	1.26
Chemical Analysis using ICP-MS (wt.%/wt)	Si	0.01%	22.68	24.9	21.3	22.8
	Fe	0.05%	12.33	8.26	12.5	11.8
	Al	0.01%	4.45	3.91	4.79	4.92
	Ca	0.01%	3.78	3.07	3.91	3.38
	Mg	0.01%	5.70	4.77	6.63	6.19
	Mn	0.001%	0.24	0.176	0.243	0.223
	K	0.1%	1.45	1.3	1.5	1.6
	Ti	0.001%	0.21	0.17	0.25	0.24
	As	0.001%	0.08	0.026	0.048	0.028
	Ni	0.001%	0.095	0.056	0.074	0.055
	Cu	0.001%	0.008	0.005	0.007	0.005
	Zn	0.001%	0.013	0.008	0.009	0.007
	Pb	0.001%	0.001	0.005	0.003	0.004
	Co	0.001%	0.007	0.005	0.006	0.006
	Cr	0.01%	0.13	0.11	0.16	0.15
	Sb	0.002%	< 0.002	< 0.002	< 0.002	< 0.002
S/C Analysis, Static & NAG tests	S_{total} (%)	0.09	1.78	0.28	0.68	0.37
	C_{total} (%)	0.09	1.44	1.52	1.48	1.54
	AP ($CaCO_3$/t)	-	55.63	8.75	21.25	11.56
	NP ($CaCO_3$/t)	-	119.95	126.62	123.28	128.28
	NNP ($CaCO_3$/t)	-	64.33	117.87	102.03	116.72
	NPR (NP/AP)	-	2.16	14.47	5.80	11.09
	NAGpH	-	6.65	8.24	7.85	8.13
	AGP**	-	No	No	No	No

[a]DL: detection limit

[b]DDMS: Desulphurized material using DMS

[c]DST: Desulphurized material using spiral and shaking table

[d]DC: Desulphurized material using combination of techniques

7.4.2 Mineralogical Characterisation

7.4.2.1 Bulk Mineralogy

Optical microscopy observations of the feed sample indicated that pyrite was the main sulphide present in the examined WR, with trace amounts of gersdorffite, pyrrhotite, arsenopyrite, and chalcopyrite (Figure 7.4A). Sulphide minerals displayed different textures that could be classified as: i) free or liberated sulphides with no common boundaries with other non-sulphide minerals (NSG) (Figure 7.4A-B), ii) mid-liberated sulphides with boundaries partially shared with NSG minerals (Figure 7.4A-B), and iii) locked sulphides entirely encapsulated within NSG minerals (Figure 7.4C-D-E-F).

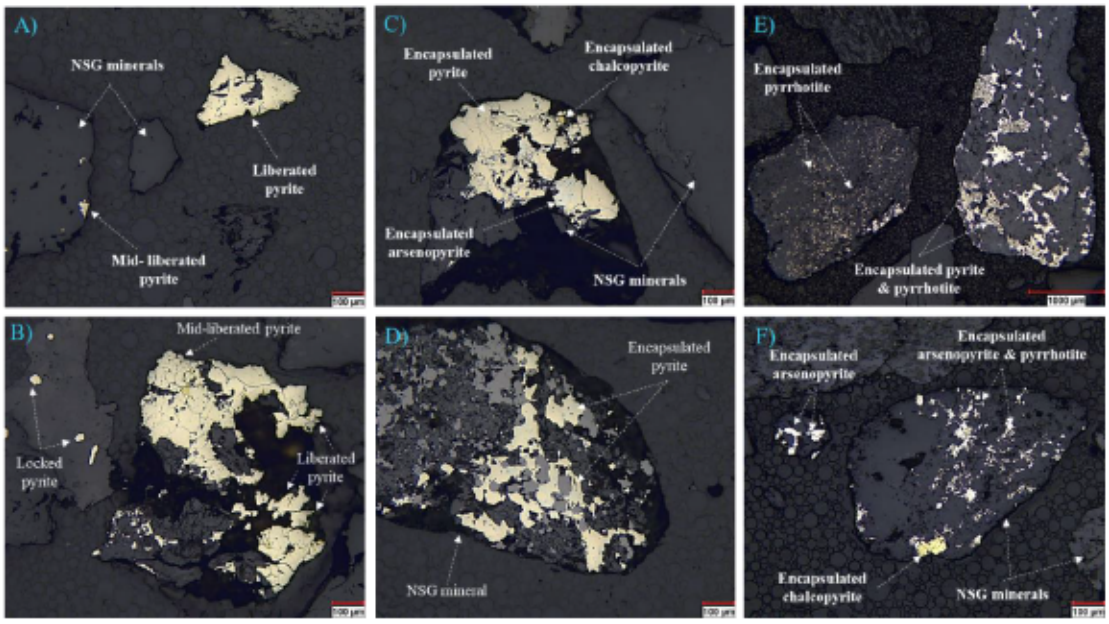

Figure 7.4 Optical microscopy (reflected light mode) photomicrographs of the studied material showing textures and mineralogical associations of sulphides. A, B) Liberated and mid-liberated sulphides, C, D, E, and F) encapsulated sulphides.

To investigate other mineralogical characteristics of the studied WR, the sample was submitted for mineralogical assessment using QEMSCAN®. The mineralogical composition results are summarized in Figure 7.5. Sulphide minerals were present in the form of iron sulphides (pyrrhotite and pyrite) with gersdorffite subordinated. Some traces of arsenopyrite, chalcopyrite, and pentlandite were also detected (Figure 7.5). Carbonates occurred mainly as calcite. The bulk mineralogical composition of the studied material was dominated by non-sulphide minerals (NSG), namely micas, chlorite, quartz, amphibole, plagioclase, and serpentine. This is in accordance with elevated Al, Si, Ca, and Mg concentrations. Quantitatively, total sulphide and carbonate contents were 4.58 wt% and 4.47 wt%, respectively. Specifically, sulphide mineral contents were ~4 wt% pyrite, 0.33 wt% gersdorffite, 0.15 wt% pyrrhotite, 0.03 wt% arsenopyrite, and 0.01 wt% chalcopyrite. Carbonate content was 4.47 wt%. Moreover, micas, chlorite, quartz, and amphibole contents were 22.3 wt%, 20.8 wt%, 17.9 wt%, and 15.4 wt%, respectively. Other minerals were identified with contents less than 5%, including plagioclase (3.2 wt%), Fe and Mg serpentine (2.6 wt%), and Fe oxide (1.2 wt%) (Figure 7.5).

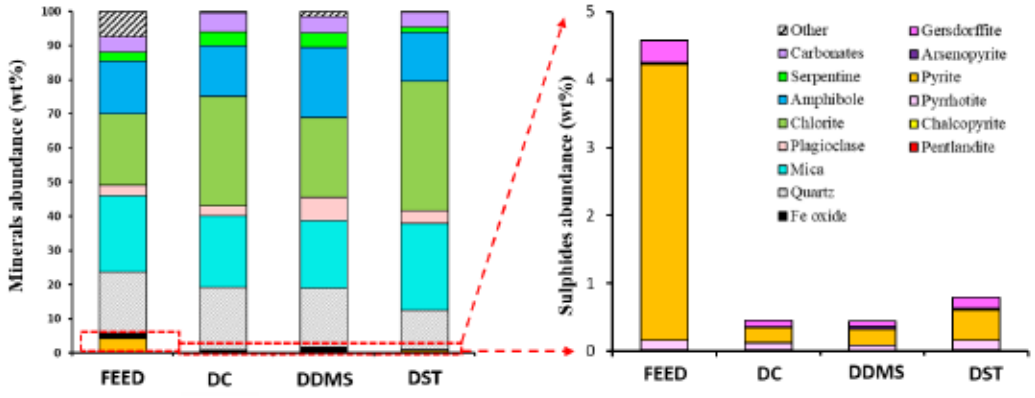

Figure 7.5 Modal mineralogy of feed sample and desulphurized materials

7.4.2.2 Textural Analysis and Mineral Liberation Quantification

Mineral liberation and mineralogical associations

Sulphide (main acid-generating minerals) and carbonate (neutralizing minerals) liberation degrees and their mineralogical associations are highlighted in Figure 7.6A; this describes the relationship of these minerals with surrounding minerals (level to which the minerals of interest are exposed in the sample) (Elghali et al., 2018). In the liberation data, a mineral is considered liberated (free) when its liberation degree is greater than 95%, and it is considered locked when its liberation is less than 10%. A mineral is considered mid-liberated (binary state) when more than 95% of the particle area composed of the mineral of interest and the associated minerals. Pyrite and pyrrhotite were combined as Fe-sulphides while gersdorffite and arsenopyrite were combined as As-sulphides. Figure 7.6A shows that carbonates and Fe-sulphides displayed approximately the same degree of liberation (30.9 and 31.5 wt%, respectively). The As-sulphide liberated fraction was about 13.9 wt%. Sulphides and carbonates were associated with NSG minerals (especially silicate minerals) as binary associations. Figure 7.6A also illustrates the mineralogical associations of the sulphides and carbonates. Fe- and As-sulphide minerals were associated with NSG minerals in proportions of about 53 wt% and 63 wt%, respectively. Carbonates were associated with NSG minerals for about 59 wt%.

Contaminant deportment (S, As, Ni, and Co)

Elemental deportment of chemical species of interest (S, Co, As, and Ni as contaminants) was calculated based on the bulk chemical composition and mineralogical composition of the studied material. Sulphur within the studied material was mainly associated with pyrite, pyrrhotite, gersdorffite, arsenopyrite, and chalcopyrite. These contaminant-bearing sulphides/sulphosalts differ in their

involvement in mine drainage processes (different reactivities). Figure 7.6B shows S, As, Ni, and Co deportment within the studied sample. The results showed that 93.35%, 3.71%, 2.44%, 0.23%, and 0.20% of the S was associated with pyrite, gersdorffite, pyrrhotite, chalcopyrite, and arsenopyrite, respectively. Cobalt within the studied sample was totally attributed to gersdorffite (100 wt%), while 91.29 wt% and 8.71 wt% of the As was associated with gersdorffite and arsenopyrite, respectively. Cobalt within the studied sample was attributed to gersdorffite (100%), while 46.58%, 41.68%, and 11.74% of the Ni was attributed to gersdorffite, pyrrhotite, and pentlandite, respectively. Arsenic was attributed to arsenopyrite (77%), gersdorffite (21.33%), and pyrrhotite (1.69%). The majority of the Ni was attributed to gersdorffite (74.41%) and pentlandite (1.39 wt%), while the remaining Ni occurred as an inclusion in the amphibole (23.21%), as confirmed by EPMA (Ait-khouia et al., 2022a).

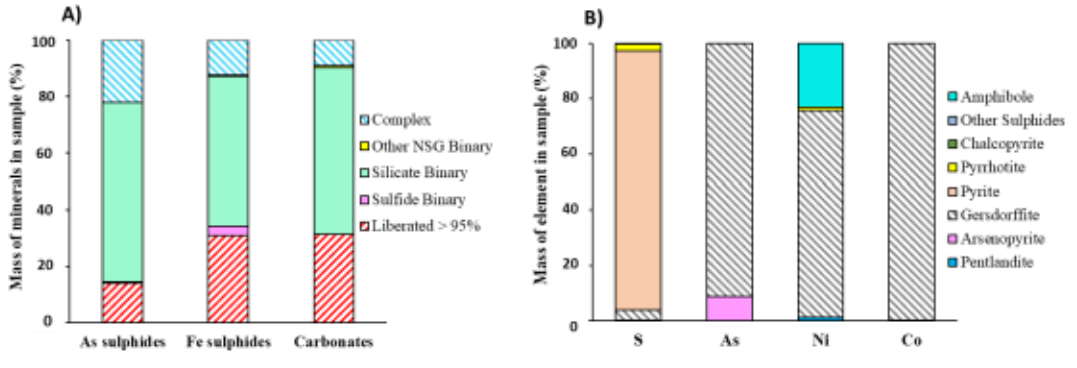

Figure 7.6 A) Mineralogical associations and B) sulphur, arsenic, nickel, and cobalt deportments for the feed sample.

7.4.3 Desulphurization Results

The aim of this section was to assess the feasibility of desulphurizing the studied WR fraction by recovering the contaminant-bearing sulphides using different approaches: i) centrifugal DMS, ii) spiral/shaking table, and iii) combined techniques including centrifugal DMS, Knelson, and flotation. The concentrate materials produced were

subjected to pyro-analysis to estimate the gold content and to evaluate the possibility to offset the costs related to the best sulphur separation process for this study.

7.4.3.1 Centrifugal Dense Medium Separation (DMS)

Results of desulphurization using the centrifugal DMS method are shown in Table 7.3. The sulphur content was depleted within the desulphurized materials from an initial value of 1.78 wt% to 0.28 wt%, leading to a sulphur recovery of 88%.

Table 7.3 Results of desulphurization processes on the studied sample.

Process	Material	S (%)	C (%)	Sulphur recovery (%)	Wt% of the concentrate
DMS	Feed Sample	1.78	1.44	**88.14**	**23.8**
	Concentrate	6.08	1.18		
	Desulphurized material	0.28	1.52		
Spiral & shaking table	Concentrate	5.2	1.31	**70.66**	**27.2**
	Desulphurized material	0.68	1.48		
Combination (DMS, Knelson, flotation)	Concentrate	6.6	1.13	**84.34**	**24.7**
	Desulphurized material	0.37	1.54		

The concentrate produced (~24 wt% of the studied WR) had a 6.08 wt% sulphur content and displayed a low carbon content (1.18 wt%). The sulphur distribution indicates that sulphides and sulphosalts (S_G ranging between 4.8 and 6.1) were concentrated and were more abundant in the heavy fraction, with an upgrade ratio of 3.7. The elemental distribution also shows that the float fraction (light) contained a low sulphur content (0.28 wt%), which implies that it was successfully desulphurized.

7.4.3.2 Gravity Separation Using Spiral/Shaking Table

Results of desulphurization using gravity separation are shown in Table 7.3. The desulphurized material was characterised by a sulphur content of 0.7 wt% and a carbon content of 1.5 wt%. The sulphur content of the concentrate was 5 wt%, corresponding to a mass of concentrate of 27 wt% with a sulphur recovery of around 71 wt%.

7.4.3.3 Combination of Gravity Separation and Flotation

As described earlier, the feed sample with a particle size < 2.5 mm was screened at 850 µm (Figure 7.3C). Grains smaller than 850 µm were processed with a Knelson separator followed by flotation. The combination of gravity methods (DMS and Knelson concentrator) and flotation ensured a high sulphur recovery (84 wt%) (Table 7.3). The sulphur content of the sulphide concentrate was 6.6 wt%, corresponding to a mass of concentrate of approximately 25 wt%. The sulphur content within the desulphurized product was 0.37 wt% (Table 7.3). The carbon content was around 1.5 wt%, meaning that the neutralization potential was mostly preserved within the final desulphurized material. In terms of deleterious elements, the most successful desulphurization test yielded 0.026% of residual arsenic in the desulphurized material for the centrifugal DMS and combination approaches. The initial arsenic concentration was 0.07 wt%, which corresponds to an arsenic recovery of approximately 72 wt% for both approaches. Removal of nickel and cobalt was lower (about 56 wt% and 45 wt%, respectively), but it also reached a low residual concentration of 0.055 wt% and 0.005 wt% in the desulphurized material for an initial Ni and Co content of 0.095 wt% and 0.007 wt%, respectively (Table 7.2). However, the spiral/shaking table approach showed arsenic, nickel, and cobalt recoveries of 48 wt%, 41 wt%, and 35 wt%, respectively, corresponding to 0.048 wt%, 0.074 wt%, and 0.006 wt% of residual As, Ni, and Co, respectively.

7.4.4 Characterisation of Desulphurized Materials

7.4.4.1 Physical and Chemical Characterisation

The results of physical and chemical analyses of the desulphurized materials using DMS (DDMS), spiral/shaking table (DST), and a combination of gravity and flotation (DC) are provided in Table 7.2. The specific gravity of the different desulphurized

materials was between 2.68 and 2.82 g/cm^3, which is typical of siliceous matrices ($S_{Gquartz}$ = 2.65 g/cm^3). DST had a slightly higher specific gravity (S_G = 2.82 g/cm^3) compared to DDMS and DC because it contained more Fe- and As-bearing sulphides, which correspond to specific gravities ranging between 4.6 and 6.1 g/cm^3 (Table 7.1). These results show that the desulphurized materials were characterised by lower metal concentrations compared to the feed sample. The chemical composition of these materials was mainly composed of Si, Fe, Al, Ca, Mg, and K at respective concentrations of 24.9 wt%, 8.26 wt%, 3.91wt%, 3.07 wt%, 4.77 wt%, and 1.3 wt% for DDMS, 21.3 wt%, 12.5 wt%, 4.79 wt%, 3.91wt%, 6.63 wt%, and 1.5 wt% for DST, and 22.8 wt%, 11.8 wt%, 4.92 wt%, 3.38 wt%, 6.19 wt%, and 1.6 wt% for DC. The high presence of Si can be explained by the mineralogical composition of the desulphurized materials, which were mostly silicates (Figure 7.5). Sulphur (as sulphides) and carbon (as carbonate) concentrations were low compared to the feed sample. Sulphur and C were found at respective concentrations of 0.28 wt% and 1.52 wt% (DDMS), 0.68 wt% and 1.48 wt% (DST), and 0.37 wt% and 1.54 wt% (DC).

7.4.4.2 Mineralogical Characteristics

The mineralogical compositions of the desulphurized materials as determined by QEMSCAN® are presented in Figure 7.6B. The bulk mineralogical composition was mostly dominated by non-sulphide gangue minerals, particularly quartz, mica, amphibole, and chlorite. Quantitatively, quartz and mica contents were 18.57 wt% and 20.72 wt% for DC, 17.22 wt% and 19.89 wt% for DDMS, and 11.68 wt% and 25.32 wt% for DST, respectively. Amphibole and chlorite contents were 10.93 wt% and 32.04 wt% for DC, 20.32 wt% and 23.43 wt% for DDMS, and 14.13 wt% and 38.80 wt% for DST, respectively. These results are in accordance with elevated Si, Fe, Al, Ca, K, and Mg concentrations (Table 7.2). Other non-sulphidic minerals were identified with contents less than 5%, including serpentine, plagioclase, and Fe-oxides.

Carbonate (as calcite) contents were 6.5 wt%, 4.7 wt%, and 3.4 wt% for DC, DDMS, and DST respectively.

The three desulphurized materials contained low sulphide contents of 0.49 wt%, 0.44 wt%, and 0.91 wt% for DC, DDMS, and DST, respectively. The feed sample contained 4.59 wt% sulphides. The small amounts of remaining sulphides were mainly in the form of pyrite (0.23 wt%, 0.24 wt%, and 0.45 wt%) and pyrrhotite (0.15 wt%, 0.08 wt%, and 0.24 wt%) for DC, DDMS, and DST, respectively. Gersdorffite was also detected at 0.09 wt%, 0.07 wt%, and 0.17 wt% for the desulphurized materials, respectively (e.g., DC, DDMS, and DST). Other remaining sulphides (chalcopyrite, arsenopyrite, and pentlandite) were also detected at lower concentrations (<0.03 wt%).

Mineral liberation is recognized to be an important parameter that influences sulphide (acid generating) reactivity (Ait-Khouia et al., 2021; Elghali et al., 2021; Mafra et al., 2020). Liberation analysis revealed that As- and Fe-sulphides remaining in the desulphurized materials displayed different degrees of liberation compared to the feed sample (Figure 7.7A-B). The Fe-sulphide liberated fractions were 3.5 wt%, 2.5 wt%, and 15.8 wt% for DC, DDMS, and DST, respectively. The As-sulphide liberated fractions were 6.1 wt%, 3.1 wt%, and 31 wt% for DC, DDMS, and DST, respectively. Sulphides were more liberated in DST than in the other desulphurized materials.

As shown in Figure 7.7A, about 96%, 88%, and 60% of the As-sulphides in DDMS, DC, and DST, respectively, had a liberation degree of less than 40%. Similarly, about 85%, 77%, and 55% of the Fe-sulphides in DDMS, DC, and DST, respectively, had a liberation degree of less than 40% (Figure 7.7B). This proves that most of the remaining contaminant-bearing sulphides were not liberated, and that the liberated sulphide particles were efficiently recovered by the different desulphurization approaches, other than the spiral and shaking table processes, which exhibited insufficient desulphurization performance. Mineralogical associations of the sulphides are shown in Figure 7.7C–D.

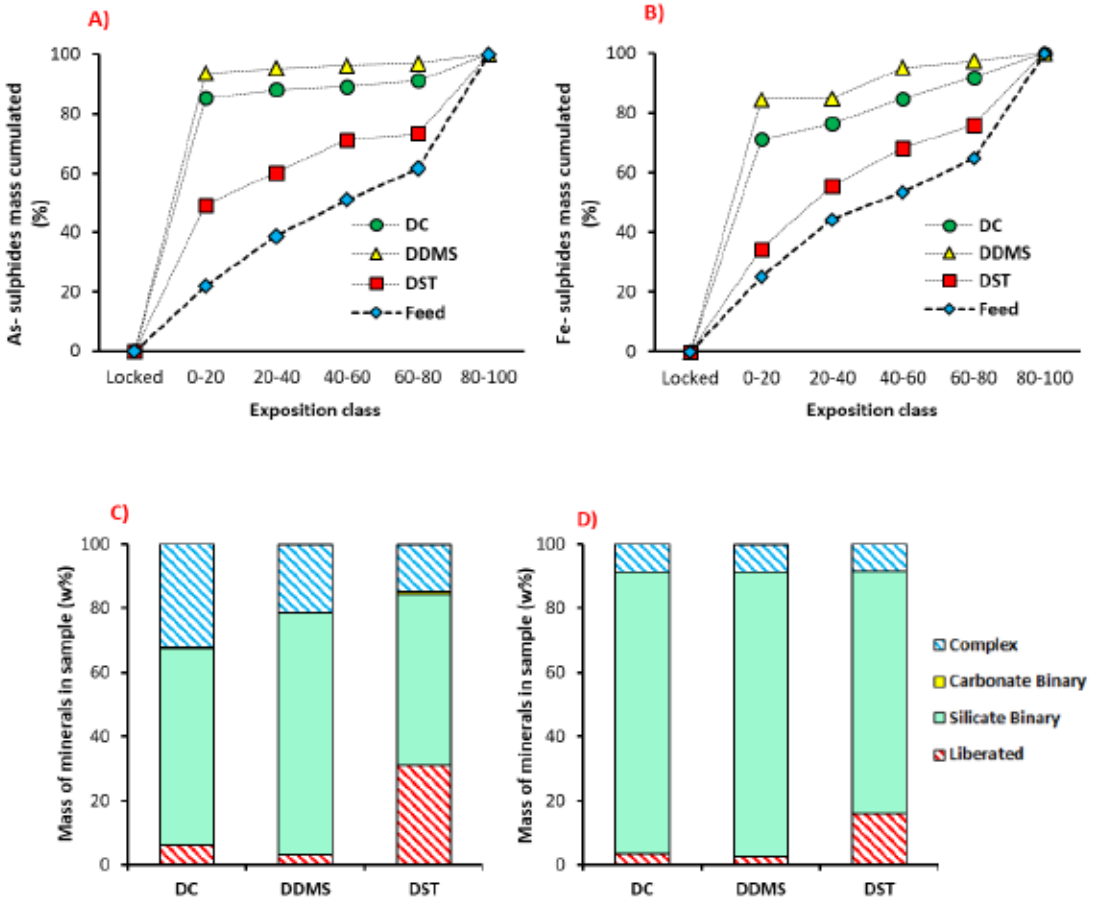

Figure 7.7 Mineral liberation degree of A) As-sulphides, B) Fe-sulphides, and mineralogical associations of C) As-sulphides and D) Fe-sulphides for the desulphurized materials.

Sulphides were mainly associated with NSG minerals as binary associations. Binary associations of Fe-sulphides with NSG minerals were 87.7 wt%, 88.8 wt%, and 75.8 wt% for DC, DDMS, and DST, respectively. Binary associations of As-sulphides with NSG minerals were about 61.4 wt%, 75.4 wt%, and 53.3 wt% for DC, DDMS, and DST, respectively.

7.4.5 Environmental Behaviour of the Feed Sample and Desulphurized Materials

7.4.5.1 Acid-Generation Potential Assessment with Static Tests

Compared to the feed sample, sulphide removal by the different techniques decreased the AP of the desulphurized materials; subsequently, the NNPs were increased due to the increase in the relative content of neutralizing minerals (e.g., carbonates, silicates) and the decrease in the sulphide content. The results of the ABA tests are presented in Table 7.2 and in Figure 7.8A. Quantitatively, the NNP of the feed sample was increased from 64.3 to 117.87, 102.03, and 116.72 kg $CaCO_3$/t for DDMS, DST, and DC, respectively. According to the classification criterion proposed by Miller et al. (1991), the desulphurized materials were non-acid generating (i.e., NNP > 20 kg $CaCO_3$/t). These results were confirmed by the NP/AP ratio criterion. The classification results are plotted in the NP vs AP graphs (Figure 7.8A).

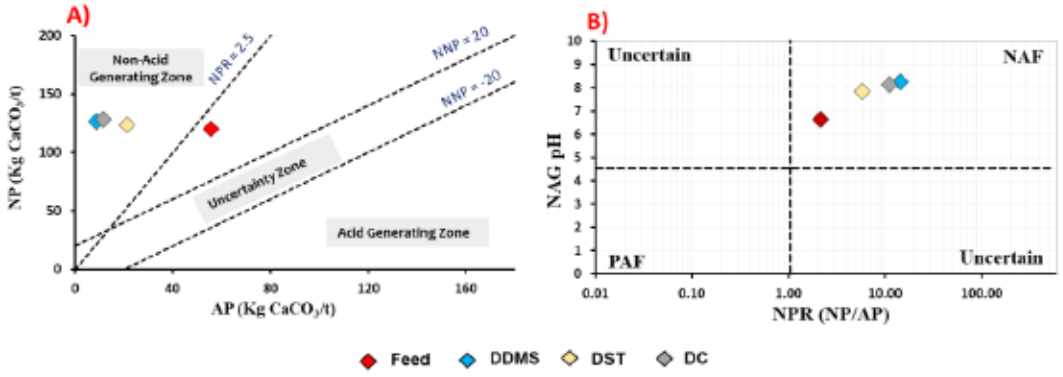

Figure 7.8 Classification of the feed sample and the desulphurized materials in terms of A) acid-base accounting tests and B) NPR versus NAG pH (NAF: non-acid forming; PAF: potentially acid-forming).

The NAG pH of the feed sample and the desulphurized materials using DMS, spiral/shaking table, and gravity combined with flotation was 6.65, 8.24, 7.85, and 8.13, respectively. For a better AGP classification as suggested by Parbhakar-Fox et al. (2018), the NAG pH values were interpreted using the NPR as shown in Figure 7.8B. Thus, the feed sample and all desulphurized materials were classified as non-acid forming (NAF).

7.4.5.2 Kinetic Leaching Tests

The geochemical behaviour of the studied fine fraction (< DPLS) and the corresponding desulphurized materials was evaluated under accelerated weathering conditions using weathering cell tests (WCs) (Cruz et al., 2001). These tests were mainly used to evaluate the effectiveness of environmental desulphurization to limit the generation of contamination by quantifying: i) the sulphide oxidation rate, and ii) the contaminant release rate. The chemical composition of the leachates from the WCs over 80 days is shown in Figure 7.9 and Figure 7.10. All the tested samples were considered to be non-acid generating over the short term according to the circumneutral pH values and low acidity values obtained during the kinetic tests (Figure 7.9A-B). The pH of the leachates was circumneutral and ranged between 7.5 and 8.1 for the feed sample and between 7.7 and 8.4 for the desulphurized materials.

The electrical conductivity (EC) showed high values for samples at the beginning of the kinetic tests (403 µS/cm for feed and 248 µS/cm, 345 µS/cm, and 469 µS/cm for DDMS, DC, and DST, respectively) and tended to stabilize at average values of 112 µS/cm for the feed sample and 80 µS/cm, 72 µS/cm, and 91 µS/cm for DDMS, DC, and DST, respectively (Figure 7.9B). This indicates a decrease in the chemical loading of the leachates. The release of weakly-bonded soluble and pre-oxidized elements was reflected in high electrical conductivity values at the earlier stages of the kinetic tests (Elghali et al., 2021; Mayer et al., 2002). Oxidation during the first ten days of the test

eliminated the oxidized surface of the particles and, consequently, exposed the non-oxidized core of the mineral.

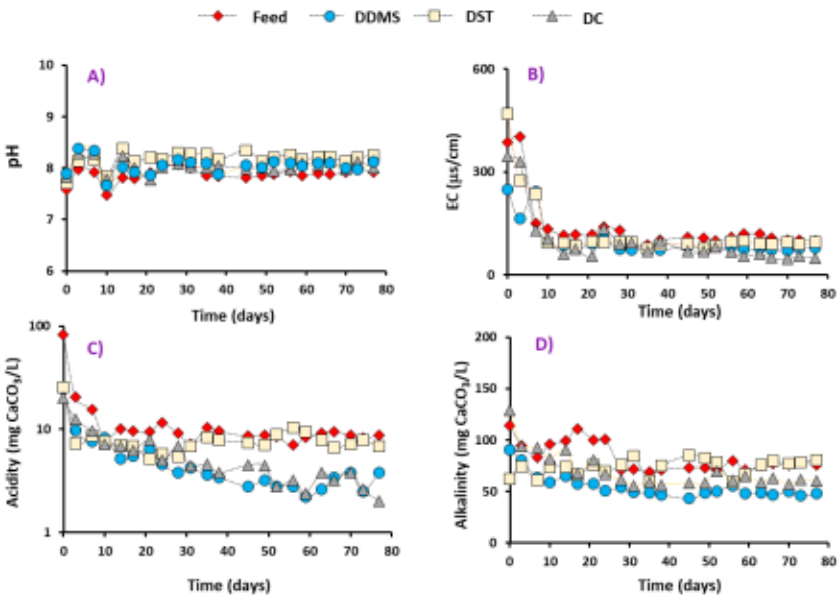

Figure 7.9 A) pH, B) electrical conductivity, C) acidity, and D) alkalinity evolution within the leachates from the feed and desulphurized materials.

The acidity generated by the feed sample was slightly higher (13.2 mg $CaCO_3$/L average) than that generated by the desulphurized materials (5.1 mg $CaCO_3$/L, 5.8 mg $CaCO_3$/L, and 8.2 mg $CaCO_3$/L averages for DDMS, DC, and DST, respectively) (Figure 7.9C); the alkalinity of the leachates was around ~83 mg $CaCO_3$/L for the feed sample and tended to decrease slightly to 54.9 mg $CaCO_3$/L, 70.2 mg $CaCO_3$/L, and 73.3 mg $CaCO_3$/L for DDMS, DC, and DST, respectively (Figure 7.9D).

The chemical composition of the leachates is presented as cumulative and mass-normalized concentrations (mg/kg). Sulphate (SO_4^{2-}) was selected as a tracer for sulphide and sulphosalt oxidation, Ca and Mg were selected to evaluate carbonate

dissolution, and Si and Al were selected to indicate aluminosilicate mineral dissolution (Benzaazoua et al., 2004). Sulphate, Fe, Ca, Mg, Mn, Si, and Al leaching from the different samples is illustrated in Figure 7.10.

The first two cycles of the weathering cell tests showed a significant increase in elements released by the samples. This increase is attributed to the leaching of elements originally present in the samples due to previous oxidation. Cumulative sulphate masses over 80 days were about 10 mg/kg for the feed sample, 2.4 mg/kg for DDMS, 4.8 mg/kg for DST, and 3.2 mg/kg for DC (Figure 7.10A). More sulphate was leached from the feed material as compared to the desulphurized materials due to the high content and high liberation degree of the sulphides within the feed sample. Moreover, calculated sulphide oxidation rates for the studied samples were: 0.125 mg/kg/day, 0.03 mg/kg/day, 0.04 mg/kg/day, and 0.06 mg/kg/day for the feed sample, DDMS, DC, and DST samples, respectively.

This difference in reactivity could be attributed to the remaining sulphide form (mineralogy), modal composition, texture, and degree of liberation (Ait-Khouia et al., 2021; Elghali et al., 2021; Mafra et al., 2020). Indeed, the remaining sulphides/sulphosalts were mostly in the form of pyrite and pyrrhotite, while the S-bearing minerals in the feed sample were essentially pyrite, pyrrhotite, arsenopyrite, and gersdorffite. When exposed to atmospheric conditions, gersdorffite and arsenopyrite have very high reactivity (Chopard et al., 2017; El-bouazzaoui et al., 2022).

The desulphurized materials released less Ca and Mg as compared to the feed material (Figure 7.10B-C). Calcium leaching was about 17.3 mg/kg for the feed sample, 9.2 mg/kg for DDMS, 11.1 mg/kg for DC, and 14.2 mg/kg for DST. Indeed, this was consistent with the expected behaviour of the samples during weathering testing: sulphides oxidize and carbonates dissolve, buffering acid production (Dold, 2017; Rimstidt and Vaughan, 2003). This is also the reason the pH values over the 80-day period remained neutral. Magnesium leaching was about 1.5 mg/kg for the feed sample,

1.3 mg/kg for DDMS, 1.2 mg/kg for DC, and 1.2 mg/kg for DST (Figure 7.10C). Less Ca and Mg was released from the desulphurized materials due to their low reactivity.

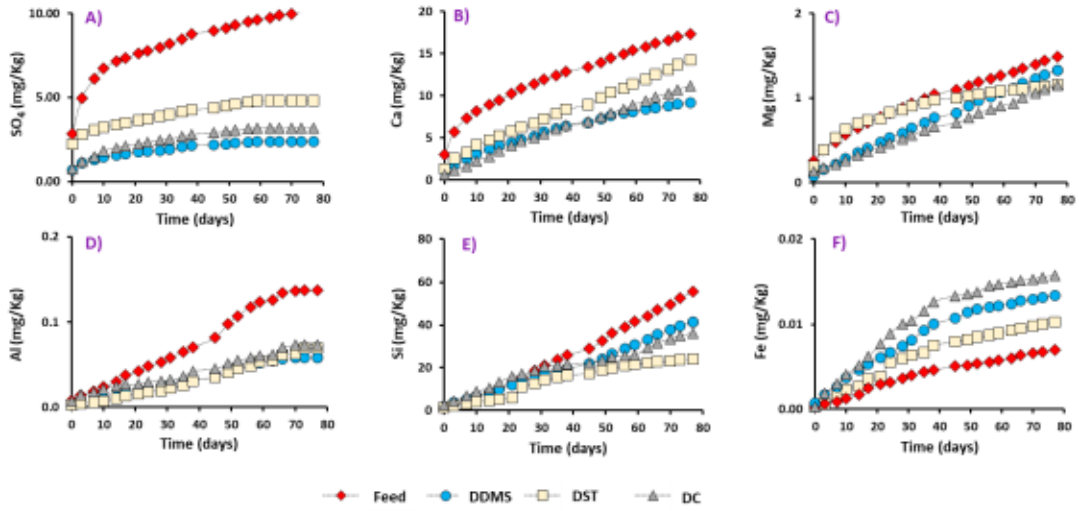

Figure 7.10 Evolution of the chemical quality of the leachates from the feed and desulphurized materials: A) SO_4^{2-}, B) Ca, C) Mg, D) Al, E) Si, and F) Fe. Concentrations are presented as cumulative and mass normalized.

More Al was released from the feed sample (0.14 mg/kg) compared to the desulphurized samples (Figure 7.10D) (aluminum leaching was about 0.06 mg/kg, 0.07 mg/ kg, and 0.07 mg/ kg for DDMS, DC, and DST, respectively). Silicon leaching was about 55.6 mg/kg for the feed sample and ranged between 41.3 mg/kg, 36.2 mg/kg, and 24.2 mg/kg for DDMS, DC, and DST, respectively (Figure 7.10E). Even if the Si- and Al-bearing minerals were enriched in the desulphurized samples through bulk sulphide removal, their release rates were lower than those from the feed sample. These differences could be linked to the lower reactivity of the desulphurized materials as compared to the feed sample.

The desulphurized samples released more Fe as compared to the feed sample (Figure 7.10F). Iron release was approximately 0.007 mg/kg for the feed sample and ranged between 0.013 mg/kg, 0.016 mg/kg, and 0.01 mg/kg for DDMS, DC, and DST, respectively. Furthermore, changes in geochemical conditions (e.g., pH, Eh, and iron concentrations) can lead to iron hydroxide precipitation. Leachates from the feed sample had circumneutral pH values ranging between 7.5 and 8.1 and an oxidation reduction potential between about 0.4 and 0.6 V. These characteristics are favourable for iron hydroxide precipitation (Cravotta III, 2008; Elghali et al., 2021) and explain the low concentrations of iron observed in the leachates. Furthermore, the mineralogical observation by optical microscopy performed on the dismantled materials revealed some sulphides coated with a fine rim of iron oxides in the feed sample and desulphurized materials (Figure 7.11).

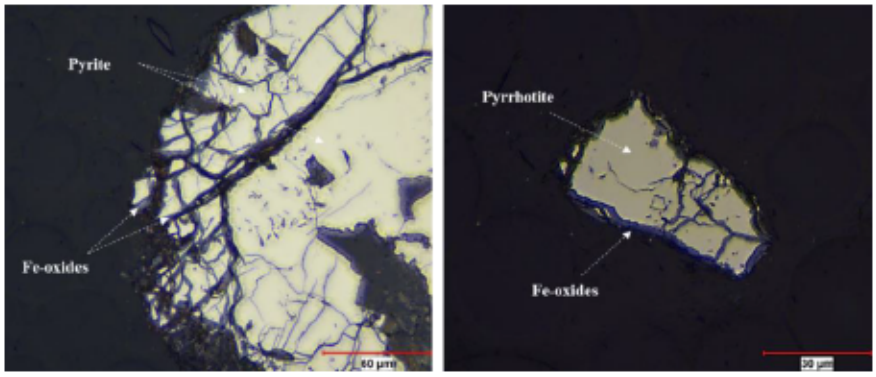

Figure 7.11 Optical microscopy images showing an example of pyrite and pyrrhotite coating with iron oxides.

Nickel, arsenic, iron, and copper were chosen as examples of contaminants. The feed sample had a non-negligible As contamination risk as compared to the desulphurized materials. Indeed, concentrations of arsenic collected immediately after each leaching

cycle exceeded the maximal accepted concentration established by Quebec provincial legislation (0.4 mg/L) (MDDEP, 2012) (Figure 7.12B).

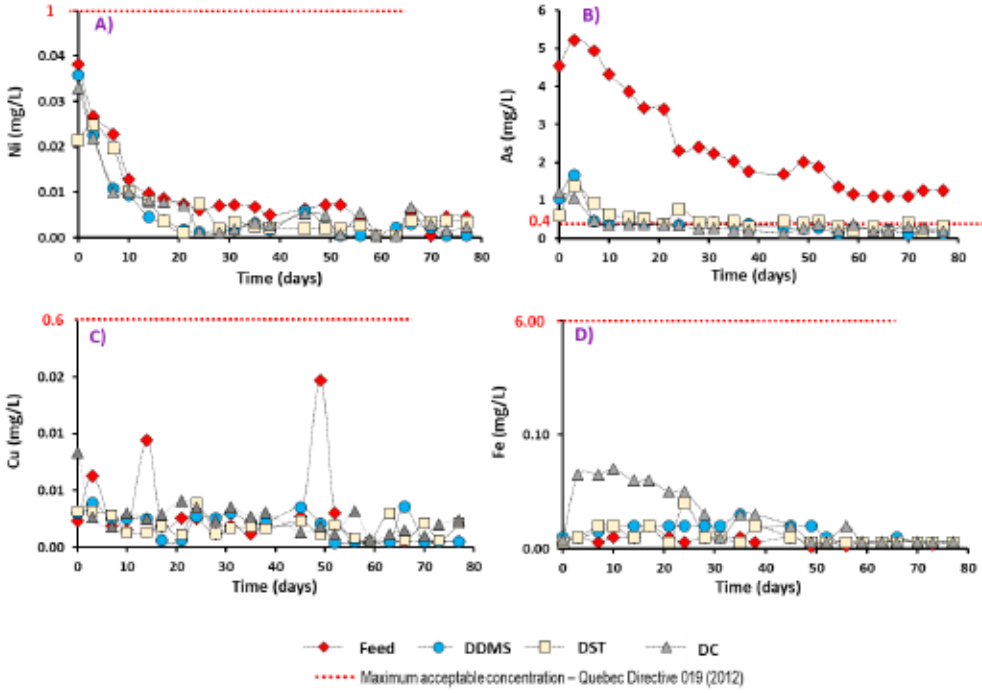

Figure 7.12 Contaminants (Fe, Cu, As, and Ni) leaching within the feed sample and desulphurized materials. A) Ni leaching, B) As leaching, C) Cu leaching, and D) Fe leaching.

The As released by the desulphurized material using the spiral/shaking table (DST) slightly exceeded regulatory criteria. This result could be linked to relatively low recovery of sulphide minerals (particularly As-sulphides) using the spiral and shaking table. The unrecovered gersdorffite and arsenopyrite exhibit very high reactivity with a strong oxidation rate when exposed to weathering (Chopard et al., 2015; El-bouazzaoui et al., 2022). Thus, the feed sample and desulphurized material using the spiral/shaking table had the potential to generate As-bearing CND.

The desulphurized materials using DMS (DDMS) and combined techniques (DC) did not pose any significant risk of CND generation at laboratory scale using weathering

cells. larger scale testing is needed to better define the risk. The instantaneous concentrations of Ni, As, Cu, and Fe (Figure 7.12) did not exceed the environmental criteria of directive 019 in Quebec (Canada), which establishes a maximum limit of 1 mg/L, 0.4 mg/L, 0.6 mg/L, and 6 mg/L, respectively (MDDEP, 2012). The release of arsenic at the beginning of the kinetic tests (first three cycles) corresponds to the leaching of the oxidized surface of the particles (e.g., sulphides and oxy-hydroxides) (Mayer et al., 2002).

7.5 Discussion

7.5.1 Efficiency of Reprocessing Techniques

The reprocessing techniques used in this study focused on the desulphurization of the reactive fraction (<DPLS) which was classified as contaminated mine drainage generating (Ait-khouia et al., 2022a). Sulphur and contaminant (i.e., As, Ni, and Co) recoveries were used to evaluate the effectiveness of the different reprocessing techniques. To qualitatively identify residual sulphides, mineralogical observations under optical microscopy were conducted on the desulphurized materials. For quantification objectives (modal composition, textural parameters, etc.), a QEMSCAN® system was used. Section 3 showed that these techniques presented different efficiencies for desulphurizing the feed sample. The DMS test results on the feed sample showed a high sulphur recovery of about 88 wt%. The sulphur contents were 6.08 wt% and 0.28 wt% in the concentrate and the desulphurized material, respectively. The low sulphur content in the light fraction suggests that a small portion of the sulphides remained locked to gangue minerals.

As the efficiency of this separation method (DMS) is dependent on the sulphide liberation degree (Ait-Khouia et al., 2021; Williford and Bricka, 2000; Wills and Finch, 2016b), a study of the textural and mineralogical characteristics of the light fraction

was performed using OM and QEMSCAN®. Based on these results, it was possible to better understand the behaviour of the studied material during the desulphurization process. As shown in Figure 7.7, most of contaminant-bearing minerals (sulphides and sulphosalts) present in the light desulphurized fraction were partially or totally associated (locked) to NSG minerals with insufficient liberation degrees. The density of the S-carrying grains was impacted and was unable to provide a significant differentiation, leading to poor separation for these grains. These results are consistent with the study conducted by Marion et al. (2017), where centrifugal DMS was used to reprocess fine material. This latest research revealed that the low recovery of iron oxide minerals in the heavy fraction (46.9%) was due to their insufficient liberation from the silicate gangue. This implies that high iron oxide recovery requires a high liberation degree. These results also corroborate the study by Khalil et al. (2019), in which lab centrifugal DMS was used as a depollution process for Pb-Zn tailings. The results indicated that the residual metallic content in the final depolluted tailings was essentially due to the textural character of Pb- and Zn-bearing minerals that were partially or totally associated to gangue minerals. Compared to the other depolluting approaches tested in this study by Khalil et al. (2019), DMS offers high sulphide recovery as it can make sharp cuts with a high degree of efficiency even if the difference between the density of the sulphides and the NSG minerals to be separated is low (<1 g/cm^3) (Wills and Finch, 2016b).

The static and kinetic tests demonstrated that the desulphurized material was non-acid and low risk of contamination. The gravity separation using spiral concentrator combined with shaking table allowed a sulphur recovery of 71 wt% with high residual sulphur content of approximately 0.7 wt% for the desulphurized material. This approach produced a slightly lower sulphur content in the concentrate as compared to the DMS approach (5.2 vs. 6.6 wt%) and did not recover sulphide minerals at a high enough level compared to the DMS approach. The relatively low recovery could be attributed to the textural character of the sulphide minerals and/or the particle size

(Gosselin et al., 1999; Williford and Bricka, 2000). Indeed, spiral/shaking table separators were unable to remove residual sulphides that were locked within NSG minerals; otherwise, their densities will be impacted (by their association with NSG minerals) and may not ensure a significant differentiation, leading to poor separation (Ait-Khouia et al., 2021; Dermont et al., 2008).

Examining the sulphide/sulphosalt liberation and association characteristics of the desulphurized material from the spiral/shaking table suggests that the low sulphide recovery was likely due to insufficient liberation. About 70% of the As-sulphides and 68% of the Fe-sulphides in DST had a liberation degree of less than 60%. Furthermore, these sulphides were mainly associated with NSG minerals as binary associations of about 53 wt% and 76 wt% for As- and Fe-sulphides, respectively. However, QEMSCAN® results also showed that a portion of the 15.8 wt% of Fe-sulphides and 31 wt% of As-sulphides present in the desulphurized material were well liberated (more than 95%). Thus, the insufficient recovery could essentially be attributed to the particle size of the feed material. The operational performance of these technologies is often limited to a specific range of particle sizes (Ait-Khouia et al., 2021; Wills and Finch, 2016a). Gravity separation using a spiral/shaking table is inefficient when undertaken to separate particles with a wide particle size distribution and/or a narrow density distribution (Williford and Bricka, 2000). Ait-Khouia et al. (2021) reported that a density difference of > 1 g/cm^3 must exist between minerals for efficient gravity separation. Conventional gravity concentrators (spiral and shaking table) are generally not suitable for fine particles (< 75 µm); they have a good applicability for the fraction ranging from 75 µm to 3,000 µm (Dermont et al., 2008; Marion et al., 2018).

Optical microscopy demonstrated that the unrecovered free portion was in the form of small particles (< 75 µm) (Figure 7.13A-B). The spiral/shaking table process was unable to remove these residual minerals (Ait-Khouia et al., 2021; Derycke et al., 2013).

According to the kinetic tests, the final desulphurized material was still slightly arsenic-generating with respect to the directive 019 limits.

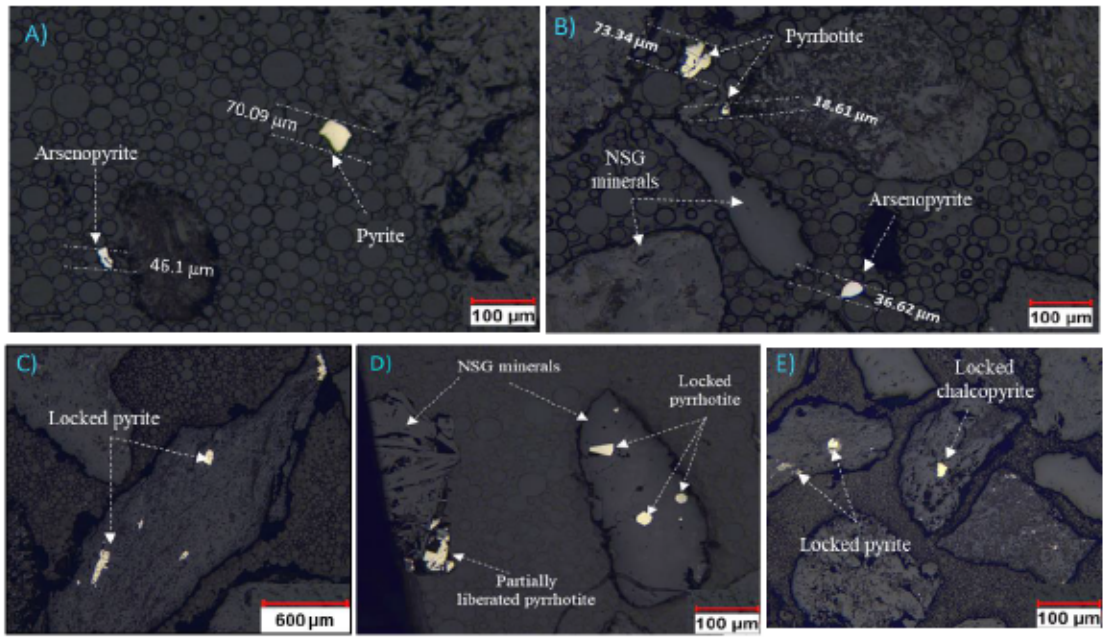

Figure 7.13 Optical microscopy of the polished section of the desulphurized material using A, B) spiral/shaking table approach and C, D, E) combination approach.

Combining gravity (DMS & Knelson concentrator) and flotation enabled the reduction of the sulphur content from 1.78 wt% (feed) to 0.37 wt% in the final desulphurized material. This approach showed a sulphur removal of about 84 wt% with a high sulphur content (6.6 wt%) in the concentrate. However, a slight decrease in the NP value was observed in the desulphurized material. This was due to the selectivity for carbonate/sulphide intergrowth particles within the concentrate material (Amar et al., 2020b). The combined techniques resulted in a final desulphurized material that was non-acid generating according to NPR and NNP criteria (Figure 7.8A-B) and low risk of contamination according to the weathering cell tests (Figure 7.12). An analysis of the mineralogical properties of the desulphurized materials revealed that residual sulphides and sulphosalts presented two main textures: partially liberated and totally

encapsulated with non-sulphide minerals (NSG) (Figure 7.13C-D-E). These reactive minerals were mineralogically considered to be unavailable for oxidation and subsequent production of contaminated leachate. Based on the sulphur removal, the approach combining DMS, Knelson, and flotation was more effective than the gravity method using a spiral and shaking table but resulted in approximately the same performance as the DMS approach. Accordingly, as suggested for mine processing tailings (Benzaazoua et al., 2000; Bois et al., 2005), the environmental desulphurization of the feed sample (< DPLS) could be considered as an effective/feasible technique that can be used to reduce the risk of water contamination by sulphides and sulphosalts. This technique should also be considered during mine WR management.

7.5.2 Reprocessing Strategy Versus Conventional Disposal of WR

The DPLS previously defined in this study, based on a combination of mineralogical characterisation and evaluation of the geochemical behaviour, could be integrated into waste rock pile management to segregate WR following mining extraction, rather than conventional bulk disposal of WR in unsaturated surface piles (Elghali et al., 2019). Based on this parameter, WR could be divided into two different fractions with completely different geochemical reactivities, resulting in the construction of two WR piles: i) a pile containing material > DPLS, which is non-reactive; and ii) a pile containing material < DPLS, which is more reactive and generates arsenic-bearing CND. This result support the findings of Amar et al. (2020b) and Elghali et al. (2018), who proposed this WR management approach. The coarser fraction (> 2.5 mm) in this study was non-reactive and could potentially be valorized in civil engineering or ceramics fields. Environmental desulphurization of the fine/reactive fraction (< 2.5 mm) using DMS or a combination of gravity and flotation would enable the reduction of the volume of CND-generating WR in surface storage (unsaturated piles) and the reduction of the contamination risk due to material oxidation (As leaching).

The desulphurized material could be valorized in situ as material for dam construction or covers to prevent and control AMD generation (Bois et al., 2004; Demers et al., 2008; Lessard et al., 2018; Rey et al., 2016), placed underground to fill open stopes, and/or stored at the surface using the conventional disposal approach. The concentrate materials can be valorized for metal (especially gold) recovery (Broadhurst and Harrison, 2015; Khalil et al., 2019), processed further into useful byproducts such as sulphuric acid (Tugrul et al., 2003), or used within underground paste backfills (Benzaazoua et al., 2008; Benzaazoua et al., 1999).

7.5.3 Feasibility of Gold Valorization and Economic Issues Related to WR Reprocessing

Desulphurization offers an opportunity to concentrate and recover gold as the remaining precious metal within the waste rock (Broadhurst and Harrison, 2015). The concentrates produced from WR reprocessing using gravity, flotation, and combined approaches were analysed for the gold content (Table 7.4).

Table 7.4 Pyro-analysis of DMS, spirals/shaking tables, and gravity combined with flotation concentrates.

Sample	Au (g/t)
Feed sample	0.35
DMS approach	1.83
Spiral/shaking table approach	1.02
Combination approach	2.05

The pyro-analysis of Au in the feed sample displays a low gold content of 0.35 g/t. The concentrate from the DMS and combination methods present a gold grade of about 1.8 g/t and 2 g/t, respectively. The gold content in the spiral/shaking table concentrate was

about 1 g/t. The DMS and combination approaches provided superior performance in terms of sulphide removal as well as gold content in the concentrate. This could be explained in part by the greater selectivity of theses methods when separating gold and sulphide grains as compared to the other techniques (Aleksandrova et al., 2019). Gold recovery could then offset some of the operating and energy costs associated with gravity methods (Knelson, DMS) and flotation. Consequently, reprocessing of the fine reactive fraction (< DPLS) directly after blasting could reduce costs related to it management. The obtained concentrate could be used in the same ore treatment process as the main plant feed. However, before implementing such a novel WR management strategy, pilot testing (including field cells) and detailed technical and economic studies are essential. The capital (equipment and installation) and operating costs are the main desulphurization costs (Alam and Shang, 2012; Benzaazoua and Kongolo, 2003; Nakhaei and Irannajad, 2017; Nuorivaara et al., 2019; Rezvanipour et al., 2018).

7.6 Conclusion

The aim of this study was to assess the feasibility of reprocessing waste rock (< 2.5 mm) to reduce its acid and metal leaching potential. Desulphurization was selected as the technique for controlling the production of CND for the studied WR. The obtained results showed that centrifugal DMS and combined gravity-flotation processes had a good potential for decontaminating WR. These processes led to the best sulphur and contaminant (As, Ni, Fe, and Cu) recoveries, and gold concentration. Furthermore, the results revealed that the analytical techniques (QEMSCAN® and optical microscopy) applied for the characterisation of the studied WR and the produced desulphurized materials clarified the behaviour of minerals during the separation processes. ICP-MS was used to determine the content of contaminant elements in the desulphurized products, while OM/QEMSCAN® was used to determine the influence of particle size, mineral liberation, and mineralogical associations on each desulphurization technique.

The contaminant grades in the desulphurized products (especially DDMS and DC) were very low, implying that: i) sulphide and sulphosalt removal using DMS or combined gravity and flotation methods performed better than the spiral/shaking table process, ii) centrifugal DMS and combined gravity and flotation could be applied as reprocessing techniques for depolluting the WR fraction < DPLS, and iii) the residual contaminant content in the desulphurized products was mainly due to the textural character of the contaminant-bearing minerals (sulphides and sulphosalts) that were partially associated to non-sulphide gangue minerals (mainly silicates).

Kinetic tests were used to compare and demonstrate the effectiveness of the adopted decontamination process. Weathering cell results showed that the feed sample posed a risk of CND (neutral pH and arsenic concentrations that exceeded the environmental guidelines for Quebec). These kinetic tests also revealed that the desulphurized materials using the DMS and combined approaches produced leachates with As concentrations below the directive 019 limits. The leachates from the desulphurized material using spiral/shaking table were slightly above the directive 019 limits for arsenic.

Pyro-analysis revealed that the concentrates of both centrifugal DMS and gravity/flotation had a Au content of > 1.8 g/t, which suggests that gold recovery evaluation could be considered.

To validate the obtained results, the exploration of centrifugal DMS and the combined gravity and flotation techniques at a pre-industrial pilot scale is important. Moreover, the desulphurized product and the concentrate should be studied to propose the best recycling or repurposing method. Finally, this study has several environmental, economic, and social implications: it will help to reduce or eliminate a significant source of environmental hazards by reprocessing and beneficiating problematic mine WR. Environmental desulphurization has been confirmed as an effective strategy for WR management and valorization.

CRediT authorship contribution statement

Yassine Ait Khouia: Conceptualization, Formal analysis, Writing - original draft;

Mostafa Benzaazoua: Conceptualization, Writing - original draft, Supervision;

Yassine Taha: Conceptualization, Writing - original draft, Writing;

Isabelle Demers: Conceptualization, Writing - original draft, Supervision.

Declaration of competing interest

The authors declare that they have no known competing financial interests or personal relationships that could have appeared to influence the work reported in this paper.

Acknowledgements

The authors would like to acknowledge the Natural Sciences and Engineering Research Council of Canada (NSERC) and industrial partners for providing funding for this work through the Collaborative Research and Development (CRD) Program granted to I. Demers. Finally, many thanks must go to the XPS laboratory in Sudbury (Canada) for their help in achieving QEMSCAN analysis and ICP-MS. Many thanks also go to CEGEP Abitibi Témiscamingue for providing spiral and shaking table used to complete the study and to Benjamin De Castro for helping to achieve OM images.

CHAPITRE 8

DISCUSSION GÉNÉRALE

8.1 Importance de la minéralogie appliquée dans le contexte de la désulfuration environnementale des rejets miniers

La désulfuration environnementale a été étudiée comme une éventuelle stratégie de gestion intégrée des rejets miniers. Les résidus Whale Tail d'Amaruq ont été caractérisés par un potentiel de contamination en Fe, As et Ni à cause de la présence de pyrite, pyrrhotite, gersdorffite et arsénopyrite. La caractérisation minéralogique a été utilisée pour suivre et contrôler l'efficacité de la désulfuration environnementale. En effet, la minéralogie automatisée QEMSCAN® a été utilisée pour quantifier le degré de libération des différents sulfures et sulfosels présents dans le résidu, ainsi que pour déterminer les occurrences de nickel et arsenic (principaux contaminants) dans le résidu frais et dans les produits désulfurés. L'objectif ultime derrière ces caractérisations minéralogiques réside dans le calcul de la réactivité absolue du résidu et le matériel désulfuré tenant compte juste des phases sulfureuses réellement exposées aux agents atmosphériques. Cette étude a montré clairement que la minéralogie appliquée pourrait être envisagée/utilisée comme moyen pour améliorer la classification des rejets miniers via les tests statiques. Elle a montré aussi que le recours à la minéralogie automatisée est de grande valeur ajoutée pour une meilleure évaluation de l'efficacité de la désulfuration environnementale comme technique de contrôle de la génération du drainage minier contaminé.

Dans notre cas, la microscopie optique et la microscopie automatisée ont démontré que le résidus désulfuré contenait des traces de pyrite (0,13 % en poids), de pyrrhotite (0,27 % en poids) et de gersdorffite (0,01 % en poids). Environ 98% de ces minéraux sont encapsulés ou associés aux minéraux de gangue (e.g., silicates); les 2% restants de ces

sulfures/sulfosels sont totalement libérés. La microscopie optique a montré que cette portion de sulfures/sulfosels libérée et non récupérée se présente sous la forme de très fines particules (<20 µm). Le processus de flottation n'a pas été en mesure de concentrer ces minéraux résiduels, car ils étaient plus fins et sortent de la plage de taille optimale (entre 20 µm et 1 mm) pour la flottation (Ait-Khouia et al., 2021 ; Derycke, 2012).

Qu'en est-il de l'apport de la minéralogie dans le cadre de la décontamination des stériles miniers par gravimétrie?

À notre connaissance, les potentiels et les limites des procédés de séparation gravimétrique des minéraux n'ont pas été suffisamment examinés jusqu'à présent dans le cadre de la désulfuration environnementale des rejets miniers. En effet, leur applicabilité dans ce contexte dépend d'une panoplie de paramètres dont la minéralogie fait partie.

La détermination de la composition minéralogique modale du stérile minier est une première information à prendre en compte. Elle est très utile afin d'anticiper au départ quelle technique de séparation pourrait être applicable efficacement pour la désulfuration. La connaissance des phases contaminantes et celles de la gangue peut aider au choix préalable d'une telle technique gravimétrique. Or, ce n'est pas suffisant. La description de la texture minéralogique (granulo-minéralogie, degré de libération et associations minéralogiques) est aussi de grande importance pour mieux outiller la base de données afin de selectionner la meilleure technique pour la désulfuration (Gosselin et al., 1999; Mercier et al., 2001).

Ces aspects minéralogiques et la spéciation des phases minérales peuvent être étudiés par la microscopie optique et par des techniques microscopiques automatisées telles que QEMSCAN® comme démontré durant cette thèse. L'applicabilité efficace des technologies de séparation gravimétrique qui ont été entreprises lors de cette thèse nécessite des conditions opératoires particulières. Ces dernières se trouvent en relation directe avec les informations obtenues grâce à la caractérisation minéralogique mais

aussi avec la distribution granulométrique (taille des particules), l'hétérogénéité de la matrice du rejet, la différence de densité entre les minéraux sulfureux et ceux de la gangue (Bouzahzah et al., 2014; Chopard et al., 2015; Dermont et al., 2008; Jamieson et al., 2015).

Le désulfuration environnementale par gravimétrie est difficile, voire parfois irréalisable, dans les cas suivants (Ait-khouia et al., 2021):

- La différence de densité entre les sulfures/sulfosels et la gangue n'est pas significative;
- Une grande variabilité des formes minéralogiques;
- Les sulfures et sulfosels sont présents dans toutes les fractions granulométriques du rejet en question.

Ce travail a mis en évidence le rôle de la minéralogie appliquée à suivre et contrôler les performances de la désulfuration environnementale par gravimétrie. En effet, la minéralogie automatisée a permis de définir la composition minéralogique modale du stérile minier en question et celle des produits désulfurés, l'abondance des sulfures/sulfosels et carbonates, leurs degrés de libération et associations minéralogiques ainsi que les occurrences de nickel et arsenic (principaux contaminants) dans le stérile minier et dans les produits désulfurés. Ces données qualitatives et quantitatives sont utilisées pour suivre l'efficacité de l'opération de la désulfuration et déterminer les défaillances de la technique utilisée. La caractérisation minéralogique a permis également d'appuyer les conclusions relatives à la prédiction du potentiel de génération d'acidité et de contamination par les tests statiques et cinétiques. Dans ce sens, les données QEMSCAN® ont été utilisées pour reclaculer la réactivité des matériaux désulfurés en considérant uniquement les surfaces exposées des sulfures/sulfosels (minéraux acidifiants et porteurs de contaminants) et carbonates (minéraux neutralisants).

8.2 Effet de la liberation minérale sur la géochimie des rejets miniers

La caractérisation minéralogique est actuellement considérée comme un outil clé et d'aide à la décision dès l'étape de l'exploration pour bien planifier le mode du traitement du minerai mais aussi pour bien prédire et comprendre le comportement environnemental des rejets miniers (Bouzahzah et al., 2014; Chopard et al., 2015; Jamieson et al., 2015). Certains auteurs ont aussi suggéré d'utiliser la minéralogie multi-techniques afin d'expliquer et de prédire les phénomènes géochimiques pouvant avoir lieu lors de l'oxydation des sulfures et sulfosels présents dans les rejets miniers (Blowes et al., 2003; Gottlieb et al., 2000; Paktunc and Davé, 2000). Cette thèse a mis en évidence l'importance de la minéralogie appliquée et surtout celle automatisée pour identifier et quantifier les paramètres texturaux des rejets miniers. En effet, elle permet de quantifier la composition minéralogique modale, la granulo-minéralogie, le degré de libération, les associations minéralogiques, etc. Ces paramètres texturaux sont de grande importance lors du processus de la désulfuration environnementale des rejets miniers ou encore lors de la gestion de ces rejets.

Le chapitre 6 de cette thèse a montré un exemple concret de l'utilisation de la minéralogie automatisée combinée à la CT (computed tomography) pour caractériser la réactivité d'un stérile minier à des fins environnementales (prédiction du potentiel polluant) et de gestion des stériles tenant compte de leur granulo-minéralogie. En effet, le paramètre lié à la libération des minéraux sulfurés et arséniés a été proposé comme suggérer par Elghali et al. (2018); il s'agit d'une approche qui consiste à définir la taille minimale des particules pour laquelle les sulfures et sulfosels sont presque complétement encapsulés dans une matrice de gangue silicatée, et donc très peu ou même non disponibles à la réaction d'oxydation en contact avec les agents atmosphériques. Ce paramètre est défini comme le diamètre d'encapsulation physique des sulfures (DPLS, diameter of physical locking of sulphides). Dans notre cas, 2,5 mm était le DPLS pour le rejet minier en question. Ce paramètre a été confirmé

cinétiquement à l'aide de tests en cellules humides monitorées sur 154 jours. Les résultats du suivi géochimique ont montré qu'effectivement la fraction >DPLS est caractérisée par une réactivité négligeable en comparaison à la réactivité de la fraction <DPLS et celle de l'échantillon total. Dans notre cas, la réactivité de l'échantillon total (stérile minier) est déterminée par la réactivité de la fraction < DPLS. L'intérêt principal derrière la détermination du DPLS réside au niveau des éventuels gains économiques et environnementaux pouvant avoir lieu s'il est intégré en amont de la gestion des stériles miniers. En effet, au lieu de gérer tout le stérile minier, il suffira juste de gérer la fraction <DPLS vu que la fraction >DPLS a un potentiel de contamination négligeable ou peu.

Il est ainsi judicieux à mentionner que la méthodologie proposée pour la détermination du DPLS est valable indépendamment du contexte géologique et lithologique des rejets en question. Cependant, quelques petites modifications peuvent avoir lieu surtout en terme du nombre de fractions granulométriques à analyser. Ce nombre dépend étroitement de la distribution granulométrique (taille maximal) du rejet étudié. En effet, plus la taille maximale des particules est grande, plus qu'il fallait augmenter le nombre de fractions granulométriques à caractériser.

8.3 Effet d'échelle

Les aspects minéralurgiques et géochimiques des résultats obtenus de cette thèse sont discutés dans les chapitres 4, 5, 6 et 7. L'effet d'échelle est abordé dans ce chapitre pour démontrer la validité d'utiliser des résultats obtenus à l'échelle laboratoire pour des perspectives de grande échelle (industrielles).

Comme il a déjà été prouvé via plusieurs études, la désulfuration environnementale des rejets miniers par flottation et gravimétrie a pu prévenir et contrôler avec succès la génération de drainage minier contaminé (Benzaazoua et al., 2017; Benzaazoua et al., 2000a; Broadhurst and Harrison, 2015; Bussière et al., 2002b; Nadeif et al., 2019; Nakhaei and Irannajad, 2017). L'étude entreprise dans ce doctorat le prouve également.

Cependant, la majorité de ces études ont été menées à l'échelle du laboratoire (petite échelle) et n'ont pas fait face aux enjeux industriels (grande échelle).

Il est ainsi intéressant de mentionner que les essais à l'échelle du laboratoire permettent généralement de s'assurer que les performances de traitement du matériel peuvent être optimisées, à l'image du procédé de la flottation (Mesa et Brito-Parada, 2019 ; Yin et al., 2018). Ces tests à petite échelle peuvent également aider à résoudre les différents problèmes du procédé pouvant affecter son efficacité. Ainsi, des essais à l'échelle pilote sont également nécessaires pour évaluer les performances du procédé sur la base des essais à l'échelle du laboratoire et éviter tout problème mécanique ou de fonctionnement qui pourrait survenir. Par exemple, l'étude menée par Seaman et al. (2012) et Yin et al. (2018) ont démontré que les réactifs utilisés pourraient améliorer la récupération du cuivre et de l'or par flottation. Cependant, les tests à l'échelle industrielle n'ont pas révélé la même efficacité qu'à l'échelle du laboratoire suite aux multiples variables qui n'étaient pas considérées à l'échelle du laboratoire telles que le type de broyage.

Pour une mise à l'échelle réussie à l'échelle industrielle, des essais à l'échelle pilote sont un bon moyen pour optimiser les opérations en mode continu (Mesa et Brito-Parada, 2019 ; Yin et al., 2018). Les essais à l'échelle pilote s'appuient fortement sur des études cinétiques pour assurer un mode de fonctionnement continu et pour aussi déterminer la fonction de transfert correcte.

Par rapport aux aspects géochimiques, il est aussi judicieux de mentionner que la prédiction de la contamination pouvant être générée par le drainage minier est généralement basée sur des essais de prédiction réalisés au laboratoire (Plante, 2010). En revanche, une panoplie de facteurs qui contrôlent le relargage des éléments chimiques (contaminants) peuvent varier considérablement entre l'échelle du laboratoire et celle du terrain (Elghali et al., 2019b; Plante, 2010a; Sapsford et al., 2008). Le pH, le ratio liquide/solide, la distribution granulométriques des particules, la

présence des minéraux secondaires, les phénomènes de sorption et d'échange d'ions à la surface des minéraux sont quelques exemples des facteurs contrôlant la réactivité des rejets miniers. Selon plusieurs études, les résultats géochimiques obtenus au laboratoire et in situ présentent des différences parfois jugées importantes en terme de concentrations des contaminants dans les lixiviats, leurs conductivités et de réactivité des matériaux étudiés (taux d'oxydation) (Plante et al., 2014; Sapsford et al., 2008). Ces différences pourraient provenir, entre autres, du ratio liquide/solide qui est généralement plus élevé au laboratoire, des conditions hydrogéologiques de l'échelle, ainsi que les conditions climatiques surtout que la température pourra avoir un impact sur l'oxydation des sulfures et sulfosels (Plante, 2010). Selon l'étude menée par Plante et al. (2014) traitant l'effet d'échelle sur les stériles de la mine Tio, il a été conclu que la mini-cellule d'altération exagère la dissolution des minéraux neutralisants versus l'oxydation des sulfures en raison du ratio liquide/solide très élevé. De même, cette recherche a pu relier les conditions du terrain et le temps de contact entre le matériau et de l'eau qui est plus long sur le terrain avec la précipitation des minéraux secondaires qui est plus favorable sur le terrain qu'au laboratoire. Ainsi, des tests de mise à l'échelle tels que des colonnes ou des cellules de terrain sont recommandés pour une confirmation finale.

8.4 Approche proposée pour la gestion intégrée des stériles miniers

Le tri des stériles par criblage, après le dynamitage, en fonction du diamètre critique DPLS pourrait être une technique efficace pour la gestion globale des stériles miniers. Basé sur ce paramètre, le coût économique lié à la gestion/restauration des haldes à stériles sera bien réduit vu la quantité réduite de stériles réactifs à gérer (moins de 40% de volume total) (Amar et al., 2020; Elghali et al., 2019).

Le schéma proposé dans la Figure 8.1 illustre les techniques de désulfuration de la fraction fine des stériles miniers (< DPLS), ainsi que la destination des matériaux désulfurés et des concentrés sulfureux et les produits désulfurés.

L'intérêt de la détermination du DPLS se situe au niveau des éventuels gains économiques qui peuvent avoir lieu s'il est intégré en amont de la gestion des stériles miniers. En effet, au lieu de gérer les stériles comme une seule entité, il est maintenant suggéré de les séparer en deux fractions dépendamment de leurs réactivités géochimiques ; une fraction réactive (<DPLS) et une fraction non réactive (> DPLS) en raison de l'encapsulation physique des sulfures dans la gangue

Tel que démontré dans cette thèse, la fraction réactive pourra être désulfurée et décontaminée tout en produisant des concentrés de sulfures/sulfosels aurifères. Ainsi, cette démarche de la gestion intégrée des rejets miniers pourra s'inscrire dans une stratégie du développement durable et d'économie circulaire surtout que les produits désulfurés peuvent être utilisés comme des matériaux de couverture pour les opérations de restauration des parcs à résidus et des haldes à stériles.

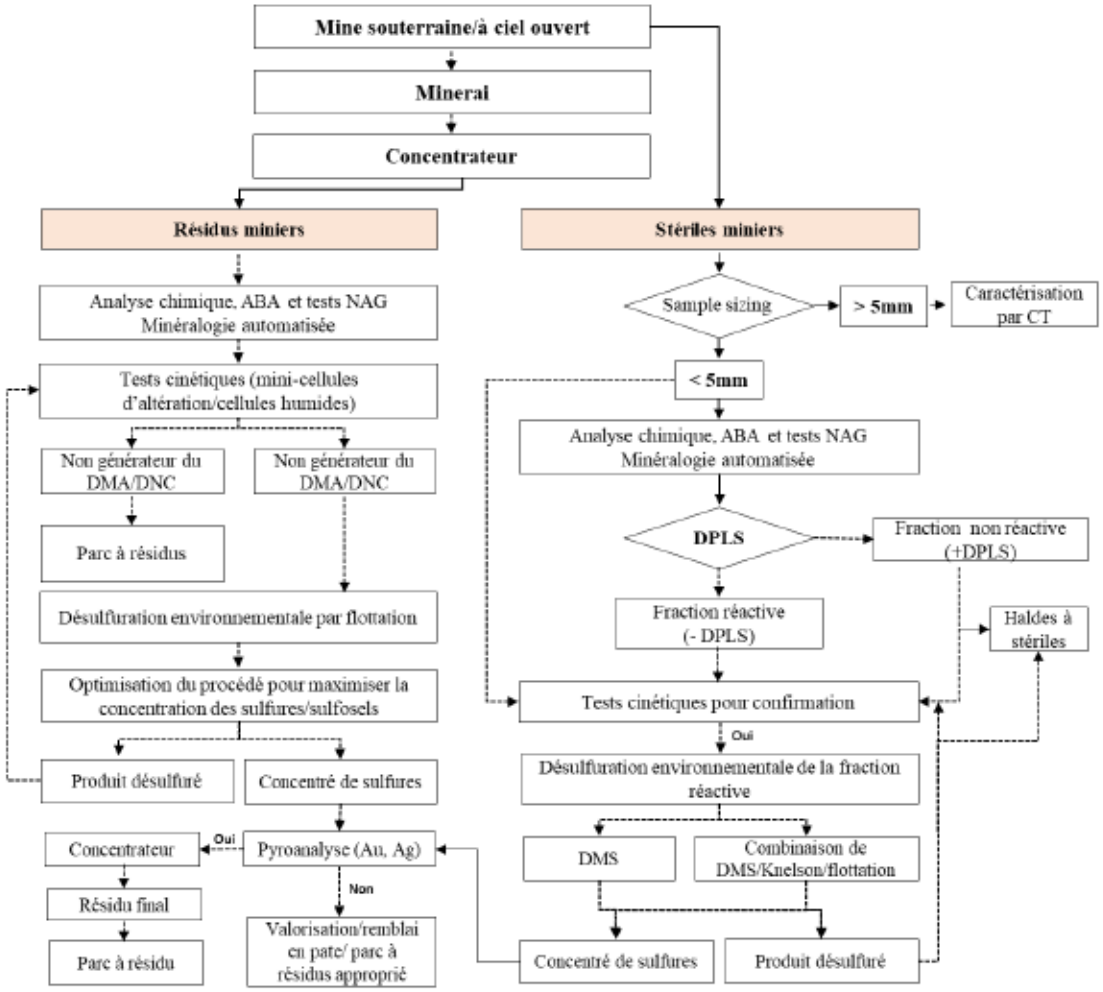

Figure 8.1 Schéma de l'approche proposée pour la gestion intégrée des rejets miniers

CHAPITRE 9

CONCLUSION ET RECOMMANDATIONS

9.1 Conclusion

De nos jours, l'industrie minière génère des quantités importantes des rejets miniers qu'il convient de gérer adéquatement surtout que cette dernière est encadrée d'un grand et croissant arsenal réglementaire. Ces rejets miniers comprennent une variété de produits dont les stériles miniers (roches stériles) et les rejets de concentrateurs (résidus) sont les plus problématiques en raison de leur volume et de leur potentiel contaminant. Différentes approches de gestion de ces rejets miniers ont été développées afin de prévenir ou minimiser les impacts sur l'environnement. Parmi celles-ci, le concept de la désulfuration environnementale comme méthode de gestion intégrée de ces rejets miniers a été proposé. En effet, ce projet de thèse s'inscrit à la suite des travaux portant sur la désulfuration environnementale des rejets pour la prévention du DMA (Benzaazoua et al., 2000a; Bois et al., 2005a; Broadhurst and Harrison, 2015; Demers et al., 2008; Mermillod-Blondin et al., 2005; Nadeif et al., 2019). La désulfuration des rejets miniers par flottation et par d'autres techniques gravimétriques est entreprise dans cette thèse pour le contrôle de la génération du drainage neutre contaminé (DNC) à l'arsenic et au nickel suite à l'oxydation de certains sulfures et sulfosels moins communs comme la gersdorffite.

Dans le cas de la désulfuration des résidus miniers par flottation non sélective, pour chaque espèce minérale (sulfure/sulfosel), l'importance de la chimie de surface et son évolution sont fonction des conditions d'opération à savoir le pH de conditionnement et, surtout, des phénomènes de dépression et de réactivation des surfaces. Les xanthates

sont les collecteurs les plus utilisés pour la flottation des sulfures, en général, et pour la désulfuration environnementale, en particulier.

Le résidu minier étudié dans cette thèse est un résidu sulfureux et arsénié (présence de la gersdorffite) issu de la mine d'Amaruq (Nunavut, Canada). L'autre matériau est un stérile minier générateur de DNC à l'arsenic et nickel issu d'un gisement aurifère au nord du Canada. Les phases arsénifères et nickélifères majoritaires de ce stérile sont la gersdorffite et l'arsénopyrite. L'étude de ces matériaux ainsi que ceux désulfurés (produits de la désulfuration environnementale) est abordée dans ce travail par une caractérisation multi-techniques alliant analyses physique, chimique et minéralogique. Cette caractérisation poussée est primordiale pour comprendre les comportements minéralurgiques et environnementaux des différents produits lors du processus de désulfuration par flottation et par gravimétrie.

Les défis associés à la flottation des résidus miniers sont aussi abordés d'un point de vue fondamental à travers la caractérisation surfacique de quelques sulfosels purs non conventiels (skuttérudite, gersdorffite et nickéline) dans différentes conditions physico-chimiques ainsi que des phases adsorbées après l'ajout du xanthate de potassium comme collecteur en solution.

L'objectif principal de cette thèse de doctorat était de réussir la désulfuration environnementale des rejets miniers aux caractéristiques différentes (résidus *vs* stériles miniers) afin de contrôler la génération du drainage minier contaminé à l'arsenic et nickel. Ainsi, l'évaluation de l'efficacité des opérations de désulfuration est réalisée à travers le calcul des récupérations en soufre/ contaminants et la caractérisation environnementale des produits désulfurés via des tests statiques et des tests cinétiques (mini-cellules d'altération, cellules humides). D'autre part, ce doctorat vise à améliorer la compréhension des mécanismes d'interaction entre les sulfosels et le collecteur de flottation de type xanthates dans différentes conditions physico-chimiques.

Pour répondre à ces objectifs, cette thèse comporte trois parties principales dont les conclusions et recommandations sont détaillées dans les prochaines sections :

1- Caractérisation des espèces superficielles présentes à la surface de la skuttérudite, la gersdorffite et la nickéline comme étant des sulfosels moins communs pouvant générer du drainage minier contaminé en As et Ni. Les caractérisations surfaciques sont menées par spectroscopie infrarouge à transformée de Fourier (DRIFTS). L'évolution des surfaces minérales après broyage, conditionnement à l'air (vieillissement) et suite à un conditionnement aqueux à différents pH (via l'utilisation de NaOH et CaO) est aussi abordée. De plus, la caractérisation des phases adsorbées à la suite d'ajout d'amyl xanthate de potassium sur ces arséniures a été également entreprise.

L'affinité des xanthates à la surface de différents arséniures a été étudiée à l'aide de la spectroscopie ultraviolet-visible (UV-Vis) dans les différentes conditions physico-chimiques en construisant les isothermes d'adsorption et en calculant les taux de recouvrements statistiques. Cette affinité/interaction a également été explorée à l'aide de mesures de potentiel zêta qui jouent un rôle fondamental dans la détermination de la charge électrique surfacique des minéraux étudiés et la détermination des meilleures conditions de flottation. La caractérisation surfacique de ces sulfosels, après broyage à sec et vieillissement révèle une variété de produits d'altération à la surface de ces minéraux qui présentaient des degrés d'oxydation différents. Pour tous les arséniures testés, la couche d'altération produite était enrichie en phases d'arsenic, notamment sous forme d'arsénite (As3+), d'arséniate (As5+), de sulfates et d'hydroxydes d'arsenic et de nickel/cobalt. En effet, l'étude de vieillissement de la skuttérudite a identifié la formation d'hydroxydes de cobalt et de nickel à sa surface. L'arsénite, en revanche, est apparu après 12 h et a disparu après 48 h, après quoi l'arséniate a commencé à se former, ce qui suggère que l'arséniate est le produit d'oxydation de l'arsénite. Le vieillissement de la gersdorffite a généré une couche d'altération hétérogène composée

principalement d'oxydes d'arsenic (arsénite et arséniate) et de sulfates de nickel (seulement après 4 h). La nickeline, quant à elle, a montré un comportement similaire, mais avec des taux d'oxydation encore plus élevés par rapport à la skutterudite, où après seulement 6 h de vieillissement, la surface a révélé la signature de l'arsénite, suivie de l'arséniate. Des hydroxydes de nickel ont également été observés à la surface de la nickeline. Le conditionnement de ces arséniures dans des conditions alcalines a amélioré l'effet d'oxydation sur les surfaces minérales comparativement aux conditions naturelles.

Par rapport aux conditionnement de ces minéraux avec le PAX, il a été conclu que des complexes nickel-, cobalt- et arsenic-xanthates se forment en surface minérale de la skutterudite et la nickéline à pH. L'augmentation de la concentration initiale des xanthates fait augmenté la quantité de chaînes d'hydrocarbures et de dixanthogène à la surface de ces minéraux. La gersdorffite, quant à elle, n'a montré que la formation du dixanthogène dans ces conditions. Cependant, des complexes nickel- ou arsenic-xanthate pourraient être présents sous forme de monocouche sur la surface de la gersdorffite mais ils ont été masqués dans les spectres DRIFTS à cause de la formation de dixanthogène en raison du taux de recouvrement statistique qui est plus élevé. Les isothermes d'adsorption et les mesures du potentiel zêta ont démontré que l'activation par les sulfates de cuivre était efficace sur les arséniures et améliorait l'adsorption du xanthate sur les surfaces d'arséniures oxydés, en particulier dans des conditions alcalines. Les résultats de cette étude ont permis de mieux comprendre la chimie de surface de ces arséniures avant et après l'adsorption du collecteur, ce qui devrait impacter leur comportement en flottation.

2- Désulfuration environnementale du résidu minier Whale Tail d'Amaruq (Agnico-Eagle Mines Ltd.) en vue de diminuer son potentiel polluant en As et Ni. La modélisation et l'optimisation du procédé de désulfuration ont été réalisées en utilisant les plans d'expériences. Plus spécifiquement, la méthodologie de surface de réponse

ainsi que la conception composite centrale comme outil statistique ont été utilisés dans ce sens. Le pH, le dosage du collecteur (PAX), le dosage de l'activateur ($CuSO_4$), le dosage du MIBC et la concentration solide étaient les facteurs de contrôle dans cette étude. Les performances ont été évaluées par le calcul des récupérations en soufre et en arsenic ainsi que sur la cinétique de flottation. Ainsi, l'évaluation de l'efficacité de la désulfuration environnementale du résidu Whale Tail à travers la caractérisation environnementale des produits désulfurés est faite par des tests statiques (PA, PN) et des tests cinétiques en mini-cellules d'altération. Cette étude constitue une application des études fondamentales développées dans le chapitre 3.

La modélisation et l'optimisation du processus de flottation des sulfures/sulfosels des résidus de Whale Tail contenant 3 % de S et 0,24 % d'As ont été réalisées en utilisant une conception expérimentale statistique et la méthodologie de surface de réponse (RSM). Le dosage du collecteur (PAX), le dosage de l'activant ($CuSO_4$), le dosage du moussant (MIBC), le pH et la concentration solide (Cs) étaient les facteurs de contrôle dans cette étude. Les propriétés minéralogiques des résidus avant et après désulfuration ont été examinées via la microscopie optique (MO) et la minéralogie automatisée (QEMSCAN®). Le comportement géochimique des résidus frais et ceux désulfurés a été évalué à l'aide des tests statiques et cinétiques en mini- cellules d'altération, déterminant ainsi l'efficacité du processus de désulfuration. Les principaux résultats ont révélé que le résidu Whale Tail d'Amaruq est constitué de particules fines à forte teneur en soufre (3% wt), principalement sous forme de pyrrhotite, pyrite et gersdorffite. Selon les tests statiques (ABA test) et le test NAG, ce résidu a été classé comme générateur d'acide. Il a été démontré également que la désulfuration environnementale par flottation dans des conditions optimales a permis la concentration/élimination d'environ 97 % des sulfures présents dans le résidu. Cette meilleure performance a permis d'atteindre des teneurs résiduelles en soufre de 0.11% et arsenic de 0.03% dans le matériau désulfuré, pour une flottation réalisée à pH=11,5; PAX= 158 g/t, CuSO4= 300 g/t, MIBC= 55 g/t, et Cs= 29,3 %. De plus, les sulfures et sulfosels résiduels

(pyrrhotite, pyrite, gersdorffite) dans les résidus désulfurés étaient complètement associés voire encapsulés dans les minéraux de gangue non sulfurés, tels qu'analysé par MO et QEMSCAN®. Ces sulfures/sulfosels résiduels ont été considérés comme non réactifs en raison de leur association avec les minéraux de gangue (principalement des silicates).

Des tests cinétiques en mini-cellules d'altération ont été effectués sur les résidus frais et ceux désulfurés pour évaluer leurs réactivités et taux de relargage de contaminants (en particulier As, Ni, Cu, Fe et Zn). En effet, le matériau désulfuré ne présente qu'un faible risque de génération de drainage minier contaminé. Tous les contaminants lixiviés étaient inférieurs aux limites fixées par la législation provinciale du Québec (Directive 019). Finalement, il a été conclu que la désulfuration environnementale par flottation pourra être considérée et utilisée comme une approche intégrée de gestion durable des résidus miniers pour la prévention et le contrôle de la génération de drainage minier contaminé.

3- Développement de pratiques permettant la décontamination, la stabilisation et le stockage des stériles miniers sulfureux porteurs de contaminants. L'introduction de la notion du degré de libération des minéraux acidifiants et neutralisants (sulfures et carbonates principalement) a permis de définir la taille des particules au-dessus de laquelle la réactivité des stériles miniers en question est négligeable. Cette taille appelée diamètre d'encapsulation physique des sulfures et sulfosels (DPLS) a été confirmée en évaluant le comportement géochimique par des essais cinétiques en cellules humides. Plus précisément, l'influence de la taille des particules et du degré de libération des sulfures/sulfosels et des carbonates sur la géochimie du drainage minier a été soigneusement examinée. Pour se faire, des techniques de caractérisation minéralogique avancées (QEMSCAN® et CT) combinées à des tests cinétiques ont été utilisées. Grace à ces techniques, il a été possible de définir le DPLS qui pourra être

utilisé pour séparer les stériles en question en deux fractions de différentes réactivités géochimiques.

Sur la base des résultats des tests minéralogiques et cinétiques, le DPLS pour le stérile minier étudié a été déterminé à 2,5 mm. Ces résultats ont montré que la fraction fine (<2,5mm) était la plus sulfurée et que les degrés de libération des sulfures/sulfosels et de carbonates étaient plus élevés par rapport à la fraction grossière (> 2,5 mm) et totale (< 10 mm). Le DPLS déterminé a été confirmé à l'aide de tests cinétiques en cellule humides surveillés pendant 154 jours. Pour les trois fractions, les carbonates étaient disponibles en quantités suffisantes et avec des degrés de libération aussi suffisants pour produire le comportement neutre observé lors des tests cinétiques. Selon les fractions granulométriques (fine, grossière ou totale), les taux d'oxydation des sulfures et de lixiviation des espèces chimiques (contaminants) étaient totalement différents. En effet, la réactivité des échantillons a montré que la fraction fine contrôlait le comportement géochimique global du stérile minier en question. Ainsi, cette fraction fine était 1,5 fois plus réactive que la fraction totale et 10 fois plus réactive que la fraction grossière. Ces différences de réactivité sont dues aux différents degrés de libération des minéraux sulfurés présents (principalement la pyrite et la gersdorffite) dans les différentes fractions. Ceci est également dû aux teneurs initiales en sulfures et carbonates dans chaque fraction. Les résultats des tests cinétiques (à l'échelle du laboratoire) ont révélé que la fraction grossière pouvait être classée comme un matériau non générateur de contaminants au regard des critères établis par la législation provinciale du Québec (Directive 019). Cependant, les fractions fines et totales risquent de générer du drainage minier neutre contaminé à l'arsenic. Le paramètre DPLS pourrait être ainsi intégré dans la gestion des haldes à stériles. En effet, le stérile minier pourrait être divisé en deux fractions granulométriques en amont de leur disposition, conduisant à la construction de deux haldes à stériles : i) une halde contenant uniquement du matériau > DPLS, non réactif (inerte) et ii) un tas contenant la fraction < DPLS, plus réactif et générateur de DNC à l'arsenic. La fraction grossière présentant

environ 60 % du stérile total pouvait potentiellement être valorisée dans le domaine du génie civil ou de la céramique ou être stockée dans une halde à stériles, ou autres. Cependant, la fraction fine pourrait être gérée différemment : elle pourrait être désulfurée (décontaminée : objet du chapitre 6), valorisée ou déposée dans un parc à résidus approprié. Sur la base de ces résultats, le fractionnement des stériles miniers selon le paramètre DPLS par un simple criblage pourrait s'avérer une approche efficace pour une gestion durable de ces rejets. Cette approche peut minimise considérablement la quantité de stériles problématiques à gérer et, par conséquent, minimiser les coûts liés à la restauration des airs d'entreposage.

La désulfuration de la fraction réactive (< 2.5 mm) du stérile minier par différentes techniques a été étudiée et a permis de réduire son potentiel contaminant et de concentrer parrallèlement l'or résiduel. Plus précisément, ce travail s'est concentré sur : i) la désulfuration environnementale (décontamination) de la fraction réactive (< 2.5 mm) en utilisant de nouvelles techniques à savoir : la DMS, le concentrateur Knelson, la spirale/table à secousses ainsi que la combinaison de la gravimétrie et flottation, ii) l'évaluation du comportement géochimique du matériel étudié et ses fractions désulfurées (prédiction de génération de drainage neutre contaminé), et iii) évaluation de la faisabilité de la concentration en or par les procédés de désulfuration.

La caractérisation chimique et minéralogique a révélé que l'échantillon d'alimentation étudié était enrichi en sulfures porteurs de contaminants (4 % en poids de pyrite, 0,33% de gersdorffite, 0,15 % en poids de pyrrhotite, etc.) et en carbonates (4,47 % de calcite). Les résultats obtenus ont montré que la DMS centrifuge et le procédé combinant la gravimétrie (DMS et knelson) et la flottation présentaient un bon potentiel de décontamination de la fraction réactive. Ces processus ont conduit aux meilleures récupérations de soufre et de contaminants (As, Ni, Fe et Cu) atteignant 88% ainsi qu'à la concentration de l'or résiduel. Avec ces performances, il a été possible de produire un rejet décontaminé dont la teneur résiduelle en soufre est seulement de 0.28% et en

arsenic de 0.026% (versus 1.78% S et 0.08% As dans l'échantillon initial). De plus, les résultats ont révélé que les techniques analytiques (QEMSCAN® et microscopie optique) appliquées pour la caractérisation du stérile minier étudié (fraction fine réactive) et des matériaux désulfurés produits ont clarifié le comportement des minéraux sulfureux lors des processus de séparation. Elles permettent d'étudier l'influence de la taille des particules, de la libération minérale et des associations minéralogiques sur chaque technique de désulfuration. En effet, la teneur en contaminants résiduels (As, Ni) dans les produits décontaminés était principalement due au caractère textural des minéraux porteurs de contaminants (sulfures et sulfosels) qui étaient partiellement associés aux minéraux de gangue non sulfurés (principalement des silicates).

Des tests cinétiques en mini-cellules d'altération ont été utilisés pour comparer et démontrer l'efficacité des processus de décontamination adoptés. Les résultats à l'échelle de laboratoire, ont prouvé que l'échantillon d'alimentation (fraction réactive) présentait un risque de DNC à l'arsenic (pH neutre et concentrations d'arsenic dépassant la limite fixée par la directive 019) et que les matériaux décontaminés par la DMS et l'approche combinant la gravimétrie et flottation, ne présentaient qu'un faible risque de génération du DNC à l'arsenic. Cependant, les lixiviats issu du matériau désulfuré via la spirale/table à secousse étaient légèrement supérieurs aux limites de la directive 019 pour l'arsenic. Par conséquent, la désulfuration environnementale de la fraction réactive des stériles miniers a été confirmée comme étant une stratégie efficace pour la gestion durable de ces rejets miniers. La pyroanalyse a révélé que les concentrés du DMS centrifuge et de la gravité/flottation présentent des teneurs appréciables en or (environ 2g/t). Avec ces teneurs, il est suggéré que la récupération d'or pourrait partiellement compenser le coût de ces processus de décontamination. Cependant, il est crucial d'évaluer la faisabilité technique et économique cette approche, compte tenu des coûts d'investissement et d'exploitation.

9.2 Recommandations

À l'issue de ce travail, il est possible d'aborder plusieures principales recommandations :

- le recours à la spectroscopie aux rayons X (XPS) comme outil d'analyse surfacique pourrait permettre une caractérisation plus approfondie des surfaces de sulfosels suite aux différents conditionnements une fois combinée à la technique DRIFTS. Ces deux techniques ont respectivement une profondeur d'analyse de quelques nanomètres (~40 Å) et de quelques microns (~25000 Å). En effet, plus de détails pourra être recueillis via l'utilisation combinée de ces deux techniques.
- dans une perspective d'établir un lien plus fort entre l'étude fondamentale et celle d'application en flottation, il serait en effet intéressant de pouvoir sonder l'état des surfaces de ces minéraux en contexte industriel afin de réaliser une évaluation de façon plus réaliste de l'influence des conditions physico-chimiques de la pulpe sur l'état de surface de ces arséniures. Ainsi, une sonde des états de surface pourra être proposée tout en immergeant l'arséniure (broyé à une granulométrie équivalente à celle des sulfures dans les résidus miniers) dans la pulpe de procédé industriel et en caractérisant les surfaces ainsi conditionnées. De même, cette caractérisation pourra être entreprise au niveau de plusieurs points stratégiques du procédé de flottation afin de préciser l'influence d'une étape spécifique du procédé sur l'état de la surface de l'arséniure en question.
- Il est aussi recommandé d'intégrer le procédé désulfuration par flottation au traitement minéralurgique/métallurgique afin d'éviter des opérations supplémentaires portant surtout sur la réactivation des surfaces des minéraux à flotter (sulfures déprimés à l'avance). Cette réactivation est couteuse et parfois difficile à réaliser en sortie de l'usine de concentration. En effet, les industriels sont appelés à optimiser à la fois la récupération des minéraux/métaux de valeur et la diminution du potentiel polluant des rejets miniers dès l'étape du développement du procédé du traitement. De plus, selon

les propriétés physico-chimiques et minéralogiques des rejets miniers à désulfurer, d'autres procédés autres que la flottation peuvent être envisagés.

- Ainsi, le recours aux procédés de séparation physique (gravimétrie par exemple) pourra être entrepris préalablement ou ultérieurement à la flottation lors de présence de fines/ultrafines particules hautement réactives (sulfures et/ou sulfosels) et qui sont difficilement récupérables par flottation vu leur finesse (Ait khouia et., 2021, Derycke et al., 2013). Ceci permettra de diminuer au maximum le volume de la partie du résidu générateur du drainage minier contaminé. En perspectives de ces travaux, une concentration des fines particules sulfureuses par un concentrateur gravimétrique avancé permettant de soumettre les particules à un champ de force centrifuge (e.g., knelson, falcon), pourrai être envisagée afin d'assurer une efficacité de désulfuration plus meilleure.

- Pour les stériles miniers et sur la base des résultats issus de objet de thèse, le fractionnement des stériles miniers selon le paramètre DPLS par un simple criblage pourrait s'avérer une approche efficace pour une gestion durable de ces rejets. Cette approche peut minimiser considérablement la quantité de stériles problématiques à gérer et, par conséquent, minimiser les coûts liés à la restauration des airs d'entreposage. En perspectives de ces travaux, il est recommandé de généraliser cette approche de gestion intégrée à d'autres stériles miniers différents de celui étudié dans le cadre de ce travail, d'un point de vue minéralogique et textural. Ceci permettra d'évaluer la validité et la performance de cette approche dans le cycle de vie de la mine. Il serait de même recommandé de passer par des tests pilote afin d'évaluer la faisabilité de l'approche proposée en dégageant les obstacles et les difficultés opérationnelles à résoudre. De plus, cette approche nécessite une étude de faisabilité technico-économique.

- Comme le DPLS déterminé dans le cas de ce doctorat, est aux environs de 2,5 mm, les techniques d'enrichissement (séparation physique) couramment utilisées dans le traitement du minerai (par exemple, la gravimétrie) pourraient combler cette lacune. Ces techniques présentent plusieurs avantages par rapport aux autres techniques de

traitement du minerai (e.g., tamisage, séparation magnétique, électrique) en raison de leur haute efficacité, de leur facilité d'utilisation, de leurs faibles coûts d'investissement et d'exploitation, de leur possibilité de traiter des granulométries grossières à des débits importants, de l'absence de l'utilisation de produits chimiques (sauf dans le cas de DMS) et, par conséquent, moins de risques environnementaux (Farrokhpay, 2020; Marion et al., 2018; Roy, 2009).

- Pour valider les résultats obtenus, l'exploration du DMS centrifuge et des techniques combinées de gravimétrie et de flottation à l'échelle pilote et industriel est importante. De plus, le produit désulfuré et le concentré doivent être étudiés plus en détail pour proposer la meilleure méthode de recyclage et/ou de valorisation. Il serait aussi intéressant de passer par des tests d'optimisation des trois approches testées dans le cadre de ce travail afin de maximiser les performances. Dans ce cadre, plus d'emphase pourra être focalisé sur l'approche spirale/table à secousse, étant donné des avantages techniques et économiques que les spirales peuvent offrir. L'espace restreint d'installation, le faible coût d'équipement, la simplicité d'opération, et l'efficacité de séparation si bien appliquées, sont quelques avantages que les spirales offrent offrent (Ait-Khouia et al., 2021; Grobler et al., 2016; Wills and Finch, 2016a).
- Les résultats obtenus des mini-cellules d'altération suggèrent que les produits désulfurés pourraient être classés comme des matériaux ne générant pas d'arsenic au regard des limites d'arsenic de la Directive 019. Cependant, des tests de mise à l'échelle tels que des colonnes ou des cellules de terrain sont recommandés pour la confirmation finale.

ANNEXE A

Supplementary materials 1

Figures

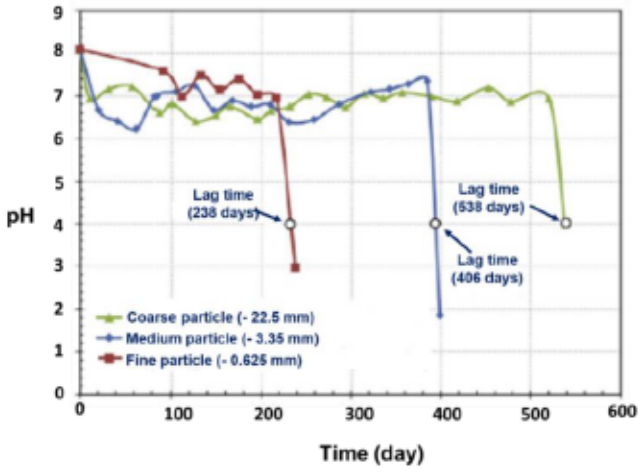

Figure 1S: Result of pH monitoring of a sample at different particle sizes. Adapted from Erguler and Erguler, (2015)

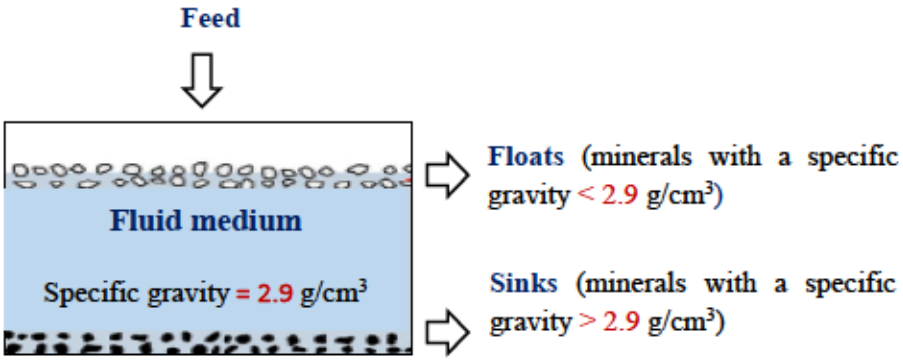

Figure 2S: Basic principle of DMS (specific gravity of fluid medium was 2.9 for illustration)

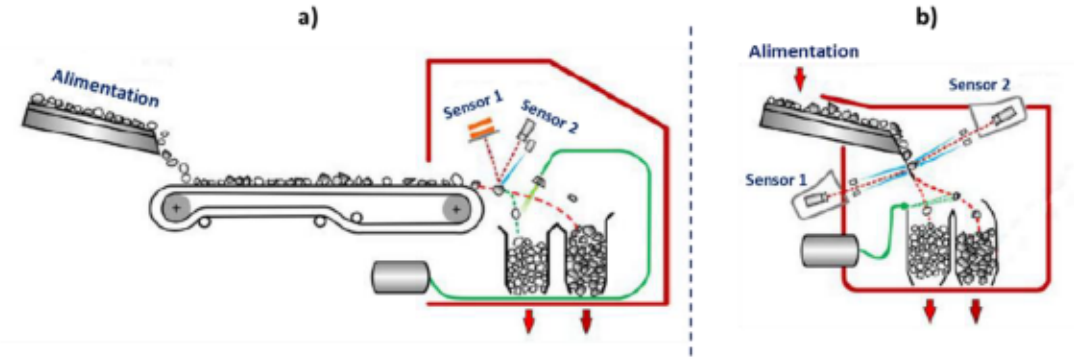

Figure 3S. Automated sorting systems **a)** belt, **b)** free fall. Adapted from Wills, (2016)

ANNEXE B

Supplementary materials 2

Tables

Table S1.1 XRD results

Minerals	Chemical formula	WTT (wt%)
Quartz	SiO_2	39.1
Stilpnomelane	-	10.2
Chlorite	$(Fe,Mg,Al)_6(SiAl)_4O_{10}(OH)_8$	8.4
Amphibole	-	9.2
Mica	-	9.8
Feldspar	$KAlSi_3O_8$	8.3
Calcite	$CaCO_3$	1.2
Pyrite	FeS_2	2.2
Pyrrhotite	$Fe_{(1-x)}S$	0.4
Cobaltite/Gersdorffite	CoAsS/NiAsS	0.5
Chalcopyrite	$CuFeS_2$	0.3
Gypsum	$CaSO_4$, $2H_2O$	0.7

Table S1.2 EPMA analysis of the grains NSG minerals observed in WTT

Analysis *LOD * (%)*	**Si** *0.02*	**Ti** *0.02*	**Al** *0.03*	**Cr** *0.02*	**Fe** *0.04*	**Ni** *0.03*	**Cu** *0.03*	**Mg** *0.03*	**Ca** *0.02*	**Mn** *0.04*	**Na** *0.05*	**K** *0.02*	**O** -	**Total** -
Quartz	46.65	0.00	0.00	0.00	0.10	0.00	0.00	0.00	0.00	0.00	0.00	0.00	*53.18*	99.94
Albite	30.69	0.01	11.02	0.00	0.28	0.00	0.00	0.09	0.67	0.01	8.30	0.77	*48.23*	100.08
Amphiboles	23.97	0.04	1.58	0.09	15.08	0.00	0.00	6.66	8.41	0.93	0.22	0.15	*41.23*	98.40
Micas	17.96	0.41	12.64	0.12	12.44	0.00	0.00	3.69	0.00	0.17	0.12	7.44	*39.61*	94.6
Chlorite	11.70	0.12	10.29	0.14	22.68	0.00	0.00	7.04	0.07	0.53	0.00	0.05	*33.97*	86.62
Epidote	18.07	0.04	14.20	0.33	7.83	0.00	0.00	0.00	16.26	0.22	0.01	0.01	*42.21*	99.21
Fe silicates	23.35	0.01	0.05	0.00	31.48	0.00	0.00	3.44	0.43	0.90	0.00	0.00	*38.37*	98.03
Magnetite	0.02	0.02	0.01	0.06	71.85	0.00	0.00	0.00	0.03	0.11	0.00	0.01	*27.80*	99.89

******LOD*: limit of ditection

Table S.1.3 Analysis of variance for sulfur recovery

Source	F-value	p-value	Source	F-value	p-value
Model	**15.5**	**< 0.0001**	BE	0.3683	0.5487
A-pH	1.76	**0.1947**	CD	2.48	0.1259
B-PAX	153.85	**< 0.0001**	CE	0.1776	0.6765
C-$CuSO_4$	0.5581	0.461	DE	0.1493	0.702
D-MIBC	3.4	**0.0756**	A^2	0.0004	0.9841
E-Cs	4.13	**0.0514**	B^2	135.71	**< 0.0001**
AB	1.13	0.297	C^2	0.0003	0.9864
AC	0.0015	0.9693	D^2	0.11	0.7426
AD	0.7981	0.379	E^2	3.24	0.0823
AE	0.0002	0.9892	**Residual**	-	-
BC	0.1131	0.7391	**Lack of Fit**	1.85	**0.2049**
BD	0.0072	0.9328	**Pure Error**	-	-

CV (%) = 2.97; R^2 = 0.91; Pred-R^2 = 0.7; Adj- R^2 = 0.86; Adeq Precision = 22.16

Figures

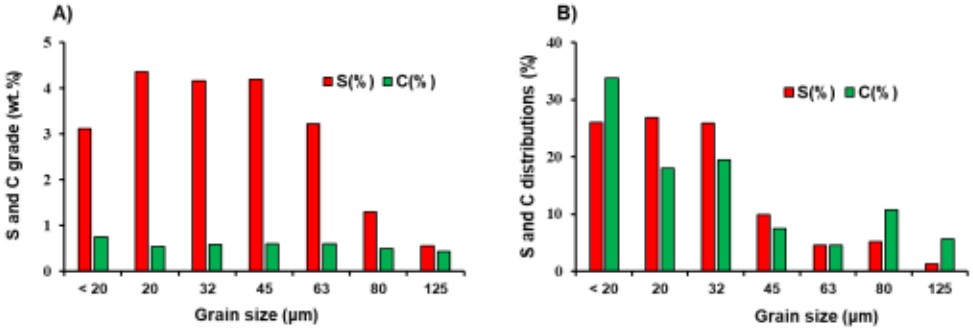

Figure S1.1 Size-by-size analyses of Whale Tail tailings. **A)** Grades of S and C in different grain size fractions. **B)** Distributions of S and C.

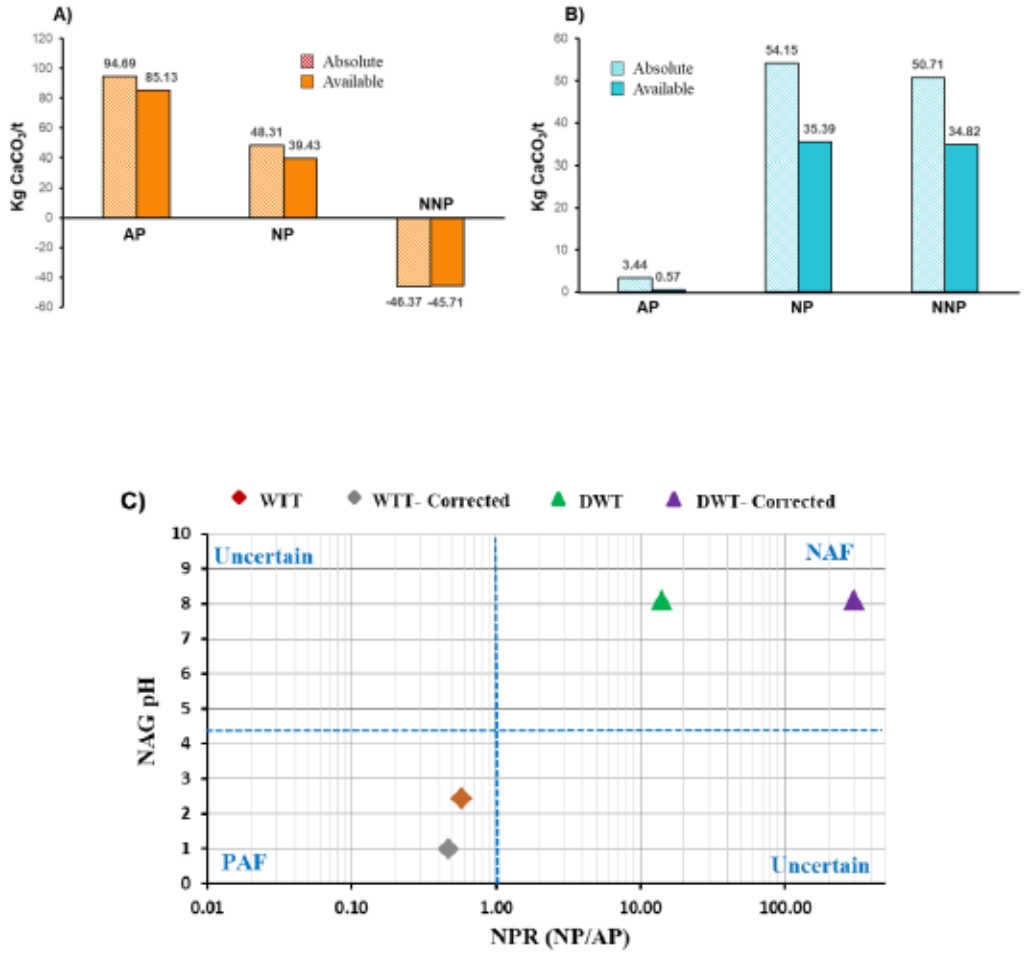

Figure S1.2 Absolute and available (after correction with liberation degree) AP, NP, and NNP for A) WTT and B) DWT. C) Results of acid generation potential from ABA and NAG tests.

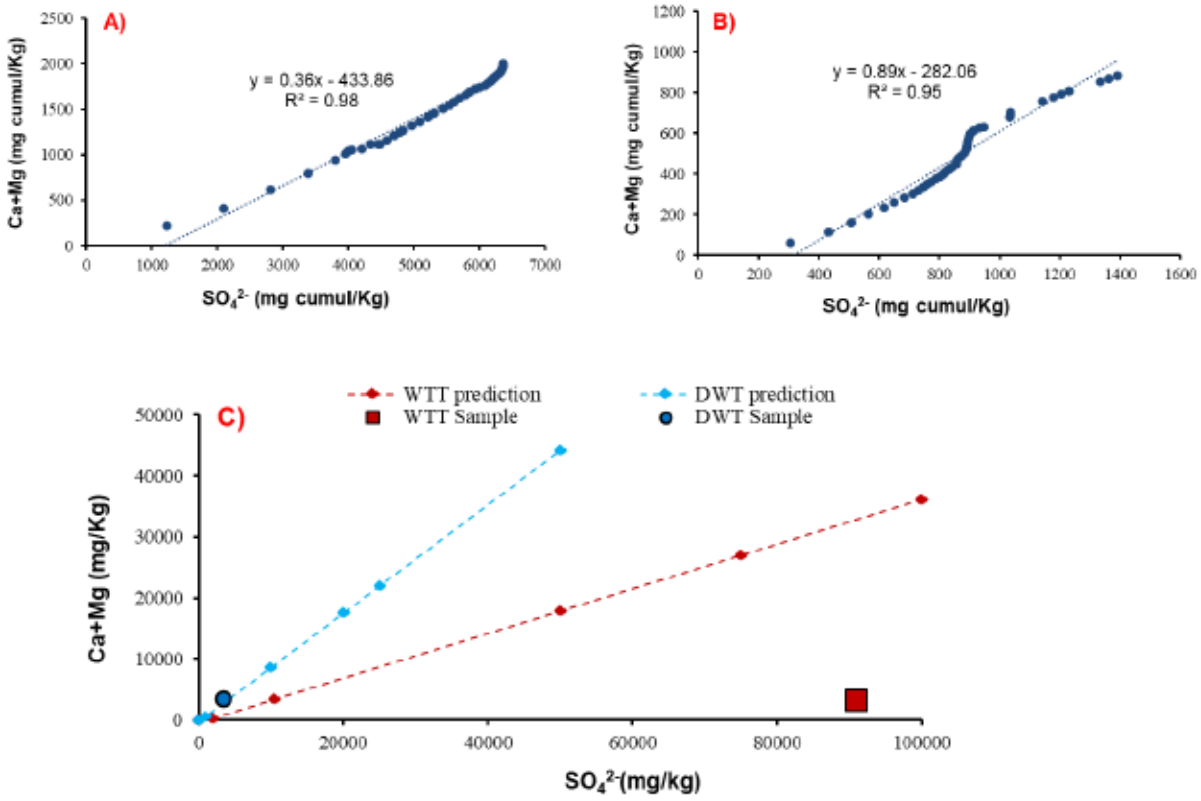

Figure S1.3 Long-term prediction of the geochemical behavior of WTT and DWT. A-B) Oxidation/neutralization predicted curves of WTT and DWT, and (C) experimental curves with projection of the initial composition of the samples.

ANNEXE C

Supplementary materials 3

Figures

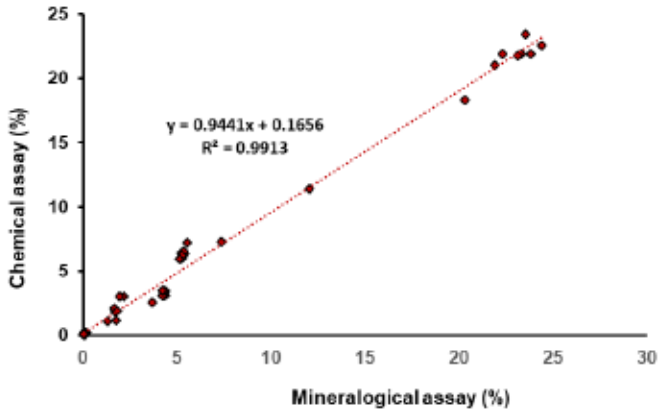

Figure S2.1 Correlation of chemical assay results versus calculated chemical compositions

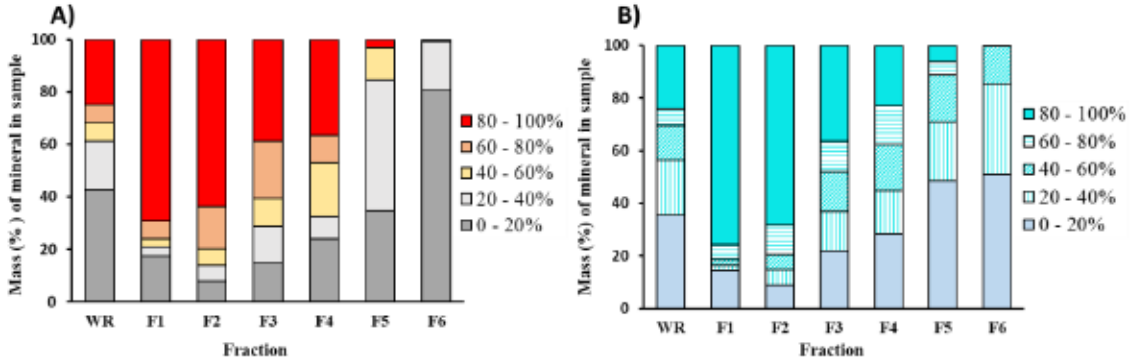

Fig. S2.2 Sulphides and carbonates liberation for all grain size fractions (mass % total sulphides in sample): **A)** Total sulphides liberation; **B)** total carbonates liberation; **C)** free sulphides and free carbonates versus grain size fractions

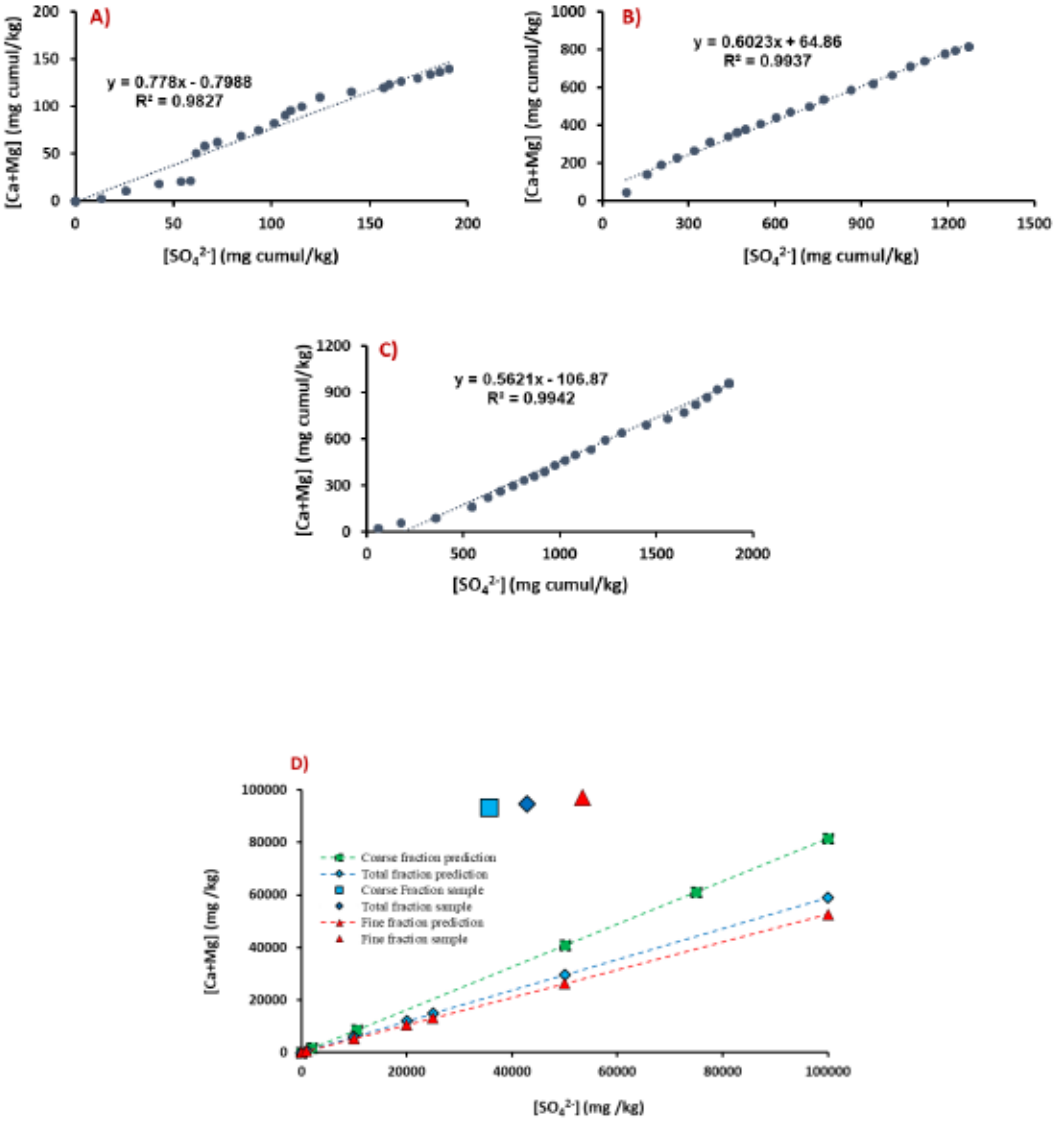

Fig. S2.3 Oxidation/neutralization curves and long-term prediction of the coarse, total and fine fractions. A), B) and C): oxidation/neutralization experimental curves of coarse, total and fine fractions respectively and (D): long-term prediction for coarse, total and fine fractions

Tables

Table S2.1 EPMA analysis of the grains NSG minerals observed

Analysis	Si	Ti	Al	Cr	Fe	Ni	Mg	Ca	Mn	Na	K	O	Total
LOD	*0.02*	*0.02*	*0.03*	*0.02*	*0.04*	*0.03*	*0.03*	*0.02*	*0.04*	*0.05*	*0.02*	-	-
Quartz	*46.83*	*0.00*	*0.05*	*0.00*	*0.18*	*0.01*	*0.02*	*0.00*	*0.00*	*0.00*	*0.00*	*53.48*	*99.94*
Orthoclase	*30.18*	*0.01*	*10.79*	*0.00*	*0.15*	*0.00*	*0.00*	*0.00*	*0.00*	*0.24*	*13.60*	*46.77*	*101.41*
Amphiboles	*20.42*	*0.16*	*4.50*	*0.15*	*19.96*	*0.09*	*5.49*	*2.25*	*0.44*	*0.12*	*2.50*	*38.38*	*98.40*
Fe-Chlorite	*12.53*	*0.07*	*10.90*	*0.09*	*23.17*	*0.02*	*7.50*	*0.03*	*0.46*	*0.00*	*0.27*	*35.84*	*90.88*
Carbonates	*0.19*	*0.00*	*0.12*	*0.00*	*2.85*	*0.00*	*0.98*	*29.06*	*0.73*	*0.00*	*0.01*	*15.60*	*99.21*
Fe silicate	*23.35*	*0.01*	*0.05*	*0.00*	*31.48*	*0.00*	*3.44*	*0.43*	*0.90*	*0.00*	*0.00*	*38.37*	*98.03*

Table S.2.2 Examples of pieces scanned using CT and calculation of liberation degree

Sample	Total volume (mm^3)	Volume of sulphides (mm^3)	Sulphides volume distribution (%)	Sulphides volume at the surface (mm^3)	Liberation degree (%)
Piece 1	3216.15	23.69	0.74	1.24	5.23
Piece 2	650.57	9.47	1.45	0.32	3.38
Piece 3	240.61	1.63	0.68	0.08	4.90
Piece 4	88.42	0.62	0.70	0.03	4.83

RÉFÉRENCES

Abeidu, A., Almahdy, A., 1980. Magnesia mixture as a regulator in the separation of pyrite from chalcopyrite and arsenopyrite. International Journal of Mineral Processing, 6(4), 285-302.

Abols, J., Grady, P., 2006. Maximizing gravity recovery through the application of multiple gravity devices. Paper presented at the Proceedings of the International Symposium on the Treatment of Gold Ores, 44 th Annual Conference of Metallurgists, Calgary.

Adam, K., Kourtis, A., Gazea, B., Kontopoulos, A., 1997. Evaluation of static tests used to predict the potential for acid drainage generation at sulphide mine sites.

Adkins, S., Pearse, M., 1992. The influences of collector chemistry on kinetics and selectivity in base-metal sulphide flotation. Minerals Engineering, 5(3-5), 295-310.

Agorhom, E., Skinner, W., Zanin, M., 2014. Diethylenetriamine depression of cu-activated pyrite hydrophobised by xanthate. Minerals Engineering, 57, 36–42.

Ahmed, A. H., Arai, S., Ikenne, M., 2009. Mineralogy and paragenesis of the co-ni arsenide ores of bou azzer, anti-atlas, morocco. Economic Geology, 104(2), 249-266.

Ait-Khouia, Y., Benzaazoua, M., Demers, I., 2021. Environmental desulfurization of mine wastes using various mineral processing techniques: Recent advances and opportunities. Minerals Engineering, 174, 107225.

Aksoy, D. O., Sagol, E., 2016. Application of central composite design method to coal flotation: Modelling, optimization and verification. Fuel, 183, 609-616.

Alam, R., Shang, J. Q., 2012. Effect of operating parameters on desulphurization of mine tailings by froth flotation. Journal of Environmental Management, 97, 122-130.

Aleksandrova, T., Talovina, I., Duryagina, A., 2019. Gold–sulphide deposits of the russian arctic zone: Mineralogical features and prospects of ore benefication. Geochemistry.

Allen, T., 2013. Particle size measurement: 4th ed. Chapman and Hall, London, 2013.

Alloway, B., 1995. Heavy metals in soils 2nd edition halsted press: John Wiley and Sons Inc, London.

Álvarez, J., Calzón, J., Fonseca, J., 2004. Chemisorption and electrochemistry of diphenyldiselenide on the hanging mercury drop electrode. Electrochimica Acta , 49, 1389-1395.

Amar, H., Benzaazoua, M., Elghali, A., Bussière, B., Duclos, M., 2020a. Upstream environmental desulphurisation and valorisation of waste rocks as a sustainable and management approach. Journal of Geochemical Exploration, 106555.

Amar, H., Elghali, A., Benzaazoua, M., 2021. Geochemical behaviour of benign desulphurised waste rocks for mine drainage control and sustainable management. Journal of Geochemical Exploration, 225, 106767.

Amar, H., Mostafa, B., Mohamed, E., Mathieu, V., Joly, M.-A., Abdellatif, E., 2020b. Reprocessing feasibility of polymetallic waste rock for cleaner and sustainable mining. Journal of Geochemical Exploration, 106683.

Amos, R. T., Blowes, D. W., Bailey, B. L., Sego, D. C., Smith, L., Ritchie, A. I. M., 2015. Waste-rock hydrogeology and geochemistry. Applied Geochemistry, 57, 140-156.

Asadi, M., Soltani, F., Mohammadi, M. R. T., Khodadadi, D. A., Abdollahy, M., 2019. A successful operational initiative in copper oxide flotation: Sequential sulphidisation-flotation technique. Physicochemical Problems of Mineral Processing, 55.

Aslan, N., Fidan, R., 2008. Optimization of pb flotation using statistical technique and quadratic programming. Separation and Purification Technology, 62(1), 160-165.

ASTM, A., 2014. C136/C136M–14, Standard test method for sieve analysis of fine and coarse aggregates. ASTM international, West Conshohocken, Pa 2014.).

Atrafi, A., Hodjatoleslami, H., Noaparast, M., Shafaei, Z., Ghorbani, A., 2012. Implementation of flotation and gravity separation, to process changarzeh sulfide-oxide lead ore. Journal of Mining and Environment, 3(2), 79-87.

Aubertin, M., Bussière, B., Bernier, L., 2002. Environnement et gestion des rejets miniers: Manuel sur cédérom: Presses International Polytechnique.

Aubertin, M., Bussière, B., Bernier, L., Chapuis, R., Julien, M., Belem, T., Simon, R., Mbonimpa, M., Benzaazoua, M., Li, L., 2002. La gestion des rejets miniers dans un contexte de développement durable et de protection de l'environnement. Congrès annuel de la société canadienne de génie civil, Montréal, Qc, Canada, 5 Juin 2002.

Aubertin, M., Fala, O., Molson, J., Chouteau, M., Anterrieu, O., Hernandez, M. A., Chapuis, R. P., Bussière, B., Lahmira, B., Lefebvre, R., 2008. Caractérisation du comportement hydrogéologique et géochimique des haldes à stériles. Paper presented at the Proceedings: Symposium sur l'environnement et les mines, Rouyn-Noranda, QC, Canada. 2–5 Nov. 2008.

Avarmaa, K., Yliaho, S., Taskinen, P., 2018. Recoveries of rare elements Ga, Ge, In and Sn from waste electric and electronic equipment through secondary copper smelting. Waste Management, 71, 400-410.

Ayawei, N., Ebelegi, A. N., Wankasi, D., 2017. Modelling and interpretation of adsorption isotherms. Journal of Chemistry, 2017, 1-11.

Benzaazoua, M., Bouzahzah, H., Taha, Y., Kormos, L., Kabombo, D., Lessard, F., Bussière, B., Demers, I., Kongolo, M., 2017. Integrated environmental management of

pyrrhotite tailings at raglan mine: Part 1 challenges of desulphurization process and reactivity prediction. Journal of Cleaner Production, 162, 86-95.

Benzaazoua, M., Bussière, B., Dagenais, A.-M., Archambault, M., 2004. Kinetic tests comparison and interpretation for prediction of the Joutel tailings acid generation potential. Environmental Geology, 46(8), 1086-1101.

Benzaazoua, M., Bussière, B., Demers, I., Aubertin, M., Fried, É., Blier, A., 2008. Integrated mine tailings management by combining environmental desulphurization and cemented paste backfill: Application to mine doyon, Quebec, Canada. Minerals Engineering, 21(4), 330-340.

Benzaazoua, M., Bussière, B., Kongolo, M., McLaughlin, J., Marion, P., 2000. Environmental desulphurization of four canadian mine tailings using froth flotation. International Journal of Mineral Processing, 60(1), 57-74.

Benzaazoua, M., Bussiëre, B., Leliëvre, J., 1998. Non-selective froth flotation of sulphide minerals for environmental tailings management. Paper presented at the Proceedings of the Annual Meeting of the Canadian Mineral Processors, Ottawa, The Canadian Institute of Mining, Metallurgy and Petroleum, 696a-696k.

Benzaazoua, M., Kongolo, M., 2003. Physico-chemical properties of tailing slurries during environmental desulphurization by froth flotation. International Journal of Mineral Processing, 69(1-4), 221-234.

Benzaazoua, M., Kongolo, M., Bussière, B., 2000b. Effect of the granulometry on desulphurization feasibility of mine tailings. ICARD 2000, 853-861.

Benzaazoua, M., Marion, P., Pinto, A., Migeon, H., Wagner, F., 2003. Tin and indium mineralogy within selected samples from the Neves Corvo ore deposit (Portugal): A multidisciplinary study. Minerals Engineering, 16(11), 1291-1302.

Benzaazoua, M., Ouellet, J., Servant, S., Newman, P., Verburg, R., 1999. Cementitious backfill with high sulfur content physical, chemical, and mineralogical characterization. Cement and Concrete Research, 29(5), 719-725.

Bergmann, C., Govender, V., Corfield, A., 2016. Using mineralogical characterisation and process modelling to simulate the gravity recovery of ferrochrome fines. Minerals Engineering, 91, 2-15.

Blowes, D. W., Jambor, J. L., Hanton-Fong, C. J., Lortie, L., Gould, W. D., 1998. Geochemical, mineralogical and microbiological characterization of a sulphide-bearing carbonate-rich gold-mine tailings impoundment, Joutel, Québec. Applied Geochemistry, 13(6), 687-705.

Blowes, D. W., Ptacek, C. J., Jambor, J. L., Weisener, C. G., Paktunc, D., Gould, W. D., Johnson, D. B., 2014. The geochemistry of acid mine drainage. 131-190.

Blowes, D., Ptacek, C., Jambor, J., Weisener, C., Paktunc, D., Gould, W., Johnson, D., 2003. The geochemistry of acid mine drainage. Environmental Geochemistry, 9, 149-204.

Boily, J.-F., Gassman, P. L., Peretyazhko, T., Szanyi, J., Zachara, J. M., 2010. Ftir spectral components of schwertmannite. Environmental Science & Technology, 44(4), 1185-1190.

Bois, D., Poirier, P., Benzaazoua, M., Bussière, B., 2004. A feasibility study on the use of desulphurized tailings to control acid mine drainage. Proceedings 2004 – 36th Annual Meeting of the Canadian Mineral Processors, January 20-22, 2004, Ottawa (Ontario), pp. 361-380.

Bois, D., Poirier, P., Benzaazoua, M., Bussière, B., Kongolo, M., 2005. A feasibility study on the use of desulphurised tailings to control acid mine drainage. CIM Bulletin, Vol. 98, No. 1087.

Bouzahzah, H., Benzaazoua, M., Bussière, B., Plante, B., 2014. Revue de littérature détaillée sur les tests statiques et les essais cinétiques comme outils de prédiction du drainage minier acide. Déchets Sciences et Techniques, 66, 14-31.

Bouzahzah, H., Benzaazoua, M., Plante, B., Bussière, B., 2015. A quantitative approach for the estimation of the "fizz rating" parameter in the acid-base accounting tests: A new adaptations of the Sobek test. Journal of Geochemical Exploration, 153, 53-65.

Broadhurst, J., Harrison, S., 2015. A desulfurization flotation approach for the integrated management of sulfide wastes and acid rock drainage risks. Paper presented at the Paper presented at the 10th International Conference on Acid Rock Drainage & IMWA Annual Conference.

Broadhurst, J., Kunene, M., von Blottnitz, H., Franzidis, J.-P., 2015. Life cycle assessment of the desulfurisation flotation process to prevent acid rock drainage: A base metal case study. Minerals Engineering, 76, 126-134.

Brough, C., Strongman, J., Bowell, R., Warrender, R., Prestia, A., Barnes, A., Fletcher, J., 2017. Automated environmental mineralogy; the use of liberation analysis in humidity cell test work. Minerals Engineering, 107, 112-122.

Brown Jr, G. E., Calas, G., 2011. Environmental mineralogy–understanding element behavior in ecosystems. Comptes Rendus Geoscience, 343(2-3), 90-112.

Bruckard, W., McCallum, D., 2007. Treatment of sulfide tailings from base metal and gold operations-a source of saleable by-products and sustainable waste management. World Gold Congress, Cairns, Australia, 22-24 October 2007, p. 85–91.

Brunauer, S., Emmett, P. H., Teller, E., 1938. Adsorption of gases in multimolecular layers. Journal of the American Chemical Society, 60(2), 309-319.

Budipramana, Y., Suprapto, S., Ersam, T., Kurniawan, F., 2014. Synthesis nickel hidroxide by electrolysis at high voltage. ARPN Journal of Engineering and Applied Sciences, 9, 2074.

Bussière, B., 2007. Colloquium 2004: Hydrogeotechnical properties of hard rock tailings from metal mines and emerging geoenvironmental disposal approaches. Canadian Geotechnical Journal, 44(9), 1019-1052.

Bussière, B., Benzaazoua, M., Aubertin, M., Mbonimpa, M., 2004. A laboratory study of covers made of low-sulphide tailings to prevent acid mine drainage. Environmental Geology, 45(5), 609-622.

Bussière, B., Benzaazoua, M., Kongolo, M., Aubertin, M., 2002b. Intégration de la désulfuration dans la restauration des sites miniers générateurs de DMA. Symposium 2002 sur l'environnement et les mines, Rouyn-Noranda, Québec, Canada.

Butcher, A., Helms, T., Gottlieb, P., Bateman, R., Ellis, S., Johnson, N., 2000. Advances in the quantification of gold deportment by Qemscan. Paper presented at the Seventh Mill Operators Conference, Kalgoorlie, WA, AusIMM.

Caldeira, C. L., Ciminelli, V. S., Osseo-Asare, K. A., 2008. Pyrite oxidation in alkaline solutions: The carbonate effect. Paper presented at the Hydrometallurgy 2008: 6th International Symposium. Society for Mining, Metallurgy and Exploration, Littleton, CO, USA.pp. 990–999

Carrasco, C., Keeney, L., Scott, M., Napier-Munn, T., 2016. Value driven methodology to assess risk and operating robustness for grade engineering strategies by means of stochastic optimisation. Minerals Engineering, 99, 76-88.

Cases, J., De Donato, P., 1991. FTIR analysis of sulphide mineral surfaces before and after collection: Galena. International Journal of Mineral Processing, 33(1-4), 49-65.

Cases, J., De Donato, P., Kongolo, M., Michot, L., 1989. An infrared investigation of amylxanthate adsorption by pyrite after wet grinding at natural and acid pH. Colloids and Surfaces, 36(3), 323-338.

Cases, J., Kongolo, M., De Donato, P., Mielczarski, J., Barres, O., Bouquet, E., Francos, A., 1995. Characterization of surface products of xanthate interactions with sulfide minerals: Influence of fine-grinding and mechanism of collector adsorption-abstraction. Proceedings Mineral Processing, Recent Advances and Future Trends. SP Mehrotra et R. Shekhar, Kanpur: Allied Published Limited, 13-28.

Chang, Y. K., Chang, J. E., Lin, T. T., Hsu, Y. M., 1999. Stability evaluations of copper ethyl xanthate and copper butyl xanthate in an acid solution. Paper presented at the Proceedings of the International Conference on Solid Waste Technology and Management, Philadelphia, PA, USA, 219-226

Charuseiam, Y., Chotpantarat, S., Sutthirat, C., 2021. Acid mine drainage potential of waste rocks in a gold mine (Thailand): Application of a weathering cell test and multivariate statistical analysis. Environmental Geochemistry and Health, 1-31.

Chatterjee, A., 1998. Role of particle size in mineral processing at tata steel. International Journal of Mineral Processing, 53(1-2), 1-14.

Chen, Y., Cao, M., Ma, C., 2019. Review of coal-fired electrification and magnetic separation desulfurization technology. Applied Sciences, 9(6), 1158.

Chen, Y.-C., Parlar, H., 2013. Enrichment behavior of immunoglobulin by foam fractionation using response surface methodology. Separation and Purification Technology, 107, 102-108.

Chopard, A., Benzaazoua, M., Bouzahzah, H., Plante, B., Marion, P., 2017. A contribution to improve the calculation of the acid generating potential of mining wastes. Chemosphere, 175, 97-107.

Chopard, A., Benzaazoua, M., Plante, B., Bouzahzah, H., Marion, P., 2015. Kinetic tests to evaluate the relative oxidation rates of various sulfides and sulfosalts. In Proceedings of the 10th international conference on acid rock drainage and IMWA annual conference 2015, Santiago, Chile.

Chopard, A., Marion, P., Mermillod-Blondin, R., Plante, B., Benzaazoua, M., 2019. Environmental impact of mine exploitation: An early predictive methodology based on ore mineralogy and contaminant speciation. Minerals, 9(7), 397.

Cravotta III, C. A., 2008. Dissolved metals and associated constituents in abandoned coal-mine discharges, Pennsylvania, USA. Part 1: Constituent quantities and correlations. Applied Geochemistry, 23(2), 166-202.

Craw, D., Bowell, R. J., 2014. The characterization of arsenic in mine waste. Reviews in Mineralogy and Geochemistry, 79(1), 473-505.

Cruz, R., Bertrand, V., Monroy, M., González, I., 2001. Effect of sulfide impurities on the reactivity of pyrite and pyritic concentrates: A multi-tool approach. Applied Geochemistry, 16(7-8), 803-819.

Dalm, M., Buxton, M. W., van Ruitenbeek, F. J., Voncken, J. H., 2014. Application of near-infrared spectroscopy to sensor based sorting of a porphyry copper ore. Minerals Engineering, 58, 7-16.

Dance, A., Morrison, R., 1992. Quantifying a black art: The electrostatic separation of mineral sands. Minerals Engineering, 5(7), 751-765.

Das, A., Sarkar, B., 2018. Advanced gravity concentration of fine particles: A review. Mineral Processing and Extractive Metallurgy Review, 39(6), 359-394.

De Donato, P., Kongolo, M., Barres, O., Yvon, J., Enderle, F., Bouquet, E., Alnot, M., Cases, J., 1999. Chemical surface modifications of sulphide minerals after comminution. Powder Technology, 105(1-3), 141-148.

De Donato, P., Mustin, C., Benoit, R., Erre, R., 1993. Spatial distribution of iron and sulphur species on the surface of pyrite. Applied Surface Science, 68(1), 81-93.

De Bronac de Vazelhes, V., Beaudoin, G., McMartin, I., Côté-Mantha, O., Boulianne-Verschelden, N., 2021. Assessment of the Amaruq gold deposit signature in glacial sediments using multivariate geochemical data analysis and indicator minerals. Journal of Geochemical Exploration, 228, 106800.

Deane, J., Nesbitt, W., Scaini, m., 2003. Gersdorffite (NiAsS) chemical state properties and reactivity toward air and aerated, distilled water. American Mineralogist, 890–900.

Demers, I., Benzaazoua, M., Bussière, B., Mbonimpa, M., Fried, E., Blier, A., 2009. Évaluation de l'application de la gestion intégrée des résidus à la mine Doyon. DÉCHE TS, 31.

Demers, I., Bussière, B., Benzaazoua, M., Mbonimpa, M., Blier, A., 2008. Column test investigation on the performance of monolayer covers made of desulphurized tailings to prevent acid mine drainage. Minerals Engineering, 21(4), 317-329.

Demers, I., Bussière, B., Mbonimpa, M., Benzaazoua, M., 2009. Oxygen diffusion and consumption in low-sulphide tailings covers. Canadian Geotechnical Journal, 46(4), 454-469.

Demers, I., Mbonimpa, M., Benzaazoua, M., Bouda, M., Awoh, S., Lortie, S., Gagnon, M., 2017. Use of acid mine drainage treatment sludge by combination with a natural soil as an oxygen barrier cover for mine waste reclamation: Laboratory column tests and intermediate scale field tests. Minerals Engineering, 107, 43-52.

Derhy, M., Taha, Y., Benzaazoua, M., El-Bahi, A., Ait-Khouia, Y., Hakkou, R., 2022. Assessment of the selective flotation of calcite, apatite and quartz using bio-based collectors: Flaxseed, nigella, and olive oils. Minerals Engineering, 182, 107589.

Dermont, G., Bergeron, M., Mercier, G., Richer-Laflèche, M., 2008. Soil washing for metal removal: A review of physical/chemical technologies and field applications. Journal of Hazardous Materials, 152(1), 1-31.

Derycke, V., 2012. Optimisation de la désulfuration de produits miniers en vue de la diminution de leur potentiel polluant: Effet de la granulométrie, du type de sulfures et évaluation de la qualité des eaux de drainage post-traitement. Rapport de thèse, Université du Québec en Abitibi-Témiscamingue, Qc, Canada.

Derycke, V., Kongolo, M., Benzaazoua, M., Mallet, M., Barrès, O., De Donato, P., Bussière, B., Mermillod-Blondin, R., 2013. Surface chemical characterization of different pyrite size fractions for flotation purposes. International Journal of Mineral Processing, 118, 1-14.

Devin, S., Bowell, R., Dey, M., Williams, C., Williams, K., 2008. A comparison of kinetic NAG tests with static and humidity cell tests for the prediction of ARD. In: Rapantova, N., Hrkal, Z. (Eds.), Mine Water and the Environment. VSB – Technical University of Ostrava, Ostrava, pp. 325–328.

Dino, G. A., Cavallo, A., Rossetti, P., Garamvölgyi, E., Sándor, R., Coulon, F., 2020. Towards sustainable mining: Exploiting raw materials from extractive waste facilities. Sustainability, 12(6), 2383.

Dold, B., 2017. Acid rock drainage prediction: A critical review. Journal of Geochemical Exploration, 172, 120-132.

Drif, B., Taha, Y., Hakkou, R., Benzaazoua, M., 2018. Recovery of residual silver-bearing minerals from low-grade tailings by froth flotation: The case of Zgounder mine, Morocco. Minerals, 8(7), 273.

Duchesne, J., Laforest, G., 2006. Remediation of electric arc furnace dust leachate by the use of cementitious materials: A column-leaching test. Acta Geochimica, 25, 99.

El-bouazzaoui, A., Ait-khouia, Y., Demers, I., Benzaazoua, M., 2022. Alternative flotation collectors for the environmental desulfurization of gersdorffite (NiAsS) bearing mine tailings: Surface chemistry. Colloids and Surfaces A: Physicochemical and Engineering Aspects, 647, 128943.

Elghali, A., Benzaazoua, M., Bouzahzah, H., Abdelmoula, M., Dynes, J. J., Jamieson, H. E., 2021a. Role of secondary minerals in the acid generating potential of weathered mine tailings: Crystal-chemistry characterization and closed mine site management involvement. Science of the Total Environment, 784, 147105.

Elghali, A., Benzaazoua, M., Bouzahzah, H., Bussière, B., 2021b. Laboratory study on the effectiveness of limestone and cementitious industrial products for acid mine drainage remediation. Minerals, 11(4), 413.

Elghali, A., Benzaazoua, M., Bouzahzah, H., Bussière, B., Villarraga-Gómez, H., 2018. Determination of the available acid-generating potential of waste rock, part I: Mineralogical approach. Applied Geochemistry, 99, 31-41.

Elghali, A., Benzaazoua, M., Bussière, B., Bouzahzah, H., 2019a. Determination of the available acid-generating potential of waste rock, part II: Waste management involvement. Applied Geochemistry, 100, 316-325.

Elghali, A., Benzaazoua, M., Bussière, B., Genty, T., 2019b. In situ effectiveness of alkaline and cementitious amendments to stabilize oxidized acid-generating tailings. Minerals, 9(5), 314.

Elghali, A., Benzaazoua, M., Bussière, B., Kennedy, C., Parwani, R., Graham, S., 2019c. The role of hardpan formation on the reactivity of sulfidic mine tailings: A case study at Joutel mine (Québec). Science of the Total Environment, 654, 118-128.

Erguler, Z. A., Erguler, G. K., 2015. The effect of particle size on acid mine drainage generation: Kinetic column tests. Minerals Engineering, 76, 154-167.

Everaert, M., Lemmens, V., Atia, T. A., Spooren, J., 2020. Sulfidic mine tailings and marl waste rock as compatible resources in a microwave-assisted roasting process. Journal of Cleaner Production, 274, 122628.

Fala, O., Molson, J., Aubertin, M., Bussière, B., 2005. Numerical modelling of flow and capillary barrier effects in unsaturated waste rock piles. Mine Water and the Environment, 24(4), 172-185.

Falconer, A., 2003. Gravity separation: Old technique/new methods. Physical Separation in Science and Engineering, 12(1), 31-48.

Fanlo, I., Subías, I., Gervilla, F., Paniagua, A., García, B., 2004. The composition of Co–Ni–Fe sulfarsenides, diarsenides and triarsenides from the San Juan de plan deposit, central pyrenees, Spain. The Canadian Mineralogist, 42(4), 1221-1240.

Farrokhpay, S., 2020. Editorial for the special issue: Physical separation and enrichment. Minerals 2020, 10, 173.

Fatahi, M., Farzanegan, A., 2018. An analysis of multiphase flow and solids separation inside knelson concentrator based on four-way coupling of CFD and DEM simulation methods. Minerals Engineering, 126, 130-144.

Ferron, C. J., Bulatovic, S. M., Salter, R. S., 1991. Beneficiation of rare earth oxide minerals. Paper presented at the Materials Science Forum (Vol. 70–72, pp. 251–270), Trans Tech Publications, Ltd., January 1991.

Förstner, U., Wittmann, G. T.W., 1981. Metal pollution in the aquatic environment. Springer Science & Business Media. Berlin Heidelberg.

Gamache-Rochette, A., 2004. Water flow characterization in unsaturated rock waste piles using in situ hydrogeological tests. M. Sc. thesis, Department of Civil, Geological, and Mining Engineering, Ecole Polytechnique, Montreal.

Ghodrati, S., Nakhaei, F., VandGhorbany, O., Hekmati, M., 2020. Modeling and optimization of chemical reagents to improve copper flotation performance using response surface methodology. Energy Sources, Part A: Recovery, Utilization, and Environmental Effects, 42(13), 1633-1648.

Gill, C. B., 1991. Electrostatic separation. In Materials Beneficiation. Materials Research and Engineering. New York, NY (pp. 141-147): Springer.

Gill, C. B., 1991. Gravity concentration. In Materials Beneficiation. Materials Research and Engineering. New York, NY (pp. 148-175): Springer.

Gillet, G., 2004. Séparation magnétique: haut gradient (SMHG) et haut champ. Techniques de l'ingénieur, Génie des procédés, Vol papier n° JB3, J3222, Mars 2004.

Goel, V., Mishra, S. K., Sharma, C., Sarangi, B., Aggarwal, S. G., Agnihotri, R., Kotnala, R. K., 2018. A non-destructive FTIR method for the determination of ammonium and sulfate in urban pm2.5 samples. MAPAN, 33(3), 209-215.

Göktepe, F., 2005. Treatment of lead mine waste by a mozley multi-gravity separator (mgs). Journal of Environmental Management, 76(4), 277-281.

Gosselin, A., Blackburn, D., Bergeron, M., 1999. Protocole d'évaluation de la traitabilité des sédiments, des sols et des boues à l'aide des technologies minéralurgiques. Sainte-Foy, QC, Canada: Ministère des Travaux Publics et Services Gouvernementaux du Canada; 1999. P 134.

Gottlieb, P., Wilkie, G., Sutherland, D., Ho-Tun, E., Suthers, S., Perera, K., Jenkins, B., Spencer, S., Butcher, A., Rayner, J., 2000. Using quantitative electron microscopy for process mineralogy applications. JOM, 52(4), 24-25.

Grewal, I., Lundt, M., Wong, D., Tse, W., 2014. Recent developments in preconcentration using dense media separation. Corpus ID: 111388136. Materials Science.

Grobler, J., Naudé, N., Zietsman, J. H., 2016. Enhanced holland-batt spline for describing spiral concentrator performance. Minerals Engineering, 92, 189-195.

Gülsoy, Ö. Y., Gülcan, E., 2019. A new method for gravity separation: Vibrating table gravity concentrator. Separation and Purification Technology, 211, 124-134.

Guntoro, P. I., Ghorbani, Y., Koch, P.-H., Rosenkranz, J., 2019. X-ray microcomputed tomography (μCT) for mineral characterization: A review of data analysis methods. Minerals, 9(3), 183.

Hakkou, R., Benzaazoua, M., Bussière, B., 2008. Acid mine drainage at the abandoned kettara mine (morocco): 1. Environmental characterization. Mine Water and the Environment, 27(3), 145-159.

Haldar, S. K., 2018. Mineral exploration: Principles and applications: 2nd ed. Elsevier: Amsterdam, The Netherlands, 2018; ISBN 978-0-12-814022-2.

Heikkinen, P., Räisänen, M., Johnson, R., 2009. Geochemical characterisation of seepage and drainage water quality from two sulphide mine tailings impoundments: Acid mine drainage versus neutral mine drainage. Mine Water and the Environment, 28(1), 30-49.

Heiskanen, K., 1993. Particle classification, 1st ed.Chapman & Hall, London, 1993.

Hesford, I., Wellings, D., 1988. Spiral and cone concentrators. Mine and Quarry, 17(12), 37-41.

Hesketh, A. H., Broadhurst, J. L., Bryan, C. G., van Hille, R. P., Harrison, S. T. L., 2010. Biokinetic test for the characterisation of AMD generation potential of sulfide mineral wastes. Hydrometallurgy, 104(3-4), 459-464.

Hirajima, T., Sasaki, K., Bissombolo, A., Hirai, H., Hamada, M., Tsunekawa, M., 2005. Feasibility of an efficient recovery of rare earth-activated phosphors from waste

fluorescent lamps through dense-medium centrifugation. Separation and Purification Technology, 44(3), 197-204.

Honaker, R., Wang, D., Ho, K., 1996. Application of the falcon concentrator for fine coal cleaning. Minerals Engineering, 9(11), 1143-1156.

Hudson-Edwards, K. A., Jamieson, H. E., Lottermoser, B. G., 2011. Mine wastes: Past, present, future. Elements, 7(6), 375-380.

Iwasaki, I., Nakazawa, H., Malicsi, A., Xiaowei, L., 1988. Recovery of platinum-group metals from gabbroic rocks. JOM, 40(6), 36-39.

Jackson, D. A., Nesbitt, H. W., Scaini, M. J., Duggal, A., Bancroft, G. M., 2003. Gersdorffite (niass) chemical state properties and reactivity toward air and aerated, distilled water. American Mineralogist, 88(5-6), 890-900.

Jambor, J., Dutrizac, J., Raudsepp, M., 2007. Measured and computed neutralization potentials from static tests of diverse rock types. Environmental Geology, 52(6), 1173-1185.

Jambor, J., Dutrizac, J., Raudsepp, M., Groat, L., 2003. Effect of peroxide on neutralization ‐ potential values of siderite and other carbonate minerals. Journal of Environmental Quality, 32(6), 2373-2378.

James, M., Aubertin, M., Bussière, B., 2013. On the use of waste rock inclusions to improve the performance of tailings impoundments. Paper presented at the Proceedings of the 18th International Conference Soil Mechanics and Geotechnical Engineering, Paris, France.

Jamieson, H. E., Walker, S. R., Parsons, M. B., 2015. Mineralogical characterization of mine waste. Applied Geochemistry, 57, 85-105.

Jiang, L., Liu, P., Zhang, Y., Yang, X., Wang, H., 2019. The effect of inlet velocity on the separation performance of a two-stage hydrocyclone. Minerals, 9(4), 209.

José Neto, D., Bergerman, M. G., Young, A. S., Petter, C. O., 2019. Pre-concentration potential evaluation for a silicate zinc ore by density and sensor-based sorting methods. REM-International Engineering Journal, 72(2), 335-343.

Jung, C., Ristau, O., Schulze, H., Sligar, S. G., 1996. The co stretching mode infrared spectrum of substrate-free cytochrome p-450cam-co: The effect of solvent conditions, temperature, and pressure. European Journal of Biochemistry, 235(3), 660-669.

Kahl, W. A., Dilissen, N., Hidas, K., Garrido, C. J., Lopez-Sanchez-Vizcaino, V., Roman-Alpiste, M., 2017. 3 ‐ D microstructure of olivine in complex geological materials reconstructed by correlative x-ray-CT and EBSD analyses. Journal of Microscopy, 268(2), 193-207.

Katwika, C. N., Kime, M.-B., Kalenga, P. N. M., Mbuya, B. I., Mwilen, T. R., 2019. Application of knelson concentrator for beneficiation of copper-cobalt ore tailings. Mineral Processing and Extractive Metallurgy Review, 40(1), 35-45.

Kelly, E. G., Spottiswood, D. J., 1982. Introduction to mineral processing. Somerset: John Wiley & Sons, New York, USA.

Khalil, A., Argane, R., Benzaazoua, M., Bouzahzah, H., Taha, Y., Hakkou, R., 2019. Pb–Zn mine tailings reprocessing using centrifugal dense media separation. Minerals Engineering, 131, 28-37.

Kojovic, T., Bergeron, Y., Leetmaa, K., 2019. The value of daily HIT ore hardness testing of SAG feed at the Meadowbank gold mine. Proceedings from SAG 2019, Vancouver, Canada. September.

Kökkılıç, O., Langlois, R., Waters, K. E., 2015. A design of experiments investigation into dry separation using a knelson concentrator. Minerals Engineering, 72, 73-86.

Kongolo, M., 1991. Interaction de l'amylxanthate de potassium avec la galène et la pyrite finement broyées: Conséquences sur la flottation. Thèse de doctorat d'État de l'Institut National Polytechnique de Lorraine, Nancy, France, 407p.

Kongolo, M., Benzaazoua, M., de Donato, P., Drouet, B. t., Barrès, O., 2004. The comparison between amine thioacetate and amyl xanthate collector performances for pyrite flotation and its application to tailings desulphurization. Minerals Engineering, 17(4), 505-515.

Koppalkar, S., 2009. Effect of operating variables in knelson concentrators: A. Pilot-scale study. McGill University.

Kwak, J.-S., 2005. Application of Taguchi and response surface methodologies for geometric error in surface grinding process. International Journal of Machine Tools and Manufacture, 45(3), 327-334.

Lamia, B., 2017. Reprocessing and environmental desulphurization of sulphide mining waste from sphalerite flotation: Case of Chaabet el Hamra mine, Algeria. World Journal of Engineering, 14(1), 42-46.

Lapakko, K. A., 1994. Evaluation of neutralization potential determinations for metal mine waste and a proposed alternative. Paper presented at the Proceeding: of the Third International Conference on the Abatement of Acidic Drainage, April.

Lapakko, K. A., Antonson, D. A., 2006. Pyrite oxidation rates from humidity cell testing of greenstone rock. Proc. 2006, 7th ICARD, March, 26-30.

Lapakko, K. A., Engstrom, J. N., Antonson, D. A., 2006. Effects of particle size on drainage quality from three lithologies. Paper presented at the Poster paper presented at the 7th International Conference on Acid Rock Drainage (ICARD).

Latief, F., Fauzi, U., Irayani, Z., Dougherty, G., 2017. The effect of x-Ray micro computed tomography image resolution on flow properties of porous rocks. Journal of Microscopy, 266(1), 69-88.

Lawrence, R. W., Scheske, M., 1997. A method to calculate the neutralization potential of mining wastes. Environmental Geology, 32(2), 100-106.

Legrand, D. L., Nesbitt, H. W., Bancroft, G. M., 1998. X-ray photoelectron spectroscopic study of a pristine millerite (NiS) surface and the effect of air and water oxidation. American Mineralogist, 83(11-12- Part 1), 1256-1265.

Lemos, M., Valente, T., Reis, P. M., Fonseca, R., Delbem, I., Ventura, J., Magalhães, M., 2021. Mineralogical and geochemical characterization of gold mining tailings and their potential to generate acid mine drainage (Minas Gerais, Brazil). Minerals, 11(1), 39.

Leppinen, J., 1990. Ftir and flotation investigation of the adsorption of ethyl xanthate on activated and non-activated sulfide minerals. International Journal of Mineral Processing, 30(3-4), 245-263.

Leppinen, J., Salonsaari, P., Palosaari, V., 1997. Flotation in acid mine drainage control: Beneficiation of concentrate. Canadian Metallurgical Quarterly, 36(4), 225-230.

Lessard, F., Bussière, B., Côté, J., Benzaazoua, M., Boulanger-Martel, V., Marcoux, L., 2018. Integrated environmental management of pyrrhotite tailings at raglan mine: Part 2 desulphurized tailings as cover material. Journal of Cleaner Production, 186, 883-893.

Li, H., Chen, W., 2019. Research on application of centrifugal circulating fluidized bed in tin mud ore separation. Paper presented at the IOP Conference Series: Earth and Environmental Science, volume 384(1):012210, Dalian, China. November 2019.

Lopéz, R., Jordão, H., Hartmann, R., Ämmälä, A., Carvalho, M. T., 2019. Study of butyl-amine nanocrystal cellulose in the flotation of complex sulphide ores. Colloids and Surfaces A: Physicochemical and Engineering Aspects, 579, 123655.

Lottermoser, B. G., 2011. Recycling, reuse and rehabilitation of mine wastes. Elements, 7(6), 405-410.

Luttrell, G., 1995. Enhanced gravity separators: New alternatives for fine coal cleaning -department of mining and minerals engineering Virginia polytechnic institute and state University.

Luttrell, G., Bethell, P., Honaker, R., 2014. Designing and operating fine coal processing circuits to meet market specifications. International Journal of Coal Preparation and Utilization, 34(3-4), 172-183.

Maest, A. S., Nordstrom, D. K., 2017. A geochemical examination of humidity cell tests. Applied Geochemistry, 81, 109-131.

Mafra, C., Bouzahzah, H., Stamenov, L., Gaydardzhiev, S., 2020. Insights on the effect of pyrite liberation degree upon the acid mine drainage potential of sulfide flotation tailings. Applied Geochemistry, 104774.

Maire, E., Withers, P. J., 2014. Quantitative x-ray tomography. International Materials Reviews, 59(1), 1-43.

Majumder, A., Barnwal, J., 2006. Modeling of enhanced gravity concentrators–present status. Mineral Processing and Extractive Metallurgy Review, 27(1), 61-86.

Majumder, A., Barnwal, J., 2011. Processing of coal fines in a water-only cyclone. Fuel, 90(2), 834-837.

Marion, C., Grammatikopoulos, T., Rudinsky, S., Langlois, R., Williams, H., Chu, P., Awais, M., Gauvin, R., Rowson, N., Waters, K., 2018. A mineralogical investigation

into the pre-concentration of the Nechalacho deposit by gravity separation. Minerals Engineering, 121, 1-13.

Marion, C., Williams, H., Langlois, R., Kökkılıç, O., Coelho, F., Awais, M., Rowson, N., Waters, K., 2017. The potential for dense medium separation of mineral fines using a laboratory falcon concentrator. Minerals Engineering, 105, 7-9.

Mayer, K. U., Frind, E. O., Blowes, D. W., 2002. Multicomponent reactive transport modeling in variably saturated porous media using a generalized formulation for kinetically controlled reactions. Water Resources Research, 38(9), 13-11-13-21.

Mayes, W. M., Potter, H. A., Jarvis, A. P., 2009. Novel approach to zinc removal from circum-neutral mine waters using pelletised recovered hydrous ferric oxide. Journal of Hazardous Materials, 162(1), 512-520.

Mbonimpa, M., Aubertin, M., Chapuis, R., Maqsoud, A., Bussière, B., 2009. Estimation of specific surface areas of coarse-grained materials with grain-size curves represented by two-parameter lognormal distributions. Proceedings of the GeoHalifax, 1607-1614.

McCoy, J. T., Auret, L., 2019. Machine learning applications in minerals processing: A review. Minerals Engineering, 132, 95-109.

McKeown, R., Barbour, L., Rowlett, D., Herasymuik, G., 2000. Characterization of the grain-size distribution for waste rock from metal mines: A review of the existing data and an evaluation of the implications for hydrogeologic behavior. Proceedings of the CSCE Annual Conference, London, Ontario, 2000.

McLemore, V. T., Donahue, K. M., Phillips, E., Dunbar, N., Walsh, P., Gutierrez, L. A., Tachie-Menson, S., Shannon, H. R., Lueth, V. W., Campbell, A. R., 2006. Characterization of goathill north mine rock pile, Questa molybdenum mine, Questa,

New Mexico. Paper presented at the International Conference of Acid Rock Drainage (ICARD). ASMR, St. Louis.

MDDEP, M. 2012. Directive 019 sur l'industrie minière. MDDEP, Québec : Gouvernement du Québec. 95 p. Online: www. mddep. gouv. qc. ca/milieu_ind/directive019/directive019. pdf.

Mehrabani, J., Noaparast, M., Mousavi, S., Dehghan, R., Ghorbani, A., 2010. Process optimization and modelling of sphalerite flotation from a low-grade Zn-Pb ore using response surface methodology. Separation and Purification Technology, 72(3), 242-249.

Mercier, G., Duchesne, J., Blackburn, D., 2001. Prediction of metal removal efficiency from contaminated soils by physical methods. Journal of Environmental Engineering, 127(4), 348-358.

Mermillod-Blondin, R., 2005. Influence des propriétés superficielles de la pyrite sur la rétention de molécules organiques soufrées: Application à la désulfuration des résidus miniers. Thèse de doctorat. Institut National Polytechnique de Lorraine en cotutelle avec Université de Montréal. 308 p.

Mermillod-Blondin, R., Kongolo, M., De Donato, P., Benzaazoua, M., Barrès, O., Bussière, B., Aubertin, M., 2005. Pyrite flotation with xanthate under alkaline conditions-application to environmental desulfurization. Paper presented at the Centenary of flotation symposium, Brisbane, QLD, Australia, 6-9 June 2005.

Mesa, D., Brito-Parada, P. R., 2019. Scale-up in froth flotation: A state-of-the-art review. Separation and Purification Technology, 210, 950-962.

Miller, S., Jeffery, J., Wong, J., 1991. Use and misuse of the acid base account for "AMD" prediction. Paper presented at the Proceedings of the 2nd International Conference on the Abatement of Acidic Drainage, Montréal, Quebec.

Miller, S., Jeffery, J., Wong, J., 1991a. In-pit identification and management of acid forming waste rock at the golden cross gold mine, New Zealand. Paper presented at the Proceedings of the Second International Conference on the Abatement of Acidic Drainage Montreal, Quebec, September.

Monte, M., Dutra, A., Albuquerque Jr, C., Tondo, L., Lins, F., 2002. The influence of the oxidation state of pyrite and arsenopyrite on the flotation of an auriferous sulphide ore. Minerals Engineering, 15(12), 1113-1120.

Muhammad, H., Shaheen, R., Akram, B., Abdin, Z., Haq, S., Mahsud, S., Ali, S., Khan, R., 2020. Green synthesis of cobalt oxide nanoparticles for potential biological applications. Materials Research Express, 7.

Nadeif, A., Taha, Y., Bouzahzah, H., Hakkou, R., Benzaazoua, M., 2019. Desulfurization of the old tailings at the Au-Ag-Cu Tiouit mine (anti-atlas Morocco). Minerals, 9(7), 401.

Nakazawa, H., Iwasaki, I., 1986. Flotation behavior of nickel arsenide. International Journal of Mineral Processing, 18(3-4), 191-202.

Nakhaei, F., Irannajad, M., 2017. Sulphur removal of iron ore tailings by flotation. Journal of Dispersion Science and Technology, 38(12), 1755-1763.

Napier-Munn, T. J., Bosman, J., Holtham, P. N., 2014. Innovations in dense medium separation technology. In C. J. Anderson, R. C. Dunne, & J. L. Uhrie (Eds.), Mineral Processing and Extractive Metallurgy: 100 Years of Innovation. Society for Mining Metallurgy & Exploration, Englewood, United States, pp. 265–275.

Napier-Munn, T., 1997. Invention and innovation in mineral processing. Minerals Engineering, 10(8), 757-773.

Ndlovu, S., Simate, G. S., Matinde, E., 2017. Waste production and utilization in the metal extraction industry: CRC Press: Boca Raton, FL, USA, 2017; ISBN 9781498767293.

Nesbitt, H. W., Reinke, M., 1999. Properties of as and s at NiAs, NiS, and Fe1-xS surfaces, and reactivity of niccolite in air and water. American Mineralogist, 84(4), 639-649.

Nesbitt, H., Muir, I., 1998. Oxidation states and speciation of secondary products on pyrite and arsenopyrite reacted with mine waste waters and air. Mineralogy and Petrology, 62(1), 123-144.

Nesbitt, H., Muir, I., Prarr, A., 1995. Oxidation of arsenopyrite by air and air-saturated, distilled water, and implications for mechanism of oxidation. Geochimica et Cosmochimica Acta, 59(9), 1773-1786.

Nesbitt, H., Schaufuss, A., Sciani, M., Hchst, H., Bancroft, G., Szargan, R., 2003. Monitoring fundamental reactions at NiAsS surfaces by synchrotron radiation x-ray photoelectron spectroscopy: As and s air oxidation by consecutive reaction schemes. Geochimica et Cosmochimica Acta, 67(5), 845-858.

Niedoba, T., Pięta, P., Surowiak, A., Şahbaz, O., 2021. Multidimensional optimization of the copper flotation in a jameson cell by means of taxonomic methods. Minerals, 11(4), 385.

Noirant, G., Benzaazoua, M., Kongolo, M., Bussière, B., Frenette, K., 2019. Alternatives to xanthate collectors for the desulphurization of ores and tailings: Pyrite surface chemistry. Colloids and Surfaces A: Physicochemical and Engineering Aspects, 577, 333-346.

Nordstrom, D. K., 2000. Advances in the hydrogeochemistry and microbiology of acid mine waters. International Geology Review, 42(6), 499-515.

Nordstrom, D. K., Blowes, D. W., Ptacek, C. J., 2015. Hydrogeochemistry and microbiology of mine drainage: An update. Applied Geochemistry, 57, 3-16.

Nuorivaara, T., Björkqvist, A., Bacher, J., Serna-Guerrero, R., 2019. Environmental remediation of sulfidic tailings with froth flotation: Reducing the consumption of additional resources by optimization of conditioning parameters and water recycling. Journal of Environmental Management, 236, 125-133.

Paktunc, A., Davé, N., 2000. Mineralogy of pyritic waste rock leached by column experiments and prediction of acid mine drainage. In: Rammlmair, D. (Eds), 6th International Congress on Applied Mineralogy in Research, Economy, Technology, Ecology and Culture, vol. I. Balkema, Rotterdam, pp. 621–623.

Parbhakar-Fox, A. K., Edraki, M., Walters, S., Bradshaw, D., 2011. Development of a textural index for the prediction of acid rock drainage. Minerals Engineering, 24(12), 1277-1287.

Parbhakar-Fox, A., Fox, N., Jackson, L., Cornelius, R., 2018. Forecasting geoenvironmental risks: Integrated applications of mineralogical and chemical data. Minerals, 8(12), 541.

Parbhakar-Fox, A., Lottermoser, B. G., 2015. A critical review of acid rock drainage prediction methods and practices. Minerals Engineering, 82, 107-124.

Peregoedova, A., 2012. Étude expérimentale des propriétés hydrogéologiques des roches stériles à une échelle intermédiaire de laboratoire. M.Sc.A. thesis, École Polytechnique de Montréal,Qc, Canada.

Pirrie, D., Butcher, A. R., Power, M. R., Gottlieb, P., Miller, G. L., 2004. Rapid quantitative mineral and phase analysis using automated scanning electron microscopy (Qemscan); potential applications in forensic geoscience. Geological Society, London, Special Publications, 232(1), 123-136.

Plante, B., 2010. Évaluation des principaux facteurs d'influence sur la prédiction du drainage neutre contaminé. Thèse de doctorat, Université du Québec à en Abitibi-Témiscamingue, Qc, Canada, 2010.

Plante, B., Benzaazoua, M., Bussière, B., 2011. Kinetic testing and sorption studies by modified weathering cells to characterize the potential to generate contaminated neutral drainage. Mine Water and the Environment, 30(1), 22-37.

Plante, B., Benzaazoua, M., Bussière, B., Biesinger, M., Pratt, A., 2010. Study of Ni sorption onto Tio mine waste rock surfaces. Applied Geochemistry, 25(12), 1830-1844.

Plante, B., Bussière, B., Benzaazoua, M., 2014. Lab to field scale effects on contaminated neutral drainage prediction from the Tio mine waste rocks. Journal of Geochemical Exploration, 137, 37-47.

Potts, P., 1987. Classical and rapid methods of analysis, In: A Handbook of Silicate Rock Analysis. Springer, pp. 47–76. Blackie Academic & Professional, London, 1987.

Qun, W., Heiskanen, K., 1990. Separation of pentlandite and nickel arsenide minerals by aeration conditioning flotation. International Journal of Mineral Processing, 29(1-2), 99-109.

Rao, S. R., 1971. Xanthates and related compounds. Marcel Dekker, New York, pp. 55-78.

Raudsepp, M., Pani, E., 2003. Application of Rietveld analysis to environmental mineralogy. Environmental Aspects of Mine Wastes, 31, 165-180.

Rey, N. J., Demers, I., Bussière, B., Mbonimpa, M., Lortie, S., 2016. Field experiments to test the elevated water table concept combined with a desulfurized tailings cover layer- Geo-Chicago 2016 (pp. 289-298).

Rezvanipour, H., Mostafavi, A., Ahmadi, A., Karimimobarakabadi, M., Khezri, M., 2018. Desulfurization of iron ores: Processes and challenges. Steel Research International, 89(7), 1700568.

Rietveld, H. M., 1969. A profile refinement method for nuclear and magnetic structures. Journal of Applied Crystallography, 2(2), 65-71.

Rikers, R., Rem, P., Dalmijn, W., 1998. Improved method for prediction of heavy metal recoveries from soil using high intensity magnetic separation (HIMS). International Journal of Mineral Processing, 54(3-4), 165-182.

Rimstidt, J. D., Vaughan, D. J., 2003. Pyrite oxidation: A state-of-the-art assessment of the reaction mechanism. Geochimica et Cosmochimica Acta, 67(5), 873-880.

Robben, C., Wotruba, H., 2019. Sensor-based ore sorting technology in mining-past, present and future. Minerals, 9(9), 523.

Roy, S., 2009. Recovery improvement of fine iron ore particles by multi gravity separation. The Open Mineral Processing Journal, 2(14), 17-30.

Salazar, J. M., Weber, G., Simon, J. M., Bezverkhyy, I., Bellat, J. P., 2015. Characterization of adsorbed water in MIL-53(Al) by FTIR spectroscopy and ab-initio calculations. The Journal of Chemical Physics, 142(12), 124702.

Sapsford, D., Bowell, R., Dey, M., Williams, C., Williams, K., 2008. A comparison of kinetic nag tests with static and humidity cell tests for the prediction of ARD. Mine Water and the Environment, 325-328.

Schaufuss, A. G., Nesbitt, H. W., Scaini, M. J., Hoechst, H., Bancroft, M. G., Szargan, R. d., 2000. Reactivity of surface sites on fractured arsenopyrite (FeAsS) toward oxygen. American Mineralogist, 85(11-12), 1754-1766.

Seaman, D., Lauten, R., Kluck, G., Stoitis, N., 2012. Usage of anionic dispersants to reduce the impact of clay particles in flotation of copper and gold at the Telfer mine.

In: 11th AusIMM Mill Operators' Conference. The Australasian Institute of Mining and Metallurgy, Hobart, Tasmania, pp. 207–216

Secco, E. A., 1988. Spectroscopic properties of SO_4 (and OH) in different molecular and crystalline environments. I. Infrared spectra of $Cu_4(OH)_6SO_4$, $Cu_4(OH)_4OSO_4$, and $Cu_3(OH)_4SO_4$. Canadian Journal of Chemistry, 66(2), 329-336.

Simate, G. S., Ndlovu, S., 2014. Acid mine drainage: Challenges and opportunities. Journal of Environmental Chemical Engineering, 2(3), 1785-1803.

Smith, L. J., Bailey, B. L., Blowes, D. W., Jambor, J. L., Smith, L., Sego, D. C., 2013. The Diavik waste rock project: Initial geochemical response from a low sulfide waste rock pile. Applied Geochemistry, 36, 210-221.

Smith, L., Senior, G., Bruckard, W., Davey, K., 2011. The flotation of millerite- a single mineral study. International Journal of Mineral Processing, 99(1-4), 27-31.

Sobek, A. A., 1978. Field and laboratory methods applicable to overburdens and minesoils: Industrial Environmental Research Laboratory. US Environmental Protection Agency, Office of Research and Development.

Soria, J., Sanz, J., Sobrados, I., Coronado, J. M., Maira, A. J., Hernández-Alonso, M. D., Fresno, F., 2007. Ftir and NMR study of the adsorbed water on nanocrystalline anatase. The Journal of Physical Chemistry C, 111(28), 10590-10596.

Stewart, A. G., 2020. Mining is bad for health: A voyage of discovery. Environ Geochem Health, 42(4), 1153-1165.

Stewart, W. A., Miller, S. D., Smart, R., 2006. Advances in acid rock drainage (ARD) characterisation of mine wastes. (Doctoral dissertation, ASMR).

Stock, S., 2008. Recent advances in X-ray microtomography applied to materials. International Materials Reviews, 53(3), 129-181.

Suarez-Fernandez, G., Vega, J., Fuertes, A., Garcia, A., Martínez-Tarazona, M., 2001. Analysis of major, minor and trace elements in coal by radioisotope x-ray fluorescence spectrometry. Fuel, 80(2), 255-261.

Svoboda, J., 1994. The effect of magnetic field strenght on the efficiency of magnetic separation. Minerals Engineering, 7(5-6), 747-757.

Taha, Y., Benarchid, Y., Benzaazoua, M., 2021. Environmental behavior of waste rocks based concrete: Leaching performance assessment. Resources Policy, 74, 101419.

Taha, Y., Benzaazoua, M., Hakkou, R., Mansori, M., 2016. Natural clay substitution by calamine processing wastes to manufacture fired bricks. Journal of Cleaner Production, 135, 847-858.

Tambwe, O., Kotsiopoulos, A., Harrison, S. T., 2020. Desulphurising high sulphur coal discards using an accelerated heap leach approach. Hydrometallurgy, 197, 105472.

Tannenbaum, R., Zubris, M., David, K., Ciprari, D., Jacob, K., Jasiuk, I., Dan, N., 2006. FTIR characterization of the reactive interface of cobalt oxide nanoparticles embedded in polymeric matrices. Journal of the Physical Chemistry B, 110(5), 2227-2232.

Taskinen, A., Kauppila, P., Tornivaara, A., Heino, N., Kurhila, M., Tiljander, M., Korhonen, T., 2018. Improving environmental properties of arsenic and sulphide rich kopsa Au–Cu ore tailings through optimised mineral processing. Improving the environmental properties, utilisation potential and long-term prediction of mining wastes. Geological Survey of Finland, Bulletin, 408.

Tripathy, A., Bagchi, S., Biswal, S., Meikap, B., 2017. Study of particle hydrodynamics and misplacement in liquid–solid fluidized bed separator. Chemical Engineering Research and Design, 117, 520-532.

Tripathy, S. K., Bhoja, S. K., Kumar, C. R., Suresh, N., 2015. A short review on hydraulic classification and its development in mineral industry. Powder Technology, 270, 205-220.

Tugrul, N., Derun, E. M., Piskin, M., Piskin, S., 2003. Evaluation of pyrite ash wastes obtained by the sulfuric acid production industry. Paper presented at the Proceedings of the 8th International Conference on Environmental Science and Technology, Lemmos Island, Vol. A, Greece.

Tukel, C., Kelebek, S., 2010. Modulation of xanthate action by sulphite ions in pyrrhotite deactivation/depression. International Journal of Mineral Processing, 95(1-4), 47-52.

Uçurum, M., Bayat, O., 2007. Effects of operating variables on modified flotation parameters in the mineral separation. Separation and Purification Technology, 55(2), 173-181.

Umpleby, R. J., 2nd, Baxter, S. C., Chen, Y., Shah, R. N., Shimizu, K. D., 2001a. Characterization of molecularly imprinted polymers with the Langmuir-Freundlich isotherm. Analytical Chemistry, 73(19), 4584.

Uslu, T., Sahinoglu, E., Yavuz, M., 2012. Desulphurization and deashing of oxidized fine coal by knelson concentrator. Fuel Processing Technology, 101, 94-100.

Valli, M., Malmensten, B., Persson, I., 1994. Interactions between sulphide minerals and alkylxanthates 9. A vibration spectroscopic study of the interaction between arsenopyrite, millerite, molybdenite, orpiment and realgar and ethylxanthate and decylxanthate ions in aqueous solution. Colloids and Surfaces A: Physicochemical and Engineering Aspects, 83(3), 219-225.

Villeneuve, M., Bussière, B., Benzaazoua, M., Aubertin, M., 2009. Assessment of interpretation methods for kinetic tests performed on tailings having a low acid

generating potential. Proceedings, Securing the Future and 8th ICARD, Skelleftea, Sweden.

Von Ketelhodt, L., 2009. Viability of optical sorting of gold waste rock dumps. Paper presented at the World Gold Conference.

Vriens, B., Plante, B., Seigneur, N., Jamieson, H., 2020. Mine waste rock: Insights for sustainable hydrogeochemical management. Minerals, 10(9), 728.

Wang, C., Harbottle, D., Liu, Q., Xu, Z., 2014. Current state of fine mineral tailings treatment: A critical review on theory and practice. Minerals Engineering, 58, 113-131.

Weber, P. A., Thomas, J. E., Skinner, W. M., Smart, R. S. C., 2004. Improved acid neutralisation capacity assessment of iron carbonates by titration and theoretical calculation. Applied Geochemistry, 19(5), 687-694.

Wiles, M., Gingras, B., Suprunchuk, T., 1967. The c=s stretching vibration in the infrared spectra of some thiosemicarbazones. Canadian Journal of Chemistry, 45(5), 469-473.

Williams, D. J., Stolberg, D. J., Currey, N. A., 2006. Long-term monitoring of kidston's "store/release" cover system over potentially acid forming waste rock piles. Proceedings of the 7th ICARD, St Louis, Mo., USA, 26-30.

Williford, C., Bricka, R. M., 2000. Physical separation of metal-contaminated soils. In: I.K. Iskandar (Ed.), Environmental Restoration of Metals Contaminated Soils, 1st ed., CRC Press LLC, Boca Raton, FL, 2000, pp. 121–165.

Wills, B. A., 2016. Physical separation: Elsevier.

Wills, B. A., Finch, J. A., 2016. Chapter 12 - froth flotation. In B. A. Wills, J. A. Finch (Eds.), Wills' mineral processing technology (8th edition) (pp. 265-380). Boston: Butterworth-Heinemann.

Wills, B. A., Finch, J. A., 2016a. Chapter 10 - gravity concentration. In B. A. Wills, J. A. Finch (Eds.), Wills' mineral processing technology (8th edition) (pp. 223-244). Boston:

Wills, B. A., Finch, J. A., 2016b. Chapter 11 - dense medium separation (DMS). In B. A. Wills, J. A. Finch (Eds.), Wills' mineral processing technology (eighth edition) (pp. 245-264). Boston: Butterworth-Heinemann.

Yin, Z., Sun, W., Hu, Y., Zhang, C., Guan, Q., Wu, K., 2018. Evaluation of the possibility of copper recovery from tailings by flotation through bench-scale, commissioning, and industrial tests. Journal of Cleaner Production, 171, 1039-1048.

Young, R., 1993. The Rietveld method, Oxford University Press, Oxford, 1993, (Vol. 5).

Yu, M., Mei, G., Li, Y., Liu, D., Peng, Y., 2017. Recovering rare earths from waste phosphors using froth flotation and selective flocculation. Minerals & Metallurgical Processing, 34(4), 161-169.

Yuvakkumar, R., Hong, S., 2015. Nd2o3: Novel synthesis and characterization. Journal of Sol-Gel Science and Technology, 73(2), 511-517.

Zhan, G., Schafer, W., Milczarek, M., Myers, K., Giraudo, J., Espell, R., 2006. The evolution of evapotranspiration cover systems at barrick goldstrike mines. Paper presented at the Proc. 7th International Conference on Acid Rock Drainage, St. Louis, MO.

Zhang, F., Yuan, C., Lu, X., Zhang, L., Che, Q., Zhang, X., 2012. Facile growth of mesoporous co3o4 nanowire arrays on ni foam for high performance electrochemical capacitors. Journal of Power Sources, 203, 250-256.

Zhang, Y., Cao, Z., Cao, Y., Sun, C., 2013. Ftir studies of xanthate adsorption on chalcopyrite, pentlandite and pyrite surfaces. Journal of Molecular Structure, 1048, 434-440.

Zhang, Y., Liu, P., Jiang, L., Yang, X., Yang, J., 2019. Numerical simulation of flow field characteristics and separation performance test of multi-product hydrocyclone. Minerals, 9(5), 300.

Zhu, X.-n., Tao, Y.-j., Sun, Q.-x., Man, Z.-p., 2017. The low efficiency of lignite separation by an enhanced gravity concentrator. Energy Sources, Part A: Recovery, Utilization, and Environmental Effects, 39(8), 835-842.